U.S. DEPARTMENT OF COMMERCE
National Technical Information Service

PB-256 903

A MODEL FOR CALCULATING EFFECTS OF LIQUID WASTE DISPOSAL IN DEEP SALINE AQUIFER

PART I - DEVELOPMENT
PART II - DOCUMENTATION

INTERCOMP RESOURCE DEVELOPMENT AND ENGINEERING, INC.

PREPARED FOR

UNITED STATES GEOLOGICAL SURVEY

JUNE 1976

A MODEL FOR CALCULATING EFFECTS OF LIQUID WASTE DISPOSAL IN DEEP SALINE AQUIFER

PART I--DEVELOPMENT

PART II--DOCUMENTATION

U.S. GEOLOGICAL SURVEY

Water-Resources Investigations 76-61

BIBLIOGRAPHIC DATA SHEET	1. Report No. USGS/WRD/WRI-76/056	2.	3. Recipient's Accession No.
4. Title and Subtitle A MODEL FOR CALCULATING EFFECTS OF LIQUID WASTE DISPOSAL IN DEEP SALINE AQUIFERS...PART I--DEVELOPMENT; PART II--DOCUMENTATION (Final report)			5. Report Date June 1976 6.
7. Author(s) INTERCOMP Resource Development and Engineering, Inc.			8. Performing Organization Rept. No. USGS/WRI-76-61
9. Performing Organization Name and Address INTERCOMP Resource Development and Engineering, Inc. 1201 Dairy Ashford Houston, Texas 77079			10. Project/Task/Work Unit No. 11. Contract/Grant No. 14-08-0001-14703
12. Sponsoring Organization Name and Address United States Geological Survey , Water Resources Division National Center Reston, Virginia 22092			13. Type of Report & Period Covered Final 14.

15. Supplementary Notes

Computer code available as NTIS TAPE NO.

16. Abstracts

A transient, three-dimensional subsurface waste-disposal model has been developed to provide methodology to design and test waste-disposal systems. The model is a finite-difference solution to the pressure, energy, and mass-transport equations. Equation parameters such as viscosity and density are allowed to be functions of the equations' dependent variables. Multiple user options allow the choice of x, y, and z cartesian or r and z radial coordinates, various finite-difference methods, iterative and direct matrix solution techniques, restart options, and various provisions for output display.

The addition of well-bore heat and pressure-loss calculations to the model makes available to the ground-water hydrologist the most recent advances from the oil and gas reservoir engineering field.

17. Key Words and Document Analysis. 17a. Descriptors

Waste disposal, computer model, water pollution, groundwater, temperature

17b. Identifiers/Open-Ended Terms

Deep-well waste-disposal model

PRICES SUBJECT

17c. COSATI Field/Group

18. Availability Statement	19. Security Class (This Report)	21. No. of Pages
No restriction on distribution	UNCLASSIFIED	
	20. Security Class (This Page) UNCLASSIFIED	

A MODEL FOR CALCULATING EFFECTS OF LIQUID WASTE DISPOSAL IN DEEP SALINE AQUIFERS, PART I--DEVELOPMENT

By INTERCOMP Resource Development and Engineering, Inc.
1201 Dairy Ashford
Houston, Texas 77079

U.S. GEOLOGICAL SURVEY

Water-Resources Investigations 76-61

Sponsored by the U.S. Geological Survey,
contract number 14-08-0001-14703
U.S. Geological Survey Technical Officer: David B. Grove

June 1976

12

UNITED STATES DEPARTMENT OF THE INTERIOR

Thomas S. Kleppe, Secretary

GEOLOGICAL SURVEY

V. E. McKelvey, Director

For additional information write to:

U.S. Geological Survey
National Center, Mail Stop 411
12201 Sunrise Valley Drive
Reston, Virginia 22092

TABLE OF CONTENTS

LIST OF ILLUSTRATIONS

LIST OF ILLUSTRATIONS (CONTINUED)

LIST OF TABLES

1.0 ABSTRACT

Injection of liquid industrial wastes into confined underground saline aquifers can offer a good disposal alternative from both environmental and economic considerations. One of the needs in choosing from among several disposal alternatives is a means of evaluating the influence such an injection will have on the aquifer system. This report describes a mathematical model to accomplish this purpose.

The objective of the contract was to develop a three-dimensional transient mathematical model which would accurately simulate behavior of waste injection into deep saline aquifers. Fluid properties, density and viscosity are functions of pressure, temperature and composition to provide a comprehensive assessment tool. The model is a finite-difference numerical solution of the partial differential equations describing

(1) single phase flow in the aquifer,

(2) energy transport by convection and conduction, and

(3) compositional changes in the aquifer fluid.

The model is not restricted to examining waste disposal operations. It can be used effectively to evaluate fresh water storage in saline aquifers, hot water storage in underground aquifers, salt water intrusion into groundwater flow systems and other similar applications.

The primary advantages of the present model can be summarized as:

(1) The model is user-oriented for easy application to full-scale evaluation needs.

(2) The model is fully three-dimensional and transient.

(3) The model is comprehensive accounting for density and viscosity variations in the aquifer due to temperature or compositional changes.

(4) The model includes the effects of hydrodynamic dispersion in both the temperature and compositional mixing between resident and injected fluids.

(5) The model energy balance includes the effects of pressure. This can be important in deep aquifer systems where the viscous pressure gradient is significant.

(6) The model uses second-order correct space and time approximations to the convective terms. This minimizes the numerical dispersion problem.

(7) The model is extremely flexible in providing a wide choice of boundary conditions. These include natural flow in the aquifer, aquifer influence functions around the perimeter of the grid in recognition that the gridded region does not have no-flow boundaries, heat losses into the overlying or underlying impermeable strata, and the wellbore heat and pressure drop calculations coupled to the aquifer flow equations.

The limitations of the present techniques are:

(1) The use of the second-order correct finite-difference approximations introduces block size and time step restrictions. These restrictions, though considerably less stringent than explicit methods cause, depend upon the magnitude of the dispersivity.

(2) The comprehensive nature of the model makes the computer time and storage requirements significant.

(3) The model, because of its complexity, is not as efficient in reducing down to solve simpler problems as a specially written model would be.

Included in the report are detailed descriptions of the approach used in the model, validation tests of the model, and a typical application of the model. A comparison volume documents the input data requirements, program structure, and an example problem for the model.

2.0 INTRODUCTION

The primary objective of this contract was to develop a three-dimensional transient mathematical model which would accurately simulate the behavior of liquid waste injection into deep saline aquifers. To provide the user an accurate simulation technique, the model recognizes fluid properties as functions of pressure, temperature, and waste concentration. In using the term "simulate the behavior," this work deals only with those aspects of waste injection which are associated with the flow of the waste fluid in the aquifer. That is, the model is not intended to answer or necessarily provide input to the environmentally related problem of potential seismic activity because of the injection. Rather, the model developed as a part of this contract delineates the pressure response and fluid displacement fronts in the vicinity of a deep waste injection well.

During the last 10 to 15 years, the use of injection wells for disposal of liquid industrial wastes has focused attention on the need to accurately describe the effect of such waste injection on the receiving aquifer. The concept of using injection wells for disposal in lieu of discharge into surface waters is that the wastes are confined to isolated geologic strata rather than released into the usable environment. These subsurface strata constitute a storage reservoir for waste material which should not be ignored at least where greater benefits to man are not feasible. Among the real needs in evaluating injection well disposal operations are:

(a) acceptable injection rates and pressures,

(b) zones of influence,

(c) potential formation capacitance to receive wastes, and

(d) degree of confinement of wastes within the aquifer.

There are additional aquifer applications in which the model could be extremely useful. Saline aquifers as future storage reservoirs for fresh water have been recently discussed[1]. This application could be a very important use of the model to evaluate the tendency of the fresh water to overrun the brine and reduce storage effectiveness. The use of heat storage wells as a total energy approach[2] also could utilize sensitivity studies performed with this model. Salt water encroachment into fresh water aquifers is another potential application of the model. Further discussion of applications of several types are in the section describing the validation of the model.

Specific Problem Areas in Developing a Model

There are several difficulties in approaching the development of a mathematical model of this type. Many of these are discussed in the following paragraphs.

One of the difficulties is that when fluid properties depend strongly upon waste injection temperature or concentration, physically unstable displacements can take place. Two examples are cited. In the first, when the waste injection has a viscosity significantly less than the resident fluid (whether due to temperature or to concentration), the displacement instability of viscous fingering takes place[3,4,5]. That is, the fluid displacement is very inefficient with the waste fluid channeling through the resident fluid. A similar displacement inefficiency can take place when a waste injection which differs in density from the resident fluid is injected into a permeability stratified porous system. When the waste is less dense and the high permeability is at the bottom, more of the less dense fluid is injected into the more permeable strata. Subsequently, a zone of more dense resident fluid can overlie the less dense injection. Under such circumstances, small convective cells of the Raleigh-Taylor instability type are set up and mix the two fluids[6,7].

The above displacement instabilities are extremely difficult to solve quantitatively. The present model is a numerical solution of the three sets of partial differential equations describing flow of fluids in porous rock. Several literature articles[8,9,10,11] have presented work using numerical models to calculate unstable miscible fluid displacement. These articles have shown that without heterogeneity or some other small scale perturbation to set up the fluid instability, the calculated instabilities are delayed in forming compared with the corresponding laboratory scale physical displacement. With the introduction of a perturbing influence in the numerical model, these unstable fluid displacements can be quantified although there is always a tendency for the calculated fluid displacement to be more efficient than the corresponding physical one.

There is, of course, a severe limitation in the fieldscale applicability of the laboratory physical displacements which have been performed. This is due to the hydrodynamic dispersion or diffusion in the laboratory scale models being much less than the value which best describes full scale field tests. Since dispersion is the stabilizing influence on the displacement, a different scale dispersion value in the laboratory can be misleading in terms of predicting field displacements. Typical dispersion values in homogeneous

laboratory displacements are in the range of 0.0001 to 0.01 feet. Some recent work[12] in matching full scale behavior of miscible constituents indicates the dispersivity may range from one to 100 feet--at least a factor of one hundred fold larger. Calculations indicate that with this magnitude dispersivity, the viscosity or density contrast must be quite large to develop a significant instability in the fluid displacement front.

Another problem area in developing a mathematical model is the difficulty in applying finite-difference techniques to first order convective problems. It is well known that the type of finite-difference approximation used can introduce numerical diffusion which is virtually indistinguishable from physical dispersion[13,14,15]. The two techniques used in the hydrology area to prevent this problem are (1) the method of characteristics[16,17,18] (other names are particle-in-a-cell, point tracking, etc.) and (2) higher order Galerkin[19,20] (other names used are variational, finite element, etc.) methods. In the present finite-difference model, we have used second order correct finite central difference approximations in both time and space. These techniques have the advantage that no numerical diffusion term of second order is introduced. The disadvantage they introduce is a limitation on block size and time step. This limitation is necessary to prevent calculated temperatures and/or concentrations from exceeding the injection levels or from being less than the initial values. The time step and block size restrictions are not overly severe for many problems. These limitations are discussed more fully in the body of the report.

As mentioned above, the basic approach in developing this model is to use finite-difference approximations for each of the three partial differential equations describing flow in the aquifer. The boundary conditions used allow water flow into and out of the finite-difference grid at any peripheral grid block in the three dimensions. Heat losses to impermeable (aquitard) strata above and below the injection interval are also included. Boundary conditions at isolated injection or production points (injection or production wells) can be specified. To permit more user flexibility, we have included the calculation of wellbore heat losses and pressure drop for flow in the injection or production wells. This overall model concept gives rise to a coupling of two separate models. These are:

(1) the reservoir model which solves the flow and energy transport in the aquifer and surrounding strata, and

5

(2) the wellbore model which solves the flow and energy transport during flow up or down the well.

Conceptually, this coupling and the factors considered are illustrated in Figure 1. The reservoir model solves the flow and energy transport throughout the set of individual grid blocks. Flow outside the region of primary interest (grid block definition) is allowed through aquifer influence functions. Essentially, this represents the coupling of an analytical concept (for example, the region of interest surrounded by an infinite aquifer) and the numerical solution. Heat transport into regions of no flow are included by finite-difference calculations in these regions coupled to the temperature profiles in the aquifer. Specified wells also impose a boundary condition. If the bottom-hole quantities were known (bottom-hole pressure, temperature, and concentration), the boundary condition could be set independent of the aquifer calculation. However, often the bottom-hole pressure and temperature have not been measured. Rather these quantities along with the rate are known at the wellhead or surface. As a consequence, the wellbore model can be required to solve for the pressure drop (rise) and temperature changes occurring during flow up or down the well. Linkage between the wellbore and reservoir models must be considered. An iterative procedure can be required and is included in the model if surface conditions are specified.

The following section describing the technical approach presents the combined model concept expressed above. The organization is to present

(1) the partial differential equations,

(2) the finite-difference approximations for both the reservoir and wellbore models,

(3) the method of solution, and

(4) the boundary conditions.

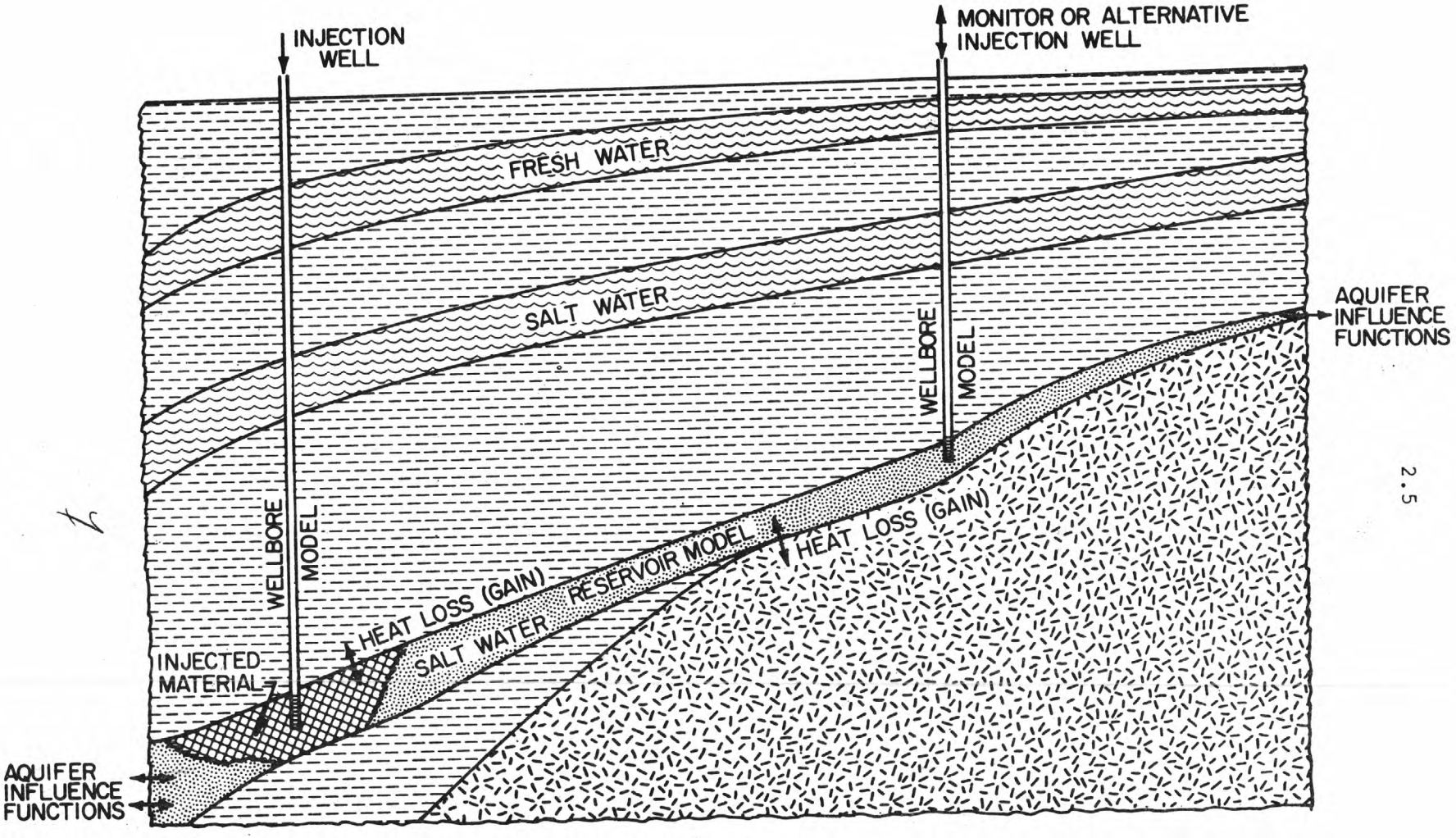

Figure 1. Schematic of the well disposal model.

3.0 TECHNICAL APPROACH

The model developed under this contract is intended to provide a user-oriented, comprehensive calculational tool for assessing the fluid displacement taking place during injection well disposal operations. The model consists basically of two parts: (1) a three-dimensional finite-difference reservoir model, and (2) a wellbore model. To the user, the two parts are indistinguishable. They are coupled closely together since the wellbore model relates the surface pressure and enthalpy to the calculated bottom-hole pressure and enthalpy from the reservoir model. At the same time, these bottom-hole quantities must also satisfy the material and energy balance relationships taking place in the reservoir.

The finite-difference reservoir model solves three coupled partial differential equations describing the behavior of a liquid phase injected into an aquifer system. The three differential equations are:

(1) conservation of total liquid mass;

(2) conservation of energy; and

(3) conservation of the mass of a specific contaminant dissolved in the injection fluid.

The first equation describes the three-dimensional Darcy flow of a single phase liquid in a porous aquifer. The density of the liquid phase can be a function of temperature, pressure, and concentration. The second equation describes the convection and dispersion of energy due to injection of a fluid of different temperature (and pressure) than the resident aquifer fluid. The third equation describes the convection and hydrodynamic dispersion of a component in the injected fluid. This allows different salinity injection from the resident aquifer water or a component which is present in the injection, but not the resident fluid. The end result is a prediction of the concentration, temperature, and pressure patterns resulting from injection of liquid wastes whose density due to temperature and/or concentration differs from the geothermally heated saline aquifer.

In addition to the three-dimensional rectangular Cartesian grid, we also have provided a two dimension (r,z) grid system. This cylindrical coordinate system is extremely well suited to single well interpretive or predictive calculations.

Basic assumptions contained in the reservoir model are:

8

(a) Three-dimensional, transient, laminar (Darcy) flow.

(b) Fluid density can be a function of pressure, temperature, and concentration. Fluid viscosity can be a function of temperature and concentration.

(c) Miscibility of the injected wastes with the in-place fluids.

(d) Aquifer properties vary with position (i.e. porosity, permeability, thickness, and elevation can be specified for each grid block in the model).

(e) Hydrodynamic dispersion is described as a function of fluid velocity.

(f) The energy equation can be described as "enthalpy in-enthalpy out = change in internal energy of the system." This is rigorous except for kinetic and potential energy which have been neglected.

(g) Boundary conditions allow natural water movement in the aquifer, heat losses to the adjacent formations, and the location of injection, production and observation points anywhere within the system.

The wellbore model simulates the injection (or production) well conditions and provides the boundary conditions for the reservoir model. The energy losses in the well are calculated to obtain the bottom-hole pressure and temperature values. The pressure drop between the well and the center of the grid block is also calculated and the rate is allocated between each vertical layer. The user may specify surface conditions or the bottom-hole temperature and pressure values. If the surface temperature and injection rate are specified, the model calculates both the surface pressure necessary to achieve the desired rate and the enthalpy of the injection stream as it enters the aquifer. The heat losses to the formation surrounding the wellbore, the frictional pressure drop, and the gravity head are calculated by the wellbore model. Alternately, one can choose to specify the surface pressure and temperature, and the model calculates the rate that can be injected limited by these specified surface conditions. In this case, an iterative procedure is required to calculate the bottom-hole pressure and the allowable injection rate. Similarly, if the well is producing, one may specify the rate or the surface pressure. The

latter case requires an iterative procedure to calculate the bottom-hole pressure and the allowable production rate.

The assumptions used in the wellbore model can be summarized as follows:

(a) Viscous heat dissipation can be neglected in the wellbore calculation.

(b) The initial ground temperature surrounding each well is known and can be expressed as a function of depth only.

(c) Flow in the well is incompressible and steady-state.

(d) For the purposes of wellbore heat loss calculations, the well is treated as a constant flux line source.

(e) Fluid properties, heat capacity, viscosity, and density are allowed to vary with pressure and temperature in the wellbore.

(f) The enthalpy of the injection fluid can be expressed as a simple proportionality to the enthalpy of pure water at the same temperature and pressure.

3.1 Reservoir Model Equations

Suppose x,y,z to be a Cartesian coordinate system and let Z(x,y,z) be the height of a point above a horizontal reference plane. Then the basic equation describing single-phase flow in a porous media results from a combination of the continuity equation

$$\nabla \cdot \rho u + q' = - \frac{\partial}{\partial t} (\phi \rho) * \qquad (3\text{-}1)$$

and Darcy's law in three dimensions.

$$u = - \frac{k}{\mu} (\nabla p - \rho g \nabla Z) . \qquad (3\text{-}2)$$

---

* Detailed definitions of all terms are given in the Nomenclature.

The result is the basic flow equation

$$\nabla\cdot\frac{\rho k}{\mu}(\nabla p - \rho g\nabla Z) - q' = \frac{\partial}{\partial t}(\phi\rho). \tag{3-3}$$

A material balance for the solute results in the solute or concentration equation

$$\nabla\cdot(\rho C\frac{k}{\mu}(\nabla p - \rho g\nabla Z)) + \nabla\cdot(\rho E)\cdot\nabla C - q'C = \frac{\partial}{\partial t}(\rho\phi C). \tag{3-4}$$

The energy balance defined as [enthalpy in-enthalpy out = change in internal energy] is described by the energy equation

$$\nabla\cdot(\frac{\rho k}{\mu} H (\nabla p - \rho g\nabla Z)) + \nabla\cdot K\cdot\nabla T - q_L - q'H \tag{3-5}$$

$$= \frac{\partial}{\partial t}[\phi\rho U + (1-\phi)(\rho C_p)_R T]$$

The system of equations (3), (4) and (5) along with the fluid property dependence on pressure, temperature, and concentration describe the reservoir flow due to injection of wastes into an aquifer. These fluid property functions are discussed in Section 4.1. This is a nonlinear system of coupled partial differential equations which must be solved numerically using high speed digital computers.

These equations are solved by dividing the region of interest into a three-dimensional grid and developing finite-difference approximations for this grid. Once the region of interest is divided into grid blocks, finite-difference equations are developed whose solution closely approximates the solution of equations (3), (4), and (5). These finite-difference approximations are:

Basic Flow Equation

$$\Delta[T_w(\Delta p - \rho g\Delta Z)] - q = \frac{V}{\Delta t}\delta(\phi\rho) \tag{3-6}$$

11

Concentration Equation

$$\Delta[T_w C(\Delta p - \rho g \Delta Z)] + \Delta(T_E \Delta C) - Cq = \frac{V}{\Delta t}(\rho \phi C) \tag{3-7}$$

Energy Equation

$$\Delta[T_w H(\Delta p - \rho g \Delta Z)] + \Delta(T_C \Delta T) - q_L - q\,H = \frac{V}{\Delta t}\,\delta[\phi \rho U + (1-\phi)(\rho C_p)_R T] \tag{3-8}$$

where the difference operators are defined by

$$\Delta(T_w \Delta p) = \Delta_x(T_w \Delta_x p) + \Delta_y(T_w \Delta_y p) + \Delta_z(T_w \Delta_z p) \tag{3-9}$$

with

$$\Delta_x(T_w \Delta_x p) = T_{w,i+1/2,j,k}\,(p^{n+1}_{i+1,j,k} - p^{n+1}_{i,j,k}) - T_{w,i-1/2,j,k}\,(p^{n+1}_{i,j,k} - p^{n+1}_{i-1,j,k}) \tag{3-10}$$

and

$$\delta\chi = \chi^{n+1} - \chi^{n} \tag{3-11}$$

The terms

$$T_w = \frac{kA\rho}{\mu \ell} \tag{3-12}$$

$$T_c = \frac{KA}{\ell} \tag{3-13}$$

$$T_E = \rho\frac{EA}{\ell} \tag{3-14}$$

have been introduced for notational convenience. Since all of the terms in equation (12) through (14) are position dependent, a further expansion is illustrated as

$$T_{w,i+1/2,j,k} = \frac{2\Delta y_j \Delta z_k}{\left(\frac{\Delta x}{k_x}\right)_i + \left(\frac{\Delta x}{k_x}\right)_{i+1}} (\rho/\mu)_{i+1/2,j,k} \qquad (3\text{-}15)$$

$$T_{E,i,j+1/2,k} = \frac{2\Delta x_i \Delta z_k}{\left(\frac{\Delta y}{E}\right)_j + \left(\frac{\Delta y}{E}\right)_{j+1}} (\rho)_{i,j+1/2,k} \qquad (3\text{-}16)$$

and $$T_{c,i,j,k+1/2} = \frac{2\Delta x_i \Delta y_j}{\left(\frac{\Delta z}{K}\right)_k + \left(\frac{\Delta z}{K}\right)_{k+1}} \qquad (3\text{-}17)$$

For radial geometry, the term $\frac{2\Delta y_j \Delta z_k}{\Delta x_i + \Delta x_{i+1}}$ becomes $2\pi \Delta z_k / \ln(r_{i+1}/r_i)$. The volume term is written as $\pi \Delta r_i^2 \Delta z_k$.

Two terms, the constituent dispersion tensor, E, and the effective heat conductivity tensor, K, need additional description. Both are taken in the present model as dependent upon the hydrodynamic dispersivity. This dispersivity is a function of the local fluid velocity. Scheidegger[21] has shown that for an isotropic porous medium there can be no more than two independent dispersivity factors. This requirement is essential so that the dispersion tensor is invariant under coordinate transformations. These two dispersivities are longitudinal, in the direction of flow, and transverse, perpendicular to flow. Generally, both are functions of the magnitude of the flow velocity. These values can be expressed as:

$$D_l = \alpha_l |\bar{u}| \qquad (3\text{-}18)$$

and

$$D_t = \alpha_t |\bar{u}|$$

When the velocity vector is divided into components along the coordinate axes, nine components of both the dispersivity and conductivity tensors occur.

These nine components (six distinct) of the dispersivity tensor can be expressed as follows:

$$
\begin{aligned}
E_{xx} &= D_l \cos^2\psi\cos^2\theta + D_t(\sin^2\theta\cos^2\psi + \sin^2\psi) \\
E_{xy} &= (D_l - D_t)\ \sin\theta\cos\theta\cos^2\psi \\
E_{xz} &= (D_l - D_t)\ \sin\psi\cos\psi\cos\theta \\
E_{yx} &= E_{xy} \\
E_{yy} &= D_l \cos^2\psi\sin^2\theta + D_t(\cos^2\theta\cos^2\psi + \sin^2\psi) \\
E_{yz} &= (D_l - D_t)\ \sin\psi\cos\psi\sin\theta \\
E_{zx} &= E_{xz} \\
E_{zy} &= E_{yz} \\
\text{and}\quad E_{zz} &= D_l \sin^2\psi + D_t \cos^2\psi
\end{aligned}
\qquad \text{(3-19)}
$$

The subscripts refer to the concentration derivatives as

$$
\frac{\partial\left(E_{xx}\frac{\partial c}{\partial x}\right)}{\partial x},\quad \frac{\partial\left(E_{xy}\frac{\partial c}{\partial y}\right)}{\partial x},\quad \frac{\partial\left(E_{yx}\frac{\partial c}{\partial x}\right)}{\partial y},\quad \text{etc.}
$$

Hydrodynamic dispersion introduces cross derivative terms into the component and energy equations. These cross terms represent component (or energy transport) in one coordinate direction due to concentration (or temperature) gradients in another direction.

As can be noted from Equations (19), when the velocity vector is oriented along the coordinate directions, the cross terms become identically zero. The maximum effect is when the velocity is along a 45° angle from one of the coordinate planes. Note also from (19) that when the transverse coefficient equals the longitudinal dispersivity, the cross terms are identically zero.

The more general expressions for the dispersivity and conductivity tensors in terms of the molecular properties as well as hydrodynamic dispersivity can be written as

$$
E \equiv \phi\ \alpha u/\phi\ + D_m
$$

and

$$
K \equiv \phi\ \alpha u/\phi\ (\rho C_p)_w + K_m \qquad \text{(3-20)}
$$

14

where the dispersivity, α, is either longitudinal or transverse. Note that the apparent conductivity due to hydrodynamic dispersion in the porous media has been taken as the product of the dispersivity, velocity and fluid volumetric heat capacity. The ordinary molecular heat conductivity of fluid plus rock, K_m, has been treated as an additive constant. The concept expressed in the two equations listed as (2) is that the microscopic heterogeneity in convective flow creates the same dispersive effect in temperature as it does in a constituent concentration.

3.2 Wellbore Model Equations

If the user elects to specify surface conditions instead of bottom-hole values, the pressure and temperature changes in the wellbore must be computed. This is done by solving the equation of energy (total) and the equation of mechanical energy simultaneously over the wellbore depth. The steady-state energy balance over a depth, ΔZ, can be written as

$$\Delta H + \frac{g\Delta Z}{g_c J} + \frac{w\Delta w}{g_c J} = \Delta Q - \frac{\Delta W_f}{J}. \qquad (3\text{-}21)$$

Assuming incompressible flow, Eq. (21) becomes:

$$\Delta H + \frac{g\Delta Z}{g_c J} = \Delta Q \qquad (3\text{-}22)$$

The heat lost to the surroundings over a depth, ΔZ, is lost through two series resistances. These include (1) heat lost from the fluid to the outside casing wall, and (2) heat lost from the casing wall temperature into the surrounding formation. The overall heat loss can be expressed as:

$$\Delta Q = \frac{2\pi R_1 U_c \Delta Z (T_{av} - T_R)}{qF(t)} \qquad (3\text{-}23)$$

In Eq. (23), the heat lost into the surrounding rock is represented by the function F(t). It can be derived assuming the wellbore is a constant heat flux line source. This overall derivation was first given by Ramey[22]. The resulting expression for F(t) is as follows:

15

$$F(t) \simeq -\ln\left(\frac{R_2}{2\sqrt{\gamma t}}\right) - 0.290 \qquad (3\text{-}24)$$

The actual expression involves the exponential integral function for which Eq. (24) is simply an excellent approximation for times greater than a fraction of one day.

The coefficient U_c in Equation (2) is a combination of the overall heat transfer coefficient for the wellbore and the conductivity of the rock. It can be expressed as:

$$\frac{1}{U_c} = \frac{1}{UF(t)} + \frac{R_1}{k} \qquad (3\text{-}25)$$

For very short times (determined by F(t) in Equation (24) <0), the function F(t) is taken as zero. This is equivalent to assuming that the outside casing wall temperature remains at the geothermal gradient until the time is sufficiently large to cause F(t)=0. Then each wellbore increment loses heat as a constant flux source.

Since enthalpy is a function of temperature and pressure, the equation of mechanical energy must be simultaneously solved to calculate the change in pressure over ΔZ. The change in pressure is the sum of the change in the gravity head and the frictional pressure drop:

$$-\Delta p = \frac{\Delta Z \rho g}{g_c} + \frac{f\rho w^2}{4g_c R_1} \qquad (3\text{-}26)$$

The friction factor is a function of Reynolds number and surface roughness. The enthalpy of the fluid is a function of both temperature and pressure:

$$H = H(p,T) \qquad (3\text{-}27)$$

The enthalpy of an arbitrary injection fluid is assumed to be proportional to the enthalpy of pure water at the same pressure and temperature according to the following relation:

$$H = C_p H_w / C_{pw} \qquad (3\text{-}28)$$

3.3 Solution of Reservoir Equations

The general finite-difference representations were listed as equations (6) through (8). These equations outline a semi-implicit finite-difference approximation in that the dependent variables, p, T, and C, appearing in the space derivatives are carried at the new time level. If the equations were linear, this results in a totally stable difference approximation. The equations are, however, nonlinear because in general the fluid properties are functions of the dependent variables. Additionally, the well-known problem of artificial numerical diffusion in finite differencing the first order convective terms requires special treatment. As a consequence, additional explanation of the finite difference approximations is in order before discussing the method of solution.

Both the component and energy balances include at user option two choices for the finite-difference approximation to the convective terms (first order space derivatives). These choices are upstream weighting (a backward difference) or central weighting (a central difference). The option is provided to give flexibility in reducing space truncation error.

It is wellknown that a backward difference introduces a space truncation error which is virtually identical in form to the desired physical diffusion[14]. The truncation errors are discussed in more detail in Sec. 5.2. Unfortunately, the space truncation error can overshadow the desired physical diffusion level for grid sizes one would desire to use. In the one-dimensional case, the space truncation error can be simply quantified as:

(1) concentration, $u\Delta x/_2$

(2) temperature, $u(\rho C_p)_w \Delta x/_2$.

These terms should be small compared to the terms E, and K, respectively. Otherwise the backward difference space truncation error can dominate the desired physical diffusion. In the case of hydrodynamic dispersion being much larger than the molecular diffusion or conduction term, the above restriction takes the form of

$$\frac{\Delta x}{2} << \alpha \text{ for either case above.} \qquad (3\text{-}29)$$

Since the value of α might typically be in the range of 30 to perhaps 100 feet, the above restriction can be a severe limitation. It should be noted that the above definition for

dispersivity factor, α, should be divided by porosity to get the value others have often used for the term dispersivity.

When a central difference finite-difference approximation is used, the space truncation error is no longer of second order (proportional to the second derivative). As a consequence, there is no artificial numerical diffusion term. There is, however, still a limitation on grid size. This particular limitation is caused by the tendency of the central difference result to overshoot and undershoot the minimum and maximum limits defined by the injection and resident fluid parameters[15]. This "oscillation" in space can be eliminated if

$$\frac{u\Delta x}{2} \leq E \tag{3-30}$$

and $$u(\rho C_p)_w \, \Delta x/_2 \leq K. \tag{3-31}$$

The above restrictions are not a mandatory requirement. Good results can be obtained even when $\frac{u\Delta x}{2}$ is somewhat greater than E. However, the user must recognize that there may be concentrations which slightly exceed the injected concentration and/or are slightly below the original resident fluid concentration.

Similarly, there is a time truncation error associated with the finite-difference approximation of the first order time derivative. Because of the convective terms in both the energy and constituent equation, the time truncation error can introduce a term which has the same effect as physical diffusion. If a backward difference in time (implicit) is used, this term can be written as:

(1) concentration, $\frac{u^2\Delta t}{2\phi}$

(2) temperature, $\frac{u^2(\rho C_p)_w \beta \, \Delta t}{2\phi}$

We have provided the user the option to choose the central difference in time Crank-Nicholson approximation. The Crank-Nicholson approximation is provided for both the energy and constituent equations, but not for the pressure equation because of the tendency for the solution to oscillate. As an example of this approximation, the concentration equation is illustrated:

$$\frac{1}{2}\Delta[T_w C^{n+1}(\Delta p^{n+1} - \rho g \Delta Z)] + \frac{1}{2}\Delta[T_w C^{n}(\Delta p^{n+1} - \rho g \Delta Z)]$$

$$+ \frac{1}{2}\Delta(T_E \Delta C^{n+1}) + \frac{1}{2}\Delta(T_E \Delta C^{n}) - \frac{1}{2}\, qC^{n+1} - \frac{1}{2}\, qC^{n} \qquad (3\text{-}32)$$

$$= \frac{V}{\Delta t}\,\delta(\rho\phi C)$$

This difference approximation has the advantage that it reduces time truncation error; however, it has the disadvantage of introducing a time step limitation to prevent slight oscillations. Our experience indicates the limitation is much less severe than the forward in time explicit approximation. In fact, it is about one-half the explicit in time first order stability criterion. The explicit criteria is:

$$\frac{u\Delta t}{\phi \Delta x} < 1 \qquad (3\text{-}33)$$

Thus, a factor of at least two larger can be used effectively with the Crank-Nicholson difference approximation.

The method of including the cross derivative terms in the temperature or concentration equations can briefly be described as follows:

(1) the cross derivative terms in the x and y directions are written at the old iterate level.

(2) in subsequent iterations after the first to update the density, the cross derivative terms are updated.

(3) the user can choose to neglect the cross derivative terms and instead use what we have termed coordinate direction diffusivity enhancement.

The coordinate direction diffusivity enhancement amounts to adding the E_{xy} and E_{xz} terms to the E_{xx} coefficient. Similarly, the E_{yx} and E_{yz} terms are added to E_{yy}. One might logically question the realism of this addition of terms. The basic problem is that if a radial flow problem is run in an xy Cartesian system, the diffusion along the 45° line in the xy plane is too low without cross terms.

As a consequence, the diffusion front looks diamond-like in shape. The front is where it should be along the coordinate directions, but is suppressed along the 45° direction. When the transverse coefficient is equal to the longitudinal, the front becomes radial again. Thus, the concept of "enhancement" of the coordinate direction terms effectively recreates this radial front. We have conducted several numerical experiments and found the enhancement approximates surprisingly well the use of the full-blown cross derivative terms as shown in Figure 2. Thus, we have provided the user the option to use either enhancement or the inclusion of the cross terms lagged at the old iterate.

The method of solving the finite-difference approximations (Equations (6), (7), and (8)) is very similar to the method used by Coats et al[23] which has been shown to work for systems even more complex than this one. This procedure provides stability and permits large time steps with a minimum amount of computer time. The actual details of the solution technique are developed in Appendix A.

3.3.1 Boundary and Initial Conditions

Specification of boundary conditions are the primary importance at

(1) injection or production wells,

(2) external periphery of the finite-difference grid definition, and

(3) at the juncture between the aquifer and the confining overburden and underburden.

The treatment of these boundary conditions is described in three separate sections included in Appendix B. The first describes the well specifications whether this specification is at the surface or at bottom-hole. The second section describes the aquifer influence functions which are used to represent the peripheral boundary. The third section describes the heat losses to overburden and underburden.

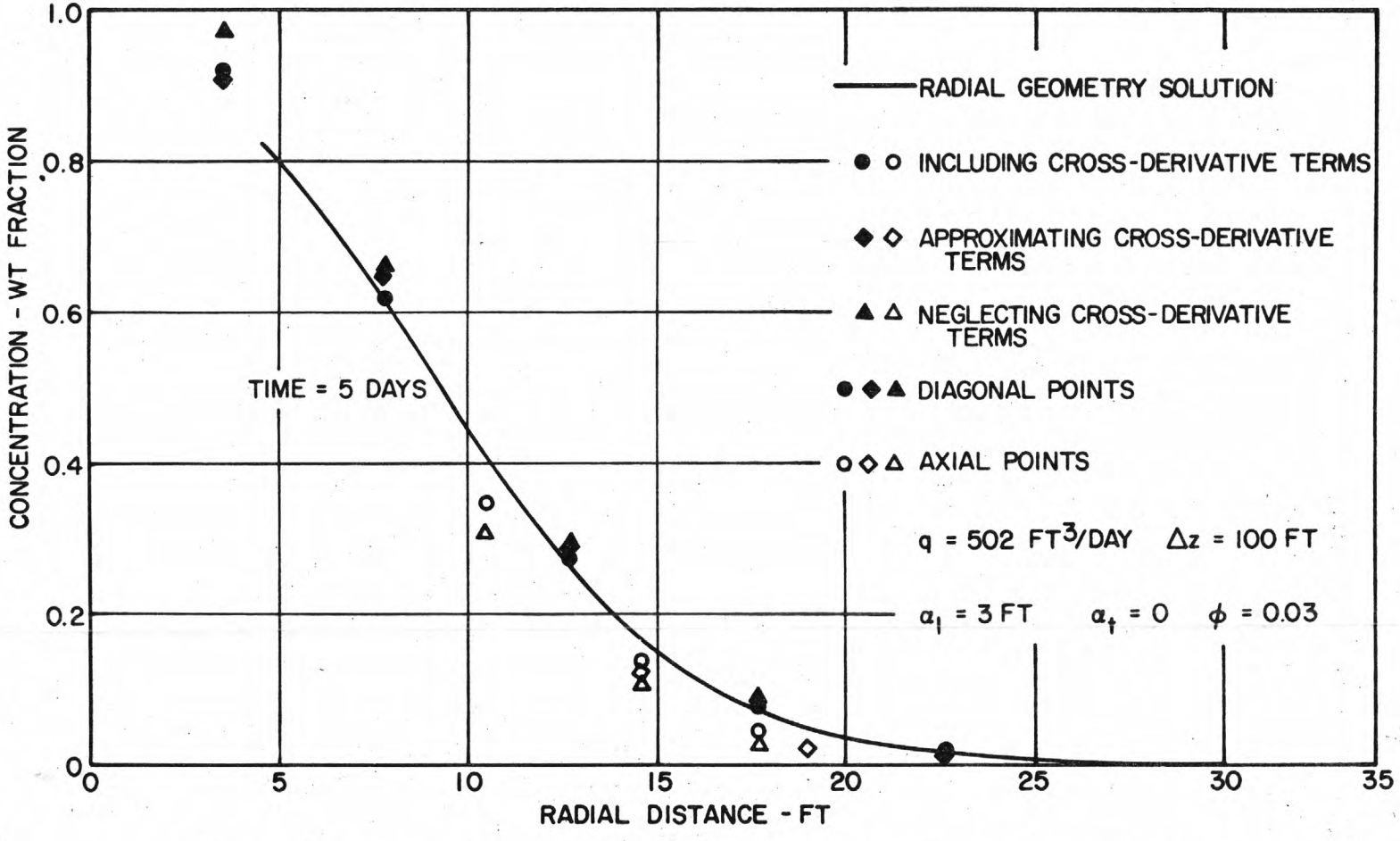

Figure 2. Importance of Including Dispersivity Cross Derivatives

4.0 MODEL TESTS

Calculational tests performed to verify the model can be categorized into four types. These are:

(1) fluid property calculation tests

(2) reservoir model tests

  (a) comparisons with simplified analytical solutions

  (b) adequacy of boundary conditions

    (i) aquifer influence functions

    (ii) overburden and underburden heat losses

(3) wellbore model tests

(4) comparison with laboratory scale model results

This section includes the details of many of the tests along with a summary of all the tests performed.

4.1 Fluid Property Calculation Tests

4.1.1 Fluid Density Model

The numerical finite-difference model includes the density as a function of composition, temperature and pressure. Fluid density, ρ, has been expanded in a three-dimensional Taylor series about the natural reservoir fluid density weight fraction (concentration = 0) at some reference temperature and pressure. For convenience, we take the initial temperature and pressure at some point in the aquifer as the reference conditions. Therefore,

$$\rho(C,T,p) = \rho_o(0,T_o,p_o) + \left[\frac{\partial\rho}{\partial C}\Big|_{C=0} C + \ldots.\right] + \left[\frac{\partial\rho}{\partial T}\Big|_{T=T_o} (T-T_o) + \ldots.\right] + \left[\frac{\partial\rho}{\partial p}\Big|_{p=p_o} (p-p_o) + \ldots.\right] \quad (4\text{-}1)$$

Neglecting the second and higher order terms, Eq. (1) can be written as follows:

$$\rho = \rho_o + a_3 C + a_2 (T-T_o) + a_1 (p-p_o) \qquad (4\text{-}2)$$

where $a_3 \equiv \left.\frac{\partial \rho}{\partial C}\right|_{C=0}$; $a_2 \equiv \left.\frac{\partial \rho}{\partial T}\right|_{T=T_o}$; $a_1 \equiv \left.\frac{\partial \rho}{\partial p}\right|_{p=p_o}$

and ρ_o is the density of the natural reservoir fluid at the initial temperature and pressure conditions.

In the model, the user is required to define both the resident fluid and the injection fluid densities at some specified value of temperature and pressure (T_1, p_1). If this specified temperature and pressure corresponded to the initial temperature and pressure at the reference point in the aquifer, then the reference density ρ_o (O, T_o, p_o) would be known. Usually this correspondence is inconvenient since the fluid densities will more likely be measured or known at a standard temperature and pressure corresponding to surface conditions. Thus, there are four values to be determined before Equation (2) defines the density of the fluid as a function of temperature and pressure.

Equation (2) assumes that the values a_1, a_2, and a_3 are independent of p, T, and C. This assumption can be tested for some fluid mixtures. Table I lists values of a_2 and a_3 for brine (NaCl) as a function of composition and temperature[24].

TABLE I

DENSITY MODEL COEFFICIENTS FOR NaCl (BRINE)

Coefficient	Wt.%	Temperature 60°F	130°F	200°F	Average over Temp.
$a_2 x10^2$ lb/ft^3°F	4	-1.34	-1.81	-2.51	-1.80
a_3 lb/ft^3%		0.43	0.43	0.42	0.43
$a_2 x10^2$ lb/ft^3°F	12	-1.66	-1.71	-1.82	-1.75
a_3 lb/ft^3%		0.46	0.46	0.45	0.46
$a_2 x\ 10^2$ lb/ft^3°F	20	-2.11	-2.22	-1.65	-1.72
a_3 lb/ft^3%		0.49	0.48	0.47	0.48
$a_2 x10^2$ lb/ft^3°F	Average over Comp.	-1.70	-1.95	-2.0	
a_3 lb/ft^3%		0.47	0.46	0.46	

Note that the thermal coefficient exhibits more variation with either composition or temperature than does the compositional coefficient. A constant average, over the range, value of a_3 introduces no more than about a 2% error in the value of a_3. Whereas, a similar average a_2 could introduce as much as a 30% error in the correct value of a_2. Still, we believe that the density model will not introduce errors outside of the normal range in uncertainty for the daily variation in density of typical waste injections. Little data on the compressibility of liquids as a function of T, p, and composition are available. Thus, it is difficult to assess whether or not a_1 is relatively constant. However, the effect of pressure on the density of liquid is significantly less than either the effect of composition or density.

The constants ρ_0, a_1, a_2, and a_3 are calculated from known values of the densities of the natural reservoir fluid and the injection fluid at some pressure (p_1) and temperature (T_1) and from the coefficients of thermal expansion and compressibility as follows:

The coefficient of thermal expansion is defined as

$$c_T \equiv -\frac{1}{\rho}\left(\frac{\partial \rho}{\partial T}\right) \tag{4-3}$$

and the compressibility as

$$c_w \equiv \frac{1}{\rho}\left(\frac{\partial \rho}{\partial p}\right) \tag{4-4}$$

Therefore, the partial derivatives of the density with respect to temperature and pressure at initial aquifer conditions are:

$$a_2 \equiv \left.\frac{\partial \rho}{\partial T}\right|_{T_o} = \rho_o\, c_T \tag{4-5}$$

and

$$a_1 \equiv \left.\frac{\partial \rho}{\partial p}\right|_{p_o} = \rho_o\, c_w. \tag{4-6}$$

The model calculates the reference fluid density, ρ_o, from the resident fluid density at (T_1, p_1) and the fluid properties c_w and c_T by the following relationship:

$$\rho_o = \rho(0,T_1,p_1)/(1 + c_w(p_1-p_o) + c_T(T_1-T_o)) \tag{4-7}$$

Subsequently, a_2 and a_1 are calculated from Eqs. (36) and (37). The coefficient, a_3, is calculated from the difference between resident and injection fluid density as:

$$a_3 \equiv \frac{\partial \rho}{\partial C} = \rho(1,T_1,p_1) - \rho(0,T_1,p_1) \tag{4-8}$$

It is helpful to inspect the relative contribution variations in temperature, pressure and concentration create in the fluid density. The compressibility of liquids is on the order of 10^{-7} - 10^{-6}/psi. As a consequence, pressure changes as large as 1000 psi would cause only a density change of roughly 0.01 to 0.1%. The thermal expansion coefficient for typical liquids varies from 10^{-4} - 10^{-3}/°F. A 100°F temperature change would then cause a density change of 1.0 to 10%. Compositional changes will generally cause the greatest effect on density. Density changes of 20% are possible over the range of fresh water to 24% NaCl. Similar density changes occur with other salts. Aqueous organic constituents probably affect the density less.

4.1.2 Fluid Viscosity Model

The viscosity included in the disposal model accounts for the influence of fluid composition and temperature on the fluid viscosity. Pressure effects have been neglected. The viscosity model was developed with the concept in mind that the user might have very little measured viscosity data for the injected fluid. Alternatively, if measured data were available, we wanted to have as accurate a model as was feasible.

The basic viscosity model dependence on concentration and temperature was expressed as:

$$\mu(T,C) = \mu_R(C) \exp[B(C)(1/T-1/T_R)] \qquad (4\text{-}9)$$

where $\mu_R(C)$ = the fluid viscosity at the reference temperature, T_R

$B(C)$ = a function of composition only

The compositional dependent factor B is taken as a linear function:

$$B(C) = CB_i + (1-C)B_r \qquad (4\text{-}10)$$

where C = mass fraction of the injection fluid, and

B_i, B_r = the "best" constants representing the temperature dependence of both injection and resident fluids

If only pure component viscosity data are available, a separate functional relationship is used.

$$\mu(T_R,C) = \mu_i(T_R)^C \mu_r(T_R)^{(1-C)} \qquad (4\text{-}11)$$

At least three different levels of measured viscosity data might be available. These can be summarized as follows:

(1) Measured

$\mu(T_R,C)$ - viscosity of fluid mixture as a function of composition at a reference temperature

$\mu_i(T)$ - viscosity of injected fluid as a function of temperature

$\mu_r(T)$ - viscosity of resident fluid as a function of temperature

Calculate

B_i, B_r as least squares fit of μ_i and μ_r

$\mu(T,C)$ from Eqs. (9) and (10)

(II) Measured

$\mu_i(T)$, $\mu_r(T)$ - viscosities of injected and resident fluids as functions of temperature

Calculate

B_i, B_r as least squares fit of μ_i, μ_r

$\mu_R(C)$ at midpoint of temperature range Eq. (11)

$\mu(T,C)$ from Eqs. (9) and (10)

(III) Measured

$\mu_i(T_R)$, $\mu_r(T_R)$ - viscosities of injected and resident fluids at single temperature

Calculate

B_i, B_r from generalized chart of Lewis & Squire[25]

$\mu_R(C)$ - Eq. (11)

$\mu(T,C)$ - Eqs. (9) and (10)

As should be obvious from the above discussion, the accuracy degrades when less measured viscosity data are available. The accuracy of each of the above approaches is discussed below.

The variation of viscosity with temperature given by Eq. (9) was tested for pure water. The reference temperature was taken as 59°F. The first two levels of viscosity data availability above include viscosities of the injection and resident fluids as a function of temperature. In the model, a least squares fit of these data is made. In the case of pure water, the maximum deviation between measured and calculated viscosities is 5% over a temperature range from freezing to boiling. In the third level of viscosity data availability described above, only the viscosity of injected and resident fluids at a specified temperature are available. In this case, the Lewis and Squire correlation[25] generates the temperature dependence. In this case, a maximum deviation, calculated to measured, of 14% was found over the same temperature range. Thus, the viscosity model temperature dependence seems to be entirely adequate.

To test the accuracy of the calculated viscosity for the three distinct levels of data availability, we have again used a brine solution. The resident fluid was taken as pure water and the injection fluid as 24% by weight NaCl. A reference temperature of 59°F was used and the aquifer temperature was taken as 150°F. The measured data for the three cases then consist of:

CASE I

(1) viscosity versus temperature for injected fluid (0% NaCl) at five temperature points: 32, 59, 100, 140 and 212°F

(2) viscosity versus temperature for resident fluid (24% NaCl)

28

(3) viscosity of mixtures of injection and resident fluids at the reference temperature, 59°F, for each one-tenth increment in concentration between 0° and 24% NaCl

CASE II

(1) same as (1) above

(2) same as (2) above

(3) no mixture viscosity data

CASE III

(1) viscosity of injected fluid (0% NaCl) at 59°F

(2) viscosity of resident fluid (24% NaCl) at 59°F

(3) no mixture viscosity data or viscosity temperature dependence

The results of calculating the viscosity for various mixtures of injection and resident fluids at a temperature of 150°F are shown in Figure 3. The maximum deviation for either Case I or II is less than 5%. For Case III, the maximum deviation is about 18%. This discrepancy occurs because the generalized Lewis-Squires extrapolation from 59°F to 150°F for pure water introduces an 18% deviation. The deviation for 24% brine due to this extrapolation was less than 5%. Even Cases I and II contain some inaccuracy in the calculation of the viscosity of water (0% NaCl) since the exponential behavior assumed is not exact.

Other fluids have been tested against the viscosity model with similar results. As an example, a 50% sucrose solution showed maximum deviations of roughly 30% over the complete concentration range from pure water to the 50% solution. We believe the viscosity model will be adequate for most cases of interest. However, other fluid property routines could be implemented into the model with minor changes.

Figure 3 - Comparison of Viscosity Model with Measured Data

Predicted Brine Viscosity @ 150°F with
Three Levels of Available Data μ (T,C)

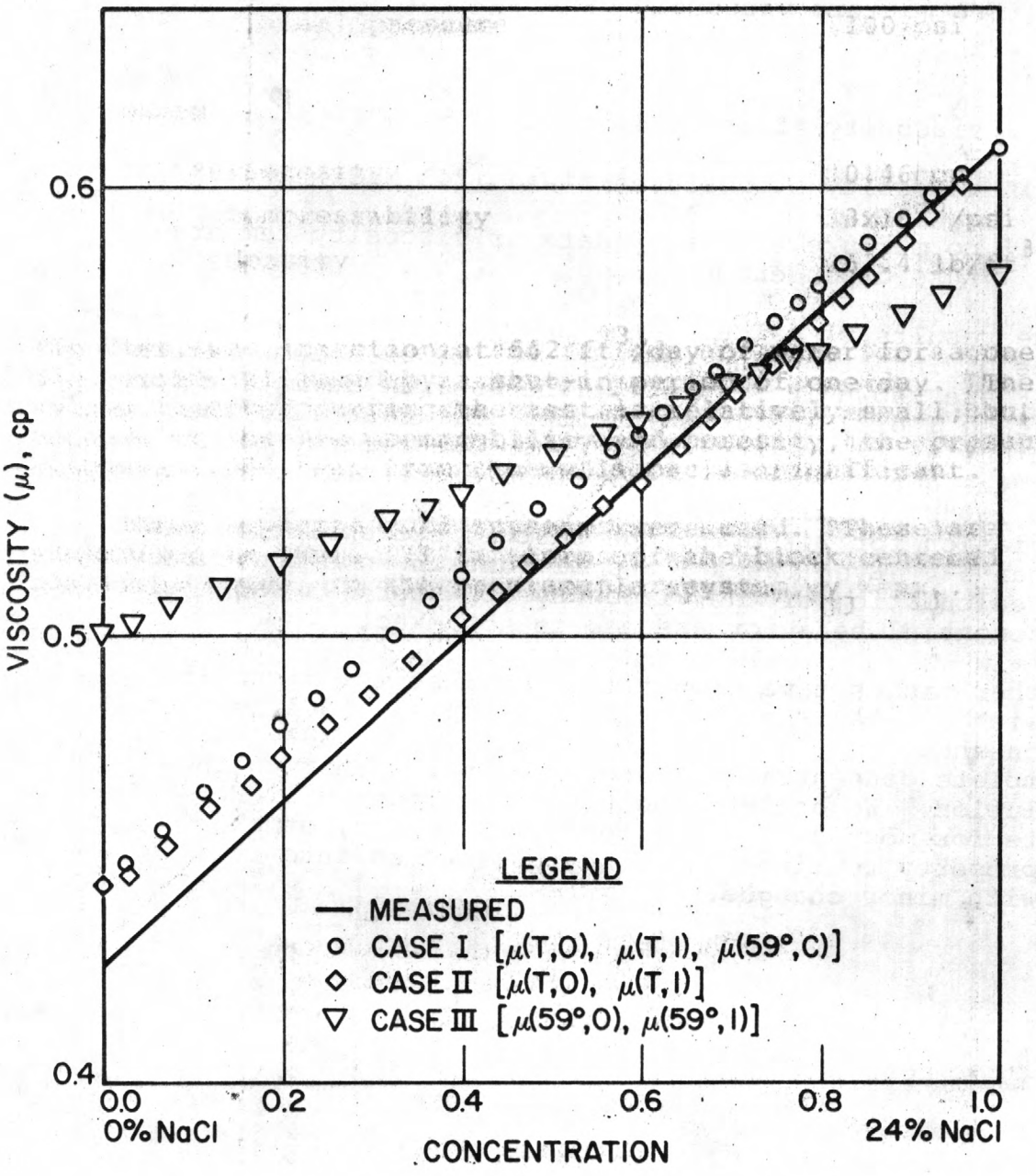

4.2 Reservoir Model Tests

The second type of testing performed on the disposal model was designed to test the reservoir model and associated boundary conditions. When density is not a function of temperature or composition, the individual equations become uncoupled. Under these circumstances, it is possible to check the numerical finite-difference solution of each equation separately against analytical solutions to these equations.

4.2.1 Comparisons with Analytical Solutions

In the comparisons with analytical solutions, we have attempted to use realistic aquifer and fluid properties to test the model. This enabled us to check not only the programmed equations, but also the importance of truncation error for realistic cases.

4.2.1.1 Flow Model Tests

Our purpose in the tests for the flow model were designed to verify not only that the equations had been debugged, but also that the combination of pressure drop in the aquifer plus pressure drop across the sand face was a good approximation. As discussed in the boundary conditions section, we have included a radial steady-state pressure drop calculation for the additional pressure drop from the average block pressure down to the wellbore pressure. In a highly transient situation such as a well test, the adequacy of this approach must be checked. Since the model has the capability of both cylindrical (r-z) and rectangular Cartesian (x,y,z) coordinates, both grid systems were checked. All runs of this type were compared with the E_i-function (exponential integral) analytical solution to radial flow subject to a specified rate as the wellbore radius approaches zero.

This solution has the form

$$\Delta p = \frac{q\mu}{4\pi kh}\left[-E_i\left(-\frac{\phi\mu c r^2}{4kt}\right)\right] \qquad (4\text{-}12)$$

where $-E_i(y) \equiv \int_y^\infty \frac{e^{-x}}{x}\,dx$.

Table II summarizes the aquifer and fluid properties used in the tests:

TABLE II - AQUIFER AND FLUID PROPERTIES
FOR FLOW MODEL TEST

Aquifer

conductivity	0.0179 ft/day(3 md)
porosity	0.03
compressibility	4×10^{-6}/psi
thickness	100 ft.
initial pressure	100 psi

Water

viscosity	0.46 cp
compressibility	3×10^{-6}/psi
density	62.4 lb/ft^3

The test was injection at 562 ft^3/day of water for a one day period followed by a shut-in period of one day. The volume injected during the test is relatively small; but, because of the low permeability and porosity, the pressure response 1,000 feet from the wellbore is significant.

Three separate grid systems were used. These are summarized in Table III in terms of the block centered positions where, in the rectangular system, $y_j = x_i$.

TABLE III - SUMMARY OF FLOW TEST GRID SYSTEMS

Block i Wellbore	Radial 16x1x1 r_i, ft 0.375	Rectangular 13x13x1 x_i, ft 0.375	Rectangular 11x11x1 x_i, ft 0.375
1	2	1	7
2	3.1	4	22
3	4.9	10	46
4	7.6	22	94
5	11.9	46	190
6	18.5	94	382
7	28.9	190	655
8	45.1	382	1000
9	70.4	655	1456
10	109.9	1000	2224
11	171.6	1456	3760
12	267.8	2224	
13	417.9	3760	
14	652.2		
15	1018.0		
16	1588.8		
External distance	2000.0	4784	4784

Each of the above grid systems was compared with the analytical solution at three different distances from the well. The first distance comparison was at the wellbore (r=0.375 feet); the second was at a distance 45 feet from the injection wellbore; and the third at a distance of 1000 feet from the wellbore. To make the comparison at the latter two distances, observation wells were placed in the appropriate blocks. Since the well rates from these blocks are zero, no additional pressure drop from the grid block average to the wellbore is present. The well index calculation of Equation (B-1) is not essential. For the injection well, however, this calculation is quite important during the injection phase of the test.

For the radial geometry, the additional pressure drop from the block center of two feet down to the wellbore of 0.375 feet requires a well index equal to (6.28)(3)(100)(.00632)/ln(2/0.375) or 7.12 ft^3cp/psi day (see illustration below).

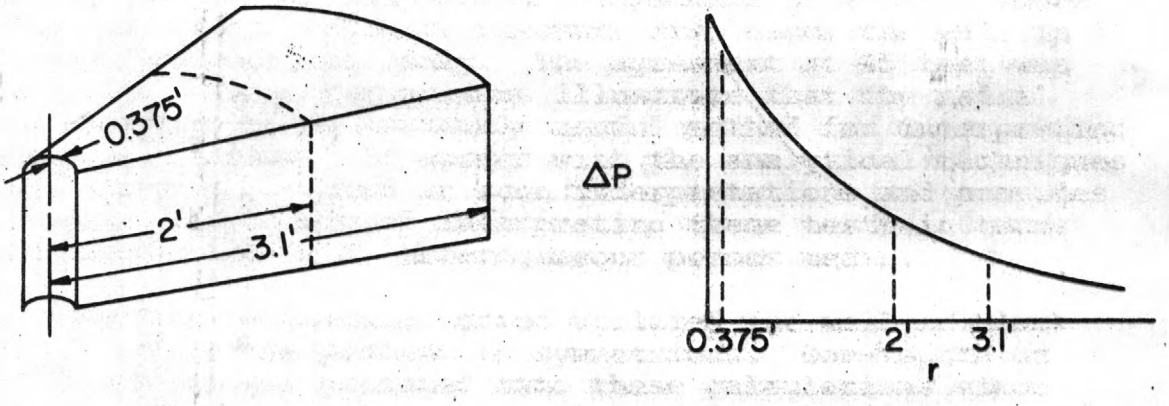

At the injection rate of 562 ft^3/day, this additional pressure drop is slightly more than 36 psi. This is the steady-state pressure drop which would exist for the specified flow between 0.375 feet and two feet. Figure 3 plots the comparison between the calculated and analytical solution results at the wellbore (r_w = 0.375 feet). Note that the additional pressure drop calculated from the well index is important in providing agreement between the two. The total pressure buildup in the aquifer grid is roughly 130 psi while the well index adds the additional 36 psi.

Since a 0.1 day increment was used in calculating the E_i-solution, there is no comparison in the very early transient period. By 0.1 day, excellent agreement is obtained between the E_i-function and the finite-difference result. However, it is the early transient period where the wellbore approximation used in the finite-difference model might be expected to give higher results than the analytical solution. This is due to the wellbore model assuming an instantaneous steady-state between the well block and the wellbore.

FIGURE 4. Comparison of Radial Geometry Numerical Result with E_i-Function
r = 0.375 ft.

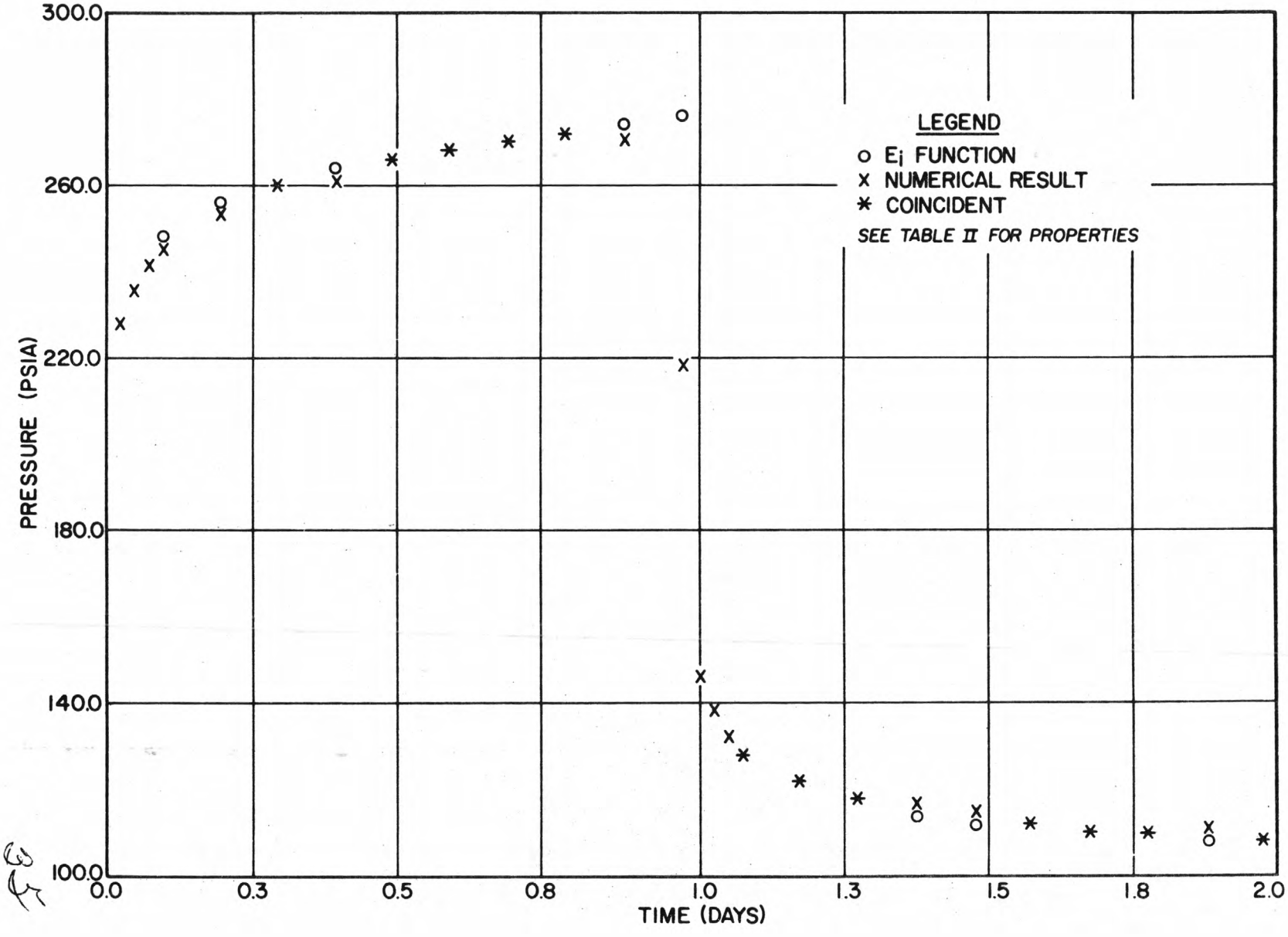

In the comparison between the finite-difference model and the analytical solution at a distance of 45 ft., there is no additional wellbore pressure drop since the well is an observational well only. The agreement at 45 feet was excellent. These comparisons illustrate that the radial flow geometry is an extremely useful method for interpreting single well tests. It agrees with the analytical techniques which are usually used in such interpretations and provides the added capability of interpreting these tests in terms of a stratified (r,z) heterogeneous porous media.

The two rectangular grids utilized the well in block (1,1,1) since the problem is symmetrical. One-fourth of the injection was prorated into these calculations since only one-fourth of the area is included. The only difference between the two grids was that in the 13x13 grid, the well block was two feet on a side. In the 11x11 grid, the well block was 14 feet on each side. The two tests were done primarily to distinguish the accuracy of the linear well index formulation. This well index is intended to calculate the additional pressure drop from the average block pressure down to the wellbore (see the illustration below). Unlike the radial case where the well index is exact (except for the steady-state assumption), the linear case involves an approximation going from the linear geometry down to the radial wellbore geometry. The well index calculation in this case is $(1/4)(6.28)(3)(100)(.00632)(2.257-.375)/.375[1./1-2.257/.375(1.-\ln 2.257/.375)] = 2.584$ ft^3 cp/psi/day. At an injection rate of 1/4 of 562 ft^3/day, the additional pressure drop is about 25 psi.

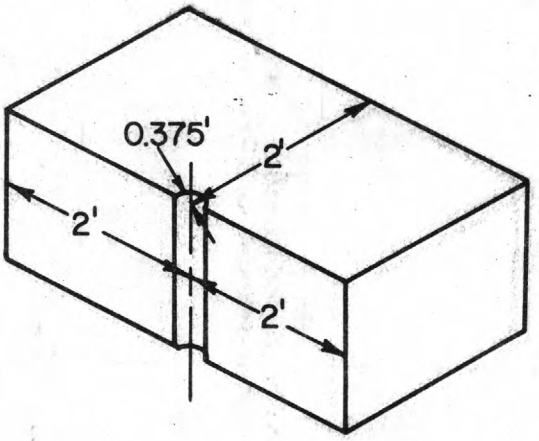

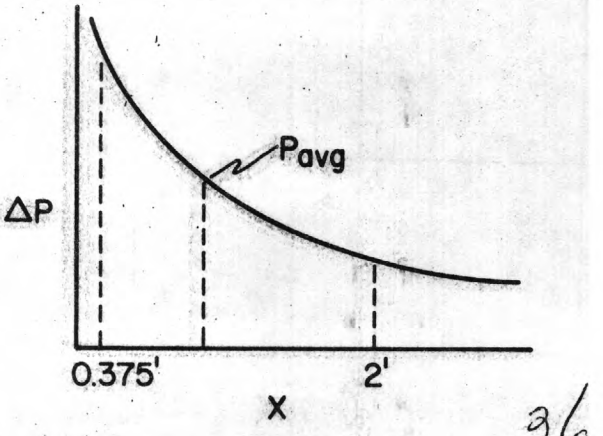

In this case the numerical result tended to be high during the injection phase by about 2-5 psi. This is a considerable improvement over what would have been calculated using the WI expression of the previous radial case. If that WI had been used, one might have assumed the necessary calculated pressure drop was over a radius of two ft. (equal to the linear block size) down to 0.375 ft. This would have given a $\Delta P = 36$ psi as before and would introduce a significantly greater error.

In the 11x11 linear geometry, the well block is now appreciably larger. The calculated well index is 1.05 ft^3 cp/psi/day. In this case, the additional pressure drop is about 61 psi. The calculated result for this block size appears to be about 2-5 psi lower than the analytical result. Again, using the radial result with an effective radius equal to one-half the overall block size, the calculated ΔP from the well index would be about 71 psi. This would give a total calculated result greater than the observed analytical result by about 5 psi. That is, about the same error, but in the opposite direction from the WI determined using the block pressure as representing the average pressure instead of the external radius pressure.

Our conclusion from the above results is that the wellbore pressure drop is a necessary addition to account for if calculated bottom-hole pressures at an injection or production well are to be compared with measured levels. Observation well results should not be sensitive to the wellbore effects unless well fillup volume was significant.

4.2.1.2 Tests of the Temperature and Concentration Equations

The analytical solutions used are well known[26]. Boundary conditions for which analytical solutions are known include:

(1) $x=0,\ C=C_0$ $\qquad$ $x\to\infty,\ C\to 0$

$T=T_0$ $\qquad$ $T\to 0$

(2) $x=0,\ uC_0 = uC-E\frac{\partial C}{\partial c}$ $\qquad$ $x\to\infty,\ C\to 0$

$uT_0 = uT-E\frac{\partial T}{\partial x}$ $\qquad$ $T\to 0$

(3) $x=0$, as in (2) $\qquad$ $x=L,\ \frac{\partial C}{\partial x} = 0$

$\frac{\partial T}{\partial x} = 0$

The last set of boundary conditions generally best represent those included in the program. A radial geometry solution corresponding to the set of boundary conditions (1) is also available.

The component or energy balance equation where E (the diffusivity) is constant can be solved by taking the Laplace transform of the partial differential equation with respect to time and reducing it to an ordinary differential equation. The solution for condition (2) in the linear case[26] is as follows:

Linear

$$\frac{T}{T_o} \text{ or } \frac{c}{c_o} = \frac{1}{2}\left[\operatorname{erfc}\left(\frac{\sqrt{\gamma}}{2}\,\frac{y-I}{\sqrt{I}}\right) - e^{\gamma y}\operatorname{erfc}\left(\frac{\sqrt{\gamma}}{2}\,\frac{y+I}{\sqrt{I}}\right)\{1+\gamma(y+I)\}\right]$$

$$+\sqrt{\frac{\gamma I}{\pi}}\,\exp\left\{-\frac{\gamma}{4I}(y-I)^2\right\} \qquad (4\text{-}13)$$

where definition of the dimensionless groups is different for the component and energy equations.

Energy	Component
γ = dimensionless diffusivity $\frac{uL}{K/(\rho Cp)_w}$	γ = dimensionless diffusivity, $\frac{uL}{E}$
y = dimensionless distance, x/L	y = dimensionless distance, x/L
L = aquifer length, and	L = aquifer length, and
$I = \frac{u(\rho Cp)_w t}{(\rho Cp)_t L}$	$I = \frac{ut}{L\phi}$

Radial

Energy	Component
$T/T_o = \frac{\Gamma(\frac{q(\rho C_p)_w}{4\pi hK}, \frac{r^2(\rho C_p)_T}{4Kt})}{\Gamma(\frac{q(\rho C_p)_w}{4\pi hK})}$	$\frac{C}{C_o} = \frac{\Gamma(\frac{q}{4\pi D_r h}, \frac{r^2\phi}{4D_r t})}{\Gamma(\frac{q}{4\pi D_r h})}$

(4-14)

Note that the solutions of both concentration and energy equations for either radial or linear geometry are identical except for definition of dimensionless groups. Also note that the diffusivity, a function of velocity (due to hydrodynamic dispersion), can be checked for the linear case since the velocity is constant. An approximate solution for diffusion a function of velocity has been developed for the radial case[27]. This approximate solution for the concentration equation can be expressed as:

$$\frac{C}{C_o} = 1/2 \text{ erfc } [(r^2/2 - \frac{Qt}{2\pi h\phi})/(4/3\ \alpha_\ell r^3 + 2\pi D_m h\phi r^4/Q)^{1/2}]$$

(4-15)

A comparison of the numerical solution with this equation has also been made and showed the same kind of agreement as the authors obtained[27].

Results for the radial geometry concentration equation are shown in Figure 5. The aquifer and fluid properties are listed in Table IV.

Figure 5 - Comparison of Numerical Results with Analytical Solution of Radial Concentration Equation

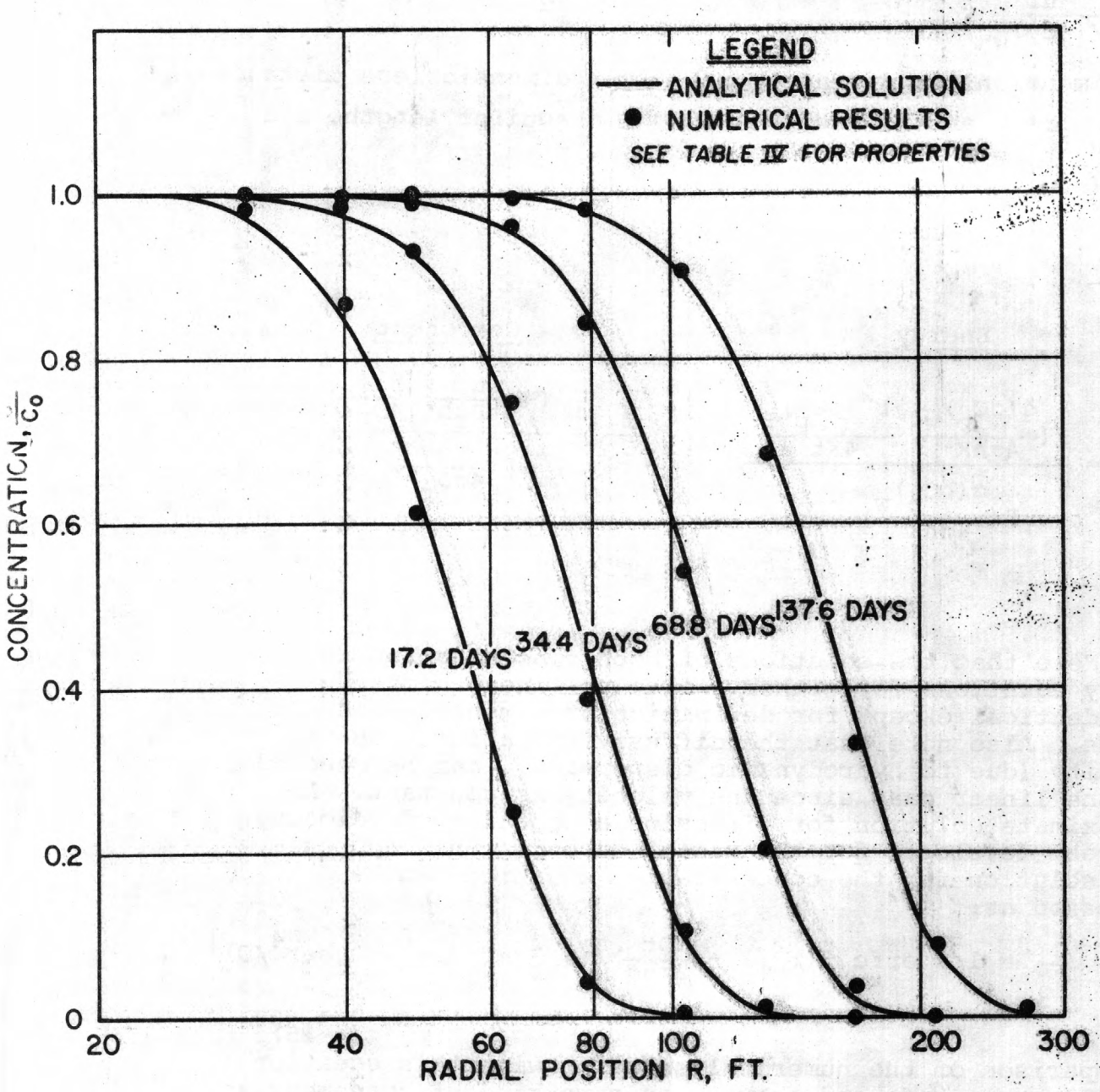

TABLE IV

AQUIFER AND FLUID PROPERTIES USED FOR THE RADIAL GEOMETRY TEST

Porosity, ϕ	0.1
Conductivity	394 ft/day (2 darcies)
Rock compressibility, C_R	~ 0
Reservoir fluid density, ρ_o	62.4 lb/ft^3
Injection fluid density, ρ_i	62.4 lb/ft^3
Viscosity, μ	2 cp
Diffusivity, D_r	1.16 ft^2/day
Flow rate, Q	58.5 ft^2/day

A total of ten grid blocks in the r-direction were used. The flow rate was maintained at 58.5 ft^2/day. The aquifer and well dimensions and grid blocks are summarized in Table V.

TABLE V

GRID BLOCK CENTERS AND OUTER BOUNDARIES

Well radius	10 ft.
Outer aquifer radius	315 ft.

Block No.	Grid Block Centers, Ft.
1	30.5
2	39.7
3	49
4	64
5	79
6	104
7	131
8	168
9	210
10	271

41

The temperature equation was tested by making the dimensionless groups appearing in (14) the same as for the concentration equation. Thermal properties for this case are shown in Table VI.

TABLE VI

THERMAL TRANSPORT PROPERTIES OF THE AQUIFER AND THE FLUID

Heat capacity of the fluid, $(C_p)_w$	1.6 Btu/lb°F
Density of the rock, ρ_R	100 lb/ft^3
Heat capacity of the rock, $(C_p)_R$	0.3 Btu/lb°F
Net thermal conductivity of the porous medium, $\bar{K}$	116 Btu/ft-day°F

Results were virtually identical to those shown in Figure 5.

One-dimensional component and energy balances were also tested for linear geometry. For constant cross-sectional area, constant flow rate also implies a constant value of the velocity. From Eq. (3), this implies a constant value of the total mass diffusivity in a homogeneous aquifer. In the radial system, a constant value of α and the flow rate q implies a decreasing $\bar{E}$ with an increase in the radius.

The aquifer and fluid properties used for the linear tests are summarized in Table VII.

TABLE VII

THE AQUIFER AND FLUID PROPERTIES USED FOR THE LINEAR TEST

Porosity, ϕ	0.1 (fraction)
Conductivity	2 ft/day (10 md)
Rock compressibility, C_R	4 x 10^{-1}/psi
Resident fluid density, ρ_o	62.4 lb/ft^3
Injection fluid density, ρ_i	62.4 lb/ft^3
Longitudinal dispersivity factor, α	52 ft
Net molecular diffusivity, D_m	1 x 10^{-5} ft^2/day
Fluid heat capacity, $(C_p)_w$	1 Btu/lb°F
Volumetric rock heat capacity, $(\rho C_p)_R$	30 Btu/ft^3°F
Apparent conductivity of the porous medium, $\bar{K}_m$	30 Btu/ft-day-°F

42

A constant superficial velocity of 0.1 ft/day was maintained (flow rate = 0.1 $ft^3/day/ft^2$). Twenty grid blocks, each of 100 ft. length, were used.

The results for the concentration at 405 and 800 days are shown in Figure 6. The results at both the times are in excellent agreement with the analytical solution. A central space difference approximation was used, as in the radial geometry. A time step of 5.6 days was used which gives a numerical truncation error of 0.28 ft^2/day. The numerical diffusivity is approximately 5% of the physical dispersivity ($\bar{E}$ = 5.2 ft^2/day).

Also on Figure 6, the results for the temperature equation are illustrated at times of 800 and 4262 days.

It is of interest to compare the results of the concentration and temperature equations at 800 days. The transport properties, dimensions of the aquifer and flow rates are the same in both cases. The dimensionless diffusivities without the molecular diffusivity and the conductivity are also the same. The net molecular diffusivity (D_m) and the thermal conductivity (K_m) are small compared to the hydrodynamic dispersivity, and their effect may be neglected for this qualitative comparison. Consider the dimensionless times:

Concentration

$$\frac{ut}{\phi L} = \frac{(0.1)(800)}{(0.1)(2000)} = 0.4$$

Temperature

$$\frac{u(\rho C_p)_w t}{(\rho C_p)_T} = \frac{(0.1)(62.4)(800)}{(33.24)(2000)} = 0.075$$

Since the dimensionless time for the temperature equation is only one-fifth of the concentration equation, the temperature front should be closer to the origin, and significantly less diffuse. This is precisely what is observed.

Now let us compare the results of the concentration equation at 800 days with the temperature equation at 4262 days. Dimensionless times are equal in this case. The only difference in the two cases is a slightly different dimensionless diffusivity because of the difference in molecular diffusivity and the thermal conductivity.

43

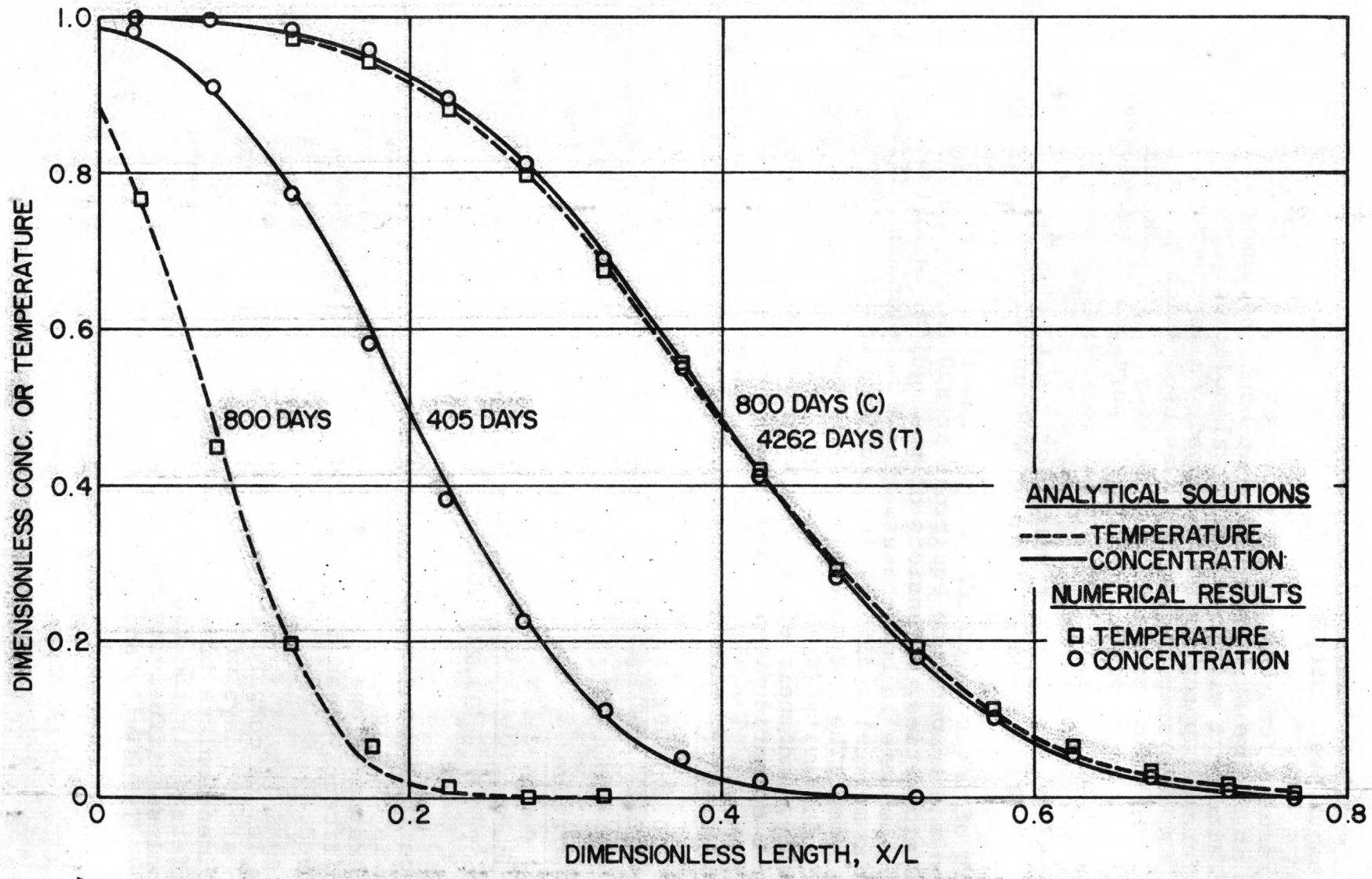

Figure 6 - Comparison of Numerical Results with Analytical Solutions of the Linear Concentration and Temperature Equations

See Table VII for properties

The dimensionless diffusivities are:

Concentration

$$\frac{\alpha u + D_m}{Lu}$$

$$\frac{(52)(0.1) + 1x10^{-5}}{(2000)(0.1)} = 2.6x10^{-2}$$

Temperature

$$\frac{\alpha u + K_m/(\rho C_p)_w}{Lu}$$

$$\frac{(52)(0.1) + (30)/(62.4)}{(2000)(0.1)} = 2.84x10^{-2}$$

Thus the fronts should be at equal distance from the source, but the thermal front should be slightly more diffuse. The results, though it is not obvious, support this conclusion.

4.2.1.3 Analytical Solution for Brine Water Intrusion

The problem of salt water encroachment into an artesian aquifer was studied by Henry (1964)[28]. He derived a steady-state analytical solution for a particular set of boundary conditions. The idealized model was a confined fresh water aquifer discharging to the ocean. The boundaries at the top and bottom of the aquifer were impermeable. A constant fresh water flux enters the aquifer along the vertical face at the fresh water end (x=0), and a constant salt water head is maintained at the ocean end (x=L). The boundary conditions used for the analytical solution are summarized below:

45

At x=0	c=0
At x=L	c=1
At z=0 and h,	$\frac{\partial c}{\partial z} = 0$

The boundary condition at x=L is an idealized condition, and difficult to achieve numerically. Since the fresh water is flowing into the ocean, there is necessarily some dilution at x=L. Numerically, the constant salt water head was maintained at x=L by a production/injection well in each vertical layer. The bottom-hole pressure in each well vertically differed by the salt water head. All wells were permitted to produce or inject depending upon the difference between the grid block pressure and the pressure head. The wells in the lower blocks injected salt water into the aquifer, and the wells in the upper blocks produced.

The numerical model without modification is not able to exactly simulate the boundary condition of C=1 at x=L. Substantial modification of the present model would be required to simulate this idealized mathematical boundary condition. To avoid this, the production/injection well in each layer described above was used. Since sea water is being injected into the lower cells, the boundary concentrations there are equal to one as desired. The boundary concentrations in the upper production cells, however, are less than one since the concentration is the cell composition. This difference in boundary condition diminishes diffusion into the top layers of the numerical model compared to the analytical result. In the comparisons presented later, this effect although small can be noted.

Henry presented analytical results[28] for the following set of parameters:

$$\zeta = \frac{L}{h} = 2$$

$$a = \frac{q\mu}{kg\Delta\rho h} = 0.263$$

$$b = \frac{D_m}{q} = 0.1$$

In the numerical model test, an aquifer 200 ft. long and 100 ft. deep was used. The aquifer and fluid properties are summarized in Table VIII.

TABLE VIII

AQUIFER AND FLUID PROPERTIES

Aquifer	
Porosity	0.5 (fractional)
Permeability	517.89 md (1.42 ft/day)
Compressibility	4×10^{-7}/psi
Dispersivity	0.1 ft^2/day
Fluid	
Fresh water density	62.43 lb/ft^3
Sea water density	64.09 lb/ft^3
Compressibility	incompressible
Viscosity	1 cp

The fresh water flow rate was maintained at 1 ft^3/day with equal allocation into each layer. The numerical grid block system consisted of five vertical layers of 20 feet each, and 12 horizontal cells of: 50, 50, 16, 16, 16, 12, 12, 8, 8, 4, 4 and 4 feet length. The smallest cells were at the ocean end.

Henry presented his steady-state analytical solution in terms of both mean salt water concentration in the vertical direction and a family of constant salt water concentration contours. However, when we integrated his concentration contours in the vertical direction, the calculated result did not agree with his mean value curve. Either set of curves could conceivably be in error. Plotting alone might account for the differences. The average over the vertical direction from Henry's contoured concentration values are shown in Figure 7. We have arbitrarily accepted his mean curve as correct and re-generated the constant concentration contours to be consistent with it. Both curves were needed for two of the three numerical model tests described in subsequent paragraphs.

47

Figure 7 - Vertical Averaged Concentration as a Function of Position in the Fresh Water Aquifer

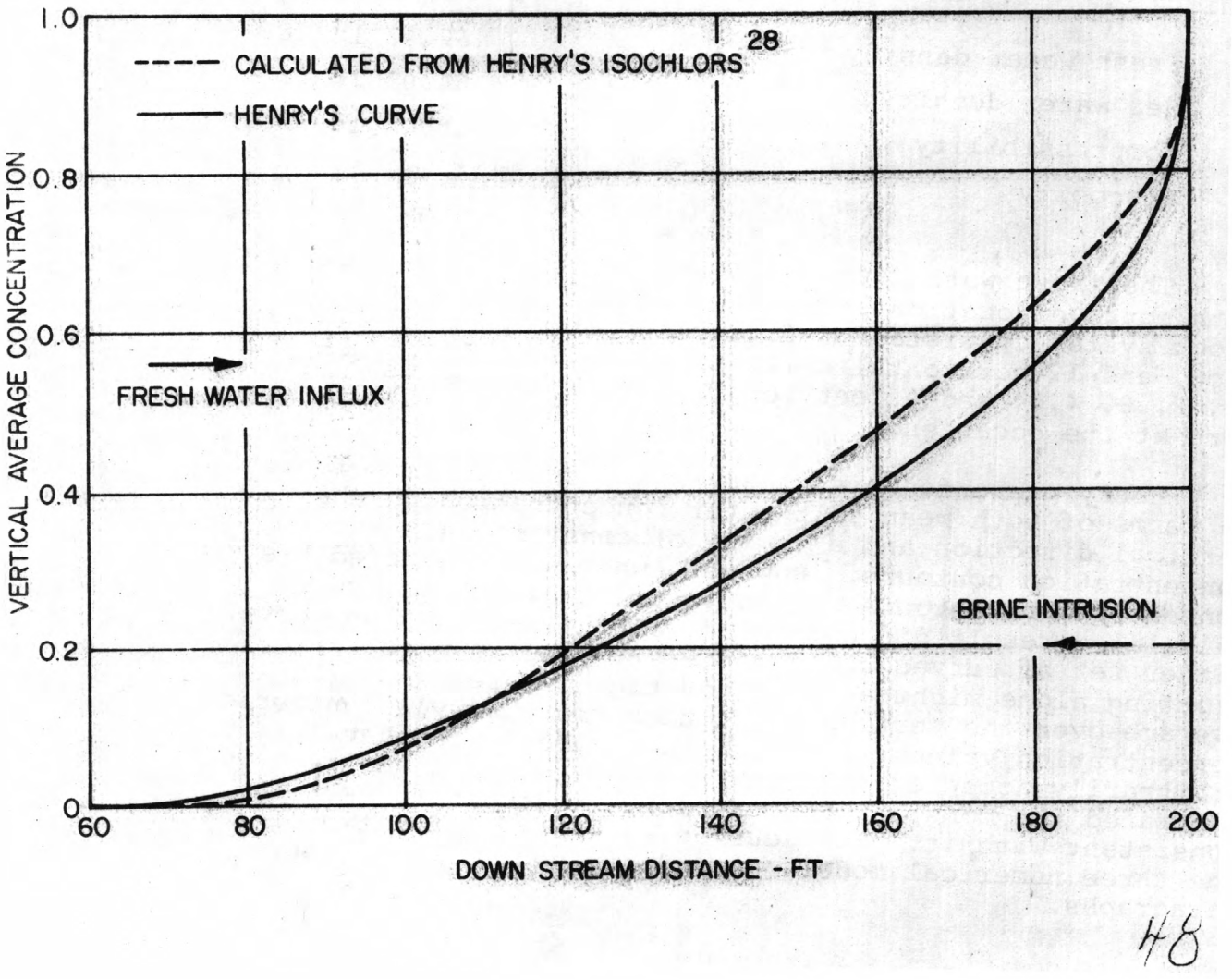

48

Three numerical model tests were made. In the first, injection was continued for 1,000 days. This corresponds to the injection of one-tenth of the total pore volume. The initial condition was taken as the aquifer being completely filled with fresh water. Because of the higher density of sea water, it intrudes into the aquifer at the bottom. After 1,000 days, the salt water front (defined as the average concentration in the vertical direction) has intruded into the aquifer much less than the steady-state solution. From Pinder and Cooper's[17] numerical solution, we estimated that injection of at least 20 pore volumes would be required to reach the steady-state. However, the qualitative behavior is similar to the steady-state solution. The mean vertical concentrations are plotted in Figure 8. The simulation was not continued after 1,000 days because of the large amount of computation time which would have been needed to reach steady-state. Instead, the two remaining tests were initialized very close to the steady-state answer, but on either side of it.

These two cases, in our opinion, constitute a rather rigorous test of the model. The two initial positions of the "front" for these cases were selected to be slightly on either side of Henry's steady-state solution. The initial vertical concentration distributions were based upon Henry's adjusted concentration profiles. The simulation was continued again for 0.1 PV (1,000 days), and the results are plotted in Figure 8. Note that the calculated salt water fronts move toward each other and toward Henry's analytical steady-state position. As a consequence, this shows that the steady-state numerical solution lies between the two simulated transient fronts. Note how slowly the simulation is approaching steady-state which verifies our earlier statement about the computer time necessary to reach this equilibrium. Based upon this work, we believe the numerical model can simulate brine intrusion accurately; however, steady-state answers such as this may require significant computer time.

4.2.2 Adequacy of Boundary Conditions

4.2.2.1 Aquifer Influence Functions

As a test of the aquifer influence functions, the same aquifer properties and rates used to test the flow model were used. The only difference is that a much smaller region of grid definition around the well was used. Instead of the 2,000 feet around the well described in the flow model test, only 337 feet was used. Each one of the three aquifer influences was used then at the periphery of this region.

Figure 8 - Comparison of Numerical Results with the Analytical Solution for Salt Water Intrusion

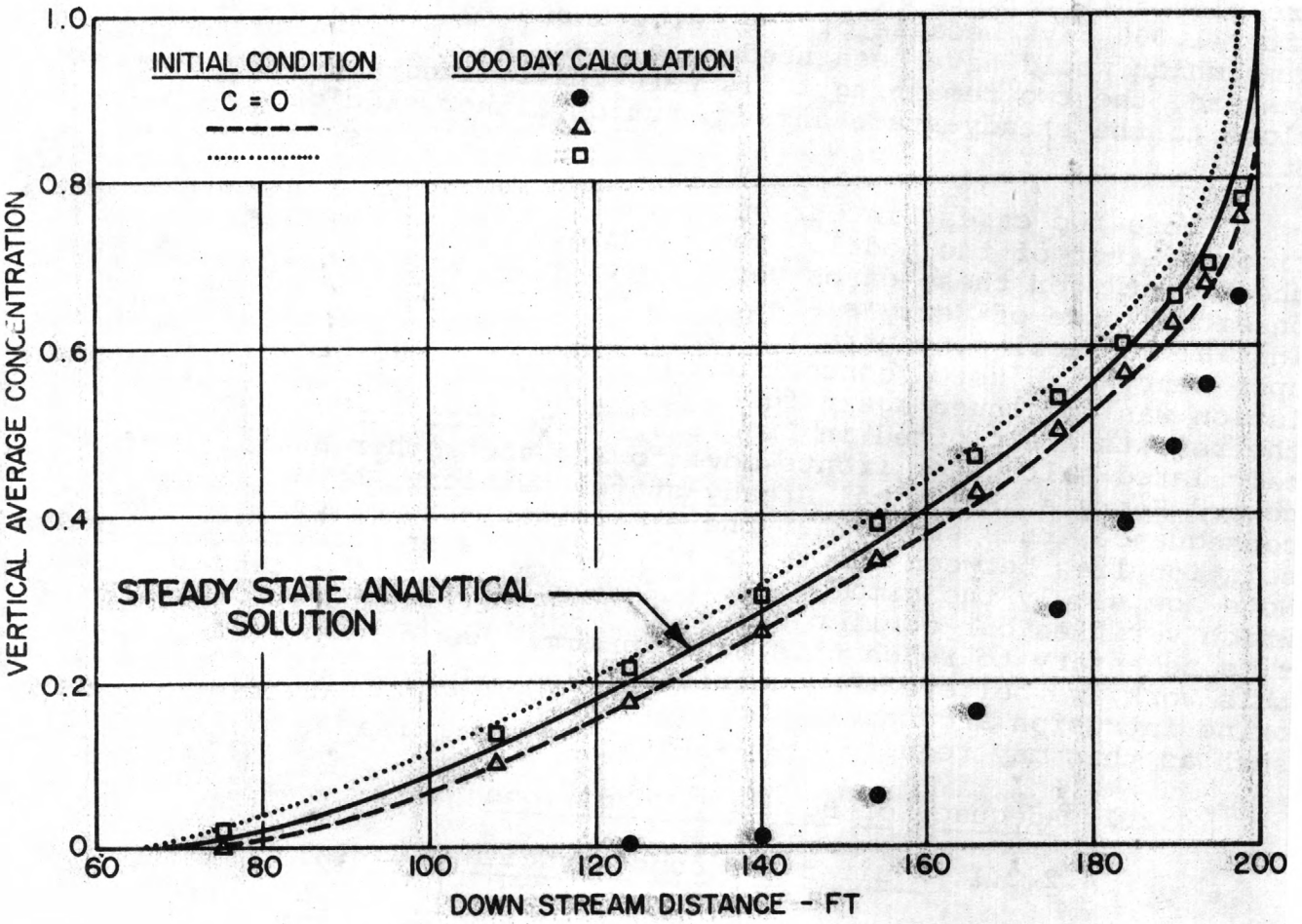

50

Four model runs were performed. In the first case, a Carter-Tracy representation[29] for an infinite aquifer was used. This should correspond most closely to the E_i analytical solution and the larger region flow model test. In the second and the third cases, the pot aquifer assumption was used--one with the aquifer influx coefficient calculated by Eq. (B-23) and the other with an arbitrarily large value of 10^6. In the fourth case, a steady-state aquifer representation was used.

The results are plotted in Figures 9 and 10. Note that the Carter-Tracy method does indeed yield a good approximation to the infinite aquifer. The two curves for the pot aquifer lie on either side of the curves for the infinite aquifer indicating that it is possible to select a value for V_1 such that it would approximate the pressure response for the infinite case. The value of 10^6 for V_1 in the third case was chosen large to keep the pressure in the edge blocks essentially constant. The pot aquifer representation is very simple and useful in history matching. The steady-state assumption shows the same qualitative behavior as an infinite aquifer, but the results are not as good as those obtained with the Carter-Tracy approximation. However, a steady-state representation is probably the best choice when the pressure along the external boundary is maintained by natural flow in the aquifer.

4.2.2.2 Overburden and Underburden Heat Losses

The top and bottom planes of a three-dimensional grid can lose or gain heat by conduction to adjacent impermeable strata as the aquifer temperature rises or falls due to injection. Discussion here is restricted to the overburden since treatment of the underlying strata is identical. We assume that thermal transport properties are constant in the overburden, and that the effects of heat conduction in the x and y direction are negligible. Two mode tests were made to check the conduction losses into overburden and underburden. In the first, the aquifer was treated as a no flow solid heated to a constant initial temperature. Heat conduction to the adjacent strata then decays this initial temperature. The second test was more appropriate to the disposal model as it will be used. In this case, there is one-dimensional flow in the aquifer due to injection of heated fluid. Heat conduction in the direction of flow is included. The heat conduction in the vertical direction in the aquifer is sufficiently large that the temperature profile in the vertical direction can be considered uniform. Conduction in the vertical direction in the adjacent strata provides heat loss from the aquifer. Avdonin[30] presented an analytical solution to the above described set of boundary conditions. His solution very similar to the more familiar case derived by Lauwerier which neglected conduction in the direction of flow in the aquifer.

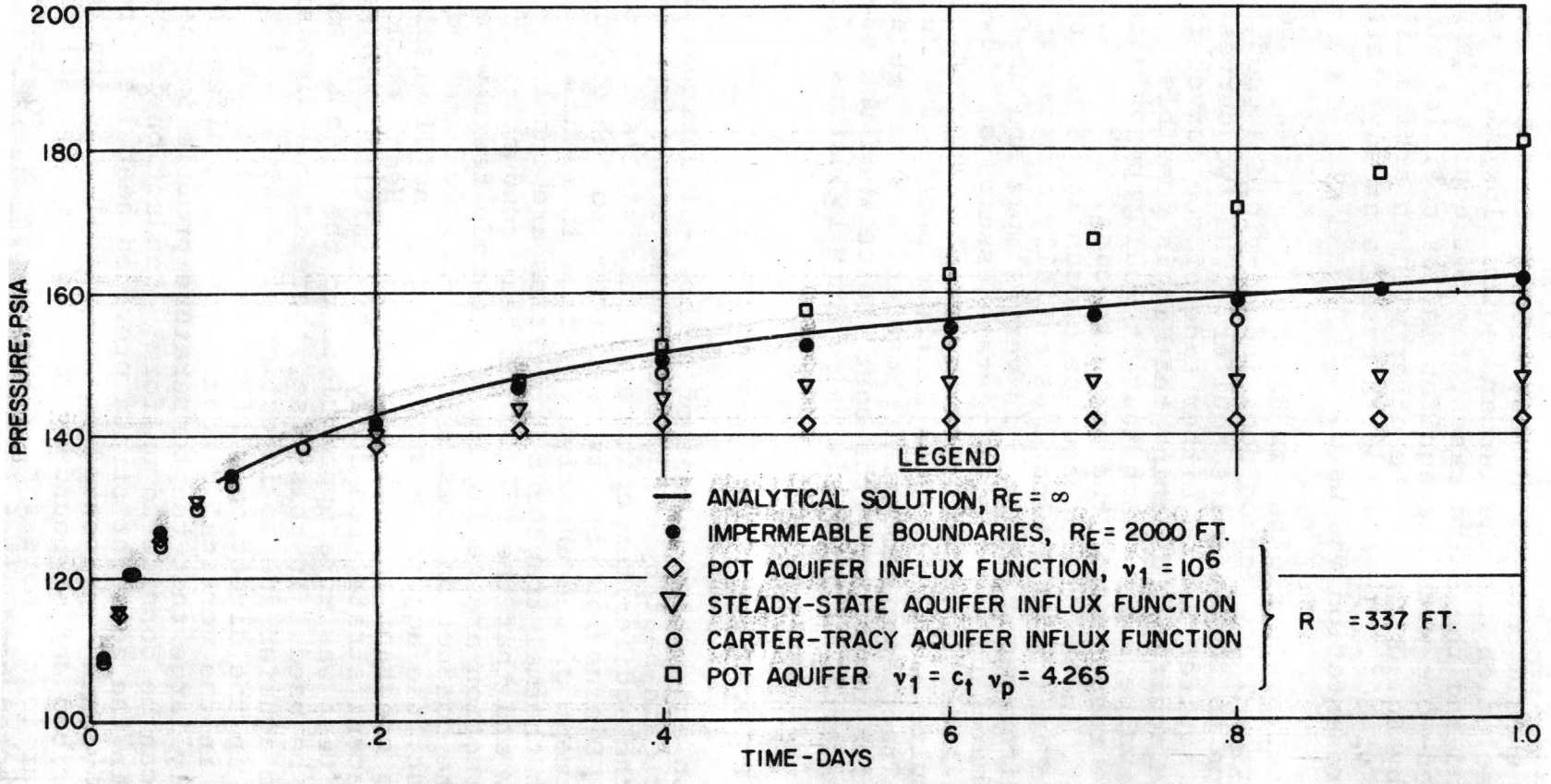

Figure 9. Test of Aquifer Influence Functions

Well No. 1
r = 0.375 ft.

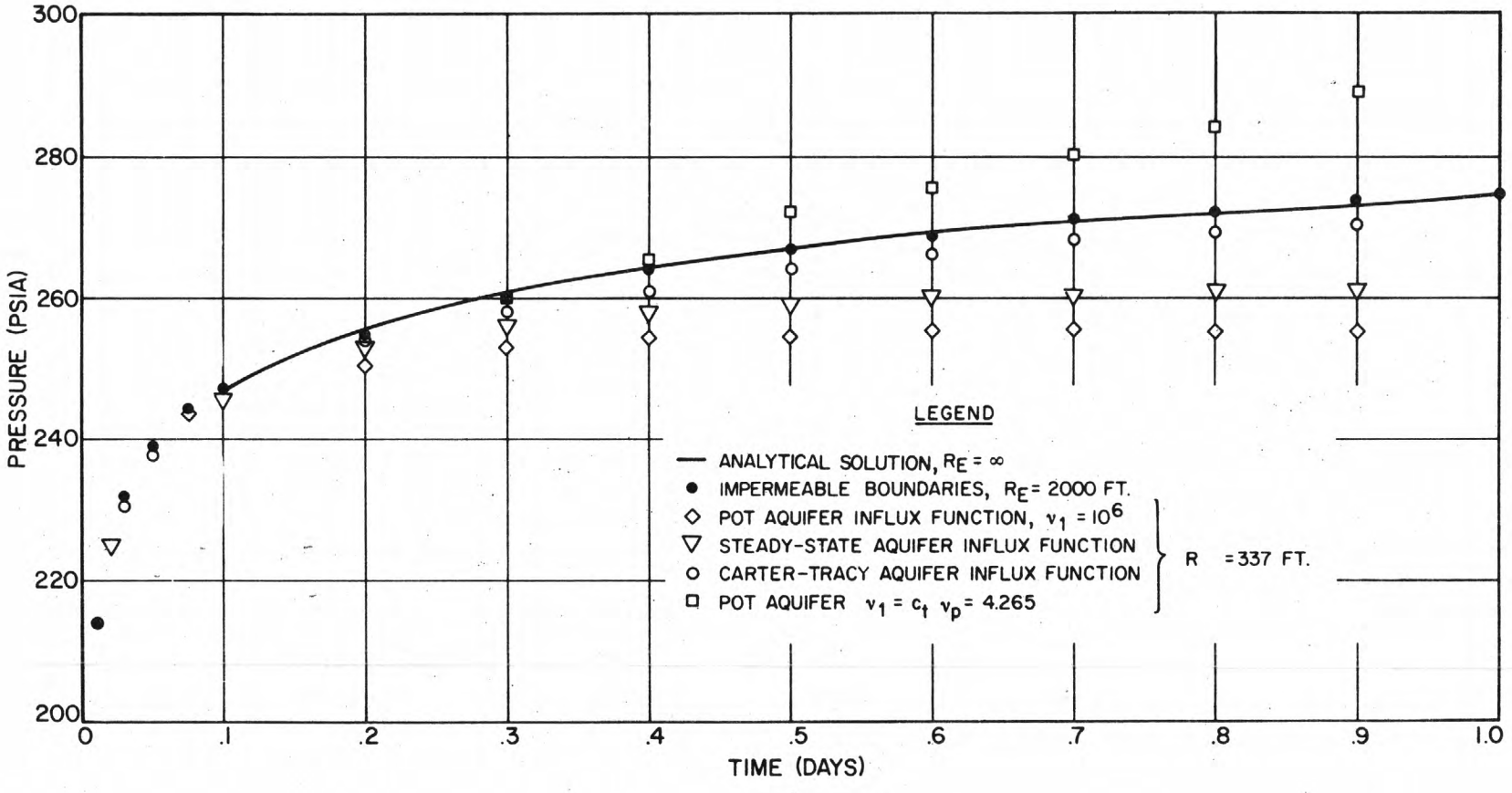

Figure 10. Test of Aquifer Influence Functions

Well No. 2
r = 45 ft.

The first model test was compared to the simple error function solution listed in Carslaw and Jaeger[32]. Calculated temperatures were in excellent agreement with the analytical solution.

The fluid and aquifer properties used in the second model test are shown in Table IX.

TABLE IX

AQUIFER AND FLUID PROPERTIES

Heat Capacities:	
Aquifer Medium	42.45 Btu/ft^3-°F
Fluid	62.4 Btu/ft^3-°F
Overburden	36.3 Btu/ft^3-°F
Thermal Conductivities, Aquifer and Overburden, $k = k_{ob}$	1.4 Btu/hr-ft-°F
Flow Rate, q	133.6 ft^3/day
Thickness, h	10.0 ft

The analytical solution [30] to this case for radial geometry can be expressed as:

$$T = \frac{1}{\Gamma(\nu)} \left(\frac{r^2}{4\lambda\tau}\right)^{\nu} \int_0^1 \exp\left(-\frac{r^2}{4\lambda\tau y}\right) \operatorname{erfc}\left(\frac{\sqrt{\tau/\lambda}\, y}{2a\sqrt{1-y}}\right) \frac{dy}{y^{(\nu+1)}} \qquad (4\text{-}16)$$

where $\nu = \dfrac{q(\rho C_p)_w}{4\pi h\, k}$

$$\lambda = k/k_{ob}$$

$$a^2 = \frac{k_{ob}(\rho C_p)_w}{k\,(\rho C)_{ob}}$$

$$\tau = \frac{4\, k_{ob} t}{h^2 (\rho C)_t}$$

The calculated aquifer temperature profiles in the radial direction are compared with the analytical solution in Figure 11. The agreement is quite good. The combined tests clearly indicate the adequacy of the calculational techniques to include heat losses to adjacent strata.

Figure 11. Test of Overburden and Underburden Heat Loss Calculations

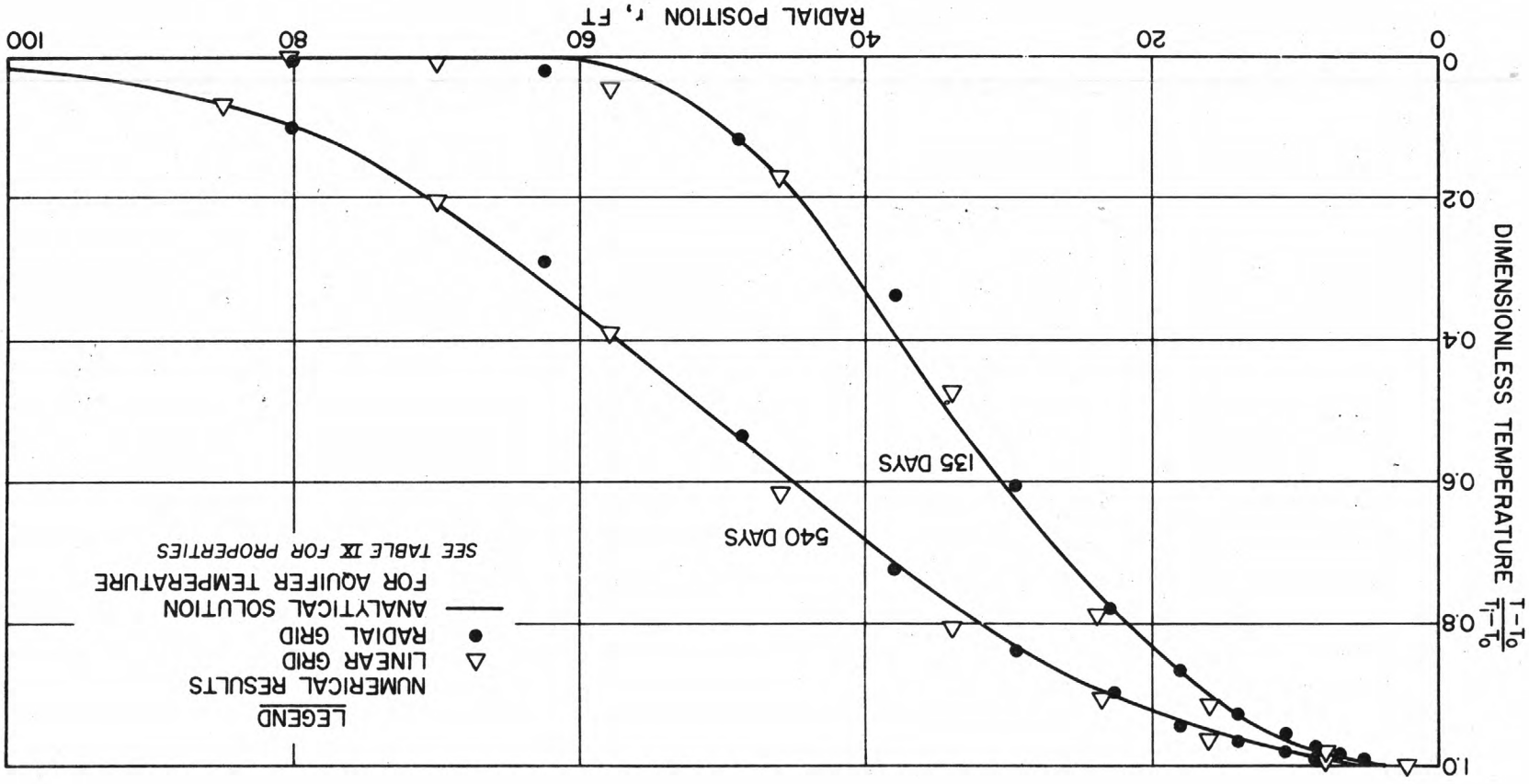

4.2.3 Test of the Wellbore Model

The wellbore model was tested against the field observation included in Ramey's paper[22] of cold water injection into an aquifer at a depth of 6500 ft. Water was injected at the rate of 4790 bbl/day (2.99×10^5 lb/day) for a period of approximately 75 days. The enthalpy of the injection fluid as it enters the aquifer and the wellhead pressures were calculated from the wellbore model. The wellbore casing was 7.0 inches outside diameter, and 6.366 inches inside diameter, and no tubing was used. Transport properties of the injection fluid, the wellbore casing, and the earth are summarized in Table X.

TABLE X

TRANSPORT PROPERTIES

Injection Fluid	
Viscosity	1.1 cp
Specific heat	1.0 Btu/lb-°F
Thermal conductivity, k_w	0.339 Btu/hr-ft°F
Casing	
Thermal conductivity, k_c	25.0 Btu/hr-ft-°F
Earth	
Thermal conductivity, k_r	1.4 Btu/hr-ft-°F
Thermal diffusivity	0.04 ft^2/hr

The temperature of the formation surrounding the wellbore was 70°F at the surface, and increased to 124°F at aquifer depth.

The overall heat transfer coefficient between the injection fluid and the surrounding rock is required for the wellbore calculations.

If h is the heat transfer coefficient between the fluid and the inner casing (or tubing) surface, then the rate of heat transfer between the fluid and the casing (tubing) can be expressed as:

$$\Delta Q = 2\pi R_1 h (T_1 - T_f)\ \Delta Z \qquad (4\text{-}17)$$

56

Similarly, the rate of heat conduction across the casing (or fluid between tubing and casing) is:

$$\Delta Q = \frac{2\pi(T_2-T_1)k\ \Delta Z}{\ln\ R_2/R_1} \quad . \tag{4-18}$$

The overall heat transfer coefficient based upon R_1 can then be written as:

$$\frac{1}{U} = \frac{1}{h} + \frac{R_1\ \ln\ R_2/R_1}{k} \tag{4-19}$$

The heat transfer coefficient, h, can be calculated from classical heat transfer equations according to the following relation:

$$\frac{hD}{k_w} = 0.023(R_e)^{0.8}(P_r)^{1/3} \tag{4-20}$$

where D = internal diameter of the tubing

k_w = Thermal conductivity of the fluid

R_e = Reynolds number

P_r = Prandtl number $\equiv (C_p\mu/k)$

For 2.69×10^4 ft^3/day of fluid flowing through a 0.531 ft. diameter casing, the Reynolds number is 63000. The Prandtl number for the injection fluid is 7.85. Therefore, the heat transfer coefficient is 201.8 Btu/hr-ft^2-°F. Then the overall heat transfer coefficient is then calculated to be 144 Btu/hr-ft^2-°F.

The temperature profile in the wellbore obtained from the model is compared with the measured temperature profile in Figure 12. The agreement is excellent. It

57

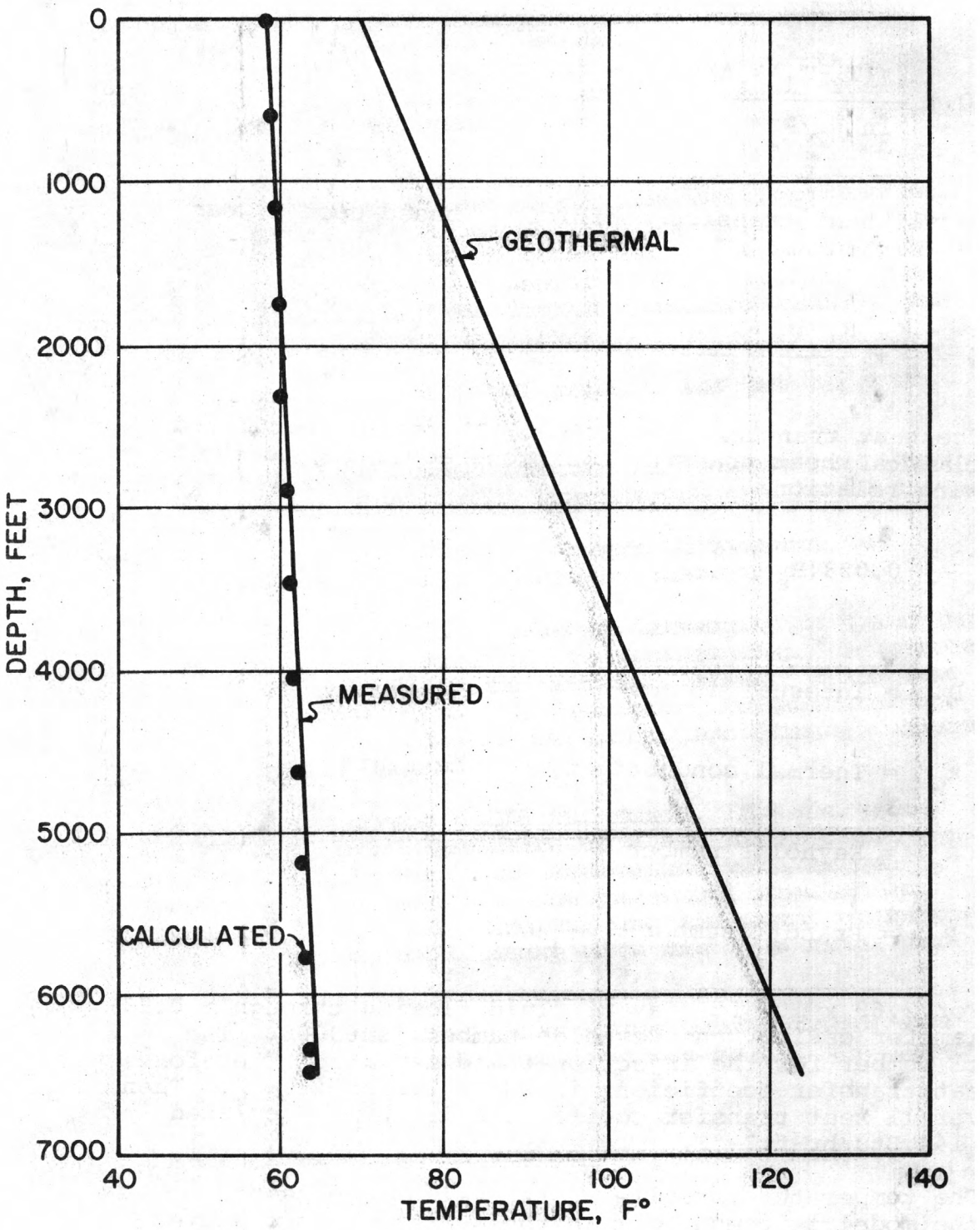

Figure 12- Comparison of Wellbore Model Results with Measured Temperature Profile

Injection well 6500 ft. depth

should be noted that the reported accuracy of the measured temperatures was ±2°F. At a depth of 6,000 ft., the measured temperature was 63.7°F and the calculated value is 63.4°F.

The wellhead pressure is calculated to be 507 psi for the initial reservoir pressure of 3000 psi. The enthalpy of the injection fluid at the surface is 28 Btu/lb, but increases to 40.3 Btu/lb as it enters the aquifer. The pressure drop due to friction is small (<<1 psi). If the fluid had been injected down two inch tubing hung inside the casing, the viscous pressure drop would have been about five hundred times larger.

4.2.4 Comparison with Laboratory Scale Model

Recent tests of laboratory scale models have been conducted at Louisiana State University to evaluate the use of saline aquifers as fresh water storage prospects[1]. Some of their tests results were made available to us for comparison with numerical model calculations.

One of the problems in using the finite-difference (or other numerical solution of the partial differential equations) model to simulate lab scale model results is that the physical dispersion is extremely small. Laboratory models are generally quite homogeneous in permeability and porosity relative to field scale application areas. As a consequence, the physical dispersion (which is enhanced by both microscale as well as macroscale heterogeneities) is much smaller in the lab models. The end result is that numerical dispersion (truncation error) is significantly more important in these simulations than it would be in field scale applications.

In the LSU miniaquifer model, the apparent dispersivity was only 0.02 cm. Reported values more typical of field scale applications are on the order of 10,000 times larger. Bredehoeft et al[12] reported a range of about 5 to 20 m for field scale determined dispersivity values. It should be mentioned that the dispersivity value above does not contain porosity implicitly in the denominator as many authors use.

As an indication of the importance of numerical truncation error, the number of blocks necessary to make the truncation error negligible can be evaluated. Even when a central space difference approximation which eliminates second order space truncation is used, the term $\frac{u\Delta x}{2}$, should be less than the physical dispersion term, αu. This eliminates the overshoot-undershoot

59

problem. If this relationship is to be satisfied, it can be noted that about 10,000 grid blocks would be required for a one-dimensional LSU miniaquifer simulation. This is clearly not feasible. Because of this, a backward difference space approximation was used in the miniaquifer simulations. This introduces more space truncation error, but the end result does not have any oscillation problem.

The question then arises as to just how important will numerical diffusion be in controlling the frontal position when density effects are also important. The results that follow tend to show that the density effects are far more important in determining the frontal position than is the artificially high diffusivity level.

We have available from LSU results for two separate miniaquifer tests. These are:

(1) a high rate, small density difference test which exhibits essentially one-dimensional behavior, and

(2) a lower rate, larger density difference test where there is considerable density effect.

The experiments at LSU involved injection of fluid into a well located at the center of the miniaquifer. A constant pressure was maintained at the external edges. Fluid was produced at the edges at a rate necessary to maintain the pressure. A dye was added to the injection fluid to observe the movement of the front.

The miniaquifer was 0.125 ft. thick, 10.0 ft. wide, and 9.6 ft. long with a wellbore of 0.006 ft. radius. An aquifer of radial geometry and equivalent pore volume (5.5 ft. radius) was used for the numerical simulation. The miniaquifer and fluid physical and transport properties are summarized in Table XI along with the flow rates for the two cases.

The value of the transverse dispersivity factor was not reported, but was arbitrarily taken as 0.1 the longitudinal dispersivity.

60

TABLE XI

THE AQUIFER AND FLUID PROPERTIES USED FOR THE MINIAQUIFER MODEL

Porosity, ϕ		0.25 (fractional)
Permeability, k		5.7 darcies (1753ft/day)
Fluid compressibility, c_w		3×10^{-6}/psi
Rock compressibility, c_R		4×10^{-6}/psi
Longitudinal dispersivity factor, α_ℓ		6.56×10^{-3} ft.
Transverse dispersivity factor, α_t		6.56×10^{-4} ft.
Net molecular diffusivity, D_m		2.3×10^{-5} ft^2/day
	Case I	Case II
Resident fluid density, ρ_o	48.57 lb/ft^3	53.32 lb/ft^3
Injected fluid density, ρ_i	48.76 lb/ft^3	48.88 lb/ft^3
Injection flow rate, q	0.037 ft^3/day	2.455 ft^3/day

Because of vertical density gradients and flow, it is necessary to use more than one vertical layer. Simulations were carried out for two, three and five layers for a portion of the total time. The results showed substantial differences between the cases of two and three layers, but only slight differences between three and five layers. The latter was chosen for the full simulation to provide more than adequate vertical definition.

Ten blocks were used in the radial direction. The centers of the blocks and the outer boundaries are listed in Table XII.

TABLE XII

GRID BLOCK CENTERS AND OUTER RADII USED FOR THE MINIAQUIFER SIMULATION

Block No.	Center, ft.	Outer Radius, ft.
1	.15	.18
2	.22	.27
3	.32	.39
4	.47	.57
5	.68	.83
6	1.00	1.21
7	1.46	1.77
8	2.13	2.59
9	3.11	3.78
10	4.54	5.52

The LSU observed data were reported in the form of frontal position plots at the top and bottom of the miniaquifer. These were observed as color fronts due to the dye in the injected fluid. The composition of the fluid at the observed frontal positions was not reported, but it would be expected that this concentration would certainly be less than 50% of injected and might be less than 10%. Because of a relatively high numerical diffusion compared to the physical dispersion, our calculated concentration profiles should be more diffuse than the observed; thus, we have compared the observed values with both the calculated 50% and 20% contours. As shown in Figure 12, this is found to be in agreement with the experimental results. The numerical concentration contours were obtained by interpolation between block centers on an r^2 basis. The calculated 20% and 50% concentrations were found to enclose the observed frontal profile. The experimental frontal positions may actually correspond to small concentration levels because of the smaller diffusivity than that simulated by the numerical model. In Figure 13 no observed frontal portion was available at the top of the model at a time of 9 days.

62

Figure 13 - Comparison of Numerical Concentration Profiles with the Observed Frontal Positions in a Laboratory Scale Aquifer

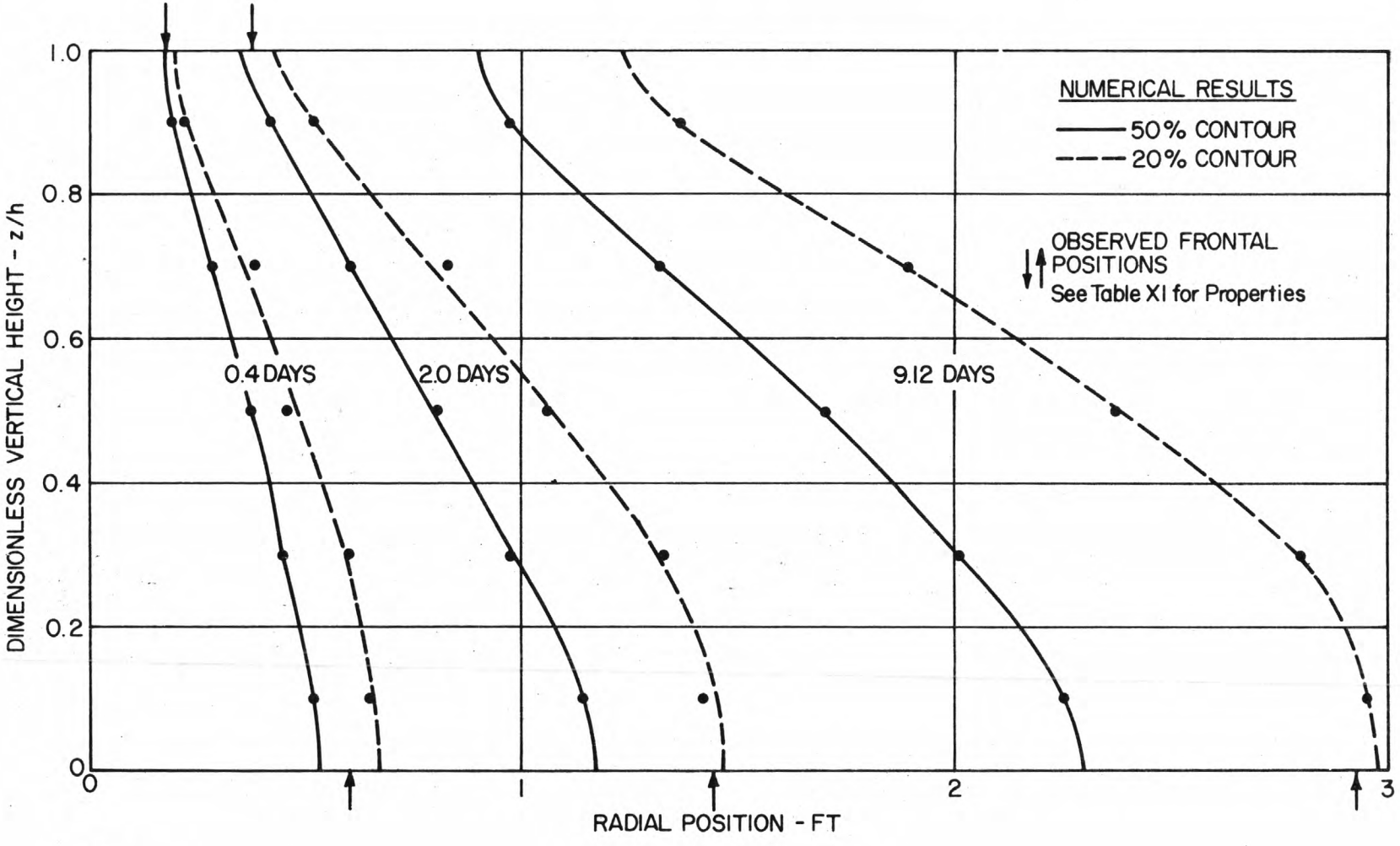

Because we have used a backward in space difference approximation, we have delineated the second order space and time truncation errors in Table XIII.

TABLE XIII

THE PHYSICAL AND NUMERICAL DIFFUSIVITIES FOR THE MINIAQUIFER SIMULATION

Radius, ft.	Diffusivities, $ft^2/day \times 10^4$				
	Physical Diffusion			Numerical Diffusion	
	αu	D_m	E	E_r	E_t
0.18	1.73	0.23	1.96	89.4	55.2
5.5	0.08	0.23	0.31	89.4	55.2

The numerical diffusivities due to both space and time truncation are much larger than the desired physical levels and yet the frontal profiles are reasonably accurate. This suggests that the density influence is so dominant that an artificially high diffusivity does not counteract this natural convective effect.

This case of small density difference (~0.25%) and higher injection rate gave observed frontal positions which lie within the 20% and 50% calculated contours. However, the calculated profiles are more vertical than the observed frontal positions. This result is due to the large numerical dispersion coefficient compared to the desired diffusion level. As a matter of fact, it would be possible to have a diffusion level sufficiently high that density effects would be overshadowed. This, of course, should be true in the numerical simulations only for cases where the physical dispersivity is extremely small such as the miniaquifer tests. In realistic field cases with much higher physical dispersion, the numerical finite-difference model should give good results.

64

To more easily see this, consider the following real size system for fresh water storage in a saline aquifer.

(1) injection-production rate = 100 gpd/ft.

(2) an external radius = 2000 ft.

(3) a porosity = 0.20

(4) a dispersivity = 100 ft.

Note than an external radius of 2000 ft. and a porosity of 0.2 would allow roughly 20×10^6 gallons of fresh water storage. The central difference requirement is that $\Delta r < 2\alpha$. Thus, Δr would have to be less than 200 ft. or 10 blocks in the horizontal (assuming equal Δr blocks). Even without the second order correct Crank-Nicholson time approximation, the time step could be as large as 100 days with the resulting numerical diffusivity only about 1% of the physical dispersivity. As a consequence, the finite-difference model can be used to accurately predict the results for fresh water storage in saline aquifer systems.

5.0 COMPUTER ASPECTS

5.1 Program Organization

The program has many features which enhance its user applicability. These include:

(a) an automatic time step feature which determines the time step based upon specified pressure, temperature, or concentration changes whichever is controlling.

(b) the three dimensions are included as singly subscripted arrays in the program and are computed during execution instead of using standard FORTRAN triple subscripts. Execution time is substantially reduced by this means.

(c) the dimensioned common area is organized so that only one routine must be recompiled if a larger problem than the original dimensions needs to be solved.

(d) the user has the flexibility to choose between a reduced band width direct solution method, ADGAUSS, or a two line successive overrelaxation iterative technique, L2SOR, in solving the finite-difference matrix equations. The L2SOR method includes a procedure for estimating the optimum acceleration parameter. Both procedures are discussed in Section 5.4.

(e) the user can choose the visual assists of plots of pressure, temperature or concentration at any well versus time and/or two-dimensional contour plots of pressure, temperature or concentration. These plots and maps are prepared on the printer to avoid time delays in plotting on another device.

5.2 Truncation Error as Related to Block Size and Time Step Restrictions

In the INTRODUCTION, the problem of truncation error was briefly discussed in connection with solving the type of equations necessary to the disposal model. Several literature articles were referenced which have recognized this problem. The energy and contaminant equations which contain convective terms are largely responsible for the importance of numerical dispersion. The pressure or total flow equation since it does not contain a convective term has truncation error which is much less significant.

Basically, the problem can be described as:

(1) A first order correct finite-difference approximation to the time or convective (first order) space derivative results in second order truncation error which is virtually identical to the physical dispersion.

(2) A second order correct finite-difference approximation eliminates the term identical to physical dispersion, but introduces a time step and block size restriction for obtaining good results.

These aspects are discussed in the following paragraphs. In this discussion, we have presented a summary of the truncation error expressions and block size-time step restrictions which would have resulted from various difference approximations which either have or could have been used. To the reader who is thoroughly familiar with these truncation error forms, we apologize and suggest he skip to section 5.3.

5.2.1 Explicit in Time

Probably the simplest set of finite-difference approximations which could have been used are those which are explicit in time, i.e. where all space derivatives are at the old time level, n. This can be considered to be a forward-in-time difference approximation. In this case, the truncation error is second order in time. However, because of the form of the differential equation, it is easy to show[14] that this second order in time error is equivalent to a second order in space error which has the same form as the physical diffusion. This truncation error can be expressed as:

$$\frac{-u^2\Delta t}{2\phi} .$$

Note that the sign of the truncation error is written as negative indicating it subtracts from or reduces the net diffusion level.

Two spatial difference approximations are commonly used for the convective term. These are a backward-in-space and a central-in-space approximation. In the former case, the numerical diffusion caused by the space approximation is:

$$\frac{u\Delta x}{2} .$$

The backward in space implies the sign of the fluid velocity must be determined and the difference taken in an up-stream direction. In the latter space approximation, there is no numerical diffusion because the truncation error is of higher order.

Explicit, forward-in-time, approximations have the disadvantage that instability can result. Round-off error in the calculation can grow and render the calculated results virtually meaningless. Two stability criteria exist for the explicit forms. The first order stability criteria is

$$\frac{u\Delta t}{\phi\Delta X} < 1. \qquad (5\text{-}1)$$

This requirement is that no more than one block volume throughput can be used in a single time step. Note also that the use of exactly this time step would cause a backward-in-space, forward-in-time approximation to have no numerical diffusion.

The second order stability criteria is that

$$\frac{E\Delta t}{\phi(\Delta X)^2} < 1/2. \qquad (5\text{-}2)$$

This criteria can be a severe limitation for many problems. When using the central-in-space explicit form, another stability limitation exists. This is that

$$\frac{u^2\Delta t}{2\phi} < E. \qquad (5\text{-}3)$$

Otherwise, the numerical diffusion (which is negative) exceeds the physical diffusion level resulting in a severe stability problem.

5.2.2 Implicit-in-Time

With the implicit or backward-in-time difference approximation, the stability criteria are removed. However, numerical diffusion due to truncation error may be as severe or even more so. In this case, the numerical

diffusion due to the space approximations is the same as listed above. The time approximation also introduces the same magnitude numerical diffusion, but of opposite sign. That is, now when using backward-in-space, backward-in-time approximations the effective numerical diffusion from each are additive.

The central-in-space difference approximation again removes the space truncation leaving only a time contribution to numerical diffusion. When the time truncation error is small compared to the physical diffusion, this approximation can give accurate results with no stability problem. However, this difference form can give rise to a spatial "oscillation"[15]. The calculated result can overshoot the maximum physically-controlled value and undershoot the minimum. The criteria which prevents this "oscillation" is given by

$$\frac{u\Delta x}{2} < E. \qquad (5\text{-}4)$$

Note that a considerable advantage still exists for using the central difference space approximation over the backward difference. In the latter case, the term, $\frac{u\Delta x}{2}$, would need to be <u>much</u> less than the desired physical diffusion, E, to give accurate results. Whereas, with the central difference, the requirement is simply that it be less. Even if the value of $\frac{u\Delta x}{2}$ exceeds the desired physical dispersion, good results can often still be obtained. For values up to perhaps $u\Delta x < 4E$, the amount of overshoot and undershoot is still acceptable even though it is not very esthetic.

5.2.3 <u>Central-in-Time</u>

The most often used second order correct time approximation is that called the Crank-Nicholson. In this case, the space truncation error terms are as before and the second order time truncation error contribution to a numerical diffusivity is removed. The disadvantage is that although stability theories show this difference form to be always stable; in actual practice, the calculated result can show an oscillation-in-time. The calculated result is better when averaged over the n and n+1 time levels and used as an intermediate time level value. However, a controlled instability can still exist. This instability appears to be tied roughly to the first and second order explicit stability criteria. However, the numerical factors in the right-hand side appear to be at least twice the explicit criteria. Even

when these values are exceeded, the calculated end result is not unstable in the classical sense of error growth without bound. However, it can be severe enough to invalidate the calculated results.

In the present model, we have provided the user the option to choose from among several difference forms. These are

(1) backward-in-space, backward-in-time

(2) backward-in-space, central-in-time

(3) central-in-space, backward-in-time

(4) central-in-space, central-in-time

As an aid to the user, we have prepared a summary table of the above described truncation error forms and stability considerations.

TABLE XIV
SUMMARY OF NUMERICAL DIFFUSION AND STABILITY

Difference Form		Numerical	
Spatial	Time	Diffusivity	Stability Consideration
BIS (upstream)	FIT (explicit)	$\frac{u\Delta x}{2} - \frac{u^2\Delta t}{2}$	$\frac{u\Delta t}{\phi\Delta x} + \frac{2E\Delta t}{\phi(\Delta x)^2} \leq 1$
CIS (centered)	FIT (explicit)	$-\frac{u^2\Delta t}{2}$	Same as above plus $\frac{u^2\Delta t}{\phi\Delta x} \leq E$
BIS (centered)	BIT (implicit)	$\frac{u\Delta x}{2} + \frac{u^2\Delta t}{2}$	None
CIS (centered)	BIT (implicit)	$\frac{u^2\Delta t}{2}$	$\frac{u\Delta x}{2} \leq E$
BIS (upstream)	CIT (Crank-Nicholson)	$\frac{u\Delta x}{2}$	$\frac{u\Delta t}{2\phi\Delta x} \leq 1$
CIS (centered)	CIT (Crank-Nicholson)	None	Same as above.

Equivalent truncation error forms or stability criteria can be derived for a radial system by substituting

$$u = q/2\pi r\Delta z$$

and $\Delta x = \Delta r = \frac{1}{r}\,\Delta \ln r$.

5.3 Computer Requirements

The model is organized to provide a relatively efficient reduction solving either a problem in less than three dimensions or without one or more of the equations. With regard to this latter comment, the complexity of the model is highly dependent upon the density and viscosity dependence upon concentration and temperature. If these properties are a function of pressure only, the three resultant equations for total flow, energy, and composition become effectively uncoupled. In such circumstances, iterations to update density are no longer required.

Similarly, energy or composition changes might be totally unimportant in a particular problem because the injection was at the same temperature or composition as the resident fluid. In such cases, the model, at user option, can be reduced to a solution of

(1) the pressure equation alone,

(2) pressure and the energy equation,

(3) pressure and the composition, or

(4) all three.

Although the reduction is certainly not as efficient as a specially written model would be, the redundant equations are not solved. Thus, much of the unneeded computer time is eliminated.

5.3.1 Storage Requirements

The model common storage is organized as one large array in blank common of the main program. Depending upon the particular problem grid dimensions, the position of each needed dimensioned array within this overall array is computed in the main program. These individual array locations are then passed to the various subroutines as arguments.

The real advantage of this approach is that there is no need to recompile if a problem larger than the original dimensions is required. If each array was in a common block

in each routine, all subroutines would need to be recompiled. On Control Data machines there is an option provided on these machines to dynamically reduce the storage from a call within the program to just that needed. Thus, on CDC machines, the size of the overall array containing all other arrays is computed as soon as the user defines the grid size. The location of the last word in the program common area is determined and added to the necessary overall array size. Then the dynamic storage reduction (or expansion) routine is called and the storage is expanded to the required size.

The above approach saves a great deal in recompilation costs if a variety of grid dimension problems are to be solved. The cost of using the dynamic allocation above is only the inclusion of a number of arguments in the call to several subroutines. In the model, five primary subroutines are called each time step. There are as many as 50-60 arguments passed in some of the routines. We have noticed little difference in running time for models written with the argument transfer and those passed by common. Thus, we believe the above arrangement does represent an overall computer saving.

Storage requirement for the program without considering the overall array is approximately

$43{,}000_{10}$ words with the subscript indicating decimal words.

A 120 grid block problem (12x5x2) requires the overall array storage at

$8{,}000_{10}$ words for L2SOR

$9{,}000_{10}$ words for ADGAUSS

A 300 grid block problem (20x5x3) requires an overall array dimension of about

$20{,}000_{10}$ words for L2SOR

and $35{,}000_{10}$ words for ADGAUSS.

Note that there is a substantial storage saving when the iterative LSOR technique is used instead of the reduced band width direct solution. A 1,000 grid block problem (20x10x5) requires an array dimension of about

$65{,}000_{10}$ words for L2SOR

and $74{,}000_{10}$ words for ADGAUSS.

77

5.3.2 Computer Timing

Time requirements for the model can vary substantially depending upon whether all three equations are being solved or whether the density is relatively constant and no iteration is required. We have attempted to provide users with some time comparisons for a range of problems.

For one iteration with all three equations being solved, the approximate timing varies from

0.015-0.025 sec/time step/grid block.

If successive iterations are required to update density, the timing may increase about 40% of the above timing for each additional time iteration is required.

Our experience has shown that a "hard" problem with significant density variations may require 3-4 iterations initially and decrease to one iteration for the majority of the time.

When the temperature or concentration equation can be deleted from the solution, there is an additional time saving. Roughly a 20% reduction of the per time step per grid block timing can be realized for each equation deleted.

Of course, the pressure or total flow equation is always solved.

5.4 Solution Techniques

The two solution techniques provided in the model are a reduced band width direction solution (ADGAUSS) method and a two line successive overrelaxation (L2SOR) iterative method. The L2SOR technique was selected over other iterative methods because of (1) its relative insensitivity to the geometric shape of the aquifer, and (2) its adaptability in choosing an optimum acceleration parameter and ordering the direction of the line orientation to minimize computer time. This latter advantage adds considerably to the ease in using the program since it removes the uncertainty in the user needing to supply iteration parameters.

5.4.1 L2SOR

In single line LSOR, the iterative method results in solving a tridiagonal system of equations directly. In the two line method, a renumbering of the points

makes this computationally more efficient. In this case, the matrix to be inverted each iterate has five diagonals. Higher multiline methods could be defined, but the gain in convergence rate is usually lost by increased work per iteration. We have found the two line SOR technique to be generally best. In terms of convergence, the LSOR technique is about 1.4 times as fast as a point SOR technique. L2SOR is about twice as fast in convergence as point SOR or 1.4 times faster than single line SOR.

The rate of convergence depends critically upon the choice of the acceleration parameter, ω. The optimum parameter can be estimated from

$$\omega = \frac{2}{1+\sqrt{1-\bar{\rho}^2(B)}} \qquad (5\text{-}5)$$

where $\bar{\rho}$ is the spectral radius of the matrix B. The method by which this can be estimated can be outlined as follows. If the equation to be solved is

$$AX = k, \qquad (5\text{-}6)$$

the spectral radius can be estimated by choosing in the SOR technique the following:

(a) $\omega = 1$

(b) $k = 0$

(c) an initial X - vector of all ones

(d) calculate

$$\underset{1\le i\le n}{\text{Min}} \frac{X_i^{\ell+1}}{X_i^{\ell}} < \rho < \underset{1\le i\le n}{\text{Max}} \frac{X_i^{\ell+1}}{X_i^{\ell}}$$

Thus, as the iteration number, ℓ, increases, a good estimate of $\bar{\rho}$ is obtained and consequently ω. Our experience has shown that three to ten iterations provide an excellent estimate of ω.

5.4.2 ADGAUSS

Until recently, iterative methods were used almost to the exclusion of direct solution techniques because

of the higher computer storage and time requirements of the latter. In 1973, Price and Coats[33] introduced some new ordering schemes for Gaussian elimination which reduces computing time and storage requirements by factors as large as six and three, respectively, when compared to more standard orderings. In their paper, they included computer time requirements based upon theory and by numerical examples. The application problems were typical diffusivity-type pressure equations such as the parabolic equation(s) solved in this model. Also presented was a comparison of work requirements with LSOR.

The work requirement for an iterative method is

$$W_{it} = C\, N_{it}\, IJK \qquad (5\text{-}7)$$

where C = the number of multiplications and divisions per iteration per grid point

N_{it} = number of iterations

For the direction solution methods, the expression can be approximated as

$$W \sim fI(JK)^3 \qquad (5\text{-}8)$$

where f is a function of the ordering scheme.

For ordinary standard ordering in the direct solution, GAUSS, f=1. For the alternating diagonal direction ordering, ADGAUSS, $0.17<f<0.5$. Practically for most three-dimensional problems, $f \sim 0.3$.

Table XV from reference (33) summarizes the work required and iterations for the same work for several iterative methods.

TABLE XV
SUMMARY OF WORK REQUIREMENTS FOR ITERATIVE METHODS

Method	Work Required C	No. Iterations for Same Work as ADGAUSS
SIP	37	$0.0081(JK)^2$
ADI	28	$0.0107(JK)^2$
LSOR	11	$0.0272(JK)^2$

The basic conclusion from the above table is that for nominal band widths (JK) of roughly 40, the ADGAUSS is equivalent to about 44 LSOR iterations. Thus, if more than 44 iterations were required, the direct solution would be faster. The authors found in testing the above expressions that often equivalent time was required for nominal band widths up to about 80. Thus, a 20x15x5 grid could probably be solved more rapidly by the direct method than by LSOR.

The disposal model includes in the direct solution option, an optimum ordering scheme of the alternating diagonal type. This ordering routine is called once when the geometry and reservoir parameters are set. We would suggest that L2SOR be considered if the minimum multiple of two dimensions is greater than about 50. Otherwise, the direct solution should be used. If storage is a problem, the iterative method should always be considered.

5.5 Visual Aids for User

The model contains both plotting and contour mapping aids to assist the user in visualizing his results. We have chosen to provide these visual aids to the user by presentation on the line printer at execution time. Thus, the visual results are available immediately to the user instead of requiring a two step process of plotting or mapping through another off-line hardware device. To also facilitate the user getting these visual aids at a time later than execution, an option is available to edit records written to tape and plot or map them. Thus, the user may run the model on a disposal problem writing records to tape (disk) and then subsequently choose to plot or map the results at desired intervals. The following subsections briefly discuss the plot and map routines.

5.5.1 Plotting Calculated Versus Observed Results

This portion of the model enables the user to plot (1) calculated pressure, temperature, or concentration versus time for any specified well or (2) plot comparative values of observed (measured) pressure, temperature or concentration with calculated values of the same variables as a function of time. Since the wellbore is made an integral part of the calculation, the user can compare these variables at surface conditions at bottom-hole, or both as desired.

This feature is especially useful during well test phases of a disposal operation. When pump tests or tracer tests are being conducted, it is particularly helpful to present a plot comparing the measured values versus the calculated values as a function of time. Then a change in permeability, porosity, dispersivity, or another variable can be made to evaluate the effect on the calculated p, T, and C.

The plotting program presents basically an x,y plot with the exception that two ordinates (observed and calculated dependent variables) are plotted versus the abscissa value (time). Two different characters are used to identify the two different ordinate values with a third character specifying coincident values. Variable spacing along the time axis is used in the plot.

5.5.2 Contour Mapping

To make the visualization of multidimensional results more comprehensible, contour maps can be prepared on the printer of pressure, temperature or concentration. These maps can be presented at any time during the calculation of the results. Since both rectangular cartesian (x,y,z) and cylindrical (r,z) coordinates can be used, maps of a cross-section or an areal plane (x,y) can be selected.

The mapping program presents a contour diagram of the dependent variable, p, T, or C, at a specified time. Up to 20 contour intervals (ranges) of the dependent variable can be described with different characters. The specific character to be mapped at each x,y point is evaluated by bilinear interpolation between the four nearest grid point values.

Arbitrary dimensions of the map width and scale can be chosen. Often it is convenient to map areal planes to scale, e.g. 1" = 100 feet in each direction. However, cross-sectional planes generally are better displayed by a distorted scale, e.g. 1" = 20 feet vertical versus 1" = 100 feet in the horizontal. If dimensions larger than a single page width or length are chosen, multiple printer pages are used with grid points specified so that superposition and alignment of the various pages is straightforward.

6.0 TYPICAL APPLICATION OF MODEL

The problem described in this section is probably representative of that for which the model would be used. The aquifer formation, plant wastes, etc., are hypothetical but are probably a realistic average of the situation which might be encountered. The application problem describes the use of the model to:

(1) interpret the injectivity tests in the potential receiving strata,

(2) design and interpret an isolated interval between-well tracer test in the formation, and

(3) make sensitivity study predictions of the fate of the injected waste.

Two deep waste injection wells were completed to dispose of inorganic constituents from a chemical plant. These wells will inject slightly acidic waste into a sandstone formation at a depth of 4020 feet. The first well, DWD-1, will carry the bulk of the injection with DWD-2 being used periodically during plant blowdown and as a backup to DWD-1. Later, plant expansion may require continuous injection into DWD-2.

A study was conducted to evaluate the alternatives for disposing of the waste aqueous phase. Among the alternatives considered were evaporation ponds, chemical treatment with subsequent release into surface water, and underground injection. The original feasibility study indicated deep well disposal was the best alternative because of (1) lower environmental impact, (2) adequate geologic strata for confinement, and (3) relative economics.

Subsequent to the feasibility study, plans were made to pursue the deep well disposal operation. Conditional permits were obtained to drill the wells and make further tests to evaluate (1) the integrity of the geological confining strata, (2) the local hydrogeological properties in the vicinity of the selected well sites, and (3) the fate of the injected constituents in the subsurface environment. The deep well disposal model was used to perform sensitivity studies and help delineate the engineering aspects concerned with the above tests and evaluations. In particular, the model was used to predict the influence region for the range in uncertainty in permeability, porosity, and dispersivity. Also of interest was to evaluate the importance of density and viscosity effects due to the higher temperature less dense injection fluid.

Hydrogeological Environment

The two injection wells were drilled through the sandstone formation reaching a total depth of about 4100 feet. Examination of the well cuttings from each well were made and a log prepared. Subsequent to the drilling of the wells, compensated neutron and formation density CNL/FDC logs were obtained to determine lithology and likely perforation intervals.

Fresh water supply in this region is obtained principally from an aquifer which has its base at roughly 500 feet. Below this depth, but above the disposal formation, are interbedded dolomite of low permeability and impermeable anhydrite. The injection zone is a sandstone of moderately good permeability with some interbedded shale stringers. The injection zone is underlain by a thick impermeable shale stringer.

Sidewall cores of the overlying anhydrite indicated permeabilities less than 1 md and generally averaging about 0.01 md. Sidewall cores were obtained for each ten feet of the potential injection interval between about 4035 and 4150 feet. The resulting permeability and porosity tests on these cores are indicated in Table XVI.

TABLE XVI

SIDEWALL CORE RESULTS

Well DWD-1			Well DWD-2		
Depth	Perm, md	Porosity,%	Depth	Perm, md	Porosity,%
4047-4057	92	10.1	4035-4045	79	9.9
4057-4067	122	9.6	4045-4055	112	10.3
4067-4077	81	9.7	4055-4065	95	10.2
4077-4087	102	11.1	4065-4075	82	9.8
4087-4097	96	10.4	4075-4085	103	10.1
4097-4107	165	11.3	4085-4095	141	10.7
4107-4117	139	10.6	4095-4105	153	11.0
4117-4127	31	9.3	4105-4115	0.1	7.6
4127-4137	42	9.9			
4137-4147	26	9.7			

Little regional water flow is known to exist under natural pressure gradients at the depth of the receiving aquifer.

Injection Facilities

Plant effluent will gravity flow to a lined storage pond connected to a large surge tank. The waste is then

pumped to the well(s). The injection rate is expected to be about 50 gpm (10,000 ft^3/day).

Both injection wells are cased and cemented to depth with nine inch casing. The casing fluid flows through four inch fiberglass tubing. A non-corrodible packer assembly is set 200 feet above the perforations in each well. Perforation density was 10 per foot. The annulus is filled with water containing a corrosion inhibitor and contains sensors to monitor pressure and conductivity which could reflect leaks in the casing or packer.

Injection and Formation Water

Injection and formation water properties are summarized in Table XVII.

TABLE XVII

INJECTION AND FORMATION WATER PROPERTIES

	Formation Water	Injection Water
Calcium (C_a)	670	50
Magnesium (M_g)	320	20
Sodium (N_a)	39,000	17,000
Potassium (K)	100	75
Sulfate (SO_4)	75	10,000
Chloride (U)	82,000	12,000
Dissolved Solids	130,000	40,000
pH	6.6	5.6
Density @ 70°F	71.77 lb/ft^3	65.27 lb/ft^3
@ 139.8°F	70.51 lb/ft^3	64.51 lb/ft^3
Viscosity @ 139.8°F	0.9 cp	0.75 cp
Tracer Metals		
Arsenic (A_s)		2000
Cadmium (C_d)		350
Copper (C_u)		600
Zinc (Z_n)		720
Mercury (H_g)		15
Iron (F_e)		2900
Nickel (N_i)		750

Well Tests

To delineate porosity and permeability, injectivity tests were made at each well. Both surface pressure bottom-hole pressure and bottom-hole temperature were monitored. Injection of 75°F water was continued for two days and then shut-in. Well pressure at both the injection

well and the untested well 625 ft. away continued to be monitored for another three days.*

Well test interpretation was performed with the model. This interpretation generally proceeds in the following way:

(1) obtain the best single layer homogeneous match of the observed pressures at both wells.

(2) Impose a skin factor at the injection well if the calculated response is significantly improved.

(3) If needed, break the injection interval into more than one layer which communicate vertically.

Figures 14 and 15 illustrate a comparison of the best single layer homogeneous calculation with the "observed results. Figure 14 compares pressures at the injection well, Figure 15 at the observation well 625 ft. away. The horizontal permeability and porosity used in the calculation were 0.22 ft/day (63 md) and 0.10 respectively. Also indicated in the figures for illustrative purposes are sensitivity results for an increase in porosity to 0.15 with the same permeability and an increase in permeability by 20% to 0.26 ft/day (76 md) with the same 10% porosity.

---

* The results of the "observed well test were calculated with the model using five communicating strata in the 100 ft. vertical direction. The horizontal permeability, porosity and thickness of each of the five strata are shown below:

	Permeability		
Thickness, ft.	md.	ft/day	Porosity, %
20	104	0.36	9.85
10	84	0.29	9.70
20	96	0.33	10.70
20	142	0.49	11.00
30	28	0.098	9.60
Average	85	0.29	10.16

The vertical permeability was one-third of the horizontal permeability. It was assumed there was an additional reduction of 50% in horizontal permeability for about 10 feet around the well due to drilling fluid invasion.

81

Figure 14 - Calculated Sensitivity for Aquifer Porosity and Permeability (Injection Well)

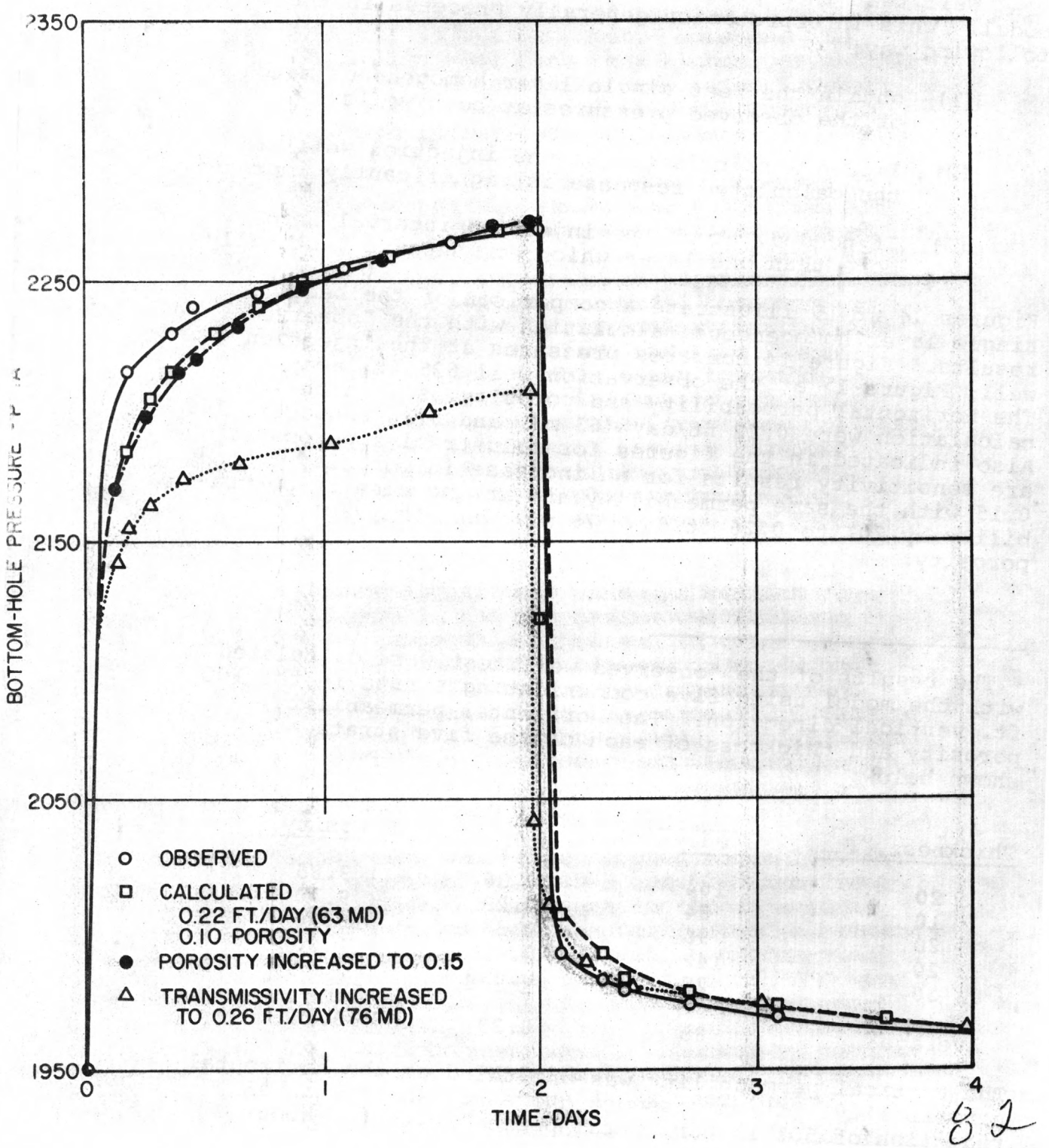

82

Figure 15 - Calculated Sensitivity for Aquifer Porosity and Permeability - Observation Well 625 Ft. from Injection Well

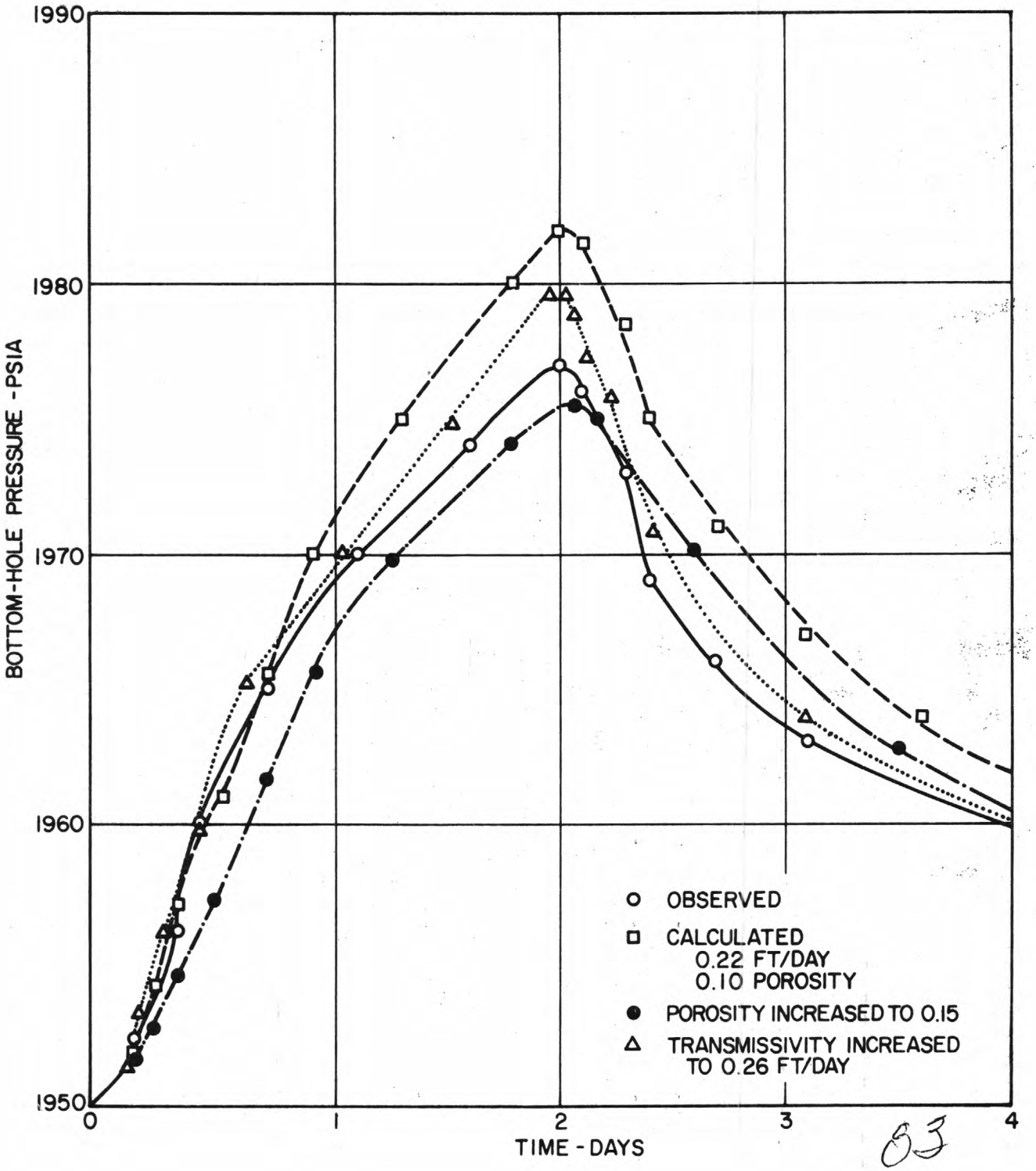

Note that the increased porosity has little effect on the injection well performance. The pressure at the well 625 feet away is much more responsive to the change in porosity. Increasing the permeability improved the agreement of calculated with observed results at the well 625 feet away from the injection point. However, the buildup at the injection well with this higher permeability is much too low. This suggested that the injection well might have a skin effect present and thus the injection well index was lowered to reflect the presence of a skin.

The end result calculation is shown in Figures 16 and 17. The formation transmissivity was 0.3 ft/day (86 md permeability) and the well index effectively reduced this permeability to 27 md to a radius of two feet around the well. As can be seen, this reduced permeability around the well has produced an adequate match of observed and calculated results at both wells indicating that further refinement is unnecessary. Note from the five layer representation table that the single layer formation transmissivity is very nearly the arithmetic composite average permeability thickness for the five layer original "observed" calculation. Although in general "history match" determined values of permeability and porosity are not totally unique, in the simple two zone model used above the values cannot be changed much and retain as adequate a match.

One of the other significant unknowns besides permeability and porosity is the dispersion coefficient. This coefficient is especially important in cases where density (or viscosity) inequality between injected and resident fluids exists. The amount of dispersion can prevent the density effects of the injection fluid tending to overrun or underrun the resident fluids. To delineate the dispersion coefficient, a tracer test was conducted in an isolated interval of the potential sandstone receiving formation (see Figure 18).

An observation well was to be located about 100 feet from the primary injection well DWD-1 and 525 feet from the secondary well DWD-2. Subsequent to the injection test above, the observation well was drilled and a between-well tracer test performed. In the test, a substantially fresher water brine at a surface temperature of 75°F was injected into the formation and the same rate was pumped from the observation well. A 10 foot injection-production interval was isolated from the overall interval by setting two packers in each well. Chloride content of the produced water was analyzed over the 20 day test period.

Figure 16 - Comparison of Calculated Injection Well Pressures with Observed Values- Reduced Transmissivity Around Injection Well

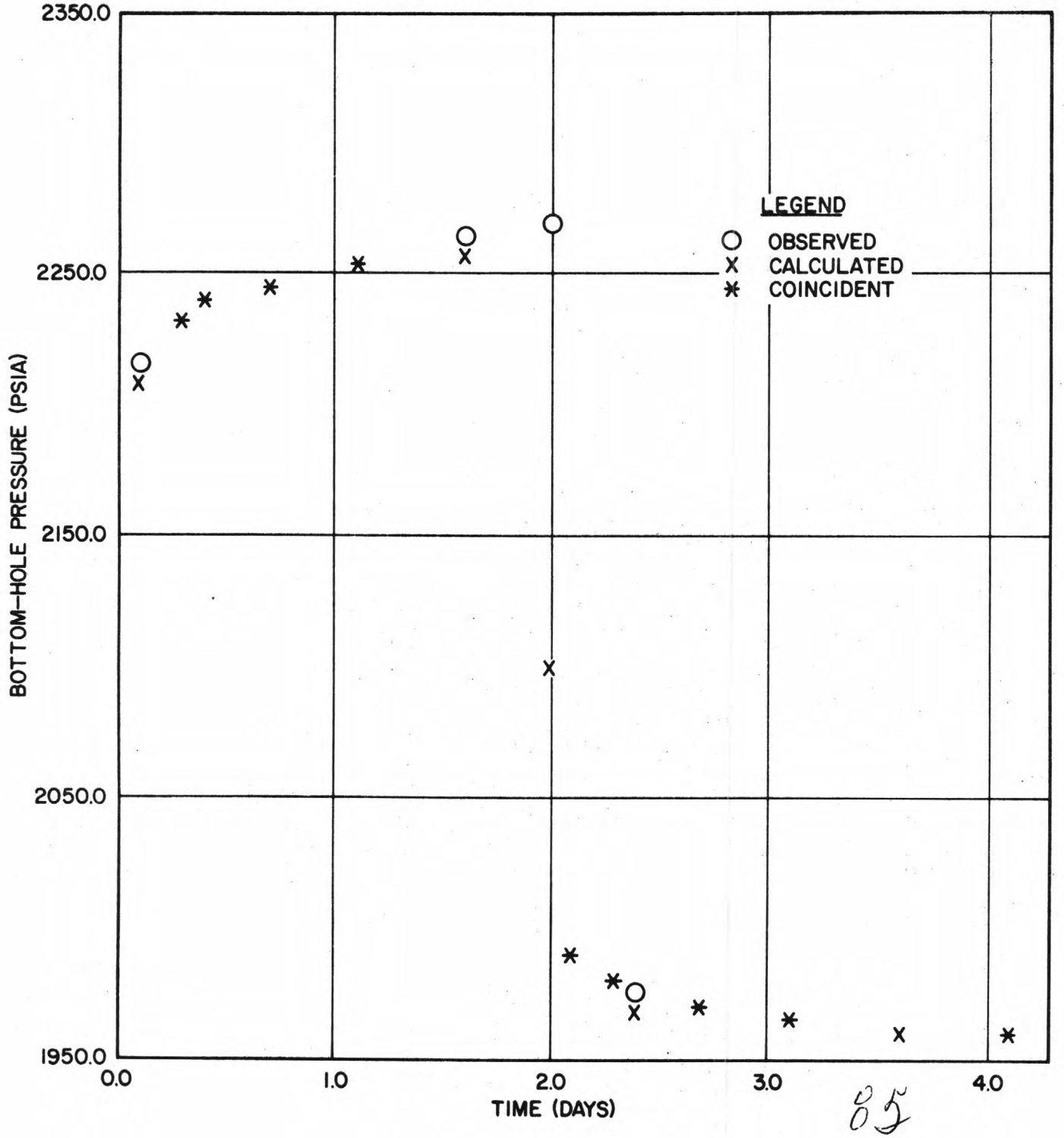

Figure 17 - Comparison of Observation Well Pressures with the Observed Results - Reduced Transmissivity Around Injection Well

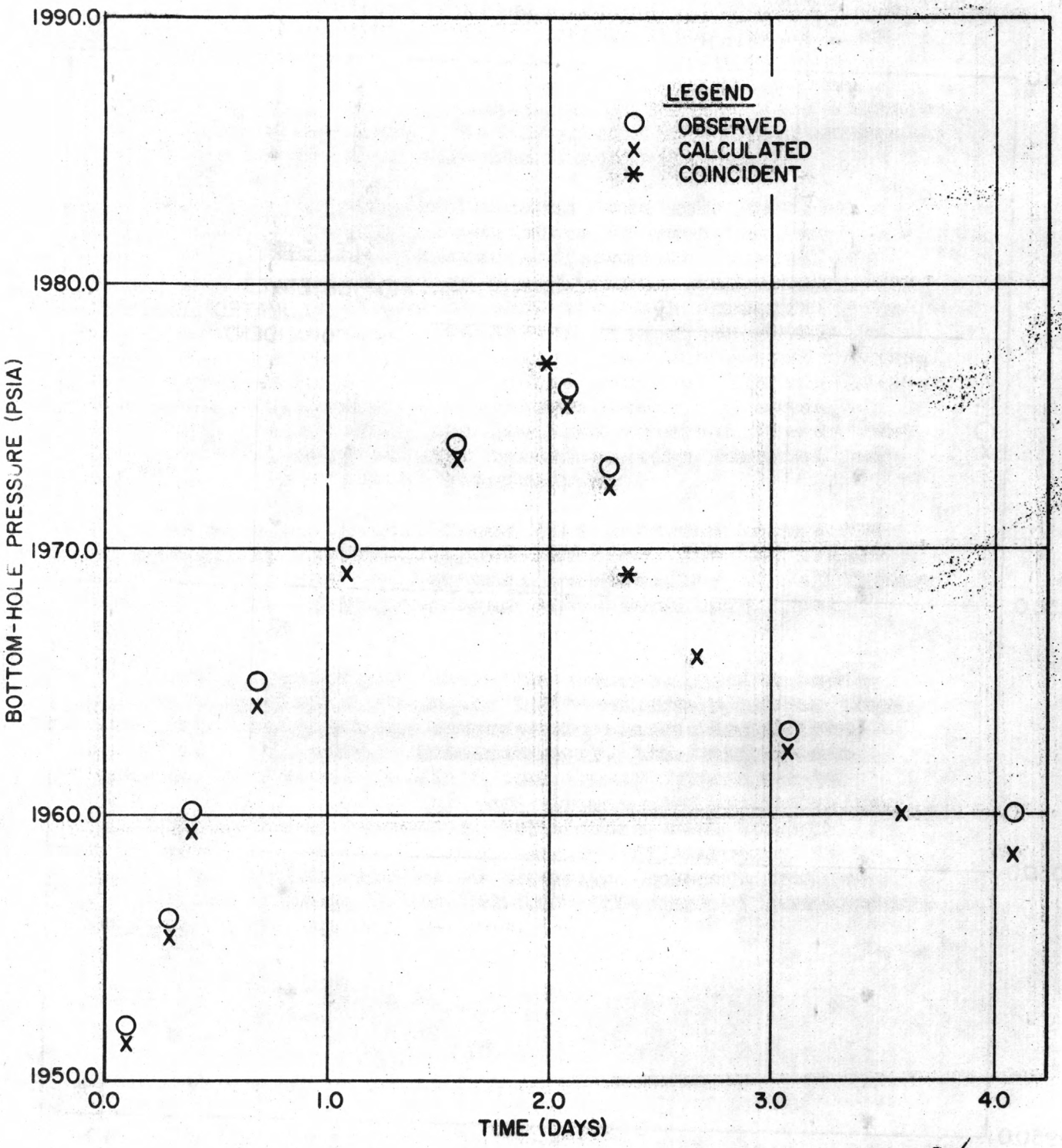

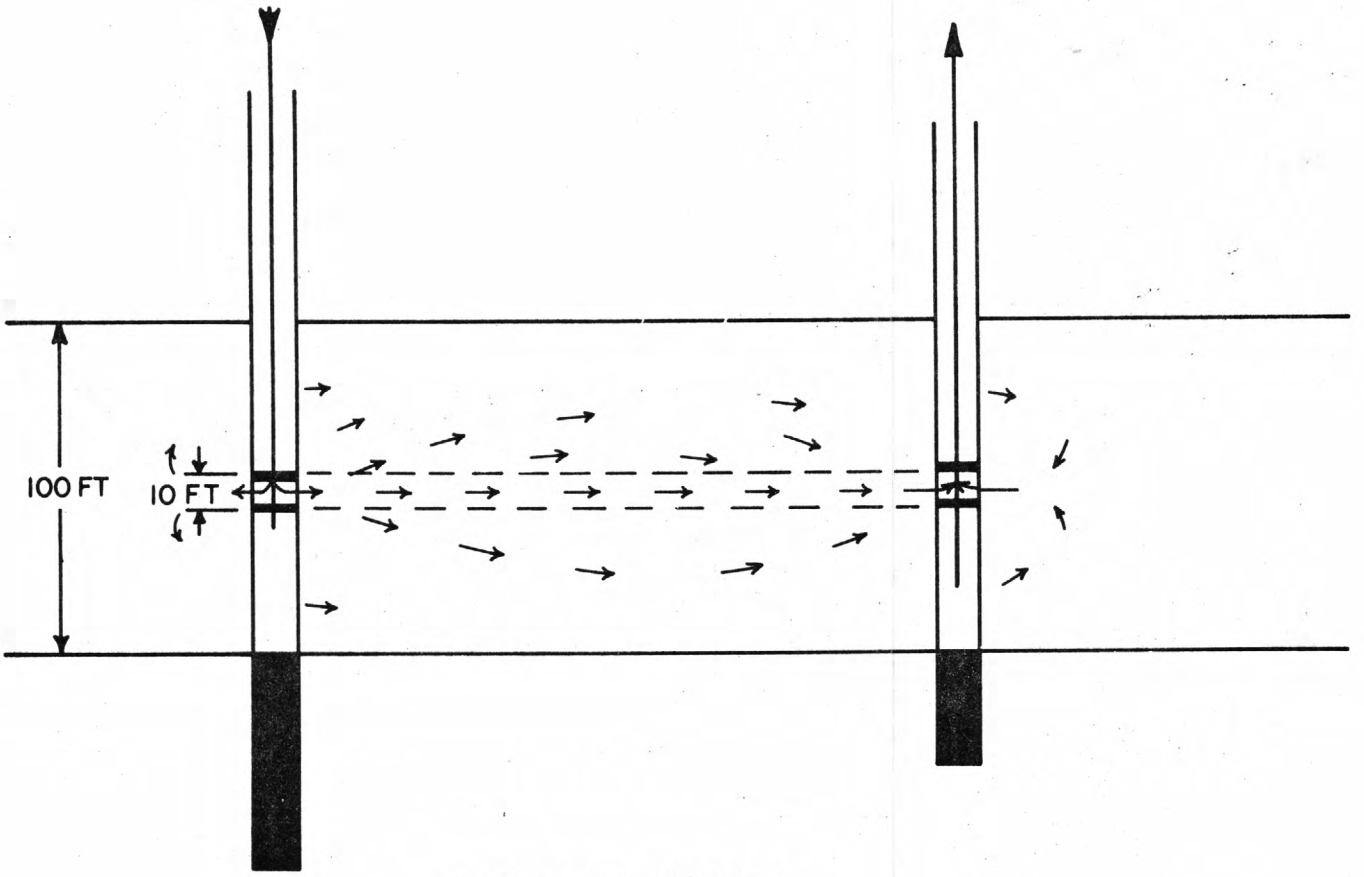

CROSS-SECTIONAL VIEW

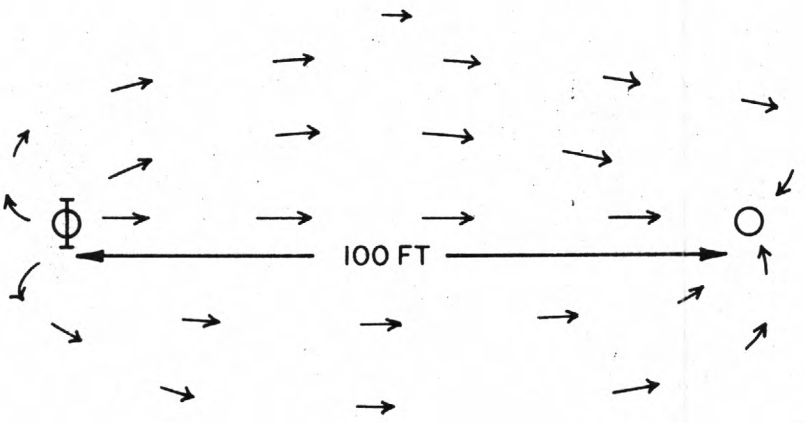

87

AREAL VIEW

Schematic of Isolated Interval Tracer Test

Figure 18

Sensitivity runs with a three vertical layer model indicated that at the dispersion level necessary to match the chloride breakout curve, the density difference had essentially no effect. This is strongly affected by the fact that the injection fluid arriving down the well at the injection interval was significantly cooler (the injection temperature ranged from 87°F initially down to 78°F) than the 140°F approximate injection zone temperature. As a consequence, the injected fluid had a viscosity about ten times higher than the formation water.

Ideally, an isolated interval test such as this tracer injection would be sensitive to vertical permeability and to the transverse dispersion as well as the longitudinal dispersion coefficient. Our sensitivity runs indicated in Figure 19 show the most sensitivity to vertical permeability. Transverse dispersion probably could not be accurately evaluated from such a test because of the small effect. Longitudinal dispersivity should be reasonably determined by the tracer test. It appears from these results that the isolated interval tracer test should be extremely helpful in delineating vertical permeability and horizontal dispersivity.

The results of the tracer test provided values for the horizontal dispersivity of 100 feet, for the transverse 20 feet, and the vertical permeability of 0.1 ft/day (~30 md). The prediction runs were based upon these results.

In the prediction runs, the waste injection had a surface temperature of about 150°F--slightly higher than the initial bottom-hole temperature which ranged from about 140°F to 141°F. Interestingly, the bottom-hole temperature started at 135°F and slowly increased to 141°F. That is, the fluid was injected slightly cooler than the original formation temperature even though it started out at the surface about 10°F warmer. At first, this might seem to be anomaly; however, the two qualitative figures below indicate the type of temperature response which can be expected.

Figure 19 - Effects of Horizontal and Vertical Dispersivity Factors and Permeabilities on Injected Fluid Concentration at a Production well 100 ft. away from the Injection Well

Sensitivity of Concentration Breakout for Vertical to Horizontal Ratios of Permeability and Dispersivity

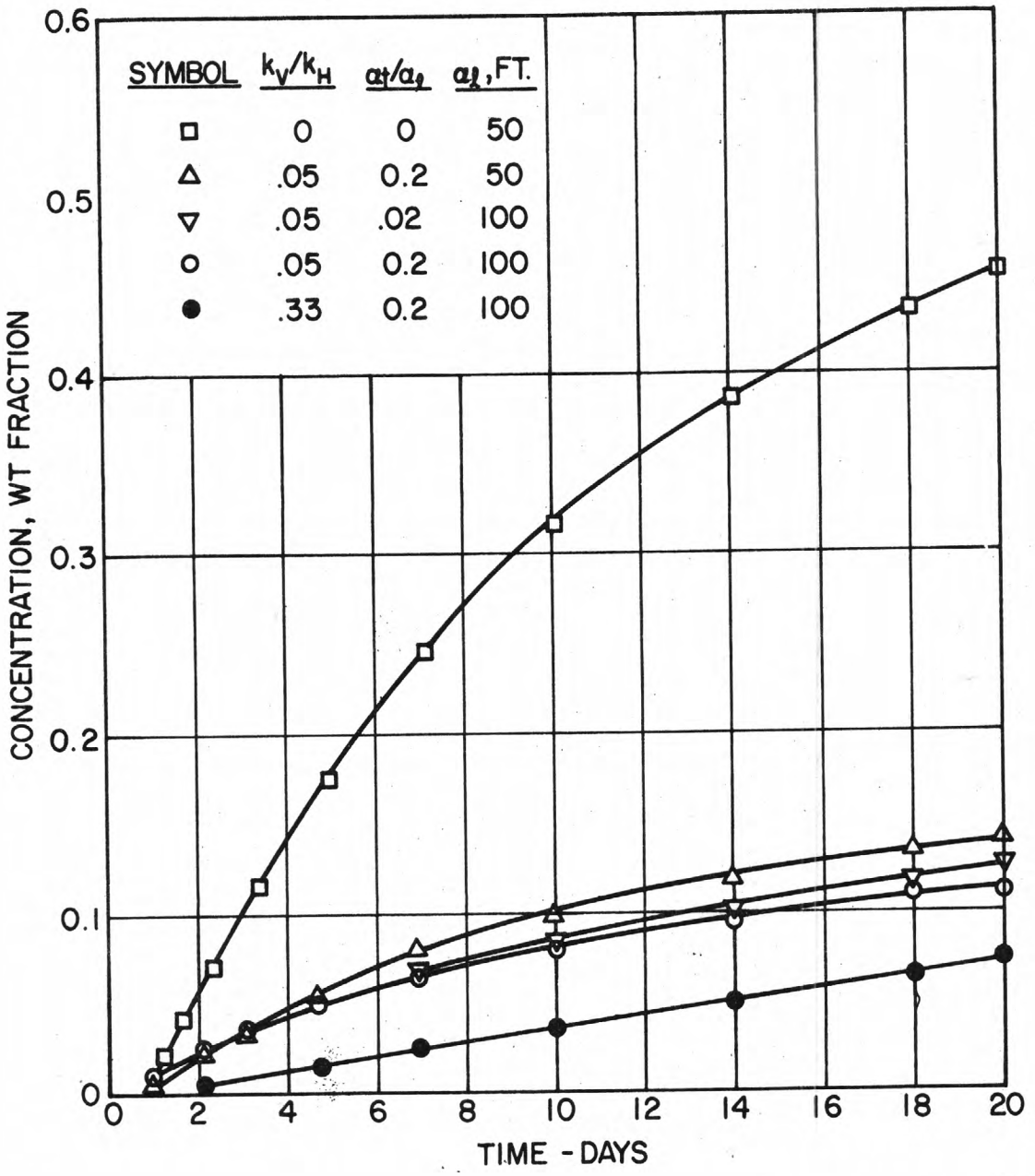

89

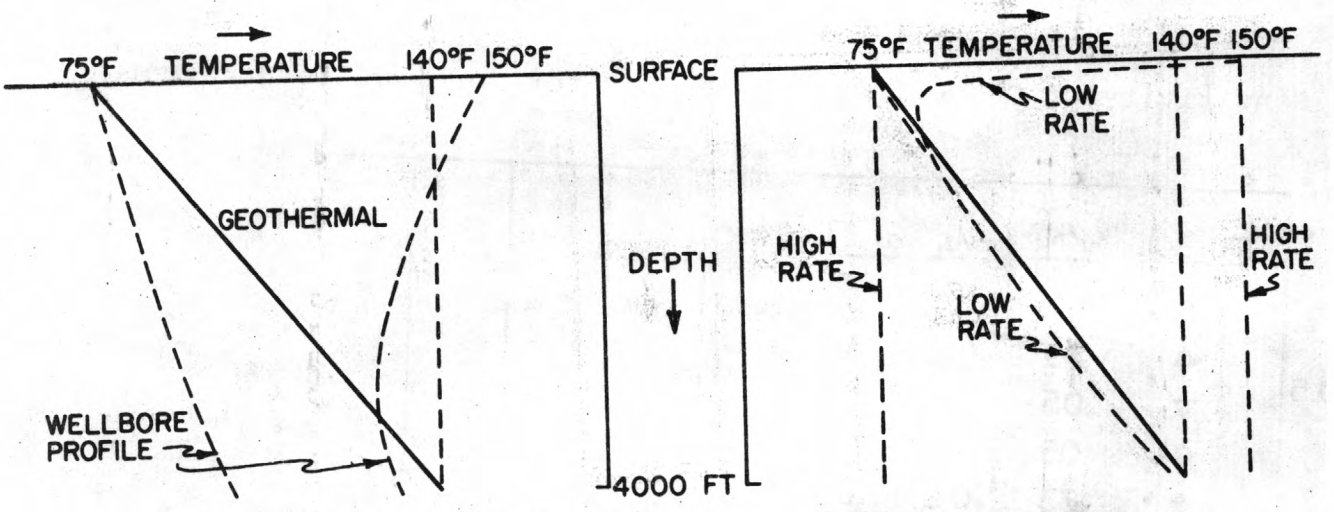

Not only is the wellbore temperature profile complicated by the interrelationship between injection temperature, injection rate, and heat transfer coefficients, but the entire heat loss is transient. Eventually, the earth surrounding the well assumes a temperature close to that of the wellbore and the bottom-hole temperature approaches the surface temperature. However, the transient may very well be important over the entire period of interest.

The slightly cooler bottom-hole injection temperature caused the injected fluid to initially have a higher viscosity than the resident water. However, the bottom-hole temperature became equal to the resident fluid temperature after roughly one month of injection. Then the viscosity of the injected water was slightly less than the formation water. Even so, the large dispersion value of 100 feet used in the prediction run prevented any significant effect of the unfavorable viscosity ratio.

A general description of the prediction run was as follows:

(1) Injection into DWD-1 was continued for 120 days. Surface temperature averaged 150°F.

(2) Subsequently, the waste was stored in a lined pond and then injected into DWD-2. The significance of the above is that the surface injection temperature dropped to 75°F due to pond storage. This period of injection continued for 60 days.

(3) After six months, injection at DWD-1 was reinitiated and the prediction continued to a time of one year.

The fluid and aquifer properties, as well as the grid description, are summarized in Table XVIII.

TABLE XVIII

FLUID AND AQUIFER PROPERTIES FOR APPLICATION PREDICTION

Aquifer	
Transmissivity (Permeability)	0.3 ft/day(90 md)
Vertical to horizontal transmissivity data	0.33
Porosity	0.10
Longitudinal dispersivity	100 ft.
Transverse dispersivity	20 ft.
Injection interval thickness	100 ft.
Temperature	139.8°F to 141°F
Geothermal gradient	1.62°F/100 ft.
Fluids-Reservoir	
Density	70.51 lb/ft^3@139.8°F
Viscosity	0.9 cp @ 139.8°F
Fluids-Injection	
Density	64.51 lb/ft^3@139.8°F
Viscosity	0.75 cp @ 139.8°F
Temperature	150°F (or 75°F)

(TABLE XVIII continued)

Grid Description (16x5x3)

x-blocks (16)

200.	200.	100.	100.	62.5	100.	100.	100.
100.	100.	100.	62.5	100.	100.	200.	200.

y-blocks (5)

100.	100.	100.	200.	200.

z-blocks (3)

33.3	33.3	33.3

Aquifer influence functions were used along all peripheral blocks except the plane, y=0. These influence functions simulate the disposal well pattern centered in an infinite extent aquifer. Since there was no known permeability heterogeneity in the y-direction, the plane y=0 was used as a symmetry plane.

A central-in-space finite difference approximation was used along with the backward-in-time. Numerical dispersion due to the space approximation was eliminated by the second-order correct space approximation. The truncation error due to the time approximation was small compared to the dispersivity. The time truncation error decreases with increased distance around the well since the velocity is smaller. At a distance of 200 feet from the well, the time truncation was less than 10% of the dispersivity value. If time truncation had been a problem, the Crank-Nicholson second-order time approximation would have been used.

The predicted results after one year for the top and bottom layers of the model are shown in Figures 20a and 20b. The amount of override due to density was insignificant. That is, the interaction of large dispersion and the temperature effect compensating for the compositional effect on density has effectively counteracted the overriding influence. Sensitivity studies would be necessary to evaluate at what dispersion level the density effect might finally become important.

Figure 20a shows that the injection zone which entered through DWD-2 has been shifted slightly away from DWD-1. The concentration contours on Figures 20a and b represent the weight fraction of injected water present at an x-y position within the reservoir. The numbered contours represented 0.05 weight fraction ranges with the band of "1's" representing 0.05 to 0.10, the "2's" represent 0.15 to 0.2, and finally the "9's" represent concentrations greater than 0.85. In the bottom plane representation, the character x simply indicates that this layer went to a zero porosity and permeability. Thus no flow is taking place.

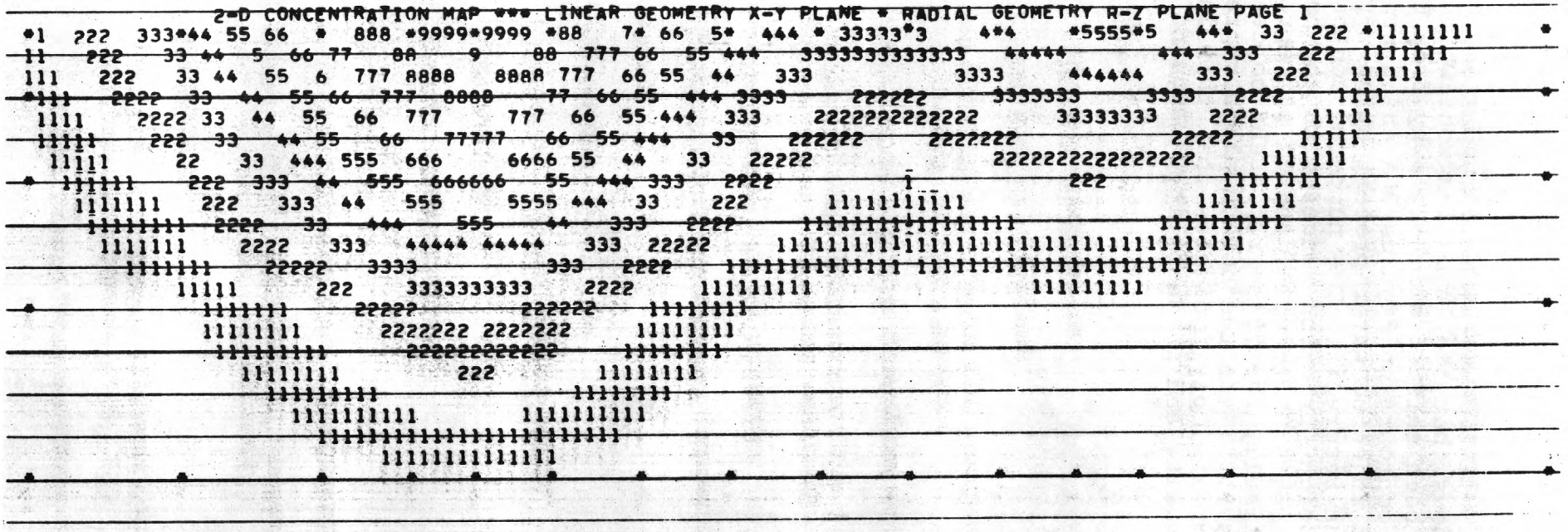

Figure 20a - Predicted Concentration Contours After One Year. Top of the Aquifer with Injection from Two Wells

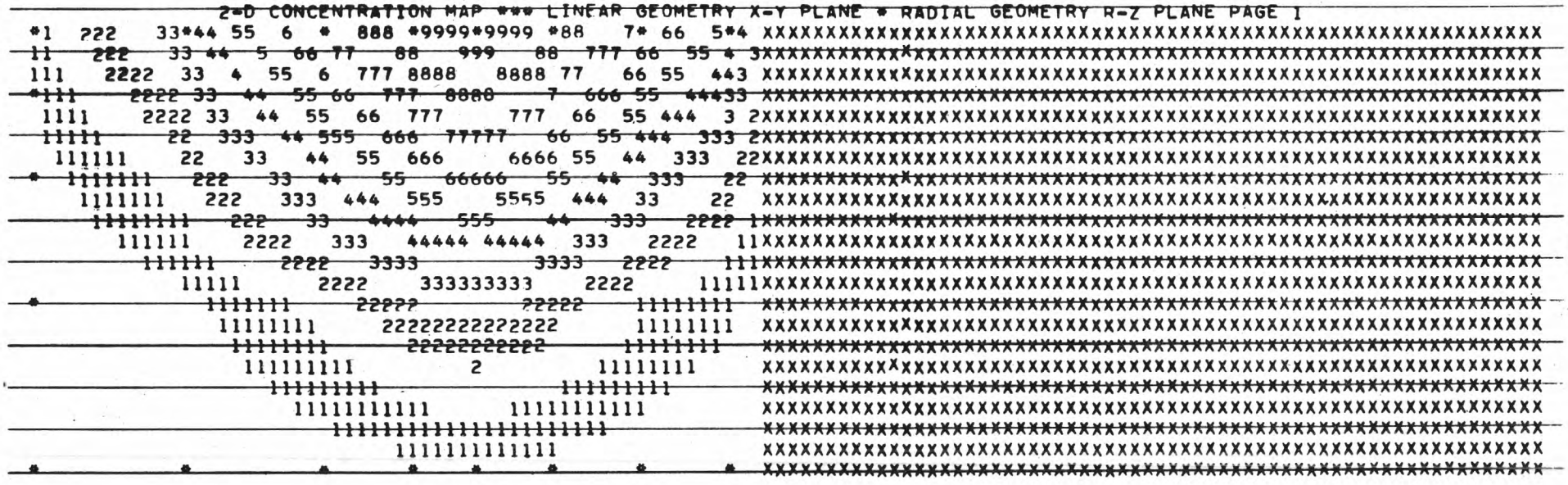

Figure 20b - Predicted Concentration Contours After One Year. Bottom of the Aquifer with Injection from Two Wells.

7.0 NOMENCLATURE

a_i, a_2, a_3	=	Coefficients in the density equation (4-2)
A	=	Area to flow--either $\Delta x \Delta y$, $\Delta x \Delta z$ or $\Delta y \Delta z$
B	=	Parameter in the viscosity model
B	=	Parameter in the Carter-Tracy aquifer influx rate expression = $2\pi \Delta Z \phi c r_e^2$ s
c	=	Compressibility
C	=	Concentration, mass fraction
C_p	=	Specific heat
D	=	Diffusion coefficient
E	=	Dispersion coefficient
e_w	=	Rate of influx across the peripheral boundaries of the aquifer
f	=	Friction factor for flow down well
F(t)	=	Transient heat conduction time function for heat loss from the wellbore
g	=	Acceleration due to gravity
g_c	=	Gravitational conversion factor
h	=	Depth
H	=	Enthalpy
J	=	Mechanical equivalent of heat
k	=	Permeability
K	=	Thermal conductivity
K_t	=	$k/\mu \phi c r_e^2$
ℓ	=	Distance between grid block centers
NX,NY,NZ	=	Numbers of grid blocks in reservoir x, y, and z directions respectively
p	=	Pressure
p^n	=	Terminal rate case influence function at dimensionless time $t_D = K_t t_n$
Q	=	Heat transferred from wellbore to surrounding earth

q	=	Mass rate of production or injection of liquid for a grid block
q'	=	Mass rate per unit volume
q_L	=	Rate of heat loss from grid block
r	=	Radial space coordinate
R_w	=	Wellbore radius
R_1, R_2	=	Inner tubing radius and outer casing radius, respectively
s	=	Fraction of a circle covered by reservoir-aquifer circular boundary
t	=	Time
T	=	Temperature
u	=	Superficial (Darcy) fluid velocity in the porous rock
U	=	Internal energy
U_c	=	Overall heat transfer coefficient
V	=	Grid block volume
V_1, V_2	=	Aquifer influence function coefficients for pot and steady-state, respectively
$W_{e,n}$	=	Cumulative water influx at time t_n
W_f	=	Work done by fluid in wellbore flow
x	=	Cartesian space coordinate
Z	=	Elevation above a reference plane

Subscripts:

av	=	Average over depth increment.
n	=	Time level t_n.
0	=	Reference level.
bh	=	Bottom-hole
ob	=	Overburden.
R	=	Rock.
i,j,k	=	Grid block indices.
w	=	Liquid.
l,t	=	Longitudinal and transverse, respectively.
m,M	=	Molecular properties in porous media and open channel, respectively.

Superscripts:

n	=	Time level ρ^n

Greek:

ϕ	=	Porosity.
ρ	=	Density.
μ	=	Viscosity.
α	=	The dispersivity proportionality to fluid velocity.
γ	=	Thermal diffusivity of rock surrounding wellbore.
θ	=	Angle of velocity vector in the x-y plane.
β	=	Lag factor in the thermal front.
ψ	=	Angle of velocity vector with the z-axis.
τ	=	Tortuosity factor
Δt	=	Time increment.
$\Delta x, \Delta y, \Delta z$	=	Grid block dimensions.

8.0 REFERENCES

(1) Kimbler, O. K., Kazmann, R. G., and Whitehead, W. R.: "Saline Aquifers--Future Storage Reservoirs for Fresh Water?" Preprints Underground Waste Management and Artificial Recharge 1 Published by American Association Pet Geologists, Tulsa, Oklahoma, 1973.

(2) Meyer, C. F. and Todd, D. K.: "Are Heat-Storage Wells the Answer?" Electrical World, August, 1973.

(3) Blackwell, R. J., Rayne, J. R., and Terry, W. M.: "Factors Influencing the Efficiency of Miscible Displacement," TRANS AIME, 216, 1959.

(4) Aronofsky, J. S.: "Mobility Rates--It's Influence on Flood Patterns during Water Encroachment," TRANS AIME, 195, 1952.

(5) Saffman, P. G., and Taylor, G. I.: "The Penetration of a Fluid Into a Porous Medium or Hele-Shaw Cell Containing a More Viscous Liquid," Proc Roy Soc, A245, 1958.

(6) Scheidegger, A. E.: "Growth of Instabilities of Displacement Fronts in Porous Media," PHYSICS OF FLUIDS, 3, 1960.

(7) Wooding, R. A.: "Stability of a Viscous Liquid in a Vertical Tube Containing Porous Material," Proc Roy Soc, A252, 1959.

(8) Peaceman, D. W. and Rachford, H. H., Jr.: "Numerical Calculation of Multidimensional Miscible Displacement," Soc. Pet. Eng. Journ., December, 1962.

(9) Perrine, R. L.: "Development of Stability Theory for Miscible Liquid-Liquid Displacement," Soc. Pet. Eng. Journ., March, 1961.

(10) Scheidegger, A. E. and Johnson E. F.: "The Statistical Behavior of Instabilities in Displacement Processes in Porous Media," Can. Journ. Phys., 39, 1961.

(11) Dougherty, E. L.: "Mathematical Model of An Unstable Miscible Displacement," Soc. Pet. Engr. Journ., June, 1963.

(12) Bredehoeft, J. D., Counts, H. B., Robson, S. G., and Robertson, J. B.: "Solute Transport in Ground-Water Systems," to be published.

99

(13) Stone, H. L. and Brian, P. L. T.: "Numerical Solution of Convective Transport Problems," AIChE Journ., 9, 1963.

(14) Lantz, R. B.: "Quantitative Evaluation of Numerical Diffusion (Truncation Error)," Soc. Pet. Eng. Journ., September, 1971.

(15) Price, H. S., Varga, R. S., and Warren, J. E.: "Application of Oscillation Matrices to Diffusion Convection Problem," J. Math. and Phys., 45, 1966.

(16) Garder, A. O., Peaceman, D. W., and Pozzi, A. L.: "Numerical Calculation of Multidimensional Miscible Displacements by Method of Characteristics," Soc. Pet. Eng. Journ., March, 1964.

(17) Pinder, G. F. and Cooper, H. H., Jr.: "A Numerical Technique for Calculating the Transient Position of the Saltwater Front," Water Resources Res., 6, 1970.

(18) Bredehoeft, J. D. and Pinder, G. F.: "Mass Transport in Flowing Ground-Water," Water Resources, 9, 1973.

(19) Price, H. S., Cavendish, J. S., and Varga, R. S.: "Numerical Methods of Higher-Order Accuracy for Diffusion Convection Equations," Soc. Pet. Eng. Journ., September, 1968.

(20) Pinder, G. W.: "A Galerkin-Finite Element Simulation of Ground-Water Contamination on Long Island, New York," Water Resources Res., 9, 1973.

(21) Scheidegger, A. E.: "General Theory of Dispersion in Porous Media," Geophys. Res. Journ., October, 1961.

(22) Ramey, H. J., Jr.: "Wellbore Heat Transmission," Journ. Pet. Tech., 1962.

(23) Coats, K. H., George, W. D., Chu, C. and Marcum, B. E.: "Three-Dimensional Simulation of Steam-flooding," SPE Journ., December, 1974.

(24) Perry, John H.: Chemical Engineer's Handbook, Third Edition, McGraw-Hill, 1950.

(25) Lewis and Squires: "Generalized Liquid Viscosity Curve," Oil and Gas Journ., 33. 1934.

(26) Coats, K. H. and Smith, B. D.: "Dead-End Pore Volume and Dispersion in Porous Media," SPE Journ., March, 1964.

100

(27) Hooper, J. A., and Harleman, D. R. F: "Dispersion in Radial Flow from a Recharge Well," J. Geophys. Res., 72, 1967.

(28) Henry, H. R.: "Effects of Dispersion on Salt Encroachment in Coastal Aquifers," U.S. Geol. Survey Water-Supply Paper 1613-C, 1964.

(29) Carter, R. D., and Tracy, G. W.: "An Improved Method for Calculating Water Influx," TRANS AIME, 415, 1960.

(30) Avdonin, N. A.: "Some Formulas for Calculating the Temperature Field of a Stratum Subject to Thermal Injection," Neft'i Gaz, 7, No. 3, 1974.

(31) Lauwerier, H. A.: "Transport of Heat on an Oil Layer Caused by Injection of Hot Fluid," App. Sic. Res., A5, 1955.

(32) Carslow, H. S., and Jaeger, J. C.: Conduction of Heat in Solids, Oxford Univ. Press, Amen House, London (1959).

(33) Price, H. S., and Coats, K. H.: "Direct Methods in Reservoir Simulation," SPE 4278 presented at the Third SPE Symposium on Numerical Simulation of Reservoir Performance of SPE of AIME, January 11-12, 1973, Houston, Texas.

(34) Van Everdingen, A. F., and Hurst, W.: "The Application of the Laplace Transformation to Flow Problems in Reservoirs," TRANS AIME, 186, 1949.

(35) Schilthius, R. J.: "Active Oil and Reservoir Energy," TRANS AIME, 118, 1936.

APPENDIX A

DETAILS OF RESERVOIR MODEL SOLUTION TECHNIQUES

The reservoir model general finite-difference approximations were developed as Equations (6) through (8). This appendix develops and discusses the details of the method of solution.

The way we shall proceed is to expand the right-hand sides of equations (6), (7), and (8) in a consistent manner. As an example, we can illustrate using equation (11) that:

$$\delta(ab) = a^{n+1}\delta b + b^{n}\delta a \qquad \text{(A-1)}$$

is consistent or exact in the sense that it satisfies the identity

$$\delta(ab) \equiv (ab)^{n+1} - (ab)^{n}$$

Following this example, the expansions for the right-hand sides of equations (6), (7), and (8) respectively are:

$$\delta(\phi\rho) = a_1\phi^{n}\delta p + a_2\phi^{n}\delta T + a_3\phi^{n}\delta C + \rho^{n+1}\phi_0 C_r\delta p, \qquad \text{(A-2)}$$

$$\delta(\phi\rho C) = a_1\phi^{n}C^{n}\delta p + a_2\phi^{n}C^{n}\delta T + a_3\phi^{n}C^{n}\delta C + \rho^{n+1}C^{n}\phi_0 C_r\delta p + \rho^{n+1}\phi^{n+1}\delta C \qquad \text{(A-3)}$$

and

$$\delta[\phi\rho U + (1-\phi)(\rho C_p)_R T] = a_1\phi^{n}U^{n}\delta p + a_2\phi^{n}U^{n}\delta T + a_3\phi^{n}U^{n}\delta C + \rho^{n+1}\phi^{n+1}U_0 C_p\delta T + \rho^{n+1}U^{n}\phi_0 C_r\delta p + (\rho C_p)_R\delta T - \phi^{n+1}(\rho C_p)_R\delta T - T^{n}(\rho C_p)_R\phi_0 C_r\delta p. \qquad \text{(A-4)}$$

where we have assumed

$$\phi \simeq \phi_0(1 + C_r(p-p_0))$$

$$u \simeq U_0 + C_p(T-T_0)$$

In addition, we have assumed that the rock density and heat capacity are essentially constant and that the liquid density ρ is a general function of pressure, temperature, and concentration which can be expressed as:

$$\phi\rho(p,T,C) = \frac{\partial\rho}{\partial p}\Big)_{T,C} \delta p + \frac{\partial\rho}{\partial T}\Big)_{p,C} \delta T + \frac{\partial\rho}{\partial C}\Big)_{p,T} \delta C \qquad \text{(A-5)}$$

and the a_1, a_2 and a_3 in equations (A-1), (A-2) and (A-3) are partial derivatives of the liquid density with respect to pressure, temperature, and concentration, respectively. These values can be obtained from tabular or functional data of liquid density as a function of pressure, temperature, and concentration.

We can now substitute the expansions from equations (A-1), (A-2) and (A-3) into (6), (7) and (8), giving

$$\Delta[T_w(\Delta p - \rho g\Delta Z)] - q = a_1\phi^n\delta p + a_2\phi^n\delta T + a_3\phi^n\delta C + \rho^{n+1}\phi_0 C_r\delta p \qquad \text{(A-6)}$$

$$\Delta[T_w C(\Delta p - \rho g\Delta Z)] + \Delta(T_E\Delta C) - Cq = a_1\phi^n C^n\delta p + a_2\phi^n C^n\delta T + a_3\phi^n C^n\delta C + \rho^{n+1}C^n\phi_0 C_r\delta p + \rho^{n+1}\phi^{n+1}\delta C \qquad \text{(A-7)}$$

$$\Delta[T_w H(\Delta p - \rho g\Delta Z)] + \Delta(T_c\Delta T) - q_L - qC_pT = a_1\phi^n U^n\delta p + a_2\phi^n U^n\delta T + a_3\phi^n U^n\delta C + \rho^{n+1}\phi^{n+1}U_0 C_{pw}\delta T + \rho^{n+1}U^n\phi_0 C_r\delta p + (\rho C_p)_R\delta T - \phi^{n+1}(\rho C_p)_R\delta T - T^n(\rho C_p)_R\phi_0 C_r\delta p. \qquad \text{(A-8)}$$

Equations (A-6), (A-7) and (A-8) represent three equations to be solved for the three unknowns--pressure, temperature and concentration.

Because of numerical stability considerations, it is important how these equations are solved. The method which we have used here has been shown by Coats et al[23] to be very stable as well as efficient. We begin by rewriting equations (A-6), (A-7) and (A-8) as

$$C_{31}\delta C + C_{32}\delta T + C_{33}\delta p = \Delta T_w \Delta\bar{p} + (q_i + \frac{dq_i}{dp})\ \delta p - (q_o + \frac{dq_o}{dp}\delta p) \qquad \text{(A-9)}$$

$$C_{21}\delta C + C_{22}\delta T + C_{23}\delta p = \Delta HT_w \Delta\bar{p} + \Delta T_c\ \Delta T - q_L + H_i(q_i + \frac{dq_i}{dp}\ \delta p) - H(q_o + \frac{dq_o}{dp}\delta p) \qquad \text{(A-10)}$$

$$C_{11}\delta C + C_{12}\delta T + C_{13}\delta p = \Delta CT_w \Delta\bar{p} + \Delta T_E \Delta C + C_i(q_i + \frac{dq_i}{dp}\ \delta p) - C(q_o + \frac{dq_o}{dp}\delta p) \qquad \text{(A-11)}$$

where the dynamic pressure $\bar{p}$ is defined as:

$$\bar{p} \equiv p - \rho g Z \qquad \text{(A-12)}$$

A list of the definitions of the coefficients C_{ij} and residuals R_i is as follows:

$$C_{11} = a_3\phi^n C^n + \rho^{n+1}\phi^{n+1}$$
$$C_{12} = a_2\phi^n C^n$$
$$C_{13} = a_1\phi^n C^n + \rho^{n+1}\phi_o C_r C^n$$
$$C_{21} = a_3\phi^n U^n$$
$$C_{22} = a_2\phi^n U^n + \phi^{n+1}\rho^{n+1}C_p + (\rho C_p)_R(1-\phi^n)$$
$$C_{23} = a_1\phi^n U^n + \rho^{n+1}\phi_o C_r U^n - (\rho C_p)_R\phi_o C_r T^n$$
$$C_{31} = a_3\phi^n$$
$$C_{32} = a_2\phi^n$$
$$C_{33} = a_1\phi^n + \rho^{n+1}\phi_o C_r$$

$$R_1 = q_i C_i - q_o C^n + \Delta C^n T_w \Delta p^n + \Delta T_E \Delta C^n$$

$$R_2 = q_i H_i - q_o H^n + \Delta H^n T_w \Delta p^n + \Delta T_c \Delta T^n$$

$$R_3 = q_i - q_o + \Delta T_w \Delta p^n$$

Equations (A-9) through (A-11) are three equations in the three unknowns δC, δT, and δp. They can be expressed in matrix form as

$$\underline{A}\underline{X} = \underline{I}\underline{Y} + \underline{R} \qquad \text{(A-13)}$$

where a is the 3x3 matrix $[C_{ij}]$, I is the identity matrix and

$$\underline{X} = \begin{bmatrix} \delta C \\ \delta T \\ \delta p \end{bmatrix}, \quad \underline{Y} = \begin{bmatrix} \Delta(T_w C \Delta p) \\ \Delta(T_w H \Delta p) \\ \Delta(T_w \Delta p) \end{bmatrix} = \begin{bmatrix} Y_1 \\ Y_2 \\ Y_3 \end{bmatrix}, \quad \underline{R} = \begin{bmatrix} R_1 \\ R_2 \\ R_3 \end{bmatrix} . \qquad \text{(A-14)}$$

Gaussian elimination reduces equation (A-13) to the form

$$\begin{bmatrix} C_{11} & C_{12} & C_{13} \\ 0 & C_{22}' & C_{23}' \\ 0 & 0 & C_{33}' \end{bmatrix} \begin{bmatrix} \Delta C \\ \Delta T \\ \Delta p \end{bmatrix} = \begin{bmatrix} 1 & 0 & 0 \\ C_{24} & 1 & 0 \\ 1 & C_{34} & C_{35} \end{bmatrix} \begin{bmatrix} Y_1 \\ Y_2 \\ Y_3 \end{bmatrix} + \begin{bmatrix} R_1' \\ R_2' \\ R_3' \end{bmatrix} . \qquad \text{(A-15)}$$

The set of equations described by Equation (A-15) are parabolic difference equations involving pressure, temperature (or enthalpy) and concentration of the type commonly encountered in problems involving flow in porous media. To obtain an efficient method of solution and minimize the computation time, the following procedure is used:

(1) The transmissibilities, T_w, T_c and T_H are evaluated using the fluid density at the old time level, n.

(2) The coefficients (C_{11}, ----, C_{33}) appearing in the accumulation terms are updated after every iteration.

(3) The spatial derivative terms (other than the transmissibilities) are evaluated at the new time level, n+1.)

(4) The concentrations and enthalpies in the sink terms are used at the new time level, n+1.

(5) The enthalpy at n+1 is approximated as follows:

$$H^{n+1} \simeq H^{n} + (c_p)_w \, \delta T \qquad \text{(A-16)}$$

(6) The dynamic pressure at n+1 is approximated as:

$$p^{n+1} \simeq p^{n+1} - \rho^{n} g Z \qquad \text{(A-17)}$$

(7) The equations are solved for the changes in pressure, concentration and temperature over the time step by either the reduced band width direct solution described by Price and Coats[33] or a two line successive overrelaxation method.

(8) An iterative procedure is used for the solution. One iteration consists of a solution of δp, δT and δC in that order.

Iterative Procedure

The values of the concentration and temperature used in the solution of δp during the $(\ell+1)^{st}$ iteration are the concentration and temperature values available after ℓ iterations. For the solution of the temperature equation, the current pressure after $(\ell+1)$ is used along with concentration at ℓ. Finally, in the concentration update, pressure and temperature values obtained after $(\ell+1)$ iterations are used.

Therefore, the last of the equations represented by (A-15) can be written as follows:

$$C_{33}'\,\delta p^{\ell+1} = \Delta T_w \Delta \bar{p}^{\ell+1} + q_i - q_o + \left(\frac{dq_i}{dp} - \frac{dq_o}{dp}\right)\delta p^{\ell+1}$$

$$+ C_{34}\left[\Delta C^{\ell} T_w \Delta \bar{p}^{\ell+1} + \Delta T_E \Delta C^{\ell} + q_i C_i - q_o C^{\ell}\right.$$

$$\left. + \frac{dq_i}{dp} C_i \delta p - \frac{dq_o}{dp} C^{\ell} \delta p\right] + C_{35}\left[\Delta H^{\ell} T_w \Delta \bar{p}^{\ell+1}\right.$$

$$+ \Delta T_c \Delta T^{\ell} + q_i H_i - q_o H^{\ell} + \frac{dq_i}{dp}\,\delta p H_i$$

$$\left. - \frac{dq_o}{dp}\,\delta p H^{\ell}\right] \qquad \text{(A-18)}$$

$$C_{22}'\,\delta T^{\ell+1} = -C_{23}\,\delta p + \Delta H^{\ell+1} T_w \Delta \bar{p}^{\ell+1}\,\Delta T_c \Delta T^{\ell+1} + q_i H_i$$

$$- q_o H^{\ell+1} + \frac{dq_i}{dp}\,\delta p H_i - \frac{dq_o}{dp}\,\delta p H^{\ell+1} + C_{24}\left[\Delta C^{\ell} T_w \Delta \bar{p}^{\ell+1}\right.$$

$$+ \Delta T_E \Delta C^{\ell} + q_i C_i - q_o C^{\ell} + \frac{dq_i}{dp}\,\delta p C_i$$

$$\left. - \frac{dq_o}{dp}\,\delta p C^{\ell}\right] \qquad \text{(A-19)}$$

and

$$C_{11}\delta C^{\ell+1} = -C_{13}\delta p - C_{12}\delta T + \Delta C^{\ell+1} T_w \Delta \bar{p}^{\ell+1} + \Delta T_E \Delta C^{\ell+1}$$

$$+ q_i C_i - q_o C^{\ell+1} + \frac{dq_i}{dp}\,\delta p C_i - \frac{dq_o}{dp}\,\delta p C^{\ell+1} \qquad \text{(A-20)}$$

where

$$\delta p^{\ell+1} \equiv p^{\ell+1} - p^{n} \qquad \text{(A-21)}$$

$$C_{33}' = C_{33} - \frac{C_{13}C_{31}}{C_{11}} - \frac{C_{11}(C_{23}C_{11} - C_{13}C_{21})}{(C_{22}C_{11} - C_{12}C_{21})(C_{32}C_{11} - C_{12}C_{31})} \qquad \text{(A-22)}$$

$$C_{34} = -\frac{C_{31}}{C_{11}} + \frac{C_{21}}{C_{11}} \frac{(C_{32}C_{11}-C_{12}C_{31})}{(C_{22}C_{11}-C_{12}C_{21})} \quad \text{(A-23)}$$

$$C_{35} = \frac{C_{32}C_{11}-C_{12}C_{31}}{C_{22}C_{11}-C_{12}C_{21}} \quad \text{(A-24)}$$

$$C_{22}' = C_{22} - \frac{C_{12}C_{21}}{C_{11}} \quad \text{(A-25)}$$

$$C_{23}' = C_{23} - \frac{C_{13}C_{21}}{C_{11}} \quad \text{(A-26)}$$

$$C_{24} = -\frac{C_{21}}{C_{11}} \quad \text{(A-27)}$$

Expansion of some of the terms in the above equations are illustrated below:

$$\Delta T_w \Delta \bar{p}^{\ell+1} = \Delta T_w \Delta p^n + \Delta T_w \Delta \delta p^{\ell+1} - \Delta T_w \rho^n g \Delta Z \quad \text{(A-28)}$$

$$\Delta C^{\ell} T_w \Delta \bar{p}^{\ell+1} = \Delta C^n T_w \Delta \bar{p}^n + \Delta C^n T_w \Delta \delta p^{\ell+1} + \Delta \delta C^{\ell} T_w \Delta \bar{p}^n + \Delta \delta C^{\ell} T_w \Delta p^{\ell+1} \quad \text{(A-29)}$$

$$\Delta H^{\ell+1} T_w \Delta \bar{p}^{\ell+1} = \Delta H^n T_w \Delta \bar{p}^n + \Delta H^n T_w \Delta \delta p^{\ell+1} + \Delta (c_p)_w \delta T^{\ell+1} T_w \Delta \bar{p}^n + \Delta (c_p)_w \delta T^{\ell+1} T_w \Delta \delta p^{\ell+1} \quad \text{(A-30)}$$

Equations (A-18) through (A-20) are solved for $\delta p^{\ell+1}$, $\delta T^{\ell+1}$, and $\delta C^{\ell+1}$, respectively, by a reduced band width direct solution or a two line successive overrelaxation (L2SOR) method. The convergence criterion is based upon the change in density over an iteration. If the solution has converged

$$p^{n+1} = p^n + \delta p \quad \text{(A-31)}$$

and similarly for C^{n+1} and T^{n+1}.

Convergence Criteria

The concentration and temperature equations are coupled through the fluid density. The velocities calculated from the pressure solution are used in the solution of the concentration and temperature equations. If the fluid density in any grid block changes substantially due to a change in either temperature or concentration, it becomes necessary to resolve the flow equation to get a new pressure solution. These new velocities are then used to resolve the concentration and temperature equations. This procedure must be continued until the change in fluid density in every grid block is below a certain allowable tolerance.

Consider a case where the change in density over a time step due to a temperature change is small, but the change in the density due to the change in concentration is significant. In this case, there is no need to iterate over the temperature solution. This principle is used in testing the convergence on density. Separate checks are made on the change in density due to the change in temperature and concentration.

A tolerance of 0.001 (fractional) is used on the change in density during an iteration. During the first iteration, all three equations are solved, and the change in density is calculated. The solution is said to have converged if the following condition is satisfied:

$$(1)\quad \frac{\Delta\rho^T + \Delta\rho^C}{\rho_o} \leq 0.001 \qquad \text{(A-32)}$$

where $\Delta\rho^T$ = the maximum change in density in any grid block due to the change in temperature over an iteration,

and $\Delta\rho^C$ = the maximum change in density in any grid block due to the change in concentration over an iteration.

However, if condition (1) is not satisfied, the following two individual convergence tests are made:

$$(2)\quad \frac{\Delta\rho^T}{\rho_o} \leq 0.0005 \qquad \text{(A-33)}$$

$$(3)\quad \frac{\Delta\rho^C}{\rho_o} \leq 0.0005 \qquad \text{(A-34)}$$

If neither of the two above written conditions are satisfied, all three equations are resolved during the next iteration and a similar set of convergence tests are made. If condition (2) is satisfied, but not (3), the next iteration includes the pressure and concentration solutions only. These iterations are carried out until condition (3) is satisfied. After convergence is obtained, the temperature equation is solved. A similar procedure is used if condition (3) is satisfied, but not (2).

It should be noted that a constant density problem will always require only one iteration. Our experience has shown that generally three iterations or less are required for the solution even for problems with large density changes.

APPENDIX B

TREATMENT OF RESERVOIR MODEL BOUNDARY CONDITIONS

WELL SPECIFICATION

Waste may be injected at any grid block in the aquifer at any specified concentration and temperature. Generally, the total waste fluid rate would be specified as well; however, other well specifications are possible. To make the model more usable, wellbore effects can be classified in three separate parts. These are (1) the pressure drop across the sand face between the grid block containing the well and the wellbore, (2) specification at bottom-hole conditions of temperature and pressure, and (3) specification of surface conditions.

The latter part, involving specification of surface conditions, requires the wellbore model. Each of the three parts is discussed separately.

Wellbore to Grid Block Pressure Drop

Pressure drop between the grid block and the wellbore is quite important in using the model to match measured bottom-hole (or water level) pressures. Often it is impractical to refine the grid to the extent necessary that this additional pressure drop could be negligible. Thus, an external means must be used in adding on this pressure. We have used the concept of adding on the steady-state radial flow pressure drop from the average block pressure down to the wellbore pressure. This expression takes the form of

$$q = \frac{WI}{\mu} \Delta p \qquad \text{(B-1)}$$

where in radial coordinates, the overall well index can be approximated by

$$WI = \frac{2\pi k \Sigma \Delta z_k}{\ln(r_i / r_w)}$$

and in rectangular Cartesian coordinates by

$$WI = 2\pi k \Sigma \Delta z_k \left(\frac{\bar{r} - r_w}{r_w}\right) \left[\frac{1}{1-\bar{r}/r_w(1-\ln \bar{r}/r_w)}\right] \qquad ///$$

$$\text{with } \bar{r} = \sqrt{\frac{\Delta x_i \Delta y_j}{\pi}} .$$

Specifications of Bottom-hole Conditions

In this case, the wellbore pressure drop and heat losses to surrounding rock are not calculated. The model offers the following options for bottom-hole specifications:

(1) The injection (or production) rate is specified and allocated between different layers based upon the layer mobilities alone. A bottom-hole pressure necessary to achieve the desired rate is calculated, and the enthalpy of injection is based upon the injection temperature and this calculated bottom-hole pressure.

The layer mobility is related to the overall well index, WI, by:

$$M_{i,j,k} = \left(\frac{k_\ell}{\mu}\right)_{i,j,k} (WI)_{i,j} \qquad \text{(B-2)}$$

where k_ℓ is a user defined fractional allocation factor. In general, this allocation factor should be proportional to the relative layer permeability-thickness product over the total injection interval permeability-thickness. Therefore, the rate of injection into each layer, k, is:

$$q_{i,j,k} = \frac{M_{i,j,k}\, q_{i,j}}{\Sigma M_{i,j,k}} \qquad \text{(B-3)}$$

where $q_{i,j}$ is the specified rate for the entire well located in the block i,j.

(2) The specified rate is injected (or produced), and this rate is allocated between different layers based upon the layer mobility times the pressure drop between the calculated bottom-hole pressure and grid block pressure. The rate of injection into each layer can then be expressed as:

$$q_{i,j,k} = [p_{bh} + \rho_w g(h_{i,j,k} - h_{i,j,1}) - p_{i,j,k}]M_{i,j,k} \qquad \text{(B-4)}$$

Equation (B-4) can be summed over k to evaluate the bottom-hole pressure, p_{bh}:

$$p_{by} = \frac{q_{i,j}}{\Sigma M_{i,j,k}} + \left[\frac{\Sigma\{[p_{i,j,k} - \rho_w g(h_{i,j,k} - k_{i,j,l})]M_{i,j,k}\}}{\Sigma M_{i,j,k}}\right] \qquad \text{(B-5)}$$

The injection enthalpy is calculated from the injection temperature and this bottom-hole pressure. Here again, $q_{i,j}$ is the specified well rate.

(3) The specified rate is allocated between different layers as in option (2); but, to improve computational stability in the layer allocation, the rate term in the reservoir model is expressed in terms of a semi-implicit formulation. The rate in each layer can be approximated by:

$$q^{n+1}_{i,j,k} \simeq q^{n}_{i,j,k} + \frac{dq}{dp}\,\delta p_{i,j,k} \qquad \text{(B-6)}$$

where $q^{n}_{i,j,k}$ = the explicit rate of injection, see Eq. (B-5), and $\delta p_{i,j,k}$ = the change in grid block pressure over the time step.

The rate of change of q with respect to p can be calculated from Eq. (B-4) as:

$$\frac{dq}{dp} = -M_{i,j,k} \qquad \text{(B-7)}$$

This term can then be placed on the diagonal in the coefficient matrix of the reservoir model providing a portion of the rate allocated to be implicit. The explicit portion $q^{n}_{i,j,k}$ is allocated by Eq. (B-5).

(4) Under this option, both the injection rate and the bottom-hole pressure can be specified and the limiting condition will be taken. The allocation between different layers is again done on the basis of the mobilities and the pressure drop between the well pressure and the grid block pressure. A bottom-hole pressure necessary to obtain the specified rate of injection (or

production) is calculated and compared to the specified bottom-hole pressure. For an injection well, if the calculated bottom-hole pressure is greater than specified, then the rate achieved is less than the specified rate. If the reverse is true, the specified rate is achieved. For a production well, if the calculated bottom-hole pressure is less than specified, the rate will be less than specified.

Note that under this option, the rate is expressed explicitly, and it is not changed during the reservoir calculations regardless of the pressure changes in the grid blocks.

(5) This option is similar to option (B-5), except that the rate in each layer is always expressed in a semi-implicit manner according to Eq. (B-6).

Specification of Surface Conditions

When surface conditions are specified, Equations (22) through (25), the wellbore model, must be solved along with the reservoir model. This can require an iterative procedure between the wellbore model and the reservoir model.

Different options or boundary conditions are allowable to perform the wellbore calculations. These include (1) a specified rate, (2) specification of surface pressure, or (3) a specification of rate or surface pressure whichever is limiting. Each of these options is discussed in the following section.

(1) The injection (or production) rate can be specified. Consider first the case of an injection well. For an injection well, the surface temperature should also be specified. The surface pressure cannot be specified arbitrarily since the bottom-hole pressure is determined by the reservoir calculation. Once the bottom-hole pressure is calculated from the grid block pressure and the injection rate, the wellbore calculations proceed from the surface to the aquifer by assuming a value of the surface pressure and calculating the bottom-hole pressure calculated from the wellbore is not within a tolerance limit of the bottom-hole pressure necessary to inject the specified rate, the surface pressure is corrected and the wellbore calculation is repeated. Iterations continue until the desired bottom-hole pressure is obtained.

For a production well, the bottom-hole pressure necessary to produce the specified rate is calculated from the reservoir model; and since the wellbore calculations proceed from the well bottom to the top for a production well, there is no need for iteration.

(2) The surface pressure can be specified for an injection or a production well. In the case of an injection well, the bottom-hole pressure is assumed and the rate that can be injected based upon the old time step grid block pressure is calculated. This calculated rate and the specified surface pressure and temperature are then used in the wellbore calculations to calculate a bottom-hole pressure. These bottom-hole pressures are compared; and, if they are not within a tolerance, a new value of the injection rate is calculated and the wellbore calculations are repeated. Iterations continue until the calculated bottom-hole pressure and injection rate do not change significantly over the iteration.

In the case of a production well, a similar procedure is used to calculate the rate and bottom-hole pressure.

(3) An injection (or production) rate and a surface pressure can be specified. The lower value of the rate calculated from the surface pressure, or the specified rate, is then used. The iteration procedure is a combination of the ones discussed above for the first two options. We start with the specified rate and calculate the surface pressure corresponding to this rate according to the iteration procedure for option (1). For an injection well, if this surface pressure is higher than the specified pressure, a rate is calculated from the specified surface pressure as in option (2). The specified rate is used if the calculated surface pressure is lower than the specified surface pressure. A similar procedure is used for a production well.

The options available for specifying the well conditions are summarized in Table B-1.

TABLE B-1

SUMMARY OF WELL SPECIFICATION OPTIONS

Option No.	Specification	Quantities Specified	Allocation Basis	Rate	Limiting Criterion
1	Bottom-hole	Rate	Mobilities	Explicit	None
2	Bottom-hole	Rate	Mobilities and pressure drop	Explicit	None
3	Bottom-hole	Rate	Mobilities and pressure drop	Semi-Implicit	None
4	Bottom-hole	Rate and bottom-hole pressure	Mobilities and pressure drop	Explicit	Calculated or specified bottom-hole pressure whichever is limiting
5	Bottom-hole	Rate and bottom-hole pressure	Mobilities and pressure drop	Semi-Implicit	Calculated or specified bottom-hole pressure whichever is limiting
6	Surface	Rate	Mobilities	Explicit	None
7	Surface	Rate	Mobilities and pressure drop	Explicit	None
8	Surface	Rate	Mobilities and pressure drop	Semi-Implicit	None
9	Surface	Rate and surface pressure	Mobilities and pressure drop	Explicit	Calculated or specified surface pressure whichever is limiting
10	Surface	Rate and surface pressure	Mobilities and pressure drop	Semi-Implicit	Calculated or specified surface pressure whichever is limiting

AQUIFER INFLUENCE FUNCTIONS AT GRID PERIPHERY

In general, the numerical grid system selected to describe an aquifer will be smaller than the entire aquifer. The aquifer may even be infinite for all practical considerations. If there are no pressure, concentration or temperature changes observed at the edge blocks during the time span of interest, the assumption of the exterior boundaries being impermeable adequately describes the aquifer. However, if the time span of interest is large enough that calculated changes occur in the peripheral grid blocks, aquifer influence (influx or efflux) calculations should be added to the calculations.

The numerical model offers an option to specify any one of the following three aquifer influence representations:

(1) Carter-Tracy - A homogeneous infinite aquifer can be simulated rigorously through the use of a finite region and the superposition method of Van Everdingen and Hurst[34]. However, this method requires considerable computer storage; and, so instead, the approximate method of Carter. and Tracy[29] has been included in the model. Basically, this method provides a good approximation of the superposition method for treating the finite region surrounded by an infinite or finite extent aquifer. The latter's equation for cumulative influx into a circular reservoir is

$$W_{e,n+1} = W_{e,n} + \frac{B\,\Delta p^{n+1} - W_{e,n}\,p',^{n+1}}{p^{n+1} - t_{Dn}\,p^{n+1}}\Delta t_D \qquad \text{(B-8)}$$

Thus, the rate of water influx over time (t_n, t_{n+1}) is

$$e_w = K_t\,\frac{B(p^i-p^n) - B(p^{n+1}-p^n) - W_{e,n}\,p',^{n+1}}{p^{n+1} - t_{Dn}\,p',^{n+1}} \qquad \text{(B-9)}$$

or

$$e_w = a - b\,\delta p \qquad \text{(B-10)}$$

where

$$a = \frac{B\Delta p^{n} - W_{e,n}\, p',^{n+1}}{p^{n+1} - t_{Dn}\, p',^{n+1}} K_t \qquad \text{(B-11)}$$

$$b = \frac{B\, K_t}{p^{n+1} - t_{Dn} p',^{n+1}} \qquad \text{(B-12)}$$

$$\delta p = p^{n+1} - p^{n} \qquad \text{(B-13)}$$

Van Everdingen and Hurst[34] tabulate P versus dimensionless time, t_D, for both infinite and finite aquifers. The data for an infinite aquifer has been included in the model and does not require additional parameters to be specified. If the user decides to use the Carter-Tracy method for a finite aquifer, a table for P versus t_D must be specified. Eq. (B-9) or (B-10) above gives influx rate into the entire reservoir whereas we need an equation for influx into a single grid block. Consider the ideal case of a homogeneous infinite aquifer and a square N x N grid -N blocks in the x direction and N blocks in the y direction and uniform grid spacing $\Delta x = \Delta y =$ constant. The equivalent radius r_e for this grid is calculated from

$$\pi r_e^2 = (N-1)\Delta x (N-1)\Delta y \qquad \text{(B-14)}$$

and this r_e is used in B and K_t in the equation above. That is, the rectangular grid boundary is replaced for the present purposes by an "equivalent" circle. The disposal model calculates water influx into a given boundary block (i,j) from Eq. (B-11).

$$e_{w_{ij}} = q_{ij} - b_{ij}\, \delta p_{ij} \qquad \text{(B-15)}$$

where a_{ij} and b_{ij} are as defined above except that

$$B_{ij} = 2\pi h \phi c r_e^2\, s_{ij} \qquad \text{(B-16)}$$

118

and s_{ij} is the fraction of a circle assigned to edge grid block (i,j). The total perimeter of the square grid is

$$L = 4(N-1)\Delta x \qquad \text{(B-17)}$$

The value of s_{ij} is $\Delta x/L$ for all edge blocks.

For the more general cases, we calculate equivalent radius r_e from

$$\pi r_e^2 = L_x L_y \qquad \text{(B-18)}$$

where L_x and L_y are the lengths of the rectangular grid. The grid should be as square as possible to retain validity of usage of circular reservoir influence functions. The total perimeter is

$$L = 2 \sum_{j=1}^{NY} \Delta y_j + 2 \sum_{i=1}^{NX} \Delta x_i \qquad \text{(B-19)}$$

where NX, NY are the numbers of grid blocks in the x and y directions, Δx_i and Δy_j are the grid increments. The value of s_{ij} in Equation (B-16) for edge block (i,j) is then $\Delta x_i/L$ on north and south edges, $\Delta y_j/L$ for east and west edges, and $(\Delta x_i + \Delta y_j)/L$ for corner blocks.

Smaller or larger values than those defined here could be used for s_{ij} for certain edge blocks to represent aquifer heterogeneity around the periphery. However, the rigor of this variation is not apparent and should be used with caution.

(2) Pot Aquifer - The influx rate depends upon the rate of change of pressure in any peripheral block, the compressibility of the aquifer, and the total pore volume of the selected grid system. The influx rate during a time step can be expressed as:

$$e_w = W_{e,n+1} - W_{e,n} = \frac{V_1(p^n - p^{n+1})}{\Delta t} \text{ ft}^3 \text{ water/day} \qquad \text{(B-20)}$$

where V_1 is the aquifer influx coefficient in ft^3/psi.

For the case of an injection well, the pressure in the aquifer increases with time of injection. If the external boundaries of the aquifer are impermeable, all fluid injected during a time step must be retained in the aquifer, and the increase in pressure can be expressed as:

$$\bar{p}^{n+1} - \bar{p}^{n} \quad \frac{q(\Delta t)}{c_t \, V_p} \qquad \text{(B-21)}$$

where

$$c_t = \phi c_w + (1-\phi) c_r, \text{ 1/psi} \qquad \text{(B-22)}$$

V_p = total pore volume of the aquifer, ft^3

q = rate of injection, ft^3/day

Δt = time step, days

$\bar{p}^{n}$ = average pressure in the aquifer at the beginning of the time step, psi

However, the increase in pressure is much smaller if there is efflux across the external boundaries. When the efflux rate becomes equal to the rate of injection, the pressure gradient across the aquifer does not change significantly with time, and the increase in pressure in the peripheral grid blocks is very nearly the same as the increase in the average pressure. Therefore, from Eq. (B-21) and (B-22), letting $q = -e_w$, we have:

$$V_1 = c_t \, V_p \qquad \text{(B-23)}$$

The pressure distribution in a pot aquifer is also known as semi-steady state pressure distribution. The assumption of a pot aquifer implies that the pressure can increase without any bounds. As was be shown in the aquifer influence function tests, the pressures in the aquifer obtained with the coefficient V_1 evaluated from Eq. (B-23) are higher than an infinite aquifer. However, the coefficient V_1 may be estimated from the measured pressure data in the aquifer, if available.

120

The influx rate expressed by Eq. (B-20) is for the whole aquifer and a fraction α_{ij} of this total influx is associated with the boundary block ij as:

$$e_w = \alpha_{ij} V_1 (p^n - p^{n+1}) \qquad \text{(B-24)}$$

The factor α_{ij} reflects the peripheral area of block i,j as a fraction of the field perimeter and also reflects the heterogeneity around the field boundary.

(3) Schilthuis[35] Steady-State Aquifer - Schilthuis proposed the following expression for calculating cumulative water influx into an aquifer:

$$W_e(t) = V_2 \int_0^t (p^i - \bar{p})\, dt \qquad \text{(B-25)}$$

where V_2 is the aquifer influx coefficient in $ft^3/day/psi$ and $\bar{p}$ is the average pressure at the aquifer boundary at time t. The rate of influx during a time step for the block i,j can then be written as:

$$e_w = \alpha_{ij} V_2 (p^i - p^{n+1}) \qquad \text{(B-26)}$$

When the rate of efflux becomes equal to the rate of injection, the pressure distribution in the aquifer reaches a steady-state. The pressure at the exterior boundary is equal to the initial pressure, p^i. The coefficient V_2 can be calculated by applying Darcy's law at the edge blocks. As an illustration, consider a circular aquifer with the external radius of the aquifer as R_e, and the radius of the edge block center as R_N. At steady-state

$$q = \frac{2\pi kh}{\mu} \frac{(p^{n+1} - p^i)}{\ln(\frac{R_e}{R_N})} \qquad \text{(B-27)}$$

Since $q = -e_w$, we obtain

$$V_2 = - \frac{2\pi kh}{\mu \ln(R_e/R_N)} \ ft^3/psi\text{-}day \qquad \text{(B-28)}$$

Since the efflux rate will never become greater than the rate of injection, the pressure in the edge block has an upper bound which can be evaluated from Eq. (B-27).

Natural Flow in the Aquifer

The aquifer influence functions permit us to set up a natural fluid movement in the aquifer. If a uniform rate of flow exists in the aquifer before any external source of injection (or production) is superimposed, the pressure distribution in the aquifer can be initialized to be at steady-state, but with natural flow. The additional water influx rate for the Carter-Tracy approximation or the steady-state assumption due to pressure changes within the grid area can then be superimposed upon the initial reservoir velocity. The model offers an option to specify the initial pressures along the boundaries, and the initial velocities are calculated from these pressures. Alternatively, one may specify a uniform rate of flow. To keep the computations simple, we have restricted the specification of the initial velocity to be in the x direction only. The other two directions could be included at a later time if desired. The aquifer natural flow is not available for a radial system since the grid blocks are defined as annuli.

HEAT LOSS TO OVER AND UNDERBURDEN

The top and bottom planes of a three-dimensional grid will lose or gain heat by conduction to adjacent strata as formation temperature rises or falls due to injection. Discussion here is restricted to the overburden since treatment of the underlying strata is identical. The temperature in the overburden obeys the conduction equation

$$\vec{\nabla}\cdot(K_{ob}\vec{\nabla}T) = (\rho C_p)_{ob}\frac{\partial T}{\partial t} \qquad \text{(B-29)}$$

We assume that the overburden acts as a semi-infinite medium vertically. Lateral overburden boundaries (at reservoir grid boundary) are assumed closed to heat flow. The initial and boundary conditions for equation (B-29) are thus

$$T(x,y,z,0) = T_0(z)$$

$$T(x,y,0,t) = T_R(x,y,t) \qquad z = 0,\ x,y \in R$$

$$T(x,y,\infty,t) = T_0$$

$$\vec{\nabla}T\cdot\vec{n} = 0 \qquad \text{all } t,\ x,y,z \in S \qquad \text{(B-30)}$$

122

where z is measured upward from the reservoir-overburden plane R, T_0 is initial temperature, T_R is the variable reservoir temperature at z = 0, S is the overburden lateral surface boundary coinciding in x-y dimensions with the exterior reservoir boundary and η is the normal to S.

We assume uniform or constant K_{ob} and $(\rho C_p)_{ob}$ and negligible effects of heat conduction in the x and y directions. These assumptions reduce the heat loss equation (B-29) to

$$K_{ob} \frac{\partial^2 T}{\partial z^2} = (\rho C_p)_{ob} \frac{\partial T}{\partial t} \qquad \text{(B-31)}$$

This equation is represented by the standard central-difference, implicit finite-difference form over a variably-spaced grid using small Δz at the reservoir-overburden boundary and increasing Δz away from the boundary. At the end of each time step the finite-difference equation is solved using the known boundary temperature change that occurred over the time step to yield the current temperature distribution in the overburden.

At the beginning of each time step (t_n), then, we have the finite-difference equivalent of $T(x,y,z,t_n)$. The solution T to the equation is separated into two components, T_1 and T_2. T_1 satisfies Equation (B-31) and the initial and boundary conditions

$$T_1(x,y,0,t) = T(x,y,0,t_n) \quad t_n<t<t_{n+1}$$
$$T_1(x,y,z,t_n) = T(x,y,z,t_n) \qquad \text{(B-32)}$$

while T_2 satisfies equation (43) and the conditions

$$T_2(x,y,0,t) = 1 \quad t_n<t<t_{n+1}$$
$$T_2(x,y,z,t_n) = 0 \qquad \text{(B-33)}$$

The solution $T(x,y,z,t_{n+1})$ corresponding to a temperature change of δT at the boundary over the $t_n \rightarrow t_{n+1}$ time step is then the sum:

$$T(x,y,z,t_{n+1}) = T_1(x,y,z,t_{n+1}) + T_2(x,y,z,t_{n+1})\,\delta T \qquad \text{(B-34)}$$

From the finite-difference equivalent of T_1 we calculate the rate of heat loss or gain that would occur during the time step if no boundary (reservoir) temperature change occurred, q_{Ln}. The solution T_2 allows calculation of the additional heat loss rate that will occur if boundary (k=1) temperature increases by δT. Thus, the heat loss or gain rate for each reservoir grid block in the top plane of the reservoir grid is of the form

$$q_L = q_{Ln} + \alpha\delta T \qquad \text{(B-35)}$$

The one-dimensional finite-difference solution of Equation (B-29) must be performed each time step for each column of overburden--i.e. for each reservoir grid block (i,j,1) i=1, NX, j=1, NY. If NZ=1, then the heat loss or gain calculated for the overburden is simply doubled to account for heat loss or gain to the underlying strata. If NZ>1, then this one-dimensional calculation must also be performed for each grid block in the lowest plane (i,j,NZ), i=1, NX, j=1, NY.

Storage requirements for this calculation for the three-dimensional case, using six grid blocks to represent the overburden, consist of 5·NX·NY locations for temperature in the overburden and for the underlying strata. The total requirement of 10·NX·NY locations is equivalent to only two full three-dimensional arrays in a problem where NZ=5. Thus, the storage requirement is not a serious concern. The computing time requirement for this heat loss or gain calculation is insignificant--less than 3% of total computing time.

The validity of neglecting the x and y direction conduction terms was checked by comparisons of model runs with a simple conduction-convection model in the work by Coats et al[23].

A MODEL FOR CALCULATING EFFECTS OF LIQUID WASTE DISPOSAL IN DEEP SALINE AQUIFERS, PART II--DOCUMENTATION

By INTERCOMP Resource Development and Engineering, Inc.
1201 Dairy Ashford
Houston, Texas 77079

U.S. GEOLOGICAL SURVEY

Water-Resources Investigations 76-61

Sponsored by the U.S. Geological Survey,
contract number 14-08-0001-14703
U.S. Geological Survey Technical Officer: Leonard A. Wood

June 1976

125

UNITED STATES DEPARTMENT OF THE INTERIOR

Thomas S. Kleppe, Secretary

GEOLOGICAL SURVEY

V. E. McKelvey, Director

For additional information write to:

U.S. Geological Survey
National Center, Mail Stop 411
12201 Sunrise Valley Drive
Reston, Virginia 22092

126

TABLE OF CONTENTS

LIST OF ILLUSTRATIONS

LIST OF TABLES

SECTION 1

OVERVIEW OF THE DEEP WELL DISPOSAL MODEL

This model provides a realistic and efficient simulation of the dispersion of contaminated water injected into an aquifer. The model consists of two parts: (1) a wellbore model and (2) an aquifer model. The two parts are closely coupled and are used together as one complete model. The user may specify surface pressure and temperature in an injection well and the wellbore model permits calculation of the pressure and temperature changes in the wellbore. The aquifer model is a numerical finite-difference solution of three basic partial differential equations for the conservation of mass, energy and contaminant.

The velocities (or mass flow rates) are expressed in terms of spatial pressure gradients through the use of Darcy's law for flow in a porous medium, leading to a set of three coupled partial differential equations. The independent variables are the spatial coordinates and time and the dependent variables are pressure, temperature and concentration (see Appendix A). The equations are coupled through the fluid density which is a function of pressure, temperature and concentration. The model permits the user to specify initial conditions and a number of boundary conditions along the edges of the numerical grid system. In addition, the user may specify heterogeneities in the aquifer porosity, permeability and specific heat. The net dispersion of heat and mass is expressed as the sum of hydrodynamic dispersion and molecular conduction (or diffusion).

The model includes several finite-difference approximations in space and time, and two different methods of solution. This gives the user an option to select the best solution technique for the problem. The model includes the options to compare the simulated pressure, temperature or concentration values against the observed values and to obtain two-dimensional contour maps of the calculated results.

The computer programs are organized to minimize computer time and storage requirements. This documentation includes a discussion of the overall program structure, descriptions of different subroutines, input data requirements and an example problem to illustrate the use and scope of the model.

The calculations are primarily performed in English units. The use of other units and conversion factors are discussed in Section 3.1.

SECTION 2

PROGRAM DESCRIPTION

2.1 PROGRAM STRUCTURE

The program is written in FORTRAN IV source code and consists of a main routine and subroutines. The main routine primarily serves as a control program to invoke the subroutines in proper order. The program is organized to use the storage space according to the problem size. The arrays that depend upon the problem size are stored as one large array, G, in blank common. Depending upon the particular problem grid dimensions, the position of each needed dimensional array within this overall array is computed in the main program. These individual array locations are then passed to the various subroutines as arguments.

The real advantage of this approach is that only one array needs to be redimensioned in the MAIN routine depending upon the problem size. The only limitation on the problem size is available storage. This approach is very efficient particularly for Control Data machines because of an available option to dynamically reduce the storage to just that needed from a call within the program. Thus, on CDC machines, the size of the overall array containing all other arrays is computed as soon as the user defines the grid size. The location of the last word in the program is determined and added to the necessary overall array size. Then the dynamic storage reduction (or expansion) routine is called and the storage is expanded to the required size.

The above approach saves a great deal in recompilation costs if a variety of grid dimension problems are to be solved. The cost of using the dynamic allocation above is only the inclusion of a number of arguments in the call to several subroutines. In the model, five primary subroutines are called each time step. There are as many as 50-60 arguments passed in some of the routines. We have noticed little difference in running time for models written with the argument transfer and those passed by common. Thus, we believe the above arrangement does represent an overall computer saving. The well arrays require dimensioning equal to or greater than the total number of wells in the grid system. These arrays have been dimensioned as 20; and if the number of wells in the desired grid system exceeds this dimension, all the well arrays must be redimensioned. The overburden and underburden vertical block arrays must be equal to or greater than the number of overburden and underburden layers, respectively. These arrays have been dimensioned as 7. If the number of

overburden or underburden blocks exceed this dimension, these arrays must also be redimensioned. Redimensioning instructions are outlined in Section 2.4.

Storage requirement for the program is approximately $43{,}000_{10}$ words. The overall length of the G array is calculated as follows:

IG + 3 x NX x NY x NZ for the L2SOR solution

and

IG + IA + IC for the direct solution

where

NX,NY,NZ = Number of grid blocks in the x, y and z directions, respectively

$$IG = 52 \times NB + 5 \times NX + 2 \times NY + 6 \times NZ + 2 \times (NBMX-1) \times NX \times NY + 10 \times NABLMX + 5 \times NZ \times NWMAX + 12$$

$$IA = \frac{NB(2NS+1) + NS^2 - NS(2NS^2+1)/3}{2} \times 1.02$$

or 7 x NB, whichever is larger

$$IC = 6 \times (NB/2 + NZ + 1)$$

NABLMX = Maximum number of aquifer influence function blocks

NB = Total number of blocks

= NX x NY x NZ

NBMX = Larger of the overburden or underburden layers (7 in the current version)

NBMAX = Maximum number of wells (20 in the current version)

NS = Product of the two smaller dimensions

A 300 grid block problem requires an overall array dimension of about

$20{,}000_{10}$ words for the L2SOR solution technique, and

$23{,}500_{10}$ words for the ADGAUSS (direct solution).

Note that there is a substantial storage saving when the iterative LSOR technique is used instead of the reduced band width direct solution. A 1,000 grid block problem requires an array dimension of about

$65{,}000_{10}$ words for L2SOR, and

$74{,}000_{10}$ words for ADGAUSS.

Computer time requirements for the model can vary substantially depending upon whether all three equations are being solved and whether the density is relatively constant and no iteration is required. We have attempted to provide users with some time comparisons for a range of problems.

For one iteration with all three equations being solved, the approximate timing is

0.015-0.025 sec/time step/grid block.

If subsequent iterations are required to update density, the timing may increase by about 40% of the time required for the first iteration. Our experience has shown that a "hard" problem with significant density variations may require 3-4 iterations initially and decrease to one iteration for the majority of the time.

When the temperature or concentration equation can be deleted from the solution, there is an additional time saving of roughly 20% for each equation not solved. Of course, the pressure or total flow equation is always solved.

The model contains both plotting and contour mapping aids to assist the user in visualizing his results. We have chosen to provide these visual aids to the user by presentation on the line printer at execution time. Thus, the visual results are available immediately to the user instead of requiring a two step process of plotting or mapping through another off-line hardware device. To also facilitate the user getting these visual aids at a time later than execution, an option is available to edit records written on tape and plot or map them. Thus, the user may run the model on a disposal problem writing records to tape (disks) and then subsequently choose to plot or map the results at desired intervals. As an illustration, a two-dimensional aerial map of concentrations is shown in Figure 1. This map is taken from an example problem in the final report (Volume 1).

Figure 1 - Two Well Injection Concentration Contours in a Horizontal Plane After a Total Period of One Year. (The numbers in the figure correspond to the relative concentrations of injection fluid.)

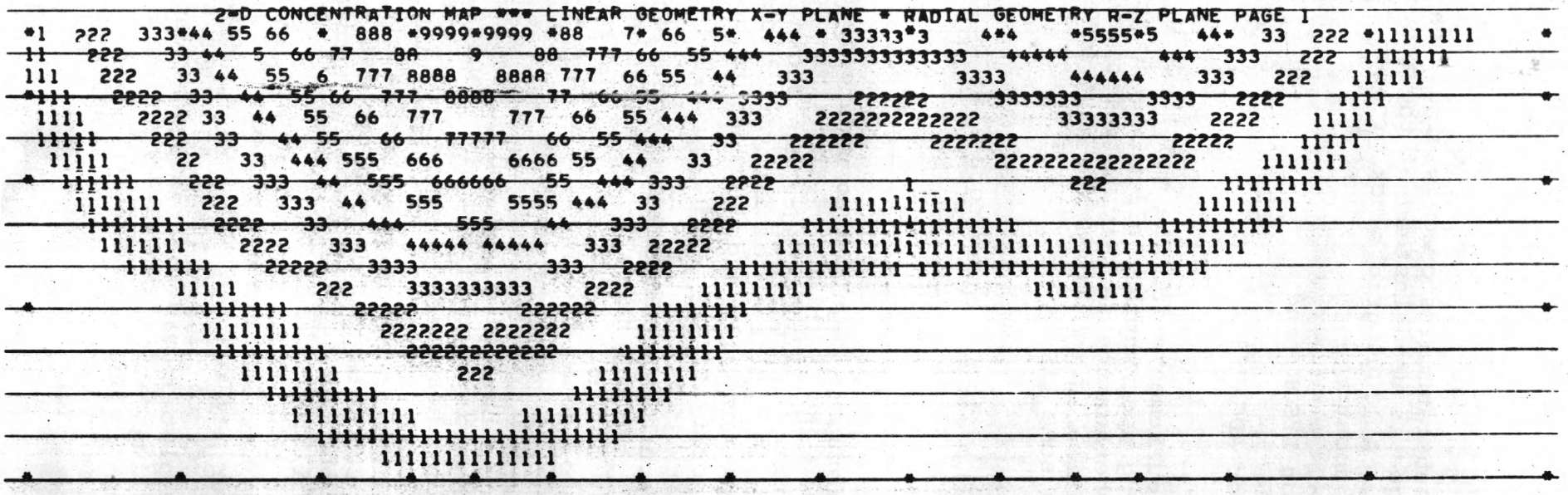

The figure shows concentration contours in an aquifer with injection from two wells. The total period of injection was one year.

The basic structure of the disposal model is shown in Figure 2. This flow chart shows the order in which different subroutines are invoked.

Three subroutines are invoked only once for each simulation. READ1 reads the aquifer description, fluid properties and other fixed data. INIT establishes initial pressure, temperature and concentration distribution according to the data furnished by the user. PRINT1 prints out the initial conditions.

Subroutine READ2 reads well data, production-injection rates and time step data. It must be invoked on the initial time step of each simulation, and may be invoked whenever changes to the well, rate, or time step data are desired.

Subroutines COEFF, PROD and ITER are the main calculation routines. They calculate transmissibilities, perform the wellbore model calculations and set up the coefficient matrices and right-hand side vector for simulating the numerical solution. The numerical solution is calculated by GAUS1D, GAUS3D or L2SOR subroutines.

Figure 2. Overall Structure of the Disposal Model with Subroutine Names and Basic Functions

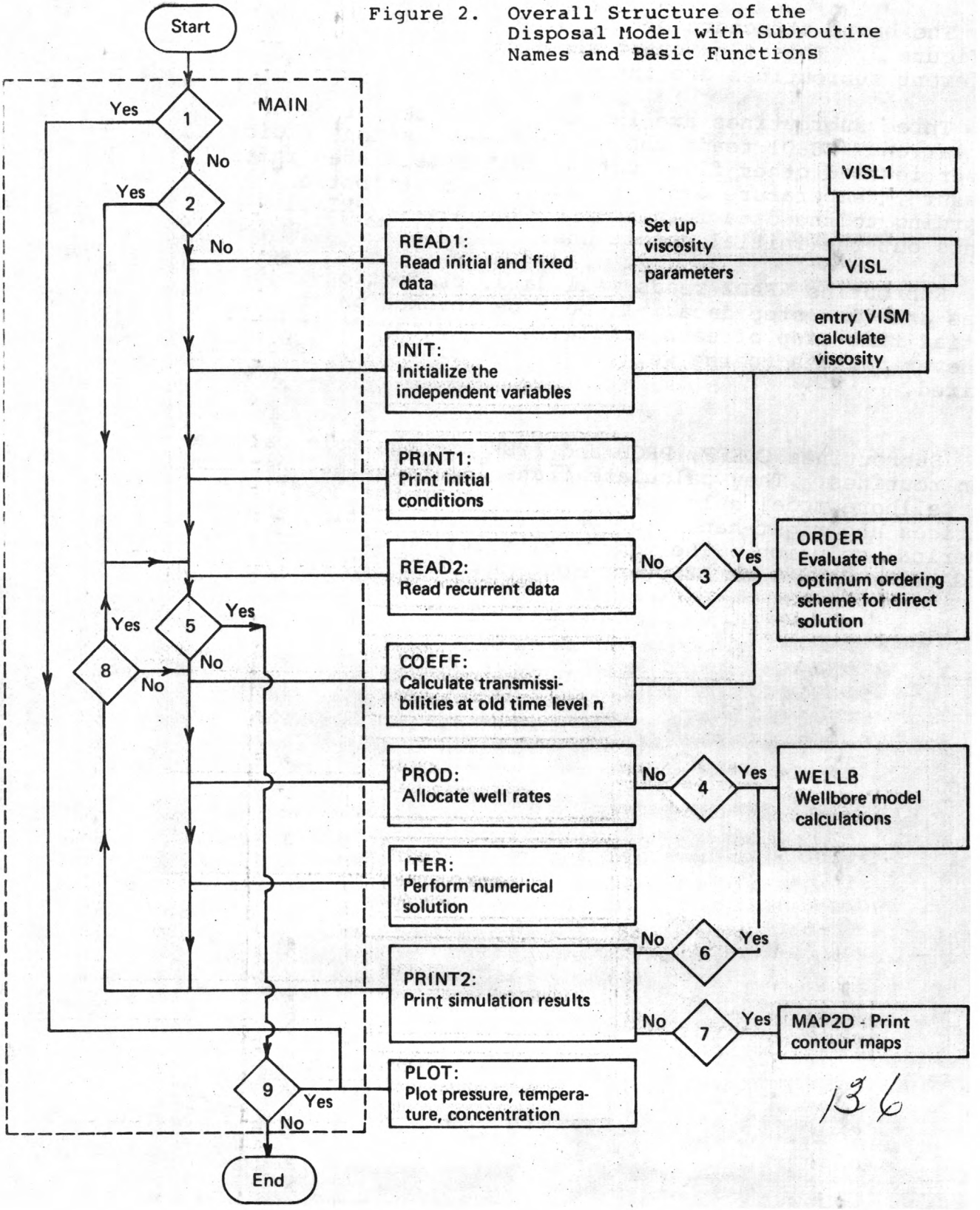

Conditions for Figure 2 are as follows:

(1) Are plots desired for a previous run?

(2) Is this a restart run?

(3) Call ORDER if it is not one-dimensional grid system and if the method of solution is reduced band width direct solution.

(4) Are wellbore calculations to be performed?

(5) Is the run to be terminated at this time step?

(6) Are wellbore calculations to be performed and is the well rate calculated semi-implicitly?

(7) Are any two-dimensional contour maps desired?

(8) Is the recurrent data read at this time step?

(9) Are any plots desired for this run?

Subroutine PRINT2 prints iteration summaries, well tables and maps at the end of each time step. MAP2D prints two-dimensional maps of pressure, temperature and concentration, and PLOT prints plots for the values of the dependent variables in the wells.

An outline of each of the subroutines is presented in the following section.

2.2 SUBROUTINES

READ1

Initial and fixed data are read in this subroutine. Pore volume and depth arrays and flow transmissibilities are set up. Thermal conduction transmissibilities in the overburden and underburden blocks are calculated, and the aquifer influence function data is read in. If the Carter-Tracy option for the aquifer influence functions has been selected and if the infinite aquifer approximation is desired, the influence coefficients are set up in this subroutine.

The subroutines VISL and VISL1 are invoked from READ1 to set up the viscosity parameters.

INIT

Pressures and concentrations in the aquifer blocks, and temperatures in the aquifer blocks and overburden-underburden blocks are initialized in this subroutine. Initial temperature gradients are permitted to exist in the vertical direction only. The temperature is read in as a function of depth and the temperature in each block is calculated based upon the depth of the grid block. A similar procedure is used for the overburden and the underburden blocks.

You may specify natural flow existing in the aquifer either by injection and production wells at the aquifer boundaries or through the use of aquifer influence functions. Under the first option, you must set the well rates and enter the well data in READ2. Under the second option, you are permitted to specify the flow velocity in the x direction only. The pressures are initialized according to the specified flow velocity.

The initial grid block values are printed in PRINT1.

READ2

Subroutine READ2 reads all recurrent data. Any part of the data entered in this subroutine can be altered at any subsequent time specified. This permits the user to change well rates, well specifications, time steps, weighting factor for finite-difference approximations and the method of solution. If the direct solution is selected as the method of solution, and if the grid system is not one-dimensional, the subroutine ORDER is invoked from READ2 to evaluate the optimum ordering scheme for the direct solution.

Before the first time step, all the data read in this subroutine must be entered. Subsequently, only the data changes need to be entered.

COEFF

Velocities and transmissibilities at time level n are calculated in this subroutine. Also, heat loss calculations are performed, and the time step is evaluated if automatic time step control is desired. The residual terms are formed from the convection and diffusion terms at time level n.

For illustration, the evaluation of the residual for the concentration equation is shown below. The net rate of convection in a block i can be written as:

$$C_{i-1/2}\, S_{i-1/2} - C_{i+1/2}\, S_{i+1/2} \qquad (2\text{-}1)$$

where S = the mass flow rate across the grid block boundary, and the subscripts (i-1/2) and (i+1/2) denote the grid block boundaries. The concentration at a block boundary is obtained by weighted averaging between the concentrations at two block centers. For example

$$C_{i-1/2} = \alpha C_{i-1} + (1-\alpha)\, C_i \qquad (2\text{-}2)$$

For a central difference approximation, $\alpha = 0.5$. For a backward difference approximation, $\alpha = 1.0$ if $u_{i-1/2} \geq 0$, and $\alpha = 0$ if $u_{i-1/2} < 0$.

Diffusion transmissibility is obtained from the "total dispersivity." Total dispersivity is the sum of the hydrodynamic dispersivity and the molecular diffusivity. The net rate of diffusion into a block can be written as:

$$T_{E_{i-1/2}}(C_{i-1}-C_i) - T_{E_{i+1/2}}(C_i-C_{i+1}) \qquad (2\text{-}3)$$

The dispersivity at the block boundary is approximated as the harmonic average of the dispersivity at the two block centers. For example, the reciprocal of dispersivity at a block edge is expressed as:

$$\frac{2}{T_{E_{i-1/2}}} = \frac{1}{\Delta x_{i-1}+\Delta x_i}\left[\frac{\Delta x_{i-1}}{T_{E_{i-1}}} + \frac{\Delta x_i}{T_{E_i}}\right] \qquad (2\text{-}4)$$

The residuals for the flow and the temperature equation are evaluated similarly.

The heat loss calculations consist of evaluation of overburden and underburden temperatures, and a coefficient to be added to the diagonal of the temperature equation matrix representing the heat loss (or gain) to the impermeable strata. These calculations are always performed implicit in time. A constant temperature boundary condition is assumed at the top of the overburden and bottom of the underburden. These boundary temperatures are calculated from the initial geothermal temperature profile.

Automatic time step control is activated if the time step is read in as zero. The user can specify maximum allowable values of pressure, temperature and concentration changes over a time step. A new value of the time step is calculated based upon the changes during the previous time step. Three values of the time step are calculated based upon the maximum changes in pressure, temperature and concentration over the previous time step. A damping factor of 0.8 is used to account for the non-linearities in the linear extrapolation of the time step. The lowest value of the calculated time step obtained from the three changes is used. If the pressure, temperature and concentration changes are smaller than the specified values, the time step is increased. The automatic time step feature is an efficient way to reduce the computation time.

PROD

This subroutine calculates the rates of injection (or production) into each layer for each well. The residual terms representing the convection and diffusion rates at time level n are incremented by the injection rates.

140

The model offers different options to specify the bottom-hole or the surface temperature and pressure conditions, allocation on the basis of mobilities or mobilities and pressure drop, and the rate term being expressed as explicit or semi-implicit in the reservoir model. The mobilities are proportional to the allocation factors which are user specified for each layer. These should be in proportion to permeability times thickness and formation damage or improvement for each layer. Only the relative values of these factors are important.

The injectivity for a layer k is expressed as follows:

$$I_k = \frac{(WI)(KHL_k)}{\sum_{i=1}^{NZ} KHL_k} \qquad (2\text{-}5)$$

where WI = well index

KHL = allocation factor for layer k.

In problems with more than one vertical layer, use of a large injectivity or productivity index can cause computational difficulty if the allocation is (INDWl=2,3) explicit and based upon mobilities and pressure drop. The rate into each layer is computed from a specified or calculated bottom-hole pressure, layer mobilities and pressure drop between the well and the grid block. A large value of mobility will result in a large allocation into that layer, and because of the large injection rate, the grid block pressure can become very close to the well pressure. This leads to a very small allocation into the layer during the next time step, and oscillation may develop from time step to time step in the allocation. This problem can be minimized or eliminated either by using a smaller time step or by simply using a smaller well index.

This problem can also be minimized by using a semi-implicit option. Under this option, the well rate is explicitly allocated on pressure at the start of the time step but an implicit pressure coefficient is retained. That is,

$$q = q^n + \frac{dq}{dp}\,\delta p \qquad (2\text{-}6)$$

where q^n is the explicit portion of production rate and δp is the change in pressure over the time step. Use of this coefficient renders the production more implicit in

pressure and stability is improved. As is obvious from the above equation, a change in pressure will result in decreasing the injection or production rate. For an injection well, the grid block pressure may increase during the time step, and the total rate of injection may drop. To overcome this problem, an iterative procedure has been set up in ITER to increase the explicit allocation such that the specified rate is achieved implicitly.

If surface conditions are specified, then the temperature and pressure changes occurring in the wellbore will also be calculated. The wellbore calculations are performed in WELLB. For an injection well, the enthalpy of injection is calculated from the temperature and pressure at the bottom of the well. The enthalpy of production is always taken as the grid block enthalpy.

WELLB

This subroutine calculates the pressure and temperature changes in the wellbores. WELLB is invoked only if you desire the wellbore calculations to be performed. The user may specify the injection or production rate, a limiting surface pressure and the surface temperature for an injection well. The surface temperature for a production well will depend upon the grid block temperature in which the well is located and the heat loss from the wellbore.

The fluid properties are permitted to vary in the wellbore. The calculations are performed over an incremental value of pressure specified by the user. The wellbore length over which the pressure change occurs and the change in temperature are calculated by an iterative procedure. The net pressure drop consists of the change in gravity head and the viscous pressure drop. For single phase flow, the frictional pressure drop is usually small. Over each increment, the first law of thermodynamics "enthalpy in-enthalpy out = change in internal energy" is applied. The temperature at any depth is calculated from the fluid enthalpy and pressure. The last increment may not be equal to the other increments and a linear extrapolation of pressure and enthalpy over the previous increment is used.

For an injection well, the temperature of injection must always be specified. If the injection rate is specified, the bottom-hole pressure is determined from the grid block pressure and the rate of injection. The surface pressure is obtained by an iterative method from the rate and the bottom-hole pressure. You may specify a limiting

surface pressure; and if the rate is determined by the limiting pressure condition, it is calculated from the surface pressure and the grid block pressure by the iterative procedure.

For a production well, if the rate is specified, the surface pressure can be obtained directly since the bottom-hole pressure and temperature are known, and the wellbore calculations have no unknown quantity proceeding from the sand face to the surface. However, if the rate is determined by a limiting surface pressure condition, an iterative procedure is required.

ITER

The numerical solution for the difference equations is obtained in this subroutine.

In a one-dimensional system, the difference equation for the dependent variable can be expressed in vector notation as:

$$\underline{\underline{A}}\ \underline{X} = \underline{R} \qquad (2\text{-}7)$$

where $\underline{X}$ is the dependent variable vector. The solution for the above equation consists of setting up the matrix A, the vector R, inverting the matrix A and operating on vector R to obtain the solution. The dependent variables in the disposal model are the changes in pressure, temperature and concentration over the time step. For a one-dimensional system, the matrix A is a tridiagonal matrix. The elements in the matrix A and the vector R are set up in subroutine ITER. Subroutine GAUS1D, GAUS3D or L2SOR can be called to obtain the solution, and a check on density is made over the iteration. An iteration consists of solving pressure, temperature and concentration equation in that order. If the maximum change in density over a grid block is below a tolerance limit, the solution is said to have converged.

The aquifer influence function calculations are performed by expressing the rate of water influx across the external boundary of the aquifer as follows:

$$e_w = a - b\delta p \qquad (2\text{-}8)$$

where the coefficients 'a' and 'b' are calculated for each peripheral block according to the aquifer influence function representation you specify. The influx rate e_w is treated as a well with semi-implicit specification. The coefficient 'a' is the explicit part of the injection rate and is added to the right-hand side of the equation,

143

and 'b' is added to the diagonal element in the matrix. Heat and contaminant influx rates are calculated explicitly, and are added on to the right-hand sides of the energy and component balance equations.

If the injection (or production) rate is allocated implicitly in a well, you may not achieve the desired rate if the pressure in the grid block changes. We have included an iterative procedure in ITER for updating the explicit parts of the well rates to achieve the specified rates. After the pressure equation has been solved during the first outer iteration, the achieved rates are compared against the specified rates. If the achieved rate is not within 5% of the specified rate, the explicit part of the rate in each layer is updated by the ratio of the specified to the achieved rate. After the explicit parts of the rates are updated, the pressure equation is solved again. A maximum of three iterations are allowed to adjust the rates.

Since the velocities may change signs with changes in the grid block pressures, it is necessary to reevaluate the weighting functions after the pressure solution. The weighting functions are used to calculate the values of the dependent variables at the grid block boundaries from the grid center values. The weighting functions are evaluated in the subroutine WTFNC. Since the pressures do not change significantly from one iteration to the next, it is assumed that the velocities do not change signs after the first iteration. Therefore, the weighting functions are not reevaluated after the first iteration.

Other subroutines called from ITER to set up the matrices and the right-hand side vectors are SCOEF, SRHA and SRHS. The coefficients C_{11}, C_{12}...etc. (see Appendix A) are evaluated in SCOEF, the right-hand side for the pressure equation is set in SRHA and the right-hand side for the energy and contaminant balance equations are set in SRHS. The off-diagonal dispersion terms are calculated at the old iterate level and added on to the right-hand sides of the temperature and concentration equations. This is done in the subroutine CRSS. A flow diagram illustrating the execution of the subroutine ITER and calling other subroutines is shown in Figure 3.

The equations are solved for changes in pressure, temperature and concentration over the time step. The total quantities are not updated until the convergence is achieved. A convergence test is made after each

144

Figure 3. Breakdown of Basic Solution Algorithm Subroutine

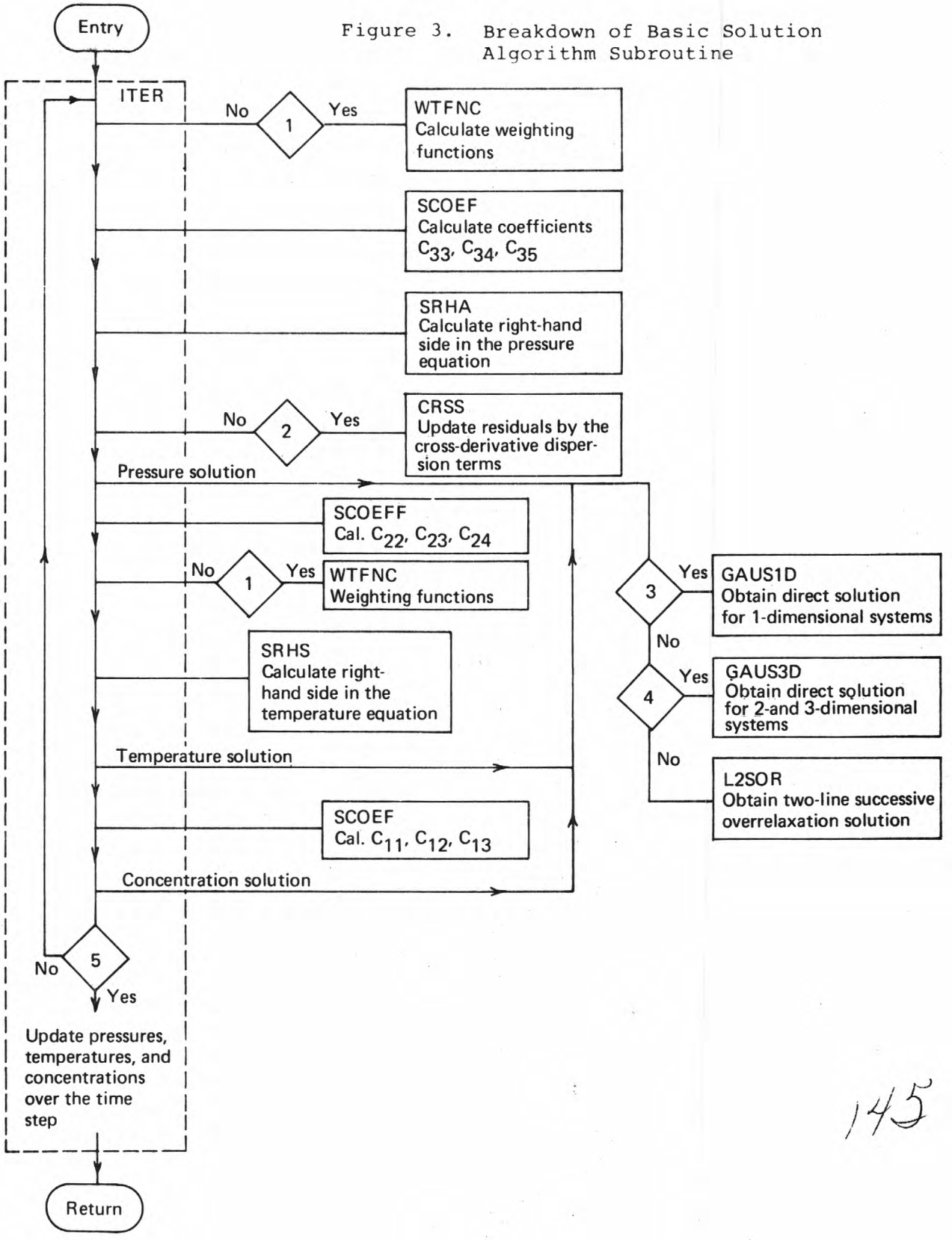

145

Conditions for Figure 3 are as follows:

(1) Is this the first iteration?

(2) Are the cross-derivative dispersion terms to be included?

(3) Is the grid block system one-dimensional?

(4) Is a direct solution desired?

(5) Has convergence been achieved?

iteration. In general, one iteration consists of solution of pressure, temperature and concentration equation in that order. However, it is not always necessary to solve all three equations. An option is provided to omit the solution of temperature and/or concentration equations. The pressure equation is always solved. The convergence criterion is the change in fluid density over an iteration. Therefore, if the maximum change in density due to a change in temperature is small, but the change in density due to a change in concentration is large enough to perform another iteration, then the energy equation is not solved during the next iteration. This procedure is carried on until convergence is reached. A similar procedure is used if the density change due to concentration change is small, but that due to temperature is large.

GAUS1D

This subroutine calculates the direct solution for one-dimensional problems. The left-hand side or the coefficient matrix is a tridiagonal matrix for one-dimensional systems. Since there is no diffusion or convection at the boundaries, a known point is available which serves as the starting point for the solution.

GAUS3D

An optimum ordering scheme developed by Price and Coats[1] is used to obtain the direct solution for two- and three-dimensional problems. This ordering scheme reduces the computer time and storage by factors as large as six and three when compared to more standard orderings and, therefore, compares favorably with two-line overrelaxation method for problems with the minimum product of two dimensions less than 50-75.

L2SOR

The two-line successive overrelaxation method is similar to a single line overrelaxation method. Instead of three diagonal terms for a single line solution, five diagonal terms are present in a double line solution. This method is generally found to be more efficient and is, therefore, included in this model. Depending upon the orientation of the optimum line, one of LSORX, LSORY or LSORZ subroutines is invoked. The program calculates optimum parameters for each equation (pressure, temperature and concentration); and therefore, a different subroutine "may" be invoked for each of the equations.

147

PLOT

This subroutine enables the user to plot (1) calculated pressure, temperature, or concentration versus time for any specified well or (2) plot comparative values of observed (measured) pressure, temperature or concentration with calculated values of the same variables as a function of time. Since the wellbore is made an integral part of the calculation, the user can compare these variables at surface and bottom-hole conditions.

This feature is especially useful during well test phases of a disposal operation. When pump tests or tracer tests are being conducted, it is particularly helpful to present a plot comparing the measured values versus the calculated values as a function of time. Then a change in permeability, porosity, dispersivity, or another variable can be made to evaluate the effect on the calculated p, T, and C.

The plotting program presents basically an x,y plot with the exception that two ordinates (observed and calculated dependent variables) are plotted versus the abscissa value (time). Two different characters are used to identify the two different ordinate values with a third character specifying coincident values. Variable spacing along the time axis is used in the plot.

MAP2D

To make the visualization of multidimensional results more comprehensible, contour maps can be prepared on the printer of pressure, temperature or concentration. These maps can be presented at any time during the calculation of the results. Since both rectangular cartesian (x,y,z) and cylindrical (r,z) coordinates can be used, maps of a cross-section or an areal plane (x,y) can be selected.

The mapping program presents a contour diagram of the dependent variable, p, T, or C, at a specified time. Up to 20 contour intervals (ranges) of the dependent variable can be described with different characters. The specific character to be mapped at each x,y point is evaluated by bilinear interpolation between the four nearest grid point values.

Arbitrary dimensions of the map width and scale can be chosen. Often it is convenient to map areal planes to scale, e.g. 1" = 100 feet in each direction. However, cross-sectional planes generally are better displayed by a distorted scale, e.g. 1" = 200 feet vertical. If

dimensions larger than a single page width or length are chosen, multiple printer pages are used with grid points specified so that superposition and alignment of the various pages is straightforward.

2.3 RESTART CAPABILITY

The program includes an optional restart feature which in many studies will reduce the total computing time and expense. By retaining intermediate results and data on magnetic tape, a problem may be interrupted and restarted at specified convenient times in the simulation run. This feature provides the ability to break a long simulation into several shorter runs and reduce the risk of wasting a large amount of computer time on a run that would be useless due to data errors or other reasons. Also, it removes the necessity of repeating the calculations for the history period for every prediction run.

The invocation of this feature is at the user's option. During history matching or for short runs it is usually more advantageous not to have to mount the restart tape. However, for the final history match run or for long simulation runs the restart feature should be used.

The procedure is set up to use two restart tapes. The unit 4 is assumed to contain the restart record, and unit 8 is written during the run to produce new restart records. The advantage of a two-tape restart is greater security. There is less chance of losing all the results of a complete run due to program, data, machine or operator error.

EXAMPLE:

Two tape restart - Assume that the input is on tape 4 and contains records from a previous run with data from time steps 5, 10, 15, 20, 25, and 30. We want to restart at time step 20 because some data were erroneously changed at the end of that step, thereby invalidating subsequent results. We want to write new restart records every 10th time step and want to continue with the data that were in effect at time step 20 (200 days) until the simulation time is 850 days.

The program will read tape 4 until it finds the record for the time step 20 on it, then will copy this one record to tape 8. Calculations resume and subsequent restart records are written on tape 8. At the end of this run, a restart record is written at time step 60. Tapes 4 and 8 contain restart records for the following time steps:

(4) 5 10 15 20 25 30

(8) 20 60

The length of a restart record is the total length of the blank common area. At the user's option, the total length can be printed out.

2.4. REDIMENSIONING THE PROGRAM

The maximum number of variables that can be transferred as arguments between different programs is limited on Control Data machines to 63. This necessitates fixed dimensioning on certain variables. The maximum number of wells, overburden and underburden layers, user specified aquifer influence functions for Carter-Tracy method, and the entries in the viscosity and temperature tables are limited only by the dimensions of the arrays with fixed dimensions. For problems that exceed the current program capacities, the program must be redimensioned and recompiled.

In the current version of the model, the simulations are subject to the following problem size limitations:

Number of wells	20
Number of overburden and underburden vertical layers	7
Number of aquifer influence functions	50
Number of entries in each of the viscosity and temperature tables	10

If you need to increase the dimensions, you should redimension the common block arrays in the following manner:

Array Names	Number of Arrays	Dimension them as:
SC, VCC	2	Number of entries in the concentration-viscosity table
TR, VISR	2	Number of entries in the temperature-viscosity table for the resident fluid
TI, VISI	2	Number of entries in the temperature-viscosity table for the injection fluid

150

ZT, TD	2	Number of entries in the depth-temperature table
PTD, TTD	2	Number of aquifer influence functions
CCOB, COB, DZOB, UOB, UUOB	5	Number of overburden layers
CCUB, CUB, DZUB, UUB, UUUB	5	Number of underburden layers
TZOB	1	Number of overburden layers +1
TZUB	1	Number of underburden layers +1
EE	1	Larger of the number of overburden and underburden layers +1
BHP through WI	31	Number of wells

If you are increasing the number of overburden or underburden blocks or the number of wells, you must also make the following changes in the main program:

Change NOBMX = 7 to number of overburden blocks or layers.

NUBMX = 7 to number of underburden blocks or layers.

NWMAX = 20 to number of wells or layer.

In actual practice, the only limitation on problem size is the core size of the machine used.

SECTION 3

APPLICATION OF THE MODEL

3.1 INPUT DATA REQUIREMENTS

This section describes the data needed to obtain as input information for using the deep well disposal model. The accuracy of simulation results depends upon the accuracy of the input data. General guidelines are presented to judge the relative importance of different parameters, minimize the numerical truncation error, and specify the numerical grid block system.

The model describes a two-component, single phase system in the absence of any chemical reactions. The two fluid components are referred to as the "resident fluid" and the "injection fluid." The two fluids may consist of entirely different chemical composition, or may represent different contaminant concentrations of the same fluid. The resident fluid refers to zero concentration and the injection fluid refers to a concentration of 1.0 (fractional). For example, the resident fluid may be "arbitrarily" taken as 2% brine solution, and the injection fluid as 20% brine solution. A concentration of 0.5 then represents 11% brine solution.

3.1.1 FLUID AND AQUIFER PROPERTIES

The physical and transport properties, in general, are expressed as functions of pressure, temperature and concentration. However, certain properties can either be assumed constant or expressed in terms of other constant properties and explicit functions of pressure, concentration and temperature. The numerical model requires, as input data, the following physical and transport properties.

(1) Compressibilities

The fluid compressibility is required in the density model to express the fluid density as a function of pressure. The fluid density is expressed as:

$$\rho(p,T,C) = \rho(p_o, T_o, 0) + \left(\frac{\partial \rho}{\partial p}\right)_{p_o,T_o,0} (p-p_o) + \left(\frac{\partial \rho}{\partial T}\right)_{p_o,T_o,0} (T-T_o) + \left(\frac{\partial \rho}{\partial C}\right)_{p_o,T_o,0} C. \quad (3\text{-}1)$$

The partial derivative of density with respect to pressure is obtained from the compressibility as follows:

$$\left(\frac{\partial \rho}{\partial p}\right)_{p_o,T_o,0} = c_w \rho(p_o,T_o,0) \qquad (3\text{-}2)$$

Therefore, the compressibility should be entered at the reference condition p_o and T_o. The reference pressure p_o is taken as the initial pressure at the top of the sand face. The reference temperature T_o is user specified and this temperature is used to calculate the fluid density and internal energy.

The model solves the equation of conservation of mass. The total mass of fluid in a grid block is simply pore volume x fluid density. The pressure effect on fluid density is included through the compressibility as discussed above. The pressure effect on pore volume is included through the rock compressibility. The dimensionless change in pore volume per unit change in pressure is the rock compressibility. The value of the rock compressibility entered should be an average value over the expected range of pressure and temperature. Units = 1/psi.

(2) Thermal Expansion Factor

This parameter is also used to calculate the fluid density (see Eq. (1)). The partial derivative of density with respect to temperature is obtained from the thermal expansion factor as follows:

$$\left(\frac{\partial \rho}{\partial T}\right)_{p_o,T_o,0} = C_T \rho(p_o,T_o,0). \qquad (3\text{-}3)$$

In general, the coefficient of thermal expansion, C_T, varies considerably with changes in pressure and temperature. If possible, the user should obtain C_T at p_o and T_o. If you expect the fluid temperature to change significantly with time, the thermal expansion factor becomes relatively more important (than compressibility) in determining the fluid density accurately. Units = 1/°F.

(3) Heat Capacities

The "total" heat capacity of the porous medium is the heat required to raise the fluid and the rock temperature per degree Fahrenheit. The total heat capacity of the porous medium per unit volume can be written as:

$$\phi(\rho C_p)_w + (1-\phi)(\rho C_p)_r \qquad (3\text{-}4)$$

153

Where ϕ is the fractional porosity, the subscripts w and r refer to the water and rock heat capacities respectively. Heat capacity, in general, is a function of temperature and pressure, but it is assumed to be constant in the aquifer model calculations. The fluid heat capacity is permitted to vary with temperature and pressure in the wellbore model calculations. The enthalpy of pure water is programmed in over the temperature range 32 - 705°F, and over the pressure range 1 - 5500 psi; and the enthalpy of the fluid in the wellbore is assumed to be proportional to the enthalpy of water. Units = Btu/lb-°F.

(4) Resident and Injection Fluid Densities

The resident and injection fluid densities must be entered at the same pressure and temperature conditions. The pressure and temperature at which the densities are available need not be the same as the aquifer conditions. Units = lb/ft^3.

(5) Resident and Injection Fluid Viscosities

The fluid viscosity is programmed as a function of fluid composition and temperature. The pressure effects are neglected. You should enter as much viscosity data as is available. You may enter the resident and injection fluid viscosities as functions of temperature, and the viscosity as a function of concentration at a reference temperature. The fluid viscosity as a function of temperature and concentration is expressed as:

$$\mu(T,c) = \mu(T_R,C) \exp \{B(C) \cdot (\frac{1}{T} - \frac{1}{T_R})\} \qquad (3\text{-}5)$$

The reference viscosity $\mu(T_R,C)$ is obtained from the viscosity-concentration data at T_R. The parameter B is obtained by linear interpolation between the B values of the resident and the injection fluid. The B values for the two fluids are obtained by a least square curve fit of Eq. (5).

If the viscosity behavior with concentration is not available, viscosity is assumed to vary with concentration as follows:

$$\mu(T,C) = [\mu(T,1)]^C \, [\mu(T,0)]^{1-C} \qquad (3\text{-}6)$$

If the viscosity dependence on temperature is not available for any fluid, generalized chart of Lewis and Squires[2] is used to extrapolate the fluid viscosity at other temperatures.

154

If you desire the fluid viscosity to be independent of temperature, you must enter the same value of viscosity at two different temperatures. Units = centipoise (cp)

$= 10^{-2}$ g/cm-sec

$= 6.72 \times 10^{-4}$ lb/ft-sec.

(6) Dispersivities

The mass and thermal dispersivities are the sums of hydrodynamic dispersivities and molecular diffusivity or conductivity. It is required to enter the hydrodynamic dispersivity factors (longitudinal and transverse) to calculate nine dispersion coefficients in the dispersivity tensor. These dispersion coefficients are evaluated at the old time level. The concentration and temperature gradients are evaluated at the new time level for all three diagonal terms. The gradients for the off-diagonal terms in the horizontal plane (E_{xy} and E_{yx}) are evaluated at the old iteration level. If convergence is reached in one iteration, and minimum iterations is one, there is no old iterate level to evaluate these terms. To offer the user an option for going back and iterating one more time to include the cross-derivative terms, we have included the off-diagonal terms in the following manner:

(a) If it is desired to include the cross-derivative terms in the horizontal plane in the simulation, the minimum number of iterations must be specified as 2 or greater.

(b) If the minimum number of iterations is entered as one, the cross-derivative terms are never calculated; but their effect is lumped together into the diagonal terms. The quantity E_{xy} evaluated at the old time level is added to E_{xx}. Similarly, E_{yx} is added to E_{yy}.

(c) The off-diagonal terms in the vertical planes (E_{xz}, E_{yz}, E_{zx}, and E_{zy}) are always lumped together with the diagonal terms to give the effective values of the dispersion terms.

The thermal conductivities should be entered for the porous media, and the molecular diffusivity should represent the net value including the effects of porosity and tortuosity. Units: Dispersivity factors = ft, Molecular diffusivity = ft^2/day.

(7) Transmission Coefficients

The velocities in the aquifer model are expressed in terms of spatial pressure gradients through the use of Darcy's law for flow in a porous medium.

$$\underline{u} = - \frac{k}{\mu} \nabla(p-\rho gh) \qquad (3\text{-}7)$$

where k = the permeability. The quantity $\frac{\mu}{k}$ represents the resistance to flow, and h = depth from a datum. The absolute pressure p can be expressed as the fluid head and, therefore,

$$\underline{u} = - \frac{k}{\mu} \nabla(\rho g h^1 - \rho gh) \qquad (3\text{-}8)$$

where

$$p \equiv \rho g h^1 \qquad (3\text{-}9)$$

or

$$\underline{u} = - \frac{k\rho g}{\mu} \nabla(h^1-h) \qquad (3\text{-}10)$$

The transmission coefficient or hydraulic conductivity is defined as

$$k = \frac{k\rho g}{\mu} \qquad (3\text{-}11)$$

The conductivity enables the expression of Darcy's law in terms of the fluid head. The permeability k is assumed to be a constant in the aquifer model, but ρ and μ are functions of temperature, concentration and pressure. Therefore, it is required to enter the conductivity at the reference conditions, viz. $T=T_o$, $C=0$ and $p=p_o$. The temperature T_o is a user specified reference temperature and p_o is the initial pressure in the grid block (1,1,1). Units = ^{o}ft/day.

The units on permeability are darcies (1 millidarcy (md) = 1.0624×10^{-11} ft^2). Permeability can be converted to hydraulic conductivity units as follows:

$$k(\text{ft/day}) = \frac{k(\text{md})\ \rho_o\ (\text{lb/ft}^3)}{\mu(\text{cp})} \times 4.4 \times 10^{-5} (\text{ft}^4\text{-cp/lb-md-day})$$

3.1.2 WELL DATA

If the wellbore calculations are not to be performed, the bottom-hole conditions must be specified. If the wellbore calculations are to be performed, specify the well head conditions and the well specifications. The user must enter the well depth, internal diameter of the tubing inside the well, outer diameter of the casing, the inner tubing roughness, and the overall heat transfer coefficient between the fluid inside the tubing and the outside surface of the casing.

The reciprocal of the overall heat transfer coefficient can be obtained by adding the individual thermal resistances. Let us consider a general case of fluid flowing inside a tubing with a static fluid in the annulus between the tubing and the casing.

The overall heat transfer coefficient U based on R_1 can be evaluated from the following expression:

$$\frac{1}{U} = \frac{1}{h} + \frac{R_1 \ln(R_2/R_1)}{K_t} + \frac{R_1 \ln(R_3/R_2)}{K_s} + \frac{R_1 \ln(R_4/R_3)}{K_c} \qquad (3\text{-}12)$$

where h = heat transfer coefficient between the injection fluid and the tubing.

K = thermal conductivity.

The subscripts t, s, and c refer to the tubing, the static fluid and the casing, respectively.

The heat transfer coefficient, h, can be calculated according to the following relation[3]:

$$\frac{2hR_1}{K_w} = 0.023\, R_e^{0.8}\, P_r^{1/3} \qquad (3\text{-}13)$$

157

where K_w = thermal conductivity of water (fluid)

R_e = Reynolds number

P_r = Prandtl number $\equiv \left(\frac{C_p \mu}{K_w}\right)$

Two options are available for allocating the rate between different layers:

(1) The injection (or production) rate is allocated between different layers based on mobilities alone.

(2) The rate is allocated on the basis of mobilities and the pressure drop between the wellbore and the grid block.

When the rate is allocated according to option (2) above, the user may elect to specify a bottom-hole or surface pressure limitation.

The mobility includes the effects of the layer thickness, permeability (or transmissivity) and skin factor. The user is required to enter the well index for each well. The well index is used to calculate the pressure drop between the wellbore and the grid block center. Using Darcy's law, we can write:

$$q = - \frac{WI}{\mu} (p - p_w) \qquad (3\text{-}14)$$

where p_w is the wellbore pressure and p is the grid block pressure. Therefore, in radial coordinates, the overall well index can be approximated by

$$WI = \frac{2\pi \Sigma k \Delta z_k}{\ln(r_{ijk}/r_w)} \qquad (3\text{-}15)$$

and in rectangular Cartesian coordinates by

$$WI = 2\pi \Sigma k z_k \left(\frac{\bar{r}-r_w}{r_w}\right) \left[\frac{1}{1-\bar{r}/r_w(1-\ln \bar{r}/r_w)}\right] \qquad (3\text{-}16)$$

with $\bar{r} = \sqrt{\frac{\Delta x_i \Delta y_j}{\pi}}$.

158

Units = ft^2/day.

3.1.3 SOLUTION TECHNIQUES

The general finite-difference equations are outlined in Appendix A. These equations outline a semi-implicit finite-difference approximation in that the dependent variables, p, T, and C, appearing in the space derivatives are expressed at the new time level. If the equations were linear, this results in a totally stable difference approximation. The equations are, however, nonlinear because in general the fluid properties are functions of the dependent variables. Additionally, the well-known problem of artificial numerical diffusion in finite differencing the first order convective terms requires special treatment.

Both the component and energy balances include at user option two choices for the finite-difference approximation to the convective terms (first order space derivatives). These choices are upstream weighting (a backward difference) or central weighting (a central difference). The option is provided to provide flexibility in reducing space truncation error. Similarly, you have an option to select the backward or central difference approximation in time. The truncation errors associated with these finite-difference approximations, and the restrictions on block size and time step are discussed in Section 3.1.5.

An iterative procedure is used for the solution. One iteration consists of a solution of the pressure, temperature and concentration equation in that order. The equations are solved for the change in the dependent variables over the time step (δp, δT, and δC). The values of the concentration and temperature used in the solution of δp during $(\ell+1)^{st}$ iteration are the concentration and temperature values available after ℓ iterations. For the solution of the temperature equation, the current pressure after $(\ell+1)$ iterations is used along with concentration at ℓ. Finally, in the concentration update, pressure and temperature values obtained after $(\ell+1)$ iterations are used. However, all the transmissibilities are evaluated using the fluid properties at the old time level n. The dispersion of heat and mass due to the off-diagonal terms are evaluated at the old "iterate" level. Thus, if the off-diagonal terms are desired to be included in the calculations, specify the minimum number of iterations as 2 or greater. If the minimum number of iterations have been specified as one, an approximation is used to enhance the diagonal terms (see Section 3.1.1).

The concentration and temperature equations are coupled through the fluid density. The velocities calculated from the pressure solution are used in the solution of the concentration and temperature equations. If the

fluid density is constant, and if the approximations for the cross-diagonal dispersion terms are considered satisfactory, there is obviously no need to iterate. Therefore, the convergence criterion is the change in density over the iteration.

A tolerance of 0.001 (fractional) is used on the change in density during an iteration. During the first iteration, all three equations are solved, and the change in density is calculated. The solution is said to have converged if the following condition is satisfied:

$$(1) \quad \frac{\Delta\rho^T + \Delta\rho^C}{\rho_o} \leq 0.001 \qquad (3\text{-}17)$$

where $\Delta\rho^T$ = the maximum change in density in any grid block due to the change in temperature over an iteration.

$\Delta\rho^C$ = the maximum change in density in any grid block due to the change in concentration over an iteration.

However, if condition (1) is not satisfied, the following two individual convergence tests are made:

$$(2) \quad \frac{\Delta\rho^T}{\rho_o} \leq 0.0005 \qquad (3\text{-}18)$$

$$(3) \quad \frac{\Delta\rho^C}{\rho_o} \leq 0.0005$$

If neither of the two above written conditions are satisfied, all three equations are resolved during the next iteration and a similar set of convergence tests are made. If condition (2) is satisfied, but not (3), the next iteration includes the pressure and concentration solutions only. These iterations are carried out until condition (3) is satisfied. After convergence is obtained, the temperature equation is solved. A similar procedure is used if condition (3) is satisfied, but not (2).

Two methods of solution have been included in the model to offer the user an option to select the most efficient method depending upon the problem. These methods are a reduced band width direct solution method (ADGAUSS) and a two line successive overrelaxation iterative method (L2SOR).

160

The model includes, on the direct solution option, an optimum ordering scheme of the alternating diagonal type. This ordering scheme was developed by Price and Coats (1973), and it reduces computing time and storage requirements by factors as large as six and three respectively when compared to more standard orderings.

A successive overrelaxation method involves solving one or more number of points explicitly and moving in space by over-correcting the values of the dependent variable at the points already solved. This procedure is carried on until the convergence is achieved. In single line successive overrelaxation, the iterative method results in solving a tridiagonal system of equations directly. In the two line method, a renumbering of the points makes this computationally more efficient. In this case, the matrix to be worked each iterate has five diagonals. Higher multiple methods could be defined, but the gain in convergence rate is usually lost by increased work per iteration and the L2SOR technique is generally the best.

You should select the method of solution depending upon the problem size. For one dimensional systems, the program internally selects the direct solution since the system of equations is only tridiagonal. For two and three dimensional systems, the nominal band width (the minimum multiple of two dimensions) should be the selection criterion. For nominal band widths of roughly 40, the ADGAUSS is equivalent to about 44 L2SOR iterations. Thus, if more than 44 iterations were required, the direct solution would be faster. Generally speaking, equivalent time is required for nominal band widths up to about 80.

If you select the L2SOR method of solution, you are required to enter the number of time steps after which a new set of iteration parameters are evaluated every time. For highly transient problems, reducing the number of these time steps could reduce the computation time, and it could be specified relatively large for conditions nearing steady-state.

3.1.4 BOUNDARY CONDITIONS

Specification of boundary conditions are the primary importance at

(1) injection or production wells,

(2) external periphery of the finite-difference grid definition, and

(3) at the juncture between the aquifer and the confining overburden and underburden.

161

The boundary conditions at the wells are described by specifying the well option. The user may specify injection or production wells at the peripheral boundaries to describe the desired boundary conditions. The user may also specify aquifer influence functions at the peripheral boundaries to simulate an aquifer larger than the finite grid system or to account for the heterogeneities existing at the aquifer boundaries. Large edge blocks can lead to error in high permeability aquifers where pressurization reaches the edge blocks. Such aquifers can be simulated by specifying a "pot" or a pseudo steady-state representation.

If it is desired to simulate an infinite or a large finite aquifer, it may not be feasible to cover the complete aquifer in the numerical grid block system. However, only a small portion of the aquifer may be needed to simulate the larger aquifer. We can estimate from Eq. (19) how far the grid system must extend to avoid exterior boundary effects:

$$r_e = 2\sqrt{kt^*/39\mu\phi c_T} \qquad (3\text{-}19)$$

where k = aquifer permeability, md

ϕ = porosity

c_T = total compressibility = $c_r + c_w$, 1/psi

μ = viscosity, cp

t^* = time span of interest, days

A grid for r_e feet external radius would act as an infinite aquifer over t^* days. If you select the grid smaller than r_e, aquifer influence function calculations for an infinite aquifer should be performed for each peripheral grid block. A rigorous superposition principle was described by Van Everdingen and Hurst[4]; but it requires considerable computer storage and the approximate method of Carter and Tracy[5] is programmed in this model. Van Everdingen and Hurst tabulate terminal rate case influence function P at dimensionless time t_D for infinite and finite aquifers. These parameters are required for Carter-Tracy calculations. The dimensionless time is defined as follows:

$$t_D = \frac{k}{\mu\phi c_T r_e^2}\, t \qquad (3\text{-}20)$$

The user may enter P versus t_D data, if available. The data for an infinite aquifer has been programmed in the

model as a default option. The rate of water influx over time t_n, t_{n+1} is given by:

$$e_w = K_t \frac{B(p^i-p^n)-B(p^{n+1}-p^n)-W_{e,n}p',n+1}{p^{n+1}-t_{Dn}\,p',n+1} \qquad (3\text{-}21)$$

where $B = 2\pi h\phi c_T r_e^2 s$

s = fraction of a circle covered by the aquifer exterior boundary

h = aquifer thickness, feet

p^i = initial pressure in the grid block, psi

p^n = grid block pressure at t_n, psi

$W_{e,n}$ = cumulative water influx at time t_n, ft^3

P' = $dP(t_D)/dt_D$

K_t = t_D/t_n

In addition to the Carter-Tracy method, the following options are included in the model:

Pot Aquifer: In this case, the influx rate during a time step is expressed as:

$$e_w = \alpha_{i,j}\, V_1 \left(\frac{p^n-p^{n+1}}{\Delta t}\right) ft^3 \text{ water/day} \qquad (3\text{-}22)$$

where the factor α_{ij} is the peripheral area of block i,j as a fraction of the field perimeter and also reflects the heterogeneity around the field boundary. The coefficient V_1 is user specified and may be calculated from the measured pressure data in the aquifer, if available. It can be calculated as follows:

$$V_1 = c_t V_p \qquad (3\text{-}23)$$

where $c_t = \phi c_w + (1-\phi)c_r$ (3-24)

V_p = total pore volume of the aquifer, ft^3

The pressure in the peripheral blocks may be kept virtually constant by specifying a large value for V_1.

Schilthuis Steady-State Aquifer: The rate of water influx during a time step for the block i,j is expressed as:

$$e_w = \alpha_{ij} V_2 (p^i - p^{n+1}) \text{ ft}^3 \text{ water/day} \quad (3\text{-}25)$$

When the rate of efflux becomes equal to the total rate of injection in the aquifer, the pressure distribution in the aquifer reaches a steady-state. The pressure at the exterior boundary is equal to the initial pressure, p^i. The coefficient V_2 can be calculated by applying Darcy's law at the edge blocks. As an illustration, consider a circular aquifer with the external radius of the aquifer as r_e, and the radius of the edge block center as r_N. At steady-state

$$q = \frac{2\pi kh}{\mu} \frac{(p^{n+1} - p^i)}{\ln (\frac{r_e}{r_N})} \quad (3\text{-}26)$$

Since $q = -e_w$, we obtain

$$V_2 = - \frac{2\pi kh}{\mu \ln (\frac{r_e}{r_N})} \text{ ft}^3/\text{psi-day} \quad (3\text{-}27)$$

For all three aquifer influx representations, the concentration and temperature outside the aquifer are assumed to be the initial concentration and temperature in the peripheral blocks. An upstream weighting is used to calculate the contaminant and heat efflux (or influx) rates. In other words, the concentration at t^n in the peripheral grid block is used for efflux calculation, and the initial concentration in the grid block is used for influx calculation.

3.1.5 SELECTION OF GRID SIZE AND TIME STEP

A backward finite-difference approximation introduces numerical diffusion, and central difference space and time approximations impose certain limitations on the grid size and time step respectively. In general, one desires to use large grid sizes and time steps to reduce the computer time and storage. Unfortunately, as is the case for desirable grid sizes, the space truncation error (numerical diffusion) can overshadow the desired

physical diffusion level. In the one-dimensional case, the space truncation error can be simply quantified as:

(1) concentration, $u\Delta x/_2$

(2) temperature, $u(\rho C_p)_w \Delta x/_2$.

These terms should be small compared to the terms E, and K, respectively. Otherwise, the backward difference space truncation error can dominate the desired physical diffusion. In the case of hydrodynamic dispersion being much larger than the molecular diffusion or conduction terms, the above restriction takes the form of

$$\frac{\Delta x}{2} << \alpha \text{ for either case above.} \qquad (3\text{-}28)$$

Since the value of α might typically be in the range of 30 to perhaps 100 feet, the above restriction can be a severe limitation. It should be noted that the above definition for dispersivity factor, α, should be divided by porosity to get the value other authors have used for the term dispersivity.

When a central difference finite-difference approximation is used, the space truncation error is no longer of second order (proportional to the second derivative). As a consequence, there is no artificial numerical diffusion term. There is, however, still a limitation on grid size. This particular limitation is caused by the tendency of the central difference result to overshoot and undershoot the minimum and maximum limits defined by the injection and resident fluid parameters. The "oscillation" in space can be eliminated if

$$\frac{u\Delta x}{2} \leq E \qquad (3\text{-}29)$$

and $u(\rho C_p)_w \Delta x/2 \leq K$.

The above restrictions are not a mandatory requirement. Good results can be obtained even when $\frac{u\Delta x}{2}$ is somewhat greater than E. However, the user may recognize that there may be concentrations which slightly exceed the injected concentration and/or slightly below the original resident fluid concentration.

Similarly, there is a time truncation error associated with the finite-difference approximation of the first order

time derivative. Because of the convective terms in both the energy and constituent equations, the time truncation error can introduce a term which has the same effect as physical diffusion. If a backward difference in time (implicit) is used, this term can be written as:

(1) concentration, $\frac{u^2 \Delta t}{2\phi}$

(2) temperature, $\frac{u^2 (\rho C_p)_w^2 \Delta t}{2[\phi(\rho C_p)_w + (1-\phi)(\rho C_p)_R]}$

We have provided the user with the option to choose the central difference in time Crank-Nicholson approximation. The Crank-Nicholson approximation is provided for both the energy and constituent equation, but not the pressure equation. This difference approximation has the advantage that it reduces time truncation error; however, it has the disadvantage of introducing a time step limitation to prevent slight oscillations. The limitation is much less severe than the forward in time explicit approximation. In fact, it is about one-half the explicit in time first order stability criterion. The explicit criteria is:

$$\frac{u\Delta t}{\phi \Delta x} + \frac{2E\Delta t}{\phi (\Delta x)^2} < 1$$

Thus, a factor of at least two larger can be used effectively with the Crank-Nicholson difference approximation.

3.2 DATA CARDS

This section defines the order of the input data and the units for each parameter. The user is referred to Section 3.1 for definitions of different physical parameters, and the execution control parameters are defined as they appear in the input statements. Each data card (or a group of data cards) is introduced in the order in which it must appear in the data deck and is assigned a reference number. The reference number also indicates the program in which the data is read:

Reference	Program
M	MAIN
R1	READ1
I	INIT
R2	READ2
P	MAIN

The program is organized to use only the actual amount of core storage required. A variable "G" in the main program is used to store all the variables that need to be dimensioned equal to the number of blocks. These variables will be referred to as full size arrays. The array "G" is stored in the blank common, and therefore, the only restriction on the number of blocks is the user specified storage on the job control card. The program is subject to a total of 20 wells, and seven overburden and underburden impermeable blocks. In actual practice, the only limitation on problem size is the core size of the machine used. The program can be easily redimensioned to the size of the actual problem.

The Fortran format associated with each input (or read) group is also noted below. For runs from initial conditions, all data described below must be prepared according to instructions. For any changes in the well rates or specifications, only the recurrent data (reference R2) should be entered. Also, the recurrent data must be entered whenever contour maps are desired or a restart record is to be written. The plotting data is entered after all the recurrent data has been read in. For a restart run, no data is read in READ1 and INIT subroutines. If you desire a plot for a previous run, all the required data is read in the main program.

A summary of all the input data cards is listed in Table 1.

TABLE I

SUMMARY OF INPUT DATA CARDS

Reference No.	Enter
M-1	Title
M-2	Control parameters
M-3	Grid system dimensions
M-4	Time at which next set of recurrent data are to be entered for a restart run.
R1-1 to R1-3	Fluid and aquifer properties
R1-4 to R1-5	Wellbore model data
R1-6	Number of entries in viscosity and temperature tables.
R1-7 to R1-10	Viscosity data
R1-11	Temperature vs depth table
R1-12	Numbers of overburden and underburden blocks
R1-13	Overburden and underburden properties
R1-14 to R1-15	Overburden and underburden blocks dimensions
R1-16	Initial pressure at a reference depth
R1-17 to R1-19	Grid block dimensions for a linear geometry aquifer
R1-20	Transmissivity and porosity data for a linear geometry, homogeneous aquifer.
R1-21	Heterogeneous aquifer data
R1-22	Radial geometry aquifer dimensions
R1-23	Radial geometry aquifer properties
R1-24 to R1-25	Data for dividing a radial geometry aquifer into regions of constant logr.

R1-26	Aquifer description (transmissibilities, pore volume, depth and thickness) modification data.
R1-27	Selection of aquifer influence function representation
R1-28	Aquifer influence coefficients for pot and steady-state aquifer representations.
R1-29	Control parameters for Carter-Tracy aquifer representation
R1-30	Aquifer influence coefficients for Carter-Tracy aquifer representation
R1-31	Average or "effective" aquifer properties for Carter-Tracy calculations
R1-32	User specified aquifer influence functions
R1-33	Modification of aquifer influence coefficients
I-1	Control parameters for initializing concentrations and natural flow
I-2	Initial concentrations
I-3	Resident aquifer fluid velocity
R2-1	Control parameters for entering recurrent data
R2-2	Solution technique
R2-3	Wellbore calculation iteration parameters
R2-4	Number of wells
R2-5 & R2-6	Well rates
R2-7	Well description
R2-8	Surface pressures at the wellbores
R2-9	Numerical solution iteration parameters
R2-10	Time step data

R2-11	Output control parameters
R2-12 to R2-15	Contour maps data
P-1	Number of wells for which plots are desired
P-2 to P-4	Data for plots

READ M1 (20A4/20A4)

LIST: TITLE

TITLE — Two cards of alphabetic data to serve as a title for this run. Any title up to 160 characters (80/card) in length may be used.

READ M-2 (8I5)

LIST: NCALL, RSTRT, ISURF, IPDIM, IIPRT, NPLP, NPLT, NPLC

NCALL — Control parameter for solving the basic partial differential equations. If you desire to simulate a solution of all three equations, enter zero. The pressure equation is always solved. The solutions of the temperature and concentration equations may be bypassed, if desired.

0 - All three equations will be solved.

-2 - The concentration equation will not be solved. The simulated solution will consist of solving a set of two coupled equations only (pressure and temperature).

1 - Only the pressure equation will be solved. The model is simplified to solving one independent partial differential equation.

2 - The temperature equation will not be solved.

RSTRT — The number of the time step at which calculations are to resume for a restart run. A restart record from a previous simulation run corresponding to the specified time step must exist on the restart tape mounted on Tape Unit Number 4.

For a nonrestart run, i.e., a run from initial conditions, read RSTRT as zero.

ISURF — Control parameter for wellbore calculations.

- 0 - No wellbore calculations will be performed. This means only rates or bottom-hole pressures may be specified.
- 1 - Wellbore calculations will be performed.

IPDIM — Blank common printing key. The total length of the blank common may be printed. This is useful in writing restart records. The length of the blank common is the storage space required on the tape every time a restart record is written.

- 0 - Blank common length is not printed.
- 1 - Blank common length is printed.

IIPRT — Transmissibilities printing key.

- 0 - No transmissibility output is activated.
- 1 - All transmissibilities calculated at old time level n are printed.

NPLP — Control parameter for plotting pressures in the wells.

- 1 - Bottom-hole and surface pressures are plotted if wellbore calculations are performed. Only the bottom-hole pressures are plotted if no wellbore calculations are performed. For an observation well, the bottom-hole pressure is the grid block pressure.
- 0 - If no pressure plots are desired.
- -1 - If pressure plots are desired for a previous run. Skip READ M-3 through R2-15, and proceed to READ P-1.

NPLT — Control parameter for plotting temperatures in the well.

1 - For an observation well, the grid block temperature is plotted. For an injection well, the bottom-hole temperature is plotted if wellbore calculations are performed. For a production well, the bottom-hole temperature is always plotted In addition, the surface temperature is plotted if the wellbore calculations are performed.

0 - If no temperature plots are desired.

-1 - If temperature plots are desired for a previous run. Skip READ M-3 through R2-15, and proceed to READ P-1.

NPLC — Control parameter for plotting concentration in the well.

1 - The concentration in the well is plotted for observation and production wells only.

0 - If no concentration plots are desired.

-1 - If concentration plots are desired for a previous run. Skip READ M-3, through R2-15 and proceed to READ P-1.

NOTE: Proceed to READ P-1 if any of NPL's are negative.

READ M-3 (8I5)

NOTE: Read this card only if RSTRT is zero. If RSTRT is non-zero, skip this card and proceed to READ M-4.

This data will be used to dimension all full size arrays (equal to total number of blocks) for the program as well as many other arrays. Because of the use of this method, very little dimensioning of input parameters and computational arrays is required throughout the remainder of the program.

LIST: NX, NY, NZ, HTG, KOUT, PRT, NABLMX, METHOD

NX — Number of grid cells in the x direction (greater than or equal to 2).

NY — Number of grid cells in the y direction (greater than or equal to 1).

NZ — Number of grid cells in the z direction (greater than or equal to 1).

HTG — Control parameter for input of reservoir description data. If you desire to specify a heterogeneous aquifer, you may either enter HTG=2 and enter data for each block, or specify a homogeneous linear or radial geometry aquifer and modify the blocks or regions in which heterogeneity is desired.

1 - Homogeneous aquifer, linear geometry.

2 - Heterogeneous aquifer, read data for each grid block, linear geometry.

3 - Radial geometry. The aquifer may be heterogeneous in the vertical direction.

KOUT — Output control.

0 - All program output activated.

1 - All program output except initial arrays (concentrations, pressures, etc.) are activated.

3 - No program output is activated. KOUT is read again in recurrent data READ R2-11. A value of KOUT here of 3 can be used to omit printing of all initialization data as is sometimes desirable in making a sequence of many history matching runs.

PRT — Output array orientation control.

-1 - Print output maps as areal layers (x-y). Block numbers in the x-direction increase from left to right and decrease down the computer page in the y-direction.

+1 - Print out is similar to above except that J-block numbers increase down the computer page.

2 - Print output maps as vertical sections (x-z).

NABLMX — Maximum number of aquifer influence function blocks. This data is used for dimensioning the aquifer influence function arrays. This number is equal to the number of peripheral blocks.

METHOD — The method of solution that you will use for the current run. The method of solution entered here is used to dimension the working arrays in numerical solution subroutines (direct solution or L2SOR). The method to be used is read again in READ R2-2. Since the amount of storage required for direct solution is always larger than for L2SOR, you may specify direct solution on this card and may actually use L2SOR, but you may not specify L2SOR on this card and use direct solution.

0, ±1 - Allocate storage for direct solution. You may specify direct solution or L2SOR in READ R2-2. The dimension of a working array "A" is printed out at this point. If you specify direct solution again in READ R2-2, the minimum length required for the array "A" will be printed. This length must be smaller than the dimension of array "A". If it is not, you must use the L2SOR method.

±2 - Allocate storage for L2SOR method. You may not specify direct solution in READ R2-2.

READ M-4 (F10.0)

NOTE: This card is read only if the run is a restart, i.e. only if the value read for RSTRT is non-zero.

LIST: TMCHG

TMCHG — Time in days at which the next set of recurrent data is to be read. If TMCHG is less than or equal to the time corresponding to the restart time step number, a set of recurrent data will be read immediately to resume the previous simulation.

175

NOTE: Proceed to READ NO. R2-1 if RSTRT is non-zero.

READ R1-1 (5E10.0)

LIST: CW, CR, CTW, CPW, CPR

CW	Compressibility of the aquifer fluid, $(psi)^{-1}$.
CR	Compressibility of rock, $(psi)^{-1}$.
CTW	Coefficient of thermal expansion of the aquifer fluid, $(°F)^{-1}$.
CPW	The fluid heat capacity, Btu/lb-°F.
CPR	The rock heat capacity per unit volume, Btu/ft^3-°F.

READ R1-2 (7E10.0)

LIST: UKTX, UKTY, UKTZ, CONV, ALPHL, ALPHT, DMEFF

UKTX	Thermal conductivity of the porous medium in the x direction (Btu/ft-°F day-see CONV).
UKTY	Thermal conductivity of the porous medium in the y direction.
UKTZ	Thermal conductivity of the porous medium in the z direction.
CONV	Conversion factor for the thermal conductivities. The entered values of the thermal conductivities are multiplied by CONV to obtain Btu/ft-day-°F units. If entered as zero, thermal conductivities should be read in Btu/ft-day-°F.
ALPHL	Longitudinal dispersivity factor, ft.
ALPHT	Transverse dispersivity factor, ft.
DMEFF	Molecular diffusivity in the porous media, ft^2/day.

176

READ R1-3 (4E10.0)

The fluid densities are entered here at concentration = 0 (natural aquifer fluid) and concentration = 1 (injection fluid). Both the densities must be entered at the same reference temperature and pressure.

LIST: PBWR, TBWR, BWRN, BWRI

PBWR	Reference pressure at which the densities are to be entered, psi.
TBWR	Reference temperature at which the densities are to be entered, °F.
BWRN	The density of the natural aquifer fluid (concentration = 0) at PBWR and TBWR, lb/ft^3.
BWRI	The density of the injection fluid (concentration = 1) at PBWR and TBWR, lb/ft^3.

READ R1-4 (I5)

NOTE: If ISURF = 0, omit READ R1-4 and R1-5 and proceed to R1-6.

LIST: NOUT

NOUT — Output control parameter for wellbore calculations.

- 0 No output is activated.
- 1 Iteration summary (number of outer iterations, flow rate and the bottom-hole pressure) is printed for each well.
- 2 The well pressure and temperature (at the surface for an injection well and at the bottom-hole for a production well) and the flow rate are printed every time subroutine WELLB is called.
- 3 The pressure and temperature in the well are printed over each increment (see DELPW in READ R1-5).

READ R1-5 (3E10.0)

LIST: PBASE, DELPW, TDIS

PBASE	Atmospheric or reference pressure at the wellheads, psi. This is used to convert absolute pressure to gauge pressure.
DELPW	Incremental value of pressure over which wellbore calculations are to be performed. The pressure and temperature calculations in the wellbores proceed in increments. The length increment corresponding to DELPW is calculated, and the temperature change over each increment is evaluated.
TDIS	Thermal diffusivity of the rock surrounding the wellbores, ft^2/hr.

READ R1-6 (4I5)

The number of entries in the viscosity and temperature tables are entered here. You should enter as much viscosity data as is available. You are required to enter at least one viscosity point for the resident fluid (conc. = 0) and one for the injection fluid (conc. = 1). These reference viscosity points should preferably be at the middle of the expected temperature range; and if possible, both the reference viscosities should be entered at the same temperature. If only one viscosity point is available, the program obtains viscosity at other temperatures according to Lewis and Squires' generalized chart.[2] If you desire to enter a constant viscosity for any of the two fluids, you must enter one more viscosity point in addition to the reference viscosity. For example, if you desire to enter constant viscosity of 0.9 cp for the injection fluid, enter NTVI=1, the reference viscosity of the injection fluid VISIR=0.9 and VISI(1)=0.9.

The temperature table describes the initial temperatures existing in the aquifer.

NOTE: Number of entries in the viscosity tables refer to the viscosity values to be entered in addition to the reference viscosities.

LIST: NCV, NTVR, NTVI, NDT

NCV	Number of entries in the concentration-viscosity table. This table is for viscosities <u>other</u> than at the reference

temperature TRR. The table should contain the viscosities of the fluid mixture at concentrations other than 0 and 1, since these two values are entered as reference viscosities. If only the two pure fluid viscosities are available, enter zero and read in the viscosities of the pure fluids as reference viscosities.

NTVR — Number of entries in the temperature-viscosity table for the aquifer resident fluid.

NTVI — Number of entries in the temperature-viscosity table for the injection fluid.

NDT — Number of entries in the depth versus temperature table.

READ R1-7 (4E10.0)

LIST: TRR, VISRR, TIR, VISIR

The reference viscosities of the injection and the resident fluids are to be entered here.

TRR — Reference temperature for the resident viscosity fluid, °F.

VISRR — Viscosity of the resident fluid at the reference temperature TRR, cp.

TIR — Reference temperature for the injection fluid viscosity, °F. If possible, this temperature should be taken equal to TRR.

VISIR — Viscosity of the injection fluid at TIR, cp.

READ R1-8 (8F10.0)

NOTE: If NCV=0, omit R1-8.

LIST: SC(I), VCC(I), I=1, NCV

SC — Concentration, fraction.

VCC — Viscosity (cp) of a fluid mixture at concentration SC, and temperature TRR.

179

READ R1-9 (8F10.0)

NOTE: If NTVR=0, skip R1-9 and proceed to READ R1-10.

LIST: TR(I), VISR(I), I=1, NTVR

TR	Temperature, °F
VISR	Viscosity (cp) of the resident fluid at the temperature TR. Do not re-enter the reference viscosity at TRR.

READ R1-10 (8F10.0)

NOTE: If NTVI=0, skip R1-10 and proceed to R1-11.

LIST: TI(I), VISI(I), I=1, NTVI

TI	Temperature, °F.
VISI	Viscosity (cp) of the injection fluid at the temperature TI. Do not enter the reference viscosity at TIR.

READ R1-11 (2F10.0)

Initial temperatures in the aquifer and the overburden-underburden blocks are to be entered here. The initial temperature is assumed to be a function of depth only.

LIST: ZT(I), TD(I), I=1, NDT

ZT	Depth, ft.
TD	Temperature, °F.

READ R1-12 (2I5)

LIST: NZOB, NZUB

NZOB	Number of overburden blocks. If NZOB $\leq$ 2, overburden heat loss calculations are not performed.
NZUB	Number of underburden blocks. If you desire the underburden heat loss calculations to be performed, a value of 3 or greater should be entered. If the number of aquifer blocks (NZ) is equal to one, the underburden heat loss is assumed to be equal to the overburden heat loss.

180

READ R1-13 (4E10.0)

LIST: KOB, CPOB, KUB, CPUB

KOB, KUB	Vertical thermal conductivities of the overburden and the underburden blocks, respectively. These conductivities should also be entered in the same units as in READ R1-2.
CPOB, CPUB	Overburden and underburden heat capacities per unit volume, Btu/ft^3-°F.

READ R1-14 (7E10.0)

NOTE: Skip this READ if NZOB=0.

DZOB	Thickness of each overburden block. The first overburden block is at the upper edge of the aquifer. The overburden block numbers increase as you go away from the aquifer.

READ R1-15 (7E10.0)

NOTE: Skip this READ if NZUB=0.

LIST: DZUB(k), k=1, NZUB

DZUB	Thickness of each underburden block. The block numbers increase as you go away from the aquifer.

READ R1-16 (4E10.0)

LIST: TO, PINIT, HINIT, HDATUM

TO	A standard temperature (°F) for calculating fluid density. Fluid density at any other temperature is calculated as the sum of the density at TO and the deviation from it.
PINIT	Initial pressure at the reference depth HINIT, psi.
HINIT	Reference depth for setting up initial conditions, ft. HINIT can be any depth within the reservoir.

HDATUM — A datum depth (ft) for printing the dynamic pressures ($p - \rho gh$). The depth h is measured from the datum depth HDATUM.

READ R1-17 (7E10.0)

NOTE: If HTG=3 (radial geometry), skip to READ R1-22.

LIST: DELX(I), I=1, NX

DELX — Length of each row of blocks in the x direction, ft.

READ R1-18 (7E10.0)

LIST: DELY(J), J=1, NY

DELY — Length of each row of blocks in the y direction, ft.

READ R1-19 (7E10.0)

LIST: DELZ(k), k=1, NZ

DELZ — Thickness of each vertical layer, ft.

If you use the "homogeneous" aquifer option (HTG=1 in READ M-3) then the reservoir is treated as a rectangular parallelepiped and the grid defined by the DELX, DELY, DELZ values are the cell dimensions in the parallelepiped. The x-y plane of the grid is horizontal only if SINX and SINY of READ R1-20 are both zero. Similarly, the z-axis in this case points downward only if SINX and SINY are both zero. DELX and DELY are measured along the x-y plane and DELZ is perpendicular to the x-y plane.

If you use the "heterogeneous" aquifer option (HTG=2 in READ M-3) then the x-y plane is a horizontal plane placed over the aquifer structure. The x-axis should be aligned with the longer dimension of the aquifer and should be as "parallel" as possible with this longer dimension.

READ R1-20 (7E10.0)

NOTE: These data are read only if HTG=1, and by themselves describe a homogeneous reservoir. Heterogeneity may be introduced by using either READ R1-21 instead of R1-20 or by regional modifications in READ R1-26.

182

LIST: KX, KY, KZ, PHI, SINX, SINY, DEPTH

KX	Hydraulic conductivity in x direction, ft/day. This quantity represents the fluid velocity obtained by a potential gradient of unity (ft. of water/ft) of the aquifer fluid at concentration zero and temperature, TO. In terms of permeability, this quantity is $(k\rho_o g/\mu_o)$. The parameters ρ_o and μ_o are the density and the viscosity of the aquifer fluid at concentration zero and temperature, TO.
KY	Hydraulic conductivity in y direction, ft/day.
KZ	Hydraulic conductivity, ft/day.
PHI	Porosity (fraction).
SINX	Sine of the reservoir dip angle along the x-axis.
SINY	Sine of the reservoir dip angle along the y-axis.
DEPTH	Depth from arbitrary reference plane (e.g. sea level) to top of grid block (1,1,1), feet.

READ R1-21 (3I3, 1X, 7E10.0)

NOTE: These data are read only if HTG=2.

LIST: I, J, K, KX, KY, KZ, PHI, UH, UTH, UCPR

I,J,K	Grid block indices.
KX	x direction hydraulic conductivity for flow, ft/day.
KY	y direction conductivity for flow, ft/day.
KZ	z direction conductivity for flow, ft/day.
PHI	Porosity, fraction.
UH	Depth (feet) measured positively downward from reference plane to top of the cell.

183

UTH — Grid block thickness in the vertical direction, feet. If the layer thickness is equal to DELZ(K) read in under READ R1-19, UTH may be entered as zero.

UCPR — Heat capacity of the rock per unit volume, Btu/ft^3-°F. If the rock heat capacity is equal to CPR (READ R1-1), UCPR may be entered as zero.

You must read one card for each non-zero pore volume grid block. Cards need not be included for zero pore volume blocks within the grid. Follow the last card with a blank card.

READ R1-22 (7E10.0)

NOTE: Skip to READ R1-26 if HTG is not equal to 3.

These data are read for a radial geometry aquifer with only one well. The well is located at the center of the numerical grid block system. The grid blocks are divided on an equal Δlogr basis, i.e. r_i/r_{i-1} is constant. If you desire to use regions of equal Δlogr instead of a constant value of Δlogr throughout the aquifer, you should specify the number of blocks in each region (READ R1-24) and the boundaries between the regions (READ R1-25).

LIST: RWW, R1, RE, DEPTH

RWW — Well radius, feet.

R1 — The first grid block center, feet.

RE — External radius of the aquifer, feet.

DEPTH — Depth from a reference plane to the top of the aquifer, feet.

READ R1-23 (5E10.0)

LIST: DELZ(K), KYY(K), KZZ(K), POROS(K), CPR1(K), k=1, NZ

DELZ — Layer thickness in the vertical direction, feet.

KYY — Horizontal hydraulic conductivity, ft/day.

KZZ — Vertical hydraulic conductivity, ft/day.

POROS — Porosity, fraction.

CPR1 — Rock heat capacity, Btu/ft^3-°F. If the rock heat capacity in the layer is equal to CPR (READ R1-1), CPR1 may be entered as zero.

You must punch one card for each vertical layer.

READ R1-24 (5I5)

NOTE: These data are read for obtaining regions of equal Δlogr. If you desire a constant value of Δlogr throughout the aquifer, insert a blank card and proceed to READ R1-26.

LIST: NXR(I), I=1,5

NXR — Number of grid blocks in each constant Δlogr region. You may specify as many as five regions. The total number of grid blocks in different regions can not exceed NX. The number of blocks in the outermost region need not be specified. For example, if you desire a total of 25 radial grid blocks and three regions of 5, 10 and 10 grid blocks, then enter NX=25 (READ M-3) and NXR's may be entered as 5, 10, 0, 0, 0 or as 5, 10, 10, 0, 0.

READ R1-25 (4E10.0)

NOTE: If NXR(1) > 0, this card is required.

LIST: RER(I), I=1,5

RER — Radii of the boundaries between different regions, feet. As an example, if the external radius of the aquifer is 5,000 ft. and you desire five grid blocks in the first 1000 ft., 10 grid blocks from 1,000 to 2,500 ft., and 10 blocks from 2,500 to 5,000 ft. and if you entered NXR's as 5 and 10 (and the rest zeroes), you should enter RER's as 1,000 ft. and 2,500 ft. only (the rest as zeroes). Alternatively, if NXR's were specified as 5, 10 and 10, then RER's should be entered as 1,000, 2,500 and 5,000.

READ R1-26 (LIST 1 - 6I5, LIST 2 - 6E10.0)

NOTE: Read as many sets of these data as necessary to describe all the reservoir description modifications desired. Follow the last set with a blank card, which the program recognizes as the end of this data set. Even if no regional modifications are desired, the blank card must nevertheless be included.

LIST 1: I1, I2, J1, J2, K1, K2

LIST 2: FTX, FTY, FTZ, FPV, HADD, THADD

I1, I2	Lower and upper limits inclusive, on the I-coordinate of the region to be modified.
J1, J2	Lower and upper limits inclusive on the J-coordinate of the region to be modified.
K1, K2	Lower and upper limits inclusive on the K-coordinates of the region to be modified.
FTX	If positive or zero, this is the factor by which the x direction transmissibilities within the defined region are to be multiplied. If negative, the absolute value of FTX will be used for the x direction transmissibilities within the region to be modified, replacing the values read earlier or determined from the permeability data read earlier.
FTY	This has the same function of FTX, but applies to the y direction transmissibilities.
FTZ	This has the same function FTX, but applies to the vertical transmissibilities.
FPV	This has the same function as FTX, but applies to the pore volumes.
HADD	This is an increment that will be added to the depths within the defined region. A positive value repositions the cell deeper, and a negative value brings it closer to the surface.

THADD — This is an increment that will be added to the thickness values within the defined region. A positive value makes the cell thicker and a negative value makes it thinner.

This data modification feature of the program provides the user with an easy way to build in reservoir heterogeneities or modify the reservoir description data during history matching. These modifications are applicable regardless of whether the data were read according to READ R1-20, R1-21 or R1-23.

The modifiers in LIST 2 above are independent in that a change effected by any one of them does not affect any of the other properties. For example, an FPV of 1.4 will increase pore volumes by 40%, but will not result in any changes in transmissibilities, depth or thickness.

The data modifications occur over rectangular regions areally as defined by the I1, I2, J1, and J2 limits. The vertical extent of the region is defined by K1 and K2. All six of these limits must be within the limits of the calculation grid. Successive regions may partially or entirely overlap other regions.

In regions in which more than one modification has been made to a parameter subject to additive modifications, the order of the modifications has no effect and the final net adjustment is simply the algebraic sum of all the additive factors that apply to the region. For the transmissibility and pore volume modifications, the order of multiple changes does not affect the final result if all the modifiers are multiplicative (positive). However, if some or all of the modifications are replacement values (negative) the order of input may affect the final result. For example, consider the following two situations in which the same modification data are applied in different orders to an original value and the final result is different.

	CASE 1	CASE 2
Original Value	100	100
Modification and Result	.50(50)	-70.(70.)
Modification and Result	-70.(70.)	.50(35.)
Modification and Result	.20(14.)	.20(7.)

The program will accept a zero modifier as a valid parameter. Therefore, if no changes are desired to data that are affected by multiplicative factors (FTX, FTY, FTZ, FPV) read the corresponding factor as 1.0, not zero. Zero additive factors (HADD and THADD) result in no changes to the depth and thickness values.

A modification to the transmissibilities over the region (I1-I2, J1-J2, K1-K2) will not affect the transmissibilities between columns I2 and I2+1, between rows J2 and J2+1 or between layers K2 and K2+1.

READ R1-27 (2I5)

NOTE: If the aquifer influence functions are zero, insert a blank card and proceed to READ I-1.

LIST: IAQ, PRTAB

IAQ — Control parameter for selecting the type of aquifer block representation.

- 0 - No aquifer influence blocks are to be used. Skip to READ I-1.
- 1 - A pot aquifer representation will be used.
- 2 - A steady-state aquifer representation will be used.
- 3 - Use the Carter-Tracy representation.

PRTAB — Print control key for the aquifer influx coefficient.

- 0 - No printing of aquifer influx coefficients will be activated.
- 1 - The locations and values of the aquifer influx coefficients will be printed.

NOTE: Aquifer influence blocks are defined as those cells in the model that communicate directly with an aquifer that is not itself modeled as part of the calculation grid, but whose effects are introduced through the aquifer terms read here. This feature can be used to introduce water influx (or efflux) from an edge

or bottom water drive without the expense that would be required to model the aquifer as part of the grid system.

READ R1-28 (LIST 1 - 6I5, LIST 2 - E10.0)

NOTE: These data are read only if IAQ is 1 or 2, meaning the pot or steady-state aquifer has been selected. If IAQ is 3, omit this READ and proceed to READ R1-30.

LIST 1: I1, I2, J1, J2, K1, K2

LIST 2: VAB

I1, I2	Lower and upper limits, inclusive, on the I-coordinate of the aquifer influx region.
J1, J2	Lower and upper limits, inclusive, on the J-coordinate of the region.
K1, K2	Lower and upper limits, inclusive, on the K-coordinate of the region.
VAB	Aquifer influence coefficient for each block within the region defined by I1, I2, etc. The units of VAB are ft^3/psi for a pot aquifer representation, and ft^3/psi-day for a steady-state representation.

NOTE: Follow the last VAB card of this data group by a blank card.

The READ group consists of two cards or any number of sets of two cards, each set defining a rectangular region and the value of VAB to be assigned that region. Overlapping of regions is permissible. The order of the sets is immaterial except that any overlapping will result in the VAB of the last set read to be assigned to the overlapped subregion. If these data are read, i.e. IAQ=1 or 2, then skip READ R1-29 through R1-32 and proceed to READ R1-33.

READ R1-29 (3I5)

NOTE: If IAQ is not equal to 3, omit these data and proceed to READ R1-33. This section is used to enter data for the Carter-Tracy method of calculating aquifer influence functions.

LIST: NCALC, NPT, PRTIF

NCALC — Control parameter for selecting how the Carter-Tracy aquifer coefficients are to be assigned.

0 - The Carter-Tracy aquifer coefficients (VAB) will be read in as input data.

1 - The VAB will be calculated by the program and assigned to each edge (perimeter) block in each areal plane, K = 1, 2, ...NZ.

2 - The VAB will be calculated by the program and assigned to each grid block in the last areal plane, K = NZ only.

NPT — Number of points in the influence function versus dimensionless time table, ($P(t_D)$ versus t_D). If NPT is zero, the program will select the Hurst-Van Everdingen infinite aquifer solution internally.

PRTIF — Print control key for the influence function table.

0 - Suppress printing.

1 - Print the table of $P(t_D)$ versus t_D.

READ R1-30 (LIST 1 - 6I5, LIST 2 - E10.0)

NOTE: Enter these data only if NCALC is zero; otherwise, skip this READ and proceed to READ R1-31.

LIST 1: I1, I2, J1, J2, K1, K2

LIST 2: VAB

I1, I2 — Lower and upper limits, inclusive, on the I-coordinate of the aquifer influence region.

J1, J2 — Lower and upper limits, inclusive, on the J-coordinate of the region.

190

K1, K2 — Lower and upper limits, inclusive, on the K-coordinate of the region.

VAB — Aquifer influence coefficient for each block within the region defined by I1, I2, etc. The aquifer influence coefficient VAB for the Carter-Tracy method is actually the fraction of the total aquifer-reservoir boundary that is represented by the length of any given grid block. For this reason it is possible to calculate the VAB from input data previously read in and the VAB does not have to be calculated externally.

NOTE: Follow the last VAB card of this data group by a blank card.

The READ group consists of two cards or any number of sets of two cards, each set defining a rectangular region and the value of VAB To be assigned that region. Overlapping of regions is permissible. The order of the sets is immaterial except that any overlapping will result in the VAB of the last set read to be assigned to the overlapped subregion.

READ R1-31 (4E10.0)

LIST: KH, PHIH, RAQ, THETAQ

KH — Conductivity-thickness for aquifer, ft^2/day. An average value of transmissivity along the edges should be used.

PHIH — Porosity-thickness for aquifer, ft.

RAQ — Equivalent aquifer radius, ft. The approximate method of Carter and Tracy is valid for circular aquifers. To retain the validity of usage of circular reservoir influence functions, the numerical grid system should be chosen as square as possible.

THETA — Angle of influence, degrees. This angle should indicate the portion of the aquifer covered by the aquifer influence boundary. If mass flow is permitted across all the boundaries, enter 360°.

191

READ R1-32 (2F10.0)

NOTE: This data is entered if NPT is not equal to zero. If NPT is zero, the program will select the aquifer influence functions for an infinite aquifer, and you do not have to read in the influence function data. Omit this READ and proceed to READ R1-33.

LIST: TD(I), PTD(I), I=1, NPT

TD — Dimensionless time, $kt/\mu\phi c_T r_e^2$.

PTD — Terminal rate case influence function as given by Van Everdingen and Hurst.

READ R1-33 (LIST 1 - 6I5, LIST 2 - E10.0)

LIST 1: I1, I2, J1, J2, K1, K2

LIST 2: FAB

NOTE: These data allow the user to modify the aquifer influx coefficient VAB by the relation

VAB(I,J,K) = VAB(I,J,K) x FAB

This is useful when a reservoir may experience no or limited water influx across one boundary. In this case, in the region where influx is limited, the FAB may be set to zero or a small number to reduce the VAB along the boundary.

I1, I2 — Lower and upper limits, inclusive, on the I-coordinate of the VAB to be modified.

J1, J2 — Similar definition for the J-coordinate.

K1, K2 — Similar definition for the K-coordinate.

FAB — Factor by which the VAB will be modified in the region I=I1, I2, J=J1, J2 and K=K1, K2.

NOTE: Follow these data with one blank card. If no modifications are desired, one blank card is still required.

READ I-1 (2I5)

NOTE: These data are read for initializing concentrations and natural flow in the aquifer. If the initial concentrations are zero everywhere in the aquifer and there is no natural flow, insert a blank card and proceed to READ R2-1.

LIST: ICOMP, INAT

ICOMP — Control parameter for initializing the concentrations.

- 0 - Initial concentrations in all the grid blocks are zero. If you enter zero, skip READ I-2.
- 1 - The initial concentrations are not zero everywhere. Non-zero concentrations will be entered in READ I-2.

INAT — Control parameter for entering natural fluid velocity.

- 0 - The aquifer fluid is static initially. If you enter zero, skip READ I-3.
- 1 - The resident fluid velocity will be entered in READ I-3.

READ I-2 (6I5, F10.0)

NOTE: Skip this READ if ICOMP is zero.

LIST: I1, I2, J1, J2, K1, K2, CINIT

I1, I2 — Lower and upper limits, inclusive, on the I-coordinate of the non-zero concentration region.

J1, J2 — Lower and upper limits, inclusive, on the J-coordinate of the non-zero concentration region.

K1, K2 — Lower and upper limits, inclusive, on the K-coordinate of the non-zero concentration region.

CINIT — Initial concentration in each of the blocks within the region defined by I1, I2, etc., dimensionless.

NOTE: Read as many of these cards as necessary to describe the concentrations everywhere in the aquifer. You need to specify only the non-zero concentrations. Follow the last card with a blank card.

READ I-3 (F10.0)

NOTE: If INAT=0, skip this card.

LIST: VEL

VEL — Initial velocity of the resident aquifer fluid in the x direction, ft/day. The initial velocities in the y and z directions are assumed to be zero.

RECURRENT DATA

The data described previously are required to describe the aquifer and fluid properties and to establish initial conditions. These data are all read before the first time step, and at subsequent time steps when you desire to change the well conditions, time step data or mapping specifications. Note that any of the data entered up to this point cannot be changed. The overburden and underburden blocks specifications or aquifer influence functions cannot be changed in any manner once they have been specified at the beginning.

READ R2-1 (7I5)

LIST: INDQ, IWELL, IMETH, ITHRU, IPROD, IOPT, INDT

INDQ — Control parameter for reading well rates.

0 - Do not read well rates.

1 - Read well rates on one card (READ R2-5). The user must enter all well rates under this option.

2 - Read one card for each well rate (READ R2-6).

IWELL — Control parameter for reading well definition data.

0 - Do not read well data.

1 - Read new or altered well data.

194

IMETH Control parameter for reading method of solution.

0 - Do not read method of solution. If you are entering data before the first time step (new run), and you enter IMETH=0, the program selects direct solution backward with time and space finite-difference approximations. The solution, under these conditions is unconditionally stable.

1 - Read new or altered method of solution.

ITHRU Run termination control.

0 - Run is to continue.

1 - Run is to terminate at this point. No more recurrent data will be read after this card. If you do not desire any plots, i.e. NPLP, NPLT and NPLC are all zero, this should be the last card in your data deck.

IPROD Control parameter for reading wellbore data.

0 - Do not read wellhead data.

1 - Read new or altered wellhead data.

IOPT Control parameter for reading wellbore iteration data.

0 - Do not read wellbore iterations data. If it is a new run and you desire the wellbore calculations to be performed, default values of the iteration parameters will be used for wellbore calculations.

1 - Read new or altered wellbore iteration data.

INDT Control parameter for reading reservoir solution iteration data.

0 - Do not read iteration data. If you are entering data before the first time step, default values of the iteration parameters will be used.

1 - Read new or altered iteration data.

READ R2-2 (I5,F10.0)

NOTE: This data is entered if IMETH is not equal to zero. If it is a new run and IMETH is equal to zero, the program selects METHOD=1 and WTFAC=1.0 (direct solution with backward space and time approximations.

LIST: METHOD, WTFAC

METHOD — Method of solution. If you enter zero, the program selects METHOD=1. You may select direct solution only if you specified direct solution in READ M-3.

1 - Reduced band width direct solution with backward finite-difference approximation in time.

2 - Two line successive overrelaxation (L2SOR) solution with backward finite-difference approximation in time.

-1 - Reduced band width direct solution with Crank-Nicholson approximation in time.

-2 - Two line successive overrelaxation solution with Crank-Nicholson approximation in time.

WTFAC — Weight factor for finite-difference approximation in space.

1.0 - Backward difference.

0.5 - Central difference.

If you enter WTFAC $\leq$ 0, the program selects WTFAC = 1.0.

READ R2-3 (I5, 4F10.0)

NOTE: This data is entered if IOPT is greater than zero. If you intend to use the default values, insert a

blank card and proceed to READ R2-4. The default values of the parameters are discussed below.

LIST: NITQ, TOLX, DOLDP, DAMPX, EPS

NITQ	Maximum number of outer iterations in the wellbore calculations. For example, if the injection rate for a well is specified, the wellhead pressure is calculated iteratively to obtain the bottom-hole pressure necessary to inject the specified rate. If entered as zero or a negative number, the program selects the default value of 20.
TOLX	The tolerance on the fractional change in pressure over an iteration. If entered as zero or a negative number, the default value of 0.001 is selected.
TOL DP	The tolerance on pressure, psi. The default value is 1 psi.
DAMPX	Damping factor in estimating the next value of the pressure (surface for an injection well and bottom-hole for a production well). If the frictional pressure drop in the well is high, a linear extrapolation may lead to oscillations around the right value. The default value is 2.0.
EPS	The tolerance on calculating temperature from given values of enthalpy and pressure. The fluid temperatures in the wellbore are calculated over each pressure increment as specified in READ R1-3. The default value is 0.001.

READ R2-4 (I5)

NOTE: If INDQ is equal to zero, skip READ R2-4 through R2-6 and proceed to R2-7.

LIST: NWT

NWT	Total number of wells.

READ R2-5 (7E10.0)

NOTE: Enter this data only if INDQ is equal to one.

LIST: Q(I), I=1, NWT

Q	Production rate, ft^3/day. If it is an injection well, enter the value as a negative production rate. You must enter all the well rates even if all of them have not changed.

READ R2-6 (I5, E10.0)

NOTE: Enter this data only if INDQ is equal to two. Read as many cards as necessary to describe all the injection and production well rates. Follow the last card with a blank card.

LIST: I, QWELL

I	Well number.
QWELL	Production rate, ft^3/day. Enter negative values for injection rates. You need to enter only the altered well rates.

READ R2-7 (LIST 1 - 6I5, LIST 2 and 4 - 7E10.0, LIST 3 - 8E10.0)

NOTE: This data is entered for IWELL equal to one. Read one set of data for each well and follow the last card with a blank card.

LIST 1: I, IIW, IJW, IIC1, IIC2, IINDW1

I	Well number.
IIW	I-coordinate of grid cell containing the well.
IJW	J-coordinate of grid cell containing the cell.
IIC1	Uppermost layer in which the well is completed.
IIC2	Lowermost layer in which the well is completed.
IINDW1	Well specification option.

198

1 - Specified rate is allocated between layers on the basis of mobilities alone.

±2 - Specified rate is allocated between layers on the basis of mobilities and the pressure drop between the wellbore and the grid block.

±3 - An injection or production rate is calculated from the specified bottom-hole or surface pressure. The lower of the specified and the calculated rate is allocated between layers on the basis of mobilities and the pressure drop between the wellbore and the grid block.

2,3 - The rate is expressed explicitly in the aquifer model equations.

-2,-3 - The rate is expressed in a semi-implicit manner in the aquifer model equations, e.g.

$$q^{n+1} = q^n + \frac{dq}{dp}\,(p^{n+1} - p^n)$$

LIST 2: WI, BHP, TINJ, CINJ

WI	Well index, ft^2/day.
BHP	Bottom-hole pressure, psi. This must be specified if IINDW1 = ±3.
TINJ	Temperature of the injection fluid, °F. If surface conditions are being specified, it is the temperature at the surface.
CINJ	Contaminant concentration in the injection fluid, dimensionless.

LIST 3: X, DW, ED, OD, TTOPW, TBOTW, UCOEF, THETA

NOTE: Skip this list if ISURF = 0.

X	Pipe (wellbore) length to top of perforations, feet.
DW	Inside wellbore (pipe) diameter, feet.
ED	Pipe roughness (inside), feet. Enter zero if it is a smooth pipe.
OD	Outside wellbore (casing) diameter, feet.
TTOP	Rock temperature surrounding the wellbore at the surface, °F.
TBOTW	Rock temperature surrounding the wellbore at the bottom-hole, °F.
UCOEF	Overall heat transfer coefficient between the inner surface of the pipe and outer surface of the casing, Btu/ft^2-°F-hr.
THETA	Angle of the wellbore with the vertical plane, degrees.

LIST 4: KHL(K), K = IC1, IC2

NOTE: Skip this READ if the well is completed in only one layer, i.e. IIC1 = IIC2.

KHL(K) Layer allocation factors for Well I. These should be in proportion to total productivity of individual layers, taking into account layer kh (absolute transmissivity x thickness) and layer formation damage or improvement (skin). Only the relative values of these factors are important. For example, if layers 3 through 6 (IC1=3, IC2=6) are completed then KHL values of .5, 2, 2.5, .1 will give the same result as values of 5, 20, 25, 1. The absolute productivity (injectivity) of completion layer k is computed as

$$WI \times KHL(k+1-IC1) \Big/ \sum_{\ell=1}^{\ell=IC2-IC1+1} KHL_{\ell}$$

READ R2-8 (7E10.0)

280

NOTE: Skip this READ if IPROD is zero.

LIST: THP(I), I=1, NWT

THP — Tubing hole or the surface pressure for each well, psi. If ISURF is one, THP must be specified for the wells with well option IINDW1=±3. A production (or injection) rate is calculated from THP, and lower of the calculated and specified rate is used for allocation between layers.

READ R2-9 (3I5)

NOTE: This data is entered if INDT is not zero. If you desire to use the default values for the data entered on this card, enter INDT as zero and skip this READ. However, if you desire to include the off-diagonal (or cross derivative) dispersion terms in the x-y plane (E_{xy} and E_{yx}), MINITN must be entered greater than or equal to 2. If MINITN is entered as one, or if the default value is used, an approximation is used to include the effect of the off-diagonal dispersion terms by enhancing the diagonal terms.

LIST: MINITN, MAXITN, IMPG

MINITN — Minimum number of outer iterations in the subroutine ITER (see Section 2.2 for explanation). The default value has been programmed as one.

MAXITN — Maximum number of outer iterations in the subroutine ITER. The default value is 5.

IMPG — Number of time steps after which the optimum parameters for the inner iterations are recalculated for the two line successive overrelaxation method. You do not have to enter this data if METHOD is not equal to ±2. The default value for IMPG is 5.

READ R2-10 (7E10.0)

LIST: TCHG, DT, DSMX, DPMX, DTPMX, DTMAX, DTMIN

TCHG — Time (days) at which next set of recurrent data will be read. The restart records can be written at TCHG only. Also, the mapping subroutine can be activated at TCHG only.

201

DT	Time step specification. If DT is positive it will be the time step (days) used from the current time to TCHG. If DT is zero, the program will select the time step automatically. DT must not be zero for the first time step of a run starting from zero time.
DSMX	Maximum (over grid) concentration change desired per time step.
DPMX	Maximum (over grid) pressure change desired per time step, psi.
DTPMX	Maximum (over grid) temperature change desired per time step, °F.
DTMAX	Maximum time step allowed (days).
DTMIN	Minimum time step required (days).

If any of the five parameters above is entered as zero, the default value is used. These values are as follows:

DSMX = 0.25

DPMX = 50.0 psi

DTPMX = 10.0 °F

DTMAX = 30.0 days

DTMIN = 1.0 day

These parameters are used only if DT equals zero. The time step DT must not be read as zero for the first time step. If DT is read as zero, the program will automatically increase or decrease the time step size every time step to seek a value such that the maximum changes in the concentration, pressure and temperature are less than or equal to the specified values.

READ R2-11 (9I5)

LIST: IO1, IO2, IO3, IO4, IO8, RSTWR, MAP, KOUT, MDAT

The program prints four types of output at the end of each time step. The parameters IO1, IO2, IO3 and IO4 control the frequency of the outputs.

IO1 — Control parameter for frequency of the time step summary output. The time step summary (7 lines) gives cumulative field injections and productions, material and heat balances, average aquifer pressure, cumulative heat loss to the overburden and the underburden, cumulative water, contaminant and heat influxes across the peripheral boundaries, and the maximum pressure, concentration and temperature changes in any block during the time step.

IO2 — Control parameter for frequency of the well summary output. This summary gives water, heat and contaminant fluid production and injection rates, cumulative production and injection, wellhead and bottom-hole pressures, wellhead and bottom-hole temperatures and the grid block pressure in which the well is located. This summary also gives the total production and injection rates and cumulative production and injection.

IO3 — Control parameter for listings of the grid block values of concentration, temperature and pressure.

IO4 — Control parameter for injection/production rate in each layer for each well.

The following values apply to all four of the above parameters:

-1 — Omit printing for all time steps from the current time through to TCHG, inclusive.

0 — Print at the end of each time step through to the step ending at TCHG.

1 — Print only at time TCHG.

n(>1) — Print at the end of every n^{th} time step and at the time TCHG.

IO8 — Control parameter for listings of the grid block values of the dependent variables. The listings are printed according to the frequency specified (IO3). This parameter gives you the option for not printing the tables you do not desire. The parameter requires a three digit specification and the first digit refers to pressure, the second to temperature and the third to concentration.

203

READ R2-12 (I5, 2F10.0)

NOTE: Enter this data only if you desire contour maps (MAP is not equal to 000), and if MDAT is equal to one.

LIST: NORIEN, XLGTH, YLGTH

NORIEN — Map orientation factor.

0 - The map is oriented with x (refers to r for radial geometry) increasing from left to right and y (z for radial geometry) increasing up the computer page, i.e. the x=0, y=0 point is the lower left hand corner.

1 - The map is oriented with x increasing from left to right and y increasing down the computer page. The origin is the upper left hand corner.

XLGTH — The length, in inches, on the computer output which is desired in the x (or r) direction.

YLGTH — The length, in inches, on the computer output which is desired in the y (or z for radial geometry) direction.

READ R2-13 (6I5, 2F10.0)

NOTE: Enter this data only if pressure contour maps are desired, and if MDAT equals one. These entries refer to pressure mapping only.

LIST: IP1, IP2, JP1, JP2, KP1, KP2, AMAXP, AMINP

IP1, IP2 — Lower and upper limits, inclusive, on the I-coordinate of the region to be mapped.

JP1, JP2 — Lower and upper limits, inclusive, on the J-coordinate of the region to be mapped.

KP1, KP2 — Lower and upper limits, inclusive, on the K-coordinate of the region to be mapped. For a linear system, you will get (KP2 - KP1 +1) aereal maps.

0 - The grid block values will be printed.

1 - The grid block values (pressure at datum or temperature or concentration) will not be printed.

2 - Refers to the first digit only. Neither the absolute pressure nor the pressure at datum will be printed.

e.g. If you desire only temperature grid block values, enter 201.

RSTWR — Restart record control parameter.

0 - No restart record will be written.

1 - Restart record will be written on Tape 8 at time TCHG.

MAP — Parameter for printing contour maps at time TCHG. Only two-dimensional maps are printed. The maps are printed for r-z coordinates in a radial system and x-y coordinates (aereal maps) in a linear system. This parameter requires a three digit specification, the first digit referring to mapping pressures, the second for mapping temperatures and the third for concentrations.

0 - The variable will not be mapped.

1 - The variable will be mapped at TCHG.

E.g. If you desire the contour maps for pressure and temperature only, enter 110.

KOUT — See READ M-3.

MDAT — Control parameter for entering the mapping specifications.

0 - The mapping specifications are not to be changed.

1 - Read new mapping specifications. If you are activating the printing of contour maps for the first time during the current run, MDAT must be entered as one.

AMINP, AMAXP — The minimum and maximum value of the pressure (psi) used to obtain 20 contour maps. If the pressure in any grid block is higher than AMAXP, it will be indicated as AMAXP, and similarly a pressure lower than AMINP is printed as AMINP. If you enter AMAXP as zero or a negative value, the program will search for a maxima and use the value as AMAXP. If you enter AMINP as a large negative number (≤ -99.0), the program will search for a minima and use the value as AMINP.

READ R2-14 (6I5, 2F10.0)

NOTE: This READ refers to temperature contour maps. Enter this data only if temperature maps are desired, and if MDAT equals one.

LIST: IT1, IT2, JT1, JT2, KT1, KT2, AMAXT, AMINT

The user is referred to READ R2-13 for definition of these parameters. This card refers to temperature mapping only as opposed to pressure mapping for R2-13.

READ R2-15 (6I5, 2F10.0)

NOTE: This READ refers to concentration contour maps. Enter this data only if concentration maps are desired, and if MDAT equals one.

LIST: IK1, IK2, JK1, JK2, KK1, KK2, AMAXK, AMINK

See READ R2-13 for definition of these parameters. This card refers to concentration mapping only as opposed to pressure mapping for READ R2-13.

NOTE: This data entered up to this point is sufficient to execute the program until time equal TCHG. The recurrent data is read again at that point. If you desire to terminate a run, enter ITHRU=1 (READ R2-1) after R2-15. If you desire any plots (if NPLP or NPLT or NPLC equals one), you should enter the plotting data (READ P-2 through P-4). If you do not desire any plots, ITHRU=1 will terminate execution at this point.

206

PLOTTING DATA

The specifications for the plots and observed data are entered here. You may obtain plots even if you do not have any observed data available. Do not enter any plotting data if you do not desire any plots. Plots can be obtained for the values of the dependent variables in the well (at the wellhead and at the bottom-hole). The quantities plotted depend upon the "type" of the well. The quantities plotted for different wells are as follows:

Type of Well	Quantities Plotted
Observation well	Bottom-hole pressure, temperature and concentration
Injection well-bottom-hole conditions specified (ISURF=0)	Bottom-hole pressure
Injection well-surface conditions specified (ISURF=1)	Bottom-hole pressure and temperature, surface pressure
Production well-bottom-hole conditions specified	Bottom-hole pressure, temperature and concentration
Production well-surface conditions specified	Bottom-hole pressure, temperature and concentration, surface pressure and temperature

You should enter READ P-1 only if you are obtaining plots for a previous run. The plotting data for one well consists of the data from READ P-2 through P-4. Enter as many sets of these data as the wells for which you desire plots. If you desire plots for all the wells, enter NWT sets of these data. If you enter less than NWT sets, follow these cards with a blank card.

READ P-1 (I5)

NOTE: Enter this data only if NPLP or NPLT or NPLC equals -1, i.e. the plots are desired for a previous run.

LIST: NWT

NWT Total number of wells

READ P-2 (I5, 5X, 10A4)

LIST: KW, ID

KW	The well number.
ID	A title for the plots for well number KW.

READ P-3 (7F10.0)

LIST: TMN, TMX, DT, PWMN, PWMX, PSMN, PSMX, TWMN, TWMX, TSMN, TSMX, CMN, CMX

These variables define the ranges of the coordinate axes for plots.

TMN	Lower limit on time.
TMX	Upper limit on time.
DT	Time step for each row. For example, if TMN=5, TMX=15, and DT=0.5, the time coordinate axis will be 20 rows long.
PWMN, PSMN, TWMN, TSMN, CMN	Lower limits on bottom-hole pressure, surface pressure, bottom-hole temperature, surface temperature and concentration, respectively.
PWMX, PSMX, TWMX, TSMX, CMX	Upper limits on bottom-hole pressure, surface pressure, bottom-hole temperature, surface temperature and concentration, respectively.

READ P-4 (6F10.0)

NOTE: Read as many cards as the observed data points (one card for each value of time at which the observed values are available). Follow the last card with a negative number in the first field specification (F10.0).

LIST: TOX, POW, POS, TOW, TOS, COS

TOX	Observation time.
POW	Bottom-hole pressure.
POS	Surface pressure.
TOW	Bottom-hole temperature.

208

TOS Surface temperature.

COS Concentration.

NOTE: The calculated data are read from tape 12. If you desire plots for a previous run, tape 12 should be attached. If you entered less than NWT sets of the plotting data, follow the last card with a blank card. This is the end of your data set.

MAPS FROM RESTART RECORDS

Restart records may be edited to obtain maps for the dependent variables. The following set of data cards are required to obtain maps for a previous run.

READ M-1 Two title cards
READ M-2 Control parameters. RSTRT must be non-zero.

READ M-3 This card must be identical to the one used for the original run.

READ M-4 Enter a negative value for TMCHG.

NOTE: Insert as many sets of mapping data (M-5 and M-6) as you desire. Follow the last set with a blank card.

READ M-5 (I5)

LIST: IMPT

IMPT The time step number at which the maps are desired. A restart record must exist corresponding to this time step.

READ M-6 (2I5)
LIST: MAP, MDAT

MAP Requires a three digit specification as in READ R2-11, except that it should be negative.

MDAT See READ R2-11.

NOTE: If MDAT has been entered as one, you should enter the mapping data R2-12 through R2-15 at this point.

3.3 ERROR DEFINITIONS

The program checks the input data for a number of possible errors to protect the user from running an entire problem with an error. A detected error will prevent execution, but the program will continue to read and check remaining data completely through the last recurrent data set.

If the number of elements in a fixed dimensioned array exceed the dimensions, you must redimension the array. This requires recompiling the program. The user is referred to Section 2.4 for redimensioning the program.

The errors detected in the data input are printed in a box; and if an error has occurred, it's number will appear in the box. Positions with zeroes do not have errors. Error numbers 1 through 50 represent the following errors:

(1) This error refers to Read M-3.
NX is less than or equal to one or
NY is less than one or
NZ is less than one.
The minimum dimensions on the grid block system are 2x1x1. The maximum size is limited only by the available computer storage.

(3) This error refers to READ R1-1.
One or more of CW, CR, CPW and CPR is negative. Physically, compressibilities and heat capacities are always equal to or greater than zero.

(4) This error refers to READ R1-2.
One or more of UKTX, UKTY, UKTZ, ALPHL, ALPHT and DMEFF is negative.

(5) This error refers to READ R1-3.
Either one or both the fluid densities (BWRN and BWRI) is zero or negative.

(6) This error refers to READ R1-7 through R1-10.
One or more of the viscosity values is entered as zero or negative.

Error numbers 7 through 9 refer to READ M-3.

(7) HTG is not within the permissible range.
HTG is less than 1 or greater than 3.

(8) The entered value for KOUT is not permissible.
KOUT is not equal to 0, 1 or 3.

(9) PRT exceeds permissible range of -1 to +2.

210

(11) This error refers to READ R1-17 through R1-19.
One or more of grid block sizes (DELX, DELY, DELZ) are zero or negative.

(12) This error refers to aquifer properties for a homogeneous aquifer (READ R1-20).
One or more of KX, KY and KZ is negative or
PHI is less than 0.001 or greater than 1.0 or
SINX or SINY is less than -1 or greater than +1.

(13) This error refers to heterogeneous aquifer data, READ R1-21.

I is greater than NX or
J is less than 1 or greater than NY or
K is less than 1 or greater than NZ or
KX or KY or KZ is negative or
PHI is less than 0.001 or greater than 1.0.

(14) This error refers to READ R1-22.
The first grid block center (R1) is less than or equal to the well radius (RWW) or R1 is greater than or equal to the aquifer boundary radius (RE).

(15) This error refers to READ R1-23.
The layer thickness (DELZ) is less than or equal to zero or
KYY or KZZ is negative or
porosity (POROS) is less than 0.001 or greater than 1.0.

(16) This error refers to READ R1-24 and R1-25.
The sum of NXR's is greater than NX or
one or more of RER's is greater than RE.

(17) This error refers to aquifer description modifications, READ R1-26.
One or more of I1, I2, J1, J2, K1, K2 are out of permissible ranges 1-NX, 1-NY and 1-NZ respectively, or
I1 is greater than I2 or
J1 is greater than J2 or
K1 is greater than K2.

(18) This error refers to READ R1-27 and R1-28.
IAQ is greater than 3 or
one or more of I1, I2, J1, J2, K1, K2 are out of permissible ranges 1-NX, 1-NY and

1-NZ respectively, or
I1 is greater than I2 or
J1 is greater than J2 or
K1 is greater than K2.

(19) The number of aquifer influence blocks (NABL) are greater than NABLMX specified in READ M-3.

(21) This error refers to READ I-2.
One or more of I1, I2, J1, J2, K1, K2 are out of permissible ranges 1-NX, 1-NY and 1-NZ respectively, or
I1 is greater than I2 or
J1 is greater than J2 or
K1 is greater than K2 or
CINIT is negative.

(23) Some grid block pore volume is non-zero and sum of transmissibilities is zero.

(24) Some grid block pore volume is negative.

(25) This error refers to READ R2-4.
Total number of wells (NWT) is less than 1 or exceeds dimension limit NWMAX.

(26) This error refers to READ R2-6.
Well number I is less than 1 or greater than NWT.

Error numbers 27 through 39 refer to READ R2-7.

(27) Well location IIW, IJW is outside aquifer, i.e.
IIW is less than 1 or greater than NX or
IJW is less than 1 or greater than NY.

(28) The well perforations are outside the aquifer, i.e. IIC1 or IIC2 is out of the range 1-NZ or
IIC1 is greater than IIC2 or
the top block of the completion interval (k=IIC1) is a zero pore volume block.

(30) The entered value of IINDW1 is not permissible. The permissible values are +1,±2 and ±3.

(32) A well index of zero is permissible only if IINDW1 is equal to one. This error occurs if IINDW1 is not equal to one and WI is zero or negative.

(33) IINDW1 is ±3 and BHP is 0. The specified value of the bottom-hole pressure is a limiting value of the well pressure if IIDW1 is ±3.

2/2

(35) All completion layers of a well are in zero pore volume blocks.

(37) One or more of KHL values are negative.

(38) All KHL values are zero for some well. At least one KHL value must be non-zero.

(39) A well number I is negative or exceeds NWT.

(40) This error refers to READ R2-2.
METHOD is less than -2 or greater than +2 or WTFAC is greater than 1.0.

Error numbers 41 and 42 refer to READ R2-9.

(41) Minimum number of outer iterations (MINITN) is less than 1 or
MINITN is greater than maximum number of outer iterations (MAXITN).

(42) Method of solution is L2SOR (METHOD = $\pm$2) and IMPG is less than or equal to zero.

Error numbers 43 through 46 refer to READ R2-10.

(43) The time at which next set of recurrent data are to be entered (TCHG) is less than or equal to current TIME.

(44) DT is zero for the first time step. Automatic time step control may not be initiated until at least the second time step.

(45) DTMAX is less than DTMIN.

(46) The value entered for MAP is not permissible. All three digits must be either 0 or 1.

Error numbers 47, 48 and 49 refer to READ R2-13, R2-14 and R2-15, respectively.

(47) IP2 is greater than NX or
KP2 is greater than NZ or
HTG is not equal to 3 and JP2 is greater than NY.

(48) IT2 is greater than NX or
KT2 is greater than NZ or
HTG is not equal 3 and JT2 is greater than NY.

213

(49) IK2 is greater than NX or
KK2 is greater than NZ or
HTG is not equal to 3 and JKZ is
greater than NY.

SECTION 4

EXAMPLE PROBLEM

4.1 INTRODUCTION

In this section an example problem utilizing the well disposal model is presented. The problem was formulated to illustrate some general features of the model and entering the data. The total number of grid blocks was taken as 50 and the method of solution was reduced band width direct solution. The total central processing time on a CDC 6600 computer was 13.7 seconds. We estimate that this run used 0.012 second central processing time per grid block per time step for the first iteration and 0.005 second per grid block per time step for each subsequent iteration. However, the concentration equation was not solved in this run; and if all three equations are solved, the central processing time required for the model is 0.015 second per grid block per time step for the first iteration and 0.006 second for each subsequent iteration.

4.2 DESCRIPTION OF THE PROBLEM

The problem consists of a single well disposal into an infinite aquifer. The injection fluid is the same as the resident fluid; and, therefore, there is no need to solve the concentration equation. The fluid being injected is at a lower temperature than the resident fluid. This fluid gains heat from the rock surrounding the wellbore and the bottom-hole temperature is higher than the surface temperature. The aquifer is at a depth of 4000 ft. and is 100 ft. thick and the porous medium is heterogeneous in the vertical direction. The total aquifer thickness is divided into five layers to describe the permeability and the porosity adequately.

The injection well is located at the center of the aquifer, and an observation well is located at a distance of 625 feet from the injection well. Since it is a single well injection problem, it can be simulated in radial geometry. We define the numerical grid block system up to a radius of 5000 feet, and divide this region into 10 radial blocks. The well radius is 4.5 inches and we take the center of the first grid block at a distance of two feet from the center. The drilling of the injection wellbore has caused damage in the aquifer and it is estimated that the horizontal and vertical permeabilities around the wellbore have been reduced by a factor of 50% up to a radius of approximately 10 feet.

The third grid block center is at 10.2 feet. Therefore, we can modify the first three transmissibilities in the x and z direction by a factor of 0.5. Since the transmissibilities are evaluated at the grid block boundaries, the third transmissibility value represents a composite value between the second and the third grid block centers. The fluid is injected at the rate of 10,000 ft^3/day for two days and then the well is shut off. The pressures and temperatures in the two wells are observed for a total period of five days.

Since we are simulating injection into an infinite aquifer, we select Carter-Tracy aquifer influence functions for an infinite aquifer at the periphery of our grid block system.

The fluid and rock properties and the well data will be described in the data input cards. The output will be discussed in Section 4.4.

4.3 EXAMPLE PROBLEM DATA INPUT FORMS

In this section, the preparation of input data forms will be illustrated for the example problem. The user is referred to Section 3.2 for the meanings of the variables.

READ M-1 (20A4/20A4)

TITLE																			
***	EXAMPLE	PROBLEM	-	WELL	DISPOSAL	MODEL	***												
WELL	TEST	FOR	SINGLE	WELL	INJECTION	INTO	AN	INFINITE	AQUIFER										

READ M-2 (8I5)

NCALL	RSTRT	ISURF	IPDIM	IIPRT	NPLP	NPLT	NPLC
-2	0	1	0	0	1	0	0

NCALL = -2 Solve only pressure and temperature equations.

ISURF = 1 Wellbore calculations are to be performed.

READ M-3 (7I5)

NX	NY	NZ	HTG	KOUT	PRT	NABLMX	METHOD
10	1	5	3	1	2	5	1

HTG = 3 Radial geometry.

KOUT = 1 All program output except initial arrays is activated.

PRT = 2 Print output maps as vertical sections (x-z).

Since RSTWR is 0, we proceed to READ R1-1.

READ R1-1 (5E10.0)

CW	CR	CTW	CPW	CPR
.000003	.000004	.0002	1.005	28.

READ R1-2 (7E10.0)

UKTX	UKTY	UKTZ	CONV	ALPHL	ALPHT	DMEFF
26.	26.	26.	0.	1.00	1.0	.001

CONV = 0 The thermal conductivities are entered in Btu/ft-day-°F.

READ R1-3 (4E10.0)

PBWR	TBWR	BWRN	BWRI
1950.	139.8	70.51	70.51

READ R1-4 (I5)

NOUT
0

NOUT = 0 No wellbore calculation output is activated.

218

READ R1-5 (3E10.0)

PBASE		DELPW		TDIS	
15.		250.		0.04	

DELPW = 250 psi

Since the wellbore is 4,000 ft. deep, and the fluid density is 70.51, the total gravity head at 4,000 ft. depth is approximately 1960 psi. Therefore, the wellbore calculations will be performed over 8 increments.

READ R1-6 (4I5)

NCV	NTVR	NTVI	NDT
0	0	0	2

NTVR = 0

The fluid viscosity is available at only one temperature.

NDT = 2

The initial temperature in the aquifer and the overburden-underburden blocks will be obtained by linear interpolation between the two data points.

6/8

READ R1-7 (4E10.0)

TRR		VISRR		TIR		VISIR	
139.8		.9		139.8		0.90	

Since NCV, NTVR and NTVI are zero, we proceed to READ R1-11.

READ R1-11 (2F10.0)

ZT(I),	TD(I),	I = 1,	NDT
0.		75.	
6000.		172.	2

READ R1-12 (2I5)

NZOB	NZUB
3	3

READ R1-13 (4E10.0)

KOB	CPOB	KUB	CPUB
26.	28.	26.	28.

READ R1-14 (7E10.0)

DZOB(K), K = 1,NZOB		
20.	40.	80.

READ R1-15 (7E10.0)

DZUB(K), K = 1,NZUB		
20.	40.	80.

READ R1-16 (4E10.0)

TO	PINIT	HINIT	HDATUM
139.8	1950.	4000.	4000.

Since HTG = 3, we proceed to READ R1-22.

220

READ R1-22 (4E10.0)

RWW	R1	RE	DEPTH
0.375	2.0	50000.	4000.

READ R1-23 (5E10.0)

DELZ(K),	KYY(K),	KZZ(K),	POROS(K),	CPR1(K),	K = 1,NZ
20.		0.36	0.12	.099	0.
10.		0.291	0.097	.097	0.
20.		0.330	0.11	.107	0.
20.		0.48	0.16	.107	0.
30.		0.099	0.033	.096	0.

CPR1 = 0 The rock heat capacity in all the layers is 28 Btu/ft-day-°F.

READ R1-24 (5I5)

NXR(I),	I = 1,5
0	

NXR(1) = 0 The grid block system will be divided into NX(=10) radial blocks on an equal Δlogr basis.

Since NXR(1) is zero, we skip READ R1-25.

READ R1-26 (LIST 1-6I5, List 2-6E10.0)

I1	I2	J1	J2	K1	K2						
FTX		FTY		FTZ		FPV		HADD		THADD	
1	3	1	1	1	5						
.5		1.0		0.5		1.		0.		0.	
0											

READ R1-27 (2I5)

IAQ	PRTAB
3	0

IAQ = 3 The Carter-Tracy aquifer influence function representation will be used.

Since IAQ is 3, we omit READ R1-28.

READ R1-29 (3I5)

NCALC	NPT	PRTIF
1	0	0

NCALC = 1 The aquifer influence function coefficients will be calculated by the program and assigned to each edge block in each areal plane.

NPT = 0 The program will select Hurst Van Everdingen infinite aquifer solution internally.

Since NCALC is not equal to zero, we omit READ R1-30.

READ R1-31 (4E10.0)

KH	PHIH	RAR	THETAR
29.28	10.11	5000.	360.

222

KH = 29.28 Summation of transmissivity x thickness of all five layers in the edge blocks = 20x0.36+10x0.291+20x0.33+20x0.48+30x0.099 = 29.28.

PHIH = 10.11 Sum of porosity x thickness = 20x0.099+10x0.097+20x0.107+20x0.107 +30x0.096 = 10.11.

Since NPT is equal to zero, we omit READ R1-32.

READ R1-33 (6I5)

I1	I2	J1	J2	K1	K2
0					

READ I-1 (2I5)

ICOMP	INAT
0	0

Since ICOMP and INAT are zero, we skip READ I-2 and I-3.

READ R2-1 (7I5)

INDQ	IWELL	IMETH	ITHRU	IPROD	IOPT	INDT
1	1	1	0	1	1	0

INDQ = 1 Read well rates on one card.

ITHRU = 0 The run is to continue.

INDT = 0 Do not read iteration data. The default values will be used.

223

READ R2-2 (I5,F10.0)

MEHTOD	WTFAC	
1	0.5	

METHOD = 1 Direct solution. Backward difference approximations in time.

WTFAC = 0.5 Central difference approximation in space.

READ R2-3 (I5,4F10.0)

NITQ	TOLX		TOLDP		DAMPX		EPS	
5	.1		1.		1.	5	.001	

READ R2-4 (I5)

NWT
2

READ R2-5 (7E10.0)

Q(I), I = 1,NWT		
-10000.	0.	

Q(1) = -10,000 Negative rate represents injection.

Since INDQ is equal to one, we skip READ R2-6.

READ R2-7 (LIST1-6I5, LIST 2 and 4-7E10.0, LIST 3-8E10.0)

I	IIW	IJW	IIC1	IIC2	IINDW1														
WI		BHP		TINJ		CINJ													
X		DW		ED		OD		TTOPW		TBOTW		UCOEF		THETA					
KHL(K), K = IC1, IC2																			
1	1	1	1	5	-2														
58.		15.		75.		0.													
40000.		.32		0.		.75		75.		139.8		2.		0.					
.25		.1		.22		.33		.1											
2	8	1	1	5	-2														
58.		15.		75.		0.													
40000.		.32		0.		.75		75.		139.8		2.		0.					
.25		.1		.22		.33		.1											
0																			

READ R2-8 (7E10.0)

THP(I), I = 1,NWT							
15.		15.					

Since INDT is equal to zero, we omit READ R2-9.

READ R2-10 (7E10.0)

TCHG		DT		DSMX		DPMX		DTPMX		DTMAX		DTMIN	
.02		.01		0.		0.		0.		0.		0.	

225

TCHG = 0.02 We intend to use automatic time step feature after the first two time steps. At TIME = 0.02, the program will read the recurrent data again.

DT = 0.01 A small time step has been selected to start the simulation.

READ R2-11 (9I5)

IO1	IO2	IO3	IO4	IO8	RSTWR	MAP	KOUT	MDAT
0	0	0	-1	001	0	000	0	0

IO1 = 0 Time step summary will be printed out at the end of each time step.

IO2 = 0 Well summary will be printed out at the end of each time step.

IO3 = 0 Lists of grid block values of the dependent variables will be printed out at the end of each time step.

IO4 = -1 We do not desire printing of injection rate for each layer.

IO8 = 001 Since we are not simulating the solution of concentration equation, there is no need to print the concentration values in every grid block.

The first set of recurrent data has been entered. Now we enter the data at TIME = TCHG = 0.02 day. The recurrent data starts from READ R2-1. We will keep the injection rate and the well data the same as before, but will activate the automatic time step feature.

READ R2-1 (7I5)

INDQ	IWELL	IMETH	ITHRU	IPROD	IOPT	INDT
0	0	0	0	0	0	0

All the values are zero because we do not desire to alter any recurrent data. The next READ to be entered is R2-10.

READ R2-10 (7E10.0)

TCHG		DT		DSMX		DPMX		DTPMX		DTMAX		DTMIN	
2.		0.		.25		50.		5.		.5		.05	

The time step is evaluated based upon the maximum values of pressure, temperature and concentration changes over the previous time step.

DPMX = 50 The maximum pressure change during a time step is permitted to be 50 psi.

DTPMX = 5 The maximum temperature change during a step is permitted to be 5 °F.

DTMAX = 0.5 We desire to limit the maximum value of the time step as 0.5 day.

DTMIN = 0.05 We limit the minimum value of the time step as 0.05 day.

READ R2-11 (9I5)

I01	I02	I03	I04	I08	RSTWR	MAP	KOUT	MDAT
0	0	0	-2	.001	0	0.0	0	0

At two days, we shut the well off; therefore, we must alter the well rate data. To do that, we must enter INDQ = 1 or 2 in READ R2-1.

READ R2-1 (7I5)

INDQ	IWELL	IMETH	ITHRU	IPROD	IOPT	INDT
2	0	0	0	0	0	0

READ R2-4 (I5)

NWT
2

Since INDQ is entered as 2, we must enter the altered well rates by READ R2-6.

READ R2-6 (I5,E10.0)

I	QWELL
1	0.

READ R2-10 (7E10.0)

TCHG	DT	DSMX	DPMX	DTPMX	DTMAX	DTMIN
.02	.01	0.	0.	0.	0.	0.

Since the well rates have been altered, we will activate the automatic time step feature after two small time steps have been taken.

READ R2-11 (9I5)

IO1	IO2	IO3	IO4	IO8	RSTWR	MAP	KOUT	MDAT
0	0	0	-1	0.01	0	000	0	0

READ R2-1 (7I5)

INDQ	IWELL	IMETH	ITHRU	IPROD	IOPT	INDT
0	0	0	0	0	0	0

READ R2-10 (7E10.0)

TCHG		DT		DSMX		DPMX		DTPMX		DTMAX		DTMIN	
5.		0.		.25		50.		5.		.5		.05	

READ R2-11 (9I5)

I01	I02	I03	I04	I08	RSTWR	MAP	KOUT	MDAT
0	0	0	-1	001	0	000	0	0

READ R2-1 (7I5)

INDQ	IWELL	IMETH	ITHRU	IPROD	IOPT	INDT
0	0	0	1	0	0	0

ITHRU = 1 We desire the run to terminate at TIME = 5 days.

Since we entered NPLP as 1, we must now enter the plotting data. Since the plots are desired for the current run (NPLP is greater than zero), we skip READ P-1.

The total number of wells is two. Therefore, we should read two sets of plotting data (P-2 through P-4).

READ P-2 (I5, 5X, 10A4)

KW	ID
1	EXAMPLE PROBLEM - INJECTION WELL

READ P-3 (7F10.0)

TMN	TMX	DT	PWMN	PWMX	PSMN	PSMX
TWMN	TWMX	TSMN	TSMX	CMN	CMX	
0.	6.	0.2	1950.	2300.	0.	0.
75.	140.	0.	0.	0.	0.	

READ P-4 (6F10.0)

TOX	POW	POS	TOW	TOS	COC
-1.					

READ P-2 (I5, 5X, 10A4)

KW	ID
2	EXAMPLE PROBLEM - OBSERVATION WELL

READ P-3 (7F10.0)

TMN	TMX	DT	PWMN	PWMX	PSMN	PSMX
TWMN	TWMX	TSMN	TSMX	CMN	CMX	
0.	6.	0.2	1950.	2000.	0.	0.
130.	150.	0.	0.	0.	0.	

READ P-4 (6F10.0)

TOX	POW	POS	TOW	TOS	COC
-1.					

230

Since we do not have any observed data available, we have entered TOX as -1. for both the wells. At 5 days, both the wells are acting as observation wells; and therefore, only bottom-hole quantities are plotted. There is no need to enter the ranges of the surface pressure and temperature.

4.4 OUTPUT

The output consists of six parts:

(1) Time step summary.

(2) Well summary.

(3) Grid block values of the dependent variables.

(4) Production or injection rate for each layer in which a well is completed.

(5) Contour maps.

(6) Dependent variables plots.

The printing of the first four outputs is controlled by I01, I02, I03 and I04. Since we entered KOUT, I01, I02 and I03 as zero, we obtain the first three outputs at every time step. The three equations solved by the model are the differential balances on total fluid, contaminant and energy. The program calculates the cumulative integral balances over the complete aquifer up to the current time step. The different quantities calculated to evaluate the integral balances are printed in the summary. Also, the maximum pressure, concentration and temperature changes in a grid block, and the average pressure calculated at the datum depth (HDEPTH) are printed. The time step summary at the end of the first time step is shown in Figure 4a.

[redacted] 4a - Well Summary at the end of the first time step [redacted]

```
TIME =     .0 DAYS  ITIME =    1  ITNS = 2  MBW = 1.0000    MBCOMP = 1.0000    HEATBL = 1.0000
TOTWP = 0.          MM LBM         TOTCP = 0.          MM LBM         TOTHP = 0.          MMBTU
TOTWI = 7.101E-03 MM LBM           TOTCI = 0.          MM LBM         TOTHI = 3.998E-01 MMBTU
TWIP  = 5.599E+04 MM LBM           TCIP  = 0.          MM LBM         THIP  = 6.208E+06 MMBTU
                                    PAVG =     1950. PSIA       HEAT LOSS = 2.022E-02 MMBTU
     DPMAX( 1, 1, 1) = 150.7  DCMAX(10, 1, 5) = 0.0000  DTEMPMAX( 1, 1, 4) = -6.35
     CUM WATER INFLUX = 1.118E-07 MM.LBM   CUM HEAT INFLUX = 1.270E-05 MMBTU
     CUM COMP. INFLUX = 0.          MM.LBM
```

where TIME = Current time (0.01 day for the current run)

ITIME = Number of time steps

ITNS = Number of outer iterations in ITER

MBW = material balance on water. This is the integral balance on the mass of aquifer fluid

$$= \frac{\text{Fluid in aquifer at the current time+Fluid produced-Initial fluid in aquifer}}{\text{Fluid injected + Fluid influx across the aquifer boundaries}}$$

MBCOMP = Material balance on component. It is calculated in a similar manner as MBW.

HEATBL = Heat balance. It is also calculated in a similar manner as MBW and MBCOMP (includes heat loss).

TOTWP = Total water, component and heat produced up to the current
TOTCP time. These quantities are printed in m.lbm, m.lbm and m.btu,

133

TOTHP — respectively. You should multiply them by 10^6 to obtain lbm. or btu figures.

TOTWI = Total water, component and heat injected. These quantities
TOTCI are also printed in m.lbm, m.lbm and m.btu, respectively.
TOTHI

PAVG = The pore volume weighted average pressure calculated at the datum depth. The grid block pressures are adjusted by $\rho_o gh$ to obtain the pressure at datum, where ρ_o is the resident fluid density at PINIT and TO, and h is the depth measured from the grid block depth to the datum.

HEAT LOSS = Cumulative heat loss to the impermeable strata above and below the aquifer, m.btu.

DPMAX = Maximum grid block pressure change over the time step, psi. The numbers in parenthesis are the grid block indices (I, J and K) in which the maximum pressure change occurred.

DCMAX = Maximum concentration and temperature changes respectively
DTEMPMAX in any grid block over the time step.

CUM WATER INFLUX = Cumulative water, component and heat influx respectively
CUM COMP. INFLUX through the peripheral boundaries. If the aquifer influence
CUM HEAT INFLUX functions are taken as zero, these quantities are always zero. A negative value represents efflux.

FIGURE 4 b - Well summary for the current run at Time = 0.01 day

THE TIME IS .010 DAYS

WELL LOCATION				PRODUCTION RATES			CUMULATIVE PRODUCTION			CUMULATIVE INJECTION			GRID	FLWG	FLWG	AH	WH
				WATER	HEAT	COMP	WATER	HEAT	COMP	WATER	HEAT	COMP	BLOCK	BHP	WHDP	TEMP	TEMP
M	I	J	K	LB/DAY	BTU/DAY	LB/DAY	LBM	BTU	LBM	LBM	BTU	LBM	PRESS	PSIA	PSIA	DG.F	DG.F
1	6	1	1- 5	-7.10E+05	-4.00E+07	0.0000	0.	0.	0.	7.10E+03	4.00E+05	0.	2101.	2185.	208.	82.	75.
2	8	1	1- 5	0.	0.	0.0000	0.	0.	0.	0.	0.	0.	1950.	1950.	0.	140.	0.
TOTALS - PROD				0.	0.	0.	0.	0.	0.								
- INJ				7.10E+05	4.00E+07	0.				7.10E+03	4.00E+05	0.					

The printout of the well summary is self-explanatory. A few parameters need some clarification. The production and injection rates are printed in the same column where the injection rates are denoted by a minus sign. The component injection or production rate for well is not printed, but instead concentration of the component in the production or injection stream is printed. The total injection and production rates are printed separately, and the total rates of production or injection of the component are also printed. The cumulative production and injection rates are printed for each well.

The well temperatures and pressures are printed explicitly (at the end of the previous time step) or implicitly (at the current time) depending upon whether the well rate was specified explicitly or implicitly. These quantities for an observation well are always printed at the current time. Since we entered IINDW1 = -2 (implicit specification), these values are printed at the current time. The quantities printed on the output are as follows:

GRID BLOCK PRESS = Grid block pressure in psi. This grid block represents the uppermost layer in which a well is open. In our case, the well is open in layers 1 through 5. Therefore, this pressure is the grid block pressure in block (1,1,1).

FLWG BHP = Flowing bottom-hole pressure, psi.

FLWG WHDP = Flowing wellhead pressure, psi.

BH TEMP = Bottom-hole temperature, °F.

WH TEMP = Wellhead temperature, °F.

For an observation well and for the other wells if the wellbore calculations are not performed, the wellhead pressure and temperature are not printed.

The third part of the output consists of listings of the grid block values. Since we specified PRT as 2 (READ M-3), the listings are printed as vertical sections. The pressure listings at 5 days are shown in Figure 4c.

FIGURE 4c

PRESSURE AT ELEVATION H (PSIA)

	1	2	3	4	5	6	7	8	9	10
1	1956.1	1956.1	1956.1	1956.1	1956.1	1956.1	1956.1	1955.9	1954.8	1950.6
2	1965.9	1965.9	1965.9	1965.9	1965.9	1965.9	1965.9	1965.7	1964.6	1960.4
3	1970.8	1970.8	1970.8	1970.8	1970.8	1970.8	1970.8	1970.6	1969.5	1965.3
4	1980.6	1980.6	1980.6	1980.6	1980.6	1980.6	1980.6	1980.3	1979.3	1975.1
5	1990.4	1990.4	1990.4	1990.4	1990.4	1990.4	1990.4	1990.2	1989.1	1984.8

The numbers at the top are the "I" values of the grid blocks, and the column at the left are "K" values of the grid blocks. The listings for the pressure at datum, temperature and concentration are similar and need no explanation.

The pressure plots for the run are shown in Figures 5 through 8. The plots are very useful in well tests and history matching runs.

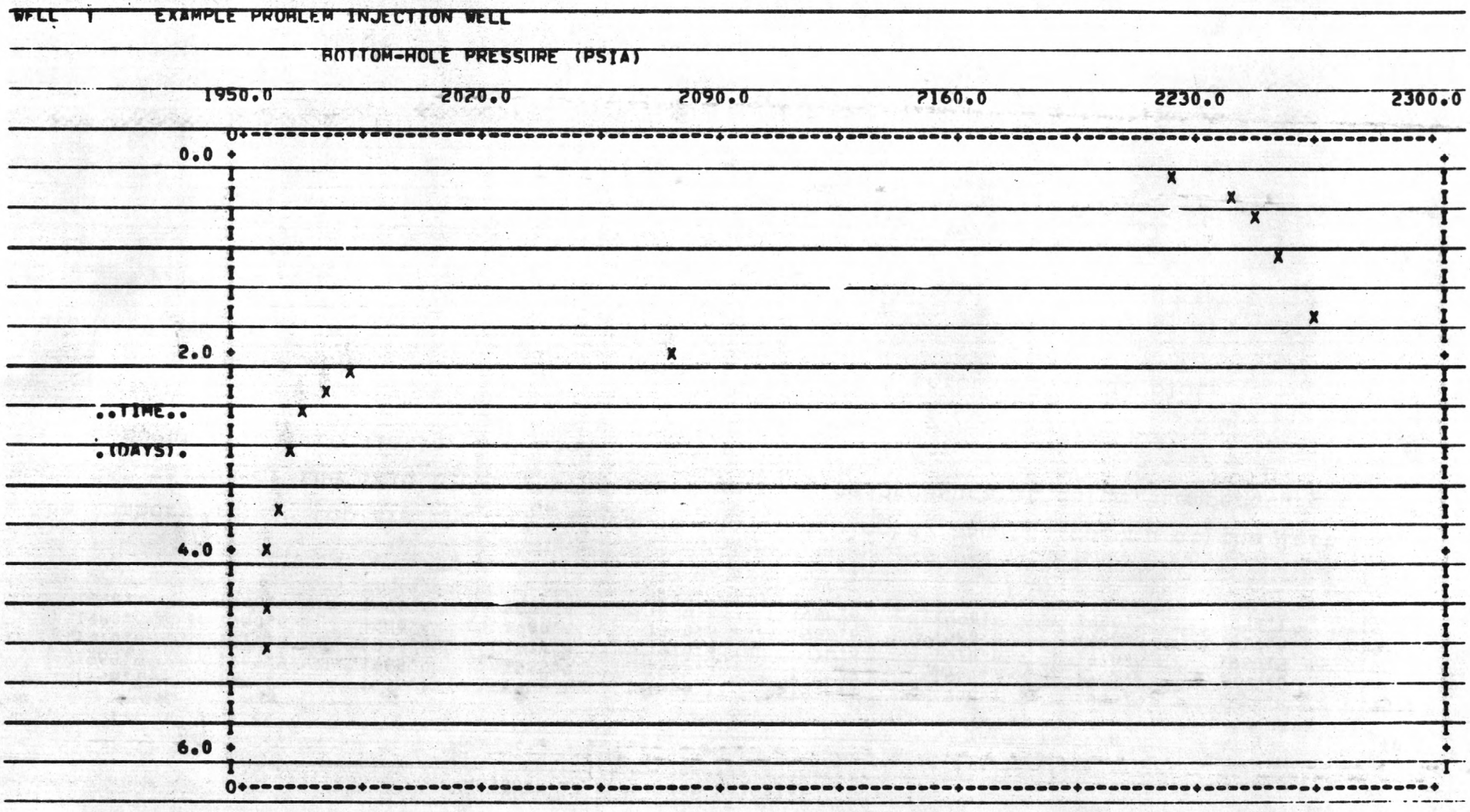

Figure 5 - Line Printer Plot of the Bottom-hole Pressure in the Injection Well for the Example Problem

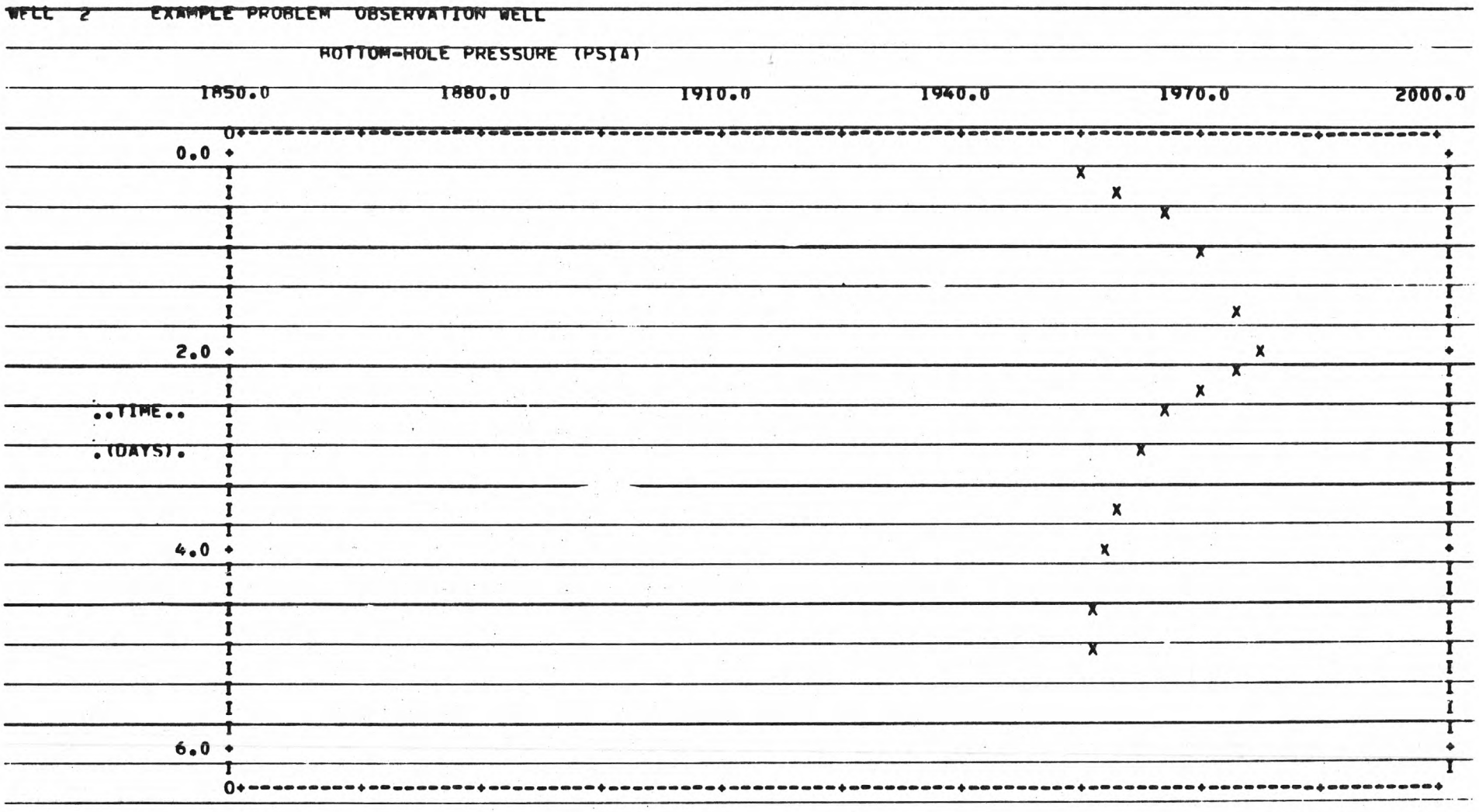

Figure 6 - Line Printer Plot of the Bottom-hole Pressure in the Observation Well for the Example Problem

SECTION 5

NOMENCLATURE

a,b	=	Aquifer influence function coefficients (Eq. 2-8)
a_1,a_2,a_3	=	Partial derivatives of density with respect to pressure, temperature and concentration, respectively.
A	=	Area to flow--either $\Delta x\Delta y$, $\Delta x\Delta z$ or $\Delta y\Delta z$.
B	=	Parameter in the viscosity model
B	=	Parameter in the Carter-Tracy aquifer influx rate expression = $2\pi\Delta Z\phi c_T r_e^2 s$.
c	=	Compressibility
C	=	Concentration, mass fraction
C_p	=	Specific heat
D	=	Diffusion coefficient
E	=	Dispersion coefficient
e_w	=	Rate of influx across the peripheral boundaries of the aquifer.
f	=	Friction factor for flow down well.
F(t)	=	Transient heat conduction time function for heat loss from the wellbore.
g	=	Acceleration due to gravity
g_c	=	Gravitational conversion factor
h	=	Depth
h	=	Heat transfer coefficient
H	=	Enthalpy
I_k	=	Injectivity for layer k
J	=	Mechanical equivalent of heat
k	=	Permeability
K	=	Thermal conductivity
K_t	=	$k/\mu\phi c_T r_e^2$
KHL	=	Allocation factor

240

ℓ	=	Distance between grid block centers
NX,NY,NZ	=	Numbers of grid blocks in reservoir x, y, and z directions respectively.
p	=	Pressure
p^n	=	Terminal rate case influence function at dimensionless time $t_D = K_t\ t_n$.
P_r	=	Prandtl number
Q	=	Heat transferred from wellbore to surrounding earth.
q	=	Mass rate of production or injection of liquid for a grid block.
q_L	=	Rate of heat loss from grid block
r	=	Radial space coordinate
R_e	=	Reynolds number
R_w	=	Wellbore radius
R_1, R_2	=	Inner tubing radius and outer casing radius, respectively.
s	=	Fraction of a circle covered by reservoir-aquifer circular boundary.
S	=	Mass flow rate across a grid block boundary
t	=	Time
T	=	Temperature
u	=	Superficial (Darcy) fluid velocity in the porous rock.
U	=	Internal energy
U_c	=	Overall heat transfer coefficient
V	=	Grid block volume
V_p	=	Pore volume
V_1, V_2	=	Aquifer influence function coefficients for pot and steady-state, respectively.
$W_{e,n}$	=	Cumulative water influx at time t_n.
W_f	=	Work done by fluid in wellbore flow.
WI	=	Well index

x	=	Cartesian space coordinate
Z	=	Elevation above a reference plane

Subscripts:

av	=	Average over depth increment
n	=	Time level t_n
0	=	Reference level
bh	=	Bottom-hole
ob	=	Overburden
R	=	Rock
i,j,k	=	Grid block indices
w	=	Liquid
l,t	=	Longitudinal and transverse, respectively
m,M	=	Molecular properties in porous media and open channel, respectively

Superscripts:

n	=	Time level ρ^n

Greek:

ϕ	=	Porosity
ρ	=	Density
μ	=	Viscosity
α	=	Weighting factor
γ	=	Thermal diffusivity of rock surrounding wellbore
Δt	=	Time increment
$\Delta x, \Delta y, \Delta z$	=	Grid block dimensions

SECTION 6

REFERENCES

(1) Price, H. S., and Coats, K. H.: "Direct Methods in Reservoir Simulation," SPE 4278 presented at the Third SPE Symposium on Numerical Simulation of Reservoir Performance of SPE of AIME, January 11-12, 1973, Houston, Texas.

(2) Lewis and Squires: "Generalized Liquid Viscosity Curve," Oil and Gas Journ., 33. 1934.

(3) McAdams, W. H.: "Heat Transmission," McGraw-Hill, New York, N. Y. (1954).

(4) Katz, D. L., Tek, M. R., Coats, K. H., Katz, M. L., Jones, S. C., and Miller, M. D.: "Movement of Underground Water in Contact with Natural Gas," AGA Monograph on Project No. 31, Am. Gas Assoc., New York, N.Y. (1963).

(5) Carter, R. D., and Tracy, G. W.: "An Improved Method for Calculating Water Influx," TRANS AIME, 415, 1960.

(6) Ramey, H. J., Jr.: "Wellbore Heat Transmission," Journ. Pet. Tech., 1962.

APPENDIX A

AQUIFER MODEL EQUATIONS

The finite-difference aquifer model solves three coupled partial differential equations describing the behavior of a liquid phase injected into an aquifer system. The finite-difference equations solved by the model are developed in this appendix.

Suppose x,y,z to be a Cartesian coordinate system and let Z(x,y,z) be the height of a point above a horizontal reference plane. Then the basic equation describing single-phase flow in a porous media results from a combination of the continuity equation

$$\nabla\cdot\rho u + q = -\frac{\partial}{\partial t}(\phi\rho)^* \qquad \text{(A-1)}$$

and Darcy's law in three dimensions.

$$u = -\frac{k}{\mu}(\nabla p - \rho g \nabla Z). \qquad \text{(A-2)}$$

The result is the basic flow equation

$$\nabla\cdot\frac{\rho k}{\mu}(\nabla p - \rho g\nabla Z) - q = \frac{\partial}{\partial t}(\phi\rho). \qquad \text{(A-3)}$$

A material balance for the solute results in the solute or concentration equation

$$\nabla\cdot(\rho C\frac{k}{\mu}(\nabla p - \rho g\nabla Z)) + \nabla\cdot(\rho E)\cdot\nabla C - qC = \frac{\partial}{\partial t}(\rho\phi C). \qquad \text{(A-4)}$$

The energy balance defined as [enthalpy in-enthalpy out = change in internal energy] is described by the energy equation

$$\nabla\cdot(\frac{\rho k}{\mu}H(\nabla p - \rho g\nabla Z)) + \nabla\cdot K\cdot\nabla T - q_L - qC_pT = \frac{\partial}{\partial t}[\phi\rho U + (1-\phi)(\rho C_p)_R T] \qquad \text{(A-5)}$$

*Detailed definitions of all terms are given in the Nomenclature.

The systems of Equations (A-3), (A-4), and (A-5) along with the fluid property dependence on pressure, temperature, and concentration describe the reservoir flow due to injection of wastes into an aquifer. This is a nonlinear system of coupled partial differential equations which must be solved numerically using high speed digital computers.

The finite-difference approximations for Equations (A-3), (A-4), and (A-5) are as follows:

Basic Flow Equation

$$\Delta[T_w(\Delta p - \rho g \Delta Z)] - q = \frac{V}{\Delta t}\,\delta(\phi\rho) \tag{A-6}$$

Solute or Concentration Equation

$$\Delta[T_w C(\Delta p - \rho g \Delta Z)] + \Delta(T_E \Delta C) - Cq = \frac{V}{\Delta t}\delta(\rho\phi C) \tag{A-7}$$

Energy Equation

$$\Delta[T_w H(\Delta p - \rho g \Delta Z)] + \Delta(T_C \Delta T) - q_L - qC_p T = \frac{V}{\Delta t}\,\delta[\phi\rho U + (1-\phi)(\rho C_p)_R T] \tag{A-8}$$

where the difference operators are defined by

$$\Delta(T_w\,\Delta p) = \Delta_x(T_w \Delta_x p) + \Delta_y(T_w \Delta_y p) + \Delta_z(T_w \Delta_z p) \tag{A-9}$$

with

$$\Delta_x(T_w \Delta_x p) = T_{w,i+1/2,j,k}\,(p^{n+1}_{i+1,j,k} - p^{n+1}_{i,j,k}) - T_{w,i-1/2,j,k}\,(p^{n+1}_{i,j,k} - p^{n+1}_{i-1,j,k}) \tag{A-10}$$

and

$$\delta\chi = \chi^{n+1} - \chi^{n}. \tag{A-11}$$

The terms

$$T_w = \frac{kA\rho}{\mu \ell} \tag{A-12}$$

$$T_c = \frac{KA}{\ell} \tag{A-13}$$

$$T_E = \rho \frac{EA}{\ell} \tag{A-14}$$

have been introduced for notational convenience. Since all of the terms in Equations (A-12) through (A-14) are position dependent, a further expansion is illustrated as

$$T_{w,i+1/2,j,k} = \frac{2\Delta y_j \Delta z_k}{(\Delta x_i + \Delta x_{i+1})} \left(\rho \frac{k_x}{\mu}\right)_{i+1/2,j,k} \tag{A-15}$$

The constituent dispersion tensor, E, and the effective heat conductivity tensor, K, in terms of the molecular properties as well as hydrodynamic dispersivity can be written as:

$$E \equiv \phi \, \alpha u/\phi + D_m \tag{A-16}$$

and

$$K \equiv \phi \, (\alpha u/\phi)(\rho C_p)_w + K_m \tag{A-17}$$

where the dispersivity factor, α, is either longitudinal or transverse for calculating the dispersivity in the direction of flow or perpendicular to it. The dispersivity along the coordinate axes must be calculated from these expressions.

For expanding the right-hand sides of Equations (A-6) through (A-8), we make the following assumptions:

(1) $$\phi \simeq \phi_o \, [1 + c_r(p-p_o)] \tag{A-18}$$

(2) $$U \simeq U_o + C_p(T-T_o) \tag{A-19}$$

(3) The rock density and heat capacity are essentially constant and that the liquid density ρ is a general function of pressure, temperature, and concentration which can be expressed as:

$$\delta\rho(p,T,C) = \frac{\partial\rho}{\partial p}\Big)_{T,C} \delta p + \frac{\partial\rho}{\partial T}\Big)_{p,C} \delta T + \frac{\partial\rho}{\partial C}\Big)_{p,T} \delta C \qquad \text{(A-20)}$$

The right-hand sides of the three equations are expanded in a consistent manner. As an example, we can illustrate using Equation (A-11) that:

$$\delta(ab) = a^{n+1}\,\delta b + b^{n}\delta a \qquad \text{(A-21)}$$

is consistent or exact in the sense that it satisfied the identity

$$\delta(ab) \equiv (ab)^{n+1} - (ab)^{n}$$

The three equations then become:

$$C_{31}\delta C + C_{32}\delta T + C_{33}\delta p = \Delta T_w \Delta\bar{p} + q_i + \frac{dq_i}{dp} - \left(q_o + \frac{dq_o}{dp}\,\delta p\right) \qquad \text{(A-22)}$$

$$C_{21}\delta C + C_{22}\delta T + C_{23}\delta p = \Delta HT_w \Delta\bar{p} + \Delta T_c\,\Delta T - q_L + H_i\left(q_i + \frac{dq_i}{dp}\,\delta p\right) - H\left(q_o + \frac{dq_o}{dp}\,\delta p\right) \qquad \text{(A-23)}$$

$$C_{11}\delta C + C_{12}\delta T + C_{13}\delta p = \Delta CT_w\,\Delta\bar{p} + \Delta T_E \Delta C + C_i\left(q_i + \frac{dq_i}{dp}\,\delta p\right) - C\left(q_o + \frac{dq_o}{dp}\,\delta p\right) \qquad \text{(A-24)}$$

where the dynamic pressure $\bar{p}$ is defined as:

$$\bar{p} \equiv p - \rho g Z \qquad \text{(A-25)}$$

A partial list of the definitions of the coefficients C_{ij} and residuals R_i is as follows:

$$C_{21} = a_3 \phi^n U^n$$

$$C_{22} = a_2 \phi^n U^n + \phi^{n+1} \rho^{n+1} C_p + (\rho C_p)_R (1-\phi^n)$$

$$C_{23} = a_1 \phi^n U^n + \rho^{n+1} \phi_o C_r U^n - (\rho C_p)_R \phi_o C_r T^n$$

$$R_2 = q_i H_i - q_o H^n + \Delta T_w H^n \Delta p^n + \Delta T_c \Delta T^n$$

where $a_1 = \frac{\partial \rho}{\partial p}$

$a_2 = \frac{\partial \rho}{\partial T}$

and $a_3 = \frac{\partial \rho}{\partial c}$

Equations (A-22) through (A-24) are three equations with three unknowns. These equations are solved by the numerical model after Gaussian elimination.

An iterative procedure is used for the solution. One iteration consists of a solution of δp, δT and δC in that order. The values of the concentration and temperature used in the solution of δp during the $(\ell+1)^{st}$ iteration are the concentration and temperature values available after ℓ iterations. For the solution of the temperature equation, the current pressure after $(\ell+1)$ is used along with concentration at ℓ. Finally, in the concentration update, pressure and temperature values obtained after $(\ell+1)$ iterations are used.

As an illustration, the temperature equation in the final form (programmed) is shown below.

$$C'_{22} \delta T^{\ell+1} = -C_{23}\, \delta p + \Delta H^{\ell+1} T_w \Delta \bar{p}^{\ell+1} + \Delta T_c \Delta T^{\ell+1} + q_i H_i$$

$$- q_o H^{\ell+1} + \frac{dq_i}{dp} \delta p H_i - \frac{dq_o}{dp} \delta p H^{\ell+1} + C_{24} [\Delta C^{\ell} T_w \Delta \bar{p}^{\ell+1}$$

$$+ \Delta T_E \Delta C^{\ell} + q_i C_i - q_o C^{\ell} + \frac{dq_i}{dp} \delta p C_i - \frac{dq_o}{dp} \delta p C^{\ell}] \qquad \text{(A-26)}$$

where

$$\delta p^{\ell+1} \equiv p^{\ell+1} - p^{n} \tag{A-27}$$

$$C'_{22} = C_{22} - \frac{C_{12}C_{21}}{C_{11}} \tag{A-28}$$

$$C'_{23} = C_{23} - \frac{C_{13}C_{21}}{C_{11}} \tag{A-29}$$

$$C_{24} = - \frac{C_{21}}{C_{11}} \tag{A-30}$$

and

$$\Delta H^{\ell+1}{}_{T_w}\Delta\bar{p}^{\ell+1} = \Delta H^{n}{}_{T_w}\Delta\bar{p}^{n} + \Delta H^{n}{}_{T_w}\Delta\delta p^{\ell+1}$$
$$+\Delta(c_p)_w\delta T^{\ell+1}{}_{T_w}\Delta\bar{p}^{n} + \Delta(c_p)_w\delta T^{\ell+1}{}_{T_w}\Delta\delta p^{\ell+1} \tag{A-31}$$

The pressure, temperature and concentration equations are solved for $\delta p^{\ell+1}$, $\delta T^{\ell+1}$ and $\delta C^{\ell+1}$, respectively, by a reduced band width direct solution or a two line successive overrelaxation method. The convergence criterion is based upon the change in density over an iteration. If the solution has converged

$$p^{n+1} = p^{n} + \delta p \tag{A-32}$$

and similarly for T^{n+1} and C^{n+1}.

APPENDIX B

WELLBORE MODEL EQUATIONS

If the user elects to specify surface conditions instead of bottom-hole values, the pressure and temperature changes in the wellbore must be computed. This is done by solving the equation of energy (total) and the equation of mechanical energy simultaneously over the wellbore depth. The energy balance over a depth, ΔZ, can be written as:

$$\Delta H + \frac{g\Delta Z}{g_c J} + \frac{wdw}{g_c J} = \Delta Q - \frac{\Delta W_f}{J}. \qquad \text{(B-1)}$$

Assuming steady-state incompressible flow, Eq. (B-1) becomes:

$$\Delta H + \frac{g\Delta Z}{g_c J} = \Delta Q \qquad \text{(B-2)}$$

The heat lost to the surroundings over a depth, ΔZ, is lost through two series resistances. These include (1) heat lost from the fluid to the outside casing wall, and (2) heat lost from the casing wall temperature into the surrounding formation. The overall heat loss can be expressed as:

$$\Delta Q = \frac{2\pi R_1 U_c \Delta Z (T_{av} - T_R)}{qF(t)} \qquad \text{(B-3)}$$

In Equation (B-3) the heat lost into the surrounding rock is represented by the function F(t). It can be derived assuming the wellbore is a constant heat flux line source. This overall derivation was first given by Ramey[6]. The resulting expression for F(t) is as follows:

$$F(t) \simeq -\ln\left(\frac{R_2}{2\sqrt{\gamma t}}\right) - 0.290 \qquad \text{(B-4)}$$

The actual expression involves the exponential integral function for which Equation (B-4) is simply an excellent approximation for times greater than a fraction of one day.

The coefficient U_c in Equation (B-3) is a combination of the overall heat transfer coefficient for the wellbore and the conductivity of the rock. It can be expressed as:

$$\frac{1}{U_c} = \frac{1}{UF(t)} + \frac{R_1}{k} \qquad \text{(B-5)}$$

For very short times (determined by F(t) in Equation (B-4) <0), the function F(t) is taken as zero. This is equivalent to assuming that the outside casing wall temperature remains at the geothermal gradient until the time is sufficiently large to cause F(t) = 0. Then each wellbore increment losses heat as a constant flux source.

Since enthalpy is a function of temperature and pressure, the equation of mechanical energy must be simultaneously solved to calculate the change in pressure over ΔZ. The change in pressure is the sum of the change in the gravity heat and the frictional pressure drop:

$$-\Delta p = \frac{\Delta Z \rho g}{g_c} + \frac{f \rho w^2}{4 g_c R_1} \qquad \text{(B-6)}$$

where ρ = density of the fluid, and f = friction factor for the flow down the well.

The friction factor is a function of Reynolds number and surface roughness. The enthalpy of the fluid is a function of both temperature and pressure:

$$H = H(p,T) \qquad \text{(B-7)}$$

The enthalpy of an arbitrary injection fluid is assumed to be proportional to the enthalpy of pure water at the same pressure and temperature according to the following relation:

$$H = C_p \, H_w / C_{pw} \qquad \text{(B-8)}$$

where C_{pw} is the heat capacity of water.

APPENDIX C

FORTRAN FORMATS

The input data for this program are conventionally prepared on standard tabulating cards. These data cards are read by the program, which is written in Fortran source code. In Fortran, the locations of various items on a data card are dictated by means of a FORMAT specification. Fortran input commands refer to a FORMAT specification in addition to a list of data items to be read, and the combination of a data list and FORMAT determines the values that the data items are assigned in the computer core storage.

The standard tabulating card is 80 columns in width. This data card can be divided into fields, where a field is defined as a group of contiguous columns which may contain a single item of data. The length of a field can be as short as one column, or as long as 80. On any card, fields of various lengths may appear. The field definition is the responsibility of the programmer. He defines fields with FORMAT specifications which are a part of his program.

In the well disposal simulation program, five types of fields are used and need to be discussed here.

The first is an "I" type field and is for integers only. Here, the definition of an integer is a quantity that must be a whole number. Decimal points may not appear in an "I" field. The second field type is "F" which is used for numbers that may assume fractional quantities (called floating point numbers). Decimal points may appear in "F" fields. The third field type is "E" which is used for floating point numbers with the option of using an exponent. The fourth field type is "X" which is used for skipping spaces on a card. Any character may appear in an "X" field because it will not be read by the program. The fifth type is "A", which is used for reading alphabetic data.

Alphabetic (A) formats are of the type Ak where k is the field length. Any alphabetic, numeric, or conventional punctuation character may appear in an A-type field.

Integer FORMAT specifications are of the type (Ik), where k is the field length. Thus, a FORMAT specification (I5) describes a data field 5 columns in length in which only

whole numbers may appear. Numbers in "I" fields must be right justified. For example, to punch the quantity 73 into an I5 field, punch blank-blank-blank-7-3. If this quantity had been punched blank-7-3-blank-blank, it would have been interpreted as 7300 because Fortran treats input blanks as zeros.

A floating point FORMAT is of the form (Fk.m), where again k is the field length. If a decimal point is not punched in the field, the program will assume that one exists m places to the left of the right-hand side of the field. If the decimal point is punched, it overrides the m specification. For example, assume we are reading a variable, A, according to the FORMAT (F5.2). The table below shows the value assigned to A for five different contents of the field.

Number punched on data card	Value assigned to A	Comments
763.1	763.1	decimal override
7.642	7.642	decimal override
83428	834.28	assumed decimal
bbb64*	.64	assumed decimal
48bbb*	480.00	assumed decimal

The floating point with exponent FORMAT is of the form (Ek.m), where again k is the field length and m is the number of decimal places put in data without a decimal. After a floating point number is entered, an E and the value of an exponent to the base 10 by which the number is to be multiplied may be added. A plus or minus can be used instead of an E and when the E is present, the absence of a sign indicates plus. Some examples may help:

Input Field	Ek.m Input Specification	Converted Value
+143.26E-03	E11.2	.14326
-12.437629E+1	E13.6	-124.37629
8936E-004	E9.10	.008936
327.625	E7.3	327.625
4.376	E5	4.376
-.0003627+5	E11.7	-36.27
-.0003627E5	E11.7	-36.27
blanks	Ek.m	-0.
lE1	E3.0	10.
E+06	E10.6	0.

The exponent must be no greater than 323 and must also be an integer.

253

*b indicates blank (space bar on keypunch, like a typewriter).

X formats are of the type kX, which simply means skip k columns on the data card.

Format specifications usually include multiple fields, e.g. (I5, I10, F10.5, 5X, F5.0). The fields are contiguous, and the first specification starts at column one on the card. Thus, this example defines a card:

col 1 - 5	integer field
col 6 - 15	integer field
col 16 - 25	floating point field
col 26 - 30	skip
col 31 - 35	floating point field

In this example, columns 36 - 80 of the card are not used and are ignored by the program; it is the same as if we had specified (I5, I10, F10.5, 5X, F5.0, 45X).

Field repitition can be indicated by prefixing the I or F with an integer that indicates the number of times that specification is to be repeated. For example, (4I5) means there are four contiguous integer fields of five columns each. This specification is the same as (I5, I5, I5, I5). As another example, (2F5.0, 3I5) is the same as (F5.0, F5.0, I5, I5, I5).

In Fortran there is a one-to-one correspondence between the items in a data list and the data fields (exclusive of X-fields). A list corresponding to (I5, I10, F10.5, 5X, F5.0) might be:

```
I, J, A, B
```

where I and J are program integers and A and B are program floating point (fractional) variables.

There are two situations in which the one-to-one correspondence between the input list and FORMAT is not strictly true--if there are fewer items in the list than the FORMAT will accommodate, and when the list has more items than the FORMAT indicates. To preserve the one-to-one correspondence in these cases, Fortran adheres to the following conventions.

In the case of a list smaller than the FORMAT, the program will ignore the unused (rightmost) specifications. For example, the input list

```
I, J, A, B
```

read on a FORMAT (2I4, 2F10.0) could be read according to (2I4, 4F10.0) with no error; the two excessive F10.0 fields are ignored.

The second situation, where the input list is longer than the FORMAT specifications, is a little more complex. Data transmission begins with the first item in the input list under control of the first field specification in the FORMAT. Data are read according to the field specifications until the end of the FORMAT is reached. At that point the next data card in the deck is automatically read. Transmission of input data continues with the next item in the input list being taken from the next card according to the first field specification of the FORMAT. That is, the scan re-initializes to the beginning of the FORMAT. A couple of examples will help clarify this.

(A) Input data list: I, J, A, K, L, B
FORMAT : (2I4, F10.0)

Variables I, J, and A are read from the first card, which exhausts the FORMAT field specifications. Then the next card is brought in and K, L, and B are read from it according to (2I4, F10.); that is, on the second card the format scan returns to the left-hand side of the FORMAT, to the first field specification.

(B) Input data list: (A(I), I = 1,N)* where N = 100
FORMAT : (8F10.0)

The first 8 values for A, i.e. A(1), A(2),..., A(8) are read from the first card, the next eight from the second, and so on, where the FORMAT of each card is (8F10.0). 13 cards are required to read this array of 100 numbers. The last card will contain only 4 values and columns 41 - 80 will not be used.

A more complete discussion of Fortran FORMAT specifications is available in any Fortran text or reference manual.

*This means that A is a subscripted variable (a one-dimensional array) and that N values are going to be read into the array starting at A(1). The mathematical expression relating to the Fortran A(1), I = 1,N) is A_i, i = 1,2,...,N.

U. S. GOVERNMENT PRINTING OFFICE 1975 - 677-365/1818 Reg. 8